Design and Synthesis of Reaction Intermediate Derivatives as Biotin Protein Ligase Inhibitors

William Tieu

A thesis submitted in total fulfilment of the requirements for

the degree of Doctor of Philosophy

THE UNIVERSITY *of* ADELAIDE

2011

Department of Chemistry

The University of Adelaide

Table of Contents

Chapter Three

Chapter Four

Chapter Five

Chapter Six

Chapter Seven

Abstract

This thesis reports the development of selective and potent small molecule inhibitors of *Staphylococcus aureus* biotin protein ligase (SaBPL) using 1,2,3-triazole and phosphodiester linkers as bioisosteric analogues of the phosphoroanhydride linker found in the reaction intermediate biotinyl-5'-AMP **1.03**.

Chapter one describes the structure and catalytic mechanism of the essential enzyme SaBPL. An overview of reaction intermediate mimics as ligase inhibitors is discussed and the utility of 1,2,3-triazole ring as a bioisosteric analogue is outlined.

Chapter two investigates the phosphodiester reaction intermediate mimic biotinol-5'-AMP **1.05** as a potential inhibitor of SaBPL. Two different synthetic approaches towards biotinol-5'-AMP **1.05** were developed with the aim of scaling up the synthesis to enable biological characterisation and animal trials. Assay results indicated biotinol-5'-AMP **1.05** is a potent but a non-selective inhibitor of SaBPL (IC$_{50}$ = 0.12 ± 0.01 μM).

Chapter three investigates the use of 1,2,3-triazole as a bioisostere of the phosphoroanhydride linker of the reaction intermediate biotinyl-5'-AMP **1.03**. Both 1,4-triazole **3.25** and 1,5-triazole **3.33** were synthesized from biotin alkyne **3.12** and adenosine azide **3.16** using CuAAC and RuAAC. Optimisation of both CuAAC and RuAAC in the synthesis of **3.25** and **3.33** were also investigated. 1,4-Triazole **3.25** is the first reported selective inhibitor of BPL, inhibiting SaBPL (K$_i$ = 1.83 ± 0.33 μM).

Chapter four extends the work described in chapter three with an investigation of 1,2,3-triazole analogues based on triazole **3.25**. Structure-activity relationships were developed and a general structure for this novel class of inhibitors was obtained. Triazole **4.01**, the lead compound from this class of inhibitors, is a potent and selective inhibitor of SaBPL (K$_i$ = 0.66 ± 0.15 μM). X-ray crystal structure of **4.01** bound to SaBPL illustrated the effective molecular recognition between the 1,2,3-triazole ring and SaBPL and emphasized the 1,2,3-triazole ring as an effective bioisostere of phosphoroanhydride linker. Additionally, a successful *in situ* click experiment was performed using a library of alkynes/azides fragments and R122G SaBPL mutant enzyme. The mutant enzyme was able

to select the appropriate fragments and selectively synthesize the potent 1,4-triazole inhibitor **4.01**.

Chapter five examines analogues of biotin alkyne **3.12**, a precursor to 1,2,3-triazole inhibitors and was found to be a potent inhibitor (SaBPL $K_i = 0.30 \pm 0.05$ µM). Norbiotin alkyne **4.16** was found as highly effective inhibitor against SaBPL ($K_i = 0.08 \pm 0.01$ µM) and an antibacterial agent against methicillin resistant *staphylococcus aureus* (MIC = 4 - 16 µg/ml).

Chapter six extends the work described in chapter four. Using the general structure developed in chapter four, a series of analogues with modifications to the ATP binding component were synthesized and assayed against a SaBPL. Triazole **6.10** containing the privileged scaffold, 2-benzoxazolone, was found as a potent and selective inhibitor against SaBPL ($K_i = 0.09 \pm 0.02$ µM).

Chapter seven details the experimental procedures used to synthesize compounds described in chapter 2 – 6.

Declaration

This work contains no material which has been accepted for the award of any other degree or diploma in any university or other tertiary institution and to the best of my knowledge and belief, contains no material published or written by another person, except where due reference has been made in the text.

I give my consent for this copy of my thesis, when deposited in the University Library, being made available for loan and photocopying, subject to the provisions of the Copyright Act *1968* (Cth).

I also give permission for the digital version of my thesis to be made available on the internet, via the University's digital research repository, the Library catalogue, the Australasian Digital Theses Program (ADTP) and also through internet search engines, unless permission has been granted by the University to restrict access for a period of time.

…………………..

William Tieu

…………………..

Date

Acknowledgement

First and foremost I would like to thank Professor Andrew Abell for his supervision and guidance during my candidature. I am indebted to his helpful advice, extensive knowledge, positive and forward thinking attitude to research and tireless efforts in drafting and revising this thesis.

I would like to thank the collaborators in the BPL project. Belinda Ng, Tatiana Soares Da Costa and Steven Polyak for performing the BPL and antimicrobial assays and *in situ* click experiments. Min Yap, Nicole Pendini and Matthew Wilce are thanked for providing the invaluable x-ray crystallographic structures of inhibitors bound to SaBPL. Particular mention goes to Grant Booker (co-supervisor) and Steven Polyak for their support, enthusiasm and tireless efforts throughout my candidature.

I would like to thank all the past and present members of the Abell group. To the post-docs (Sabrina Heng, Daniel Pedersen, Markus Pietsch and Ondrej Zvarec), thank you for the technical advice and friendship.

Thank you to my supportive parents, Hoa and Hue, for always being there for me and understanding the life of a PhD student. Thank you to my sister Joanna for the moral support and encouragement.

Unreservedly, I must thank my girlfriend Thao. She has always believed in me and has the magical ability to make me happy whenever I'm with her (especially when my experiments are not working).

Abbreviations

ABL	ATP binding loop
ACC	Acetyl CoA carboxylase
AcCN	Acetonitrile
AcOH	Acetic acid
AIBN	Azobisisobutyronitrile
AMP	Adenosine-5'-monophosphate
ATP	Adenosine-5'-triphosphate
BBL	Biotin binding loop
BCCP	Biotin carboxyl carrier protein
BOC	*tert*-Butoxycarbonyl
BPL	Biotin protein ligase
CDI	1,1' – carbonyldiimidazole
COSY	Correlation spectroscopy
^{13}C NMR	Carbon nuclear magnetic resonance
Cp*	Pentamethylcyclopentadienyl
CuAAC	Copper mediated Alkyne Azide Cycloaddition
DCC	N,N' - Dicyclohexylcarbodiimide
DCM	Dichloromethane
DDQ	2,3-dichloro-5,6-dicyano-*p*-benzoquinone
DEAD	Diethyl azodicarboxylate
DEAE	Diethylaminoethyl cellulose
DIBAL-H	Diisobutylaluminium hydride
DIPEA	N,N - Diisopropylethylamine
4-DMAP	4-Dimethylaminopyridine
DMF	Dimethylformamide
DMSO	Dimethyl sulphoxide
DMTr	4,4'-dimethoxytrityl group
DPPA	Diphenylphosphoryl azide
EcBPL	*E. coli* biotin protein ligase
EDA	Ethylenediamine
EDCI	1-Ethyl-3-(3-dimethylaminopropyl)carbodiimide

EtOAc	Ethyl acetate
EtOH	Ethanol
5-ETT	5-Ethylthiotetrazole
FTIR	Fourier transform infrared spectroscopy
^{1}H NMR	Proton nuclear magnetic resonance
HPLC	High-performance liquid chromatography
HRMS	High resolution mass spectrometry
HsBPL	*Homo sapiens* biotin protein ligase
IC$_{50}$	Half maximum inhibitory concentration
iPrOH	isopropanol
K$_i$	Dissociation constant
LCMS	Liquid chromatography mass spectrometry
*m*CPBA	*meta*-Chloroperoxybenzoic acid
Me	Methyl group
MEK	Methyl ethyl ketone (2-butanone)
MeOH	Methanol
MIC	Minimum inhibitory concentration
MRSA	Methicillin resistant *S. aureus*
MSSA	Methicillin sensitive *S. aureus*
^{31}P NMR	Phosphorous nuclear magnetic resonance
POM	pivaloyloxymethyl
p-TsOH	*para*-Toluenesulphonic acid
Py	Pyridine
RMSD	Root mean square deviation
ROESY	Rotating frame overhauser enhanced spectroscopy
RuAAC	Ruthenium mediated Alkyne Azide cycloaddition
SaBPL	*S. aureus* biotin protein ligase
SAR	Structure-activity relationship
TBAI	Tetrabutylammonium iodide
TBHP	*tert*-Butyl hydroperoxide
t-BuOH	*tert*-butanol
TEAB	Triethylamine bicarbonate buffer
TFA	Trifluoroacetic acid

THF	Tetrahydrofuran
TLC	Thin layer chromatography
TMS	Trimethylsilyl group
Ts	4-toluenesulphonyl group

Chapter One

1.1 The need for antibiotics

The spread of multidrug resistant bacteria is an unresolved threat and a heavy burden to global health services. Of particular concern are resistant strains of *Staphylococcus aureus* (*S. aureus)* such as methicillin resistant *S. aureus* (MRSA). Whilst resistance to hospital acquired MRSA (HA-MRSA) has decreased in the past decade in the USA[1], UK[2] and Australia[3], the impact of HA-MRSA is still an overwhelming and ongoing problem, accounting for over 62% of all hospital acquired infections and costing patients and hospitals up to $USD 9.7 billion annually in USA alone.[4] More concerning is the unabated increase in community acquired MRSA (CA-MRSA), which now accounts for 18% of all MRSA incidents.[1] One logical solution to this problem is to develop new classes of antibiotics with novel mechanisms of action that are directed at unexplored and viable biological targets. We present *S. aureus* biotin protein ligase (SaBPL) as one such target and the design of small molecule inhibitors thereof.

1.2 Biotin Protein Ligase

Biotin protein ligase (BPL) is a vital enzyme found in all organisms. Its primary function is to catalyze the post-translational attachment of the co-factor biotin **1.01** (vitamin B7) onto specific lysine residue on the biotin carboxyl carrier protein (BCCP) as shown in Scheme 1 (below)[5]. This species then activates key enzymes such as acetyl CoA carboxylase (ACC)[6] and pyruvate carboxylase (PC)[7]. The consequential role of ACC involves the carboxylation of acetyl-CoA to malonyl-CoA in what is the first committed step in fatty acid biosynthesis. This pathway is essential for cell membrane maintenance and biogenesis.[8] Biotin-activated PC is involved in the conversion of pyruvate to oxaloacetate to ultimately replenish the citric acid cycle. PC and the citric acid cycle is central to a number of key metabolic pathways, including amino acid biosynthesis.[9] Thus targeting BPL can affect a number of critical biochemical pathways that are essential for the survival of *S. aureus*.

BPL also has a secondary regulatory role mediated through binding with BioO and BioY genes.[10,11] Prokaryotic class II BPLs [such as *S. aureus* BPL (*Sa*BPL) and *E. coli* BPL (EcBPL)] contain a DNA binding domain. This domain is thought to bind biotin operator (BioO, which is involved in the biosynthesis of biotin) and the biotin transport protein gene

(BioY, which is involved in the cellular uptake of biotin). Thus targeting BPL will also target the ability of *S. aureus* to maintain its cellular concentration of biotin with downstream effects on biotin related biochemical pathways.
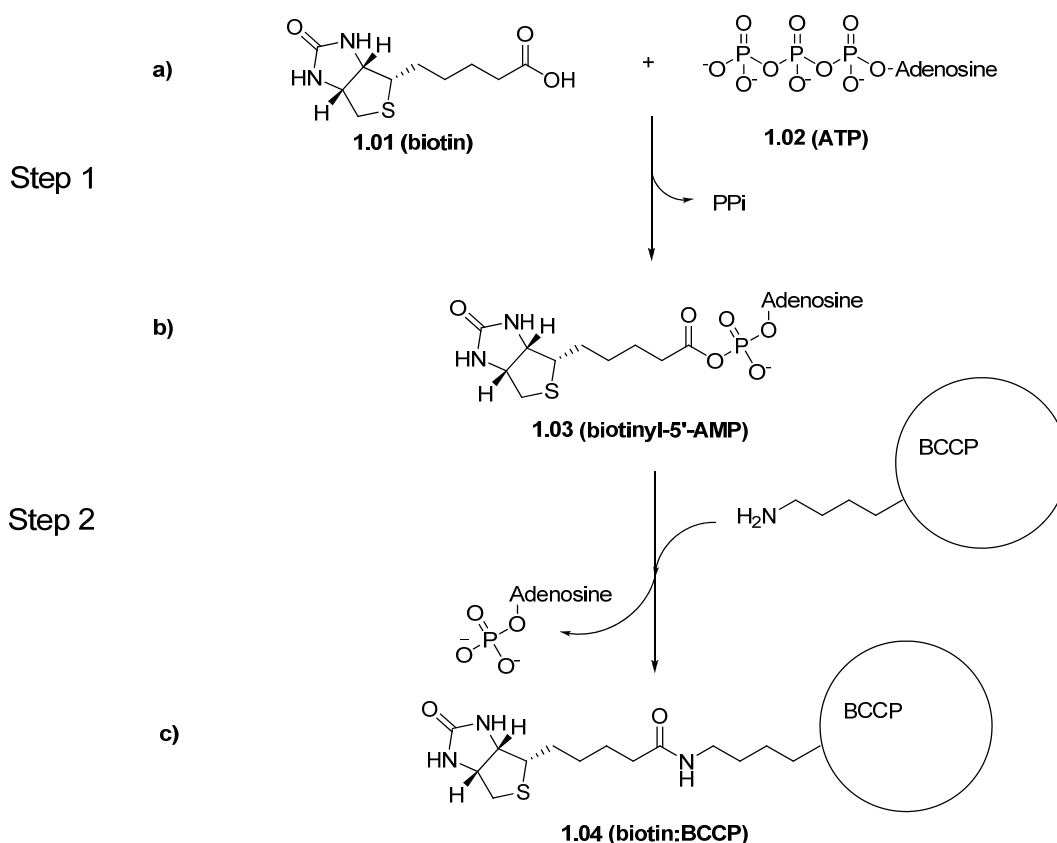
Scheme 1.1: The catalytic mechanism of biotinylation.

1.2.1 Mechanism of active site of SaBPL

The attachment of biotin to BCCP proceeds through a two step mechanism, as shown in Scheme 1.1.[12,13] In the first step, BPL catalyses the formation of biotinyl-5'-AMP **1.03** from bound biotin and ATP. This proceeds by a sequential induced fit binding of biotin to a biotin binding pocket, leading to an ordering of a biotin binding loop and ATP binding loop (see Figure 1.1 for binding loops). The subsequent binding of ATP, followed by nucleophilic attack by biotin on the α-phosphate of the ATP gives the reaction intermediate biotinyl-5'-AMP **1.03** and completes the first step. The second step involves covalent attachment of this activated biotin onto the ε-amino group of an active site lysine of BCCP. A comparison of reported structures of BPL from different species and the associated high

degree of homology suggests that this reaction proceeds in this stepwise manner in most species, i.e. activation followed by attachment.[14] Furthermore, such a stepwise mechanism is observed with other ligases such as lipoate-protein ligase A[15,16] and tRNA synthetases[12].

1.2.2 Structure of SaBPL

SaBPL has three distinct domains as depicted in Figure 1.1. It is suggested the N-terminal domain adopts a signature DNA binding helix-turn-helix motif that is involved in the regulation of both cellular uptake of biotin and the biosynthesis of biotin as described above. Additionally, Wallace and co-workers have revealed the N-terminal domain is necessary for the catalytic function of BPL, albeit within *S. cervisiae* BPL.[17] However, no study to date has determined the role of the N-terminal domain with regards to the catalytic mechanism of BPL. The C terminal domain, which is structurally similar to the ubiquitous SH3 domain, is implicated in ATP binding and protein-protein interactions. The central catalytic domain of BPL is highly conserved across all species[14], with a catalytic active site that binds both biotin and ATP. An examination of this catalytic domain reveals two disordered binding loops, an ATP binding loop (ABL-residues 218 – 230) and a biotin binding loop (BBL, residues 113 - 130) as highlighted by the blue and green ribbons, respectively, in Figure 1.1. A closer examination of the active site is detailed below.

Biotin binding pocket

The biotin binding pocket is characterised by two distinct regions, a hydrophilic pit and a hydrophobic shaft. The hydrophilic pit consists of Ser92, Thr93, Gln116 and Arg120, which hydrogen bond with the ureido ring of biotin, as shown in Figure 1.2. These residues are highly conserved in BPLs across most species.[18] The hydrophobic shaft on the other hand is defined by the induced fit binding of biotin in the first catalytic step of BPL (discussed above). This induced fit results in the valeric tail of biotin being sandwiched between 3 hydrophobic beta sheets and the hydrophobic portion of the biotin binding loop. X-ray crystal structures of biotin **1.01** and biotinyl-5'-AMP **1.03** show a high degree of conservation in the biotin binding pocket of SaBPL, EcBPL[12], AaBPL (*Aquifex aeolicus*)[19],

PhBPL (*Pyrococcus horikoshii*)[20] and MtBPL (*Mycobacterium tuberculosis*)[21] with Figure 1.2 highlighting the binding mode of biotin within this pocket for SaBPL.
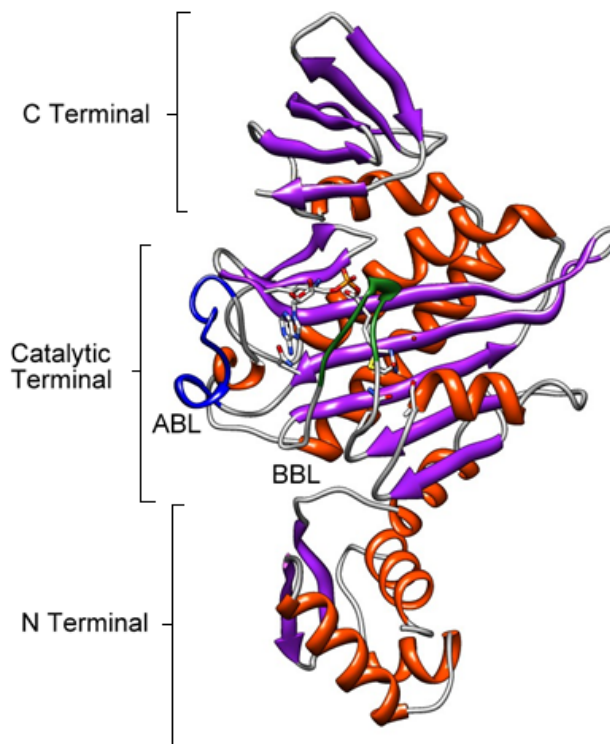
Figure 1.1: 3D depiction of SaBPL with biotinyl-5'-AMP **1.03** bound. The β sheets are shown in purple, α helices in orange, biotin binding loop (BBL) in green and ATP binding loop (ABL) in blue.
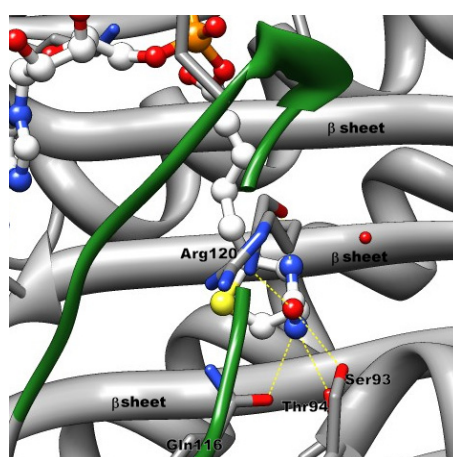
Figure 1.2: 3D depiction of reaction intermediate biotinyl-5'-AMP **1.03** bound to SaBPL with green ribbon highlighting the biotin binding loop and yellow dashes indicating hydrogen bonding interactions between the ureido ring of biotin and SaBPL.

ATP binding pocket

The ATP binding pocket is defined by a large crevasse exposed to solvent. Residues Asn212 and Ser128 at the base of the ATP binding pocket hydrogen bond with the adenine ring of ATP and also the reaction intermediate biotinyl-5'-AMP **1.03**. Trp127, situated within the biotin binding loop forms a displaced parallel π interaction with the adenine ring of biotinyl-5'-AMP **1.03** (Figure 1.3). This residue is highly conserved in BPL's across all species. Mutagenesis studies with EcBPL implicate Trp127 in binding ATP, but not binding biotin.[18,22] This suggests that intermolecular interaction with Trp127 is an important consideration for any potential SaBPL inhibitor targeting the ATP binding pocket.

Ile224, Ala228 and Phe220, situated on the ATP binding loop, create a hydrophobic region within the ATP binding pocket of SaBPL. This region is proposed to encapsulate the adenine ring of ATP. Again, mutagenesis studies in EcBPL demonstrate that modifying the hydrophobic residues results in decrease binding affinity of the ATP substrate to the ATP binding pocket of EcBPL.[22]

Figure 1.3: 3D depiction of reaction intermediate biotinyl-5'-AMP bound to SaBPL with green ribbon highlighting the biotin binding loop and blue ribbon highlighting the ATP binding loop.

Phosphate binding domain

The phosphate binding domain of SaBPL is situated between the ATP and biotin binding pockets as depicted in Figure 1.4. A ubiquitous 'Rossman fold' phosphate binding motif (GXGXXG) is located within this domain, however this binds with the phosphate groups of biotinyl-5'-AMP in an atypical mode.[12] Here, only Arg122 is involved in the binding of the phosphate group. Both Arg125 and Lys187 assist in forming a predominately positive charged phosphate domain that binds the phosphoroanhydride linker of the reaction intermediate biotinyl-5'-AMP **1.03**, as shown in Figure 1.4. There is a high degree of homology within the phosphate binding domain across most species of BPL with Arg122 universally conserved across all reported BPL species.[12]
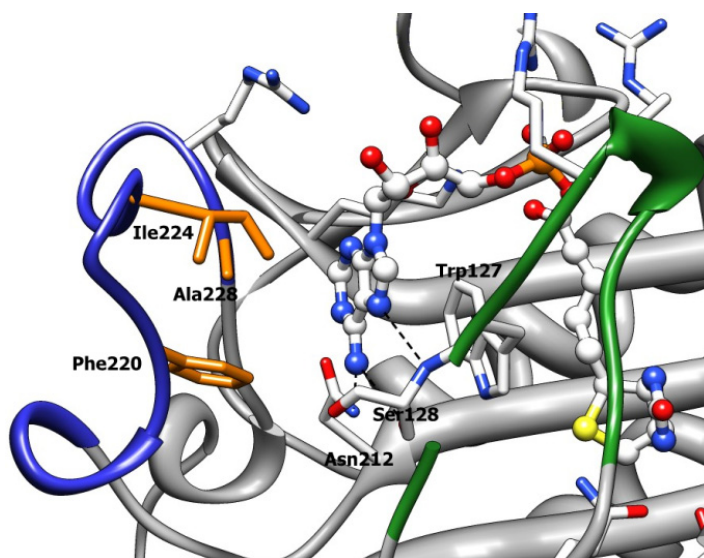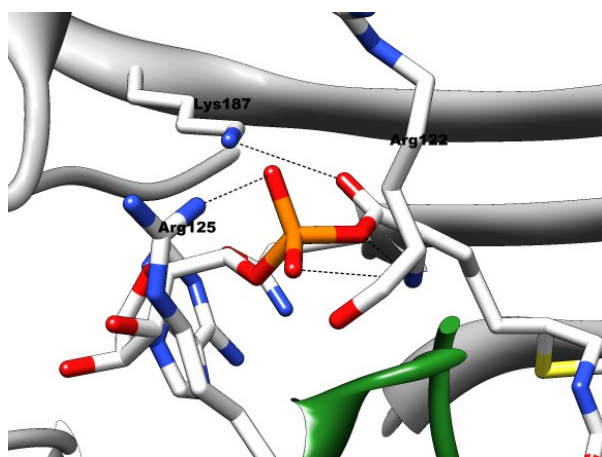

Figure 1.4: 3D depiction of reaction intermediate biotinyl-5'-AMP **1.03** bound to SaBPL with green ribbon highlighting the biotin binding loop and blue ribbon highlighting the ATP binding loop.

1.2.3 SaBPL as an antibacterial target

SaBPL is an attractive novel target for antibiotic development. Firstly, targeting SaBPL will consequently target the fatty acid pathway. SaBPL is a bi-functional enzyme that controls the biotinylation of ACC and PC. Both ACC and PC are critical to fatty acid biosynthesis and hence membrane structure. The fatty acid pathway is a proven pathway for antibacterial targets with the clinical drug isoniazid targeting enoyl-acyl carrier protein reductase, an enzyme within the fatty acid biosynthesis.[23] Secondly, SaBPL is the only enzyme in *S. aureus* that regulates biotinylation and is involved in the regulation of biotin transport (BioY) and biotin biosynthesis (BioO) genes. Thus targeting SaBPL will target

the cell's ability to source the essential metabolite, biotin. Thirdly, allelic replacement mutagenesis of individual genes in a battery of bacteria (including *S. aureus*) revealed that BPL is an essential enzyme for cell growth (i.e. the absence of BPL gene resulted in limited cell growth of *S. aureus*).[24] This result highlights that BPL is indispensable in normal cell functioning and consequently targeting BPL will result in inhibition of *S. aureus*.

Despite the attractiveness of BPL as an antibacterial target, there are limited studies examining its inhibition. The only reported BPL inhibitor is the reaction intermediate mimic, biotinol-5'-AMP **1.05** (Figure 1.5).[25] The key feature of biotinol-5'-AMP **1.05** is the non-hydrolysable and enzymatically stable bioisosteric phosphodiester linker between the biotin and adenosine component. The X-ray crystal structure of biotinol-5'-AMP **1.05** bound to EcBPL shows that this inhibitor mimics the binding mode of biotinyl-5'-AMP to EcBPL.[12] A comparison of data from kinetic and binding studies of **1.03** and **1.05** with EcBPL[25] and PhBPL[20] reveals that biotinol-5'-AMP **1.05** is capable of mimicking the allosteric regulatory function of **1.03**. Crucially and in the same studies, biotinol-5'-AMP **1.05** was found to prevent the biotinylation function of BPL. On the basis of these studies, biotinol-5'-AMP **1.05** is suggested to be a focal point for the development of inhibitors against SaBPL.
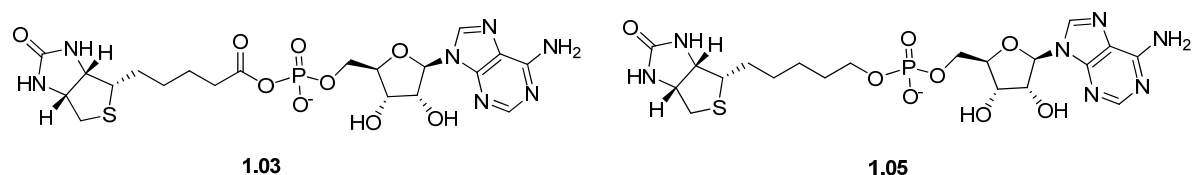
Figure 1.5: reaction intermediate biotinyl-5'-AMP **1.03** and its mimic, biotinol-5'-AMP **1.05**.

Having said this, progressing biotinol-5'-AMP **1.05** as drug is likely to be limited by at least three key features with SaBPL:

a) The high homology within the catalytic domain of BPL between species (Section 1.2.2). This suggests that biotinol-5'-AMP **1.05** will bind with all BPL in a similar fashion (this is evident from solved structures of biotinol-5'-AMP **1.05** bound to PhBPL, EcBPL and MtBPL). Thus there is a need to deviate from biotinol-5'-AMP structure in order to obtain selectivity.

b) The high specificity of BPL towards biotin.[21,26] Analogues of biotin have been developed, however small structural deviations in the ureido and thiophene ring have been shown to lack molecular recognition with the biotin binding pocket.[26] This suggests deviating from the biotinol structure will result in loss in binding affinity.

c) The ATP pocket is only formed upon biotin binding within the active site. This indicates that inhibitors must be capable of generating the ordered ATP binding pocket. It is noteworthy the ATP binding pocket contains a lower degree of sequence identity between BPL species and is suggested a focus point for developing inhibitors that are selective.

Based on this assessment, it is suggested that the design of next generation SaBPL inhibitors may require the retention of biotin component, while modifying the ATP component provide selectivity and the phosphodiester linker to provide a biostable alternative that is easy to introduce. To this end we investigated the development of a suitable bioisosteric analogue of the phosphoroanhydride linker.
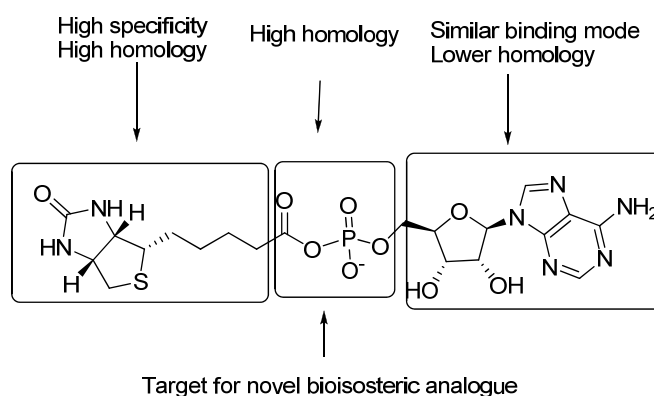
Figure 1.6: Biotinyl-5'-AMP **1.03** with boxes demarking its three components and summarising the degree of homology within each component.

1.3 Bioisosterism in drug design

Bioisosterism is a strategy employed in the rational drug design that involves exchanging fragments within a lead compound with broadly similar fragments that will elicit similar biological effects, but at the same time provide different non-biological attributes.[27-29] These attributes involve, but are not limited to, modulating the selectivity, ADME

properties, toxicophores, novelty for intellectual property purpose and ease of synthesis.[30] A focus of this thesis is to investigate phosphoroanhydride bioisosteres that allow the facile synthetic conjugation of biotin and adenosine analogues to provide structures that can selectively inhibit BPL from different species.

1.3.1 Phosphorous based bioisosteres

The phosphate groups **1.06 – 1.08** are critically associated with molecular recognition, and as such the affinity and activity of enzymes.[31] Phosphate groups **1.06 – 1.08** are ubiquitous in nature, with nearly half of all protein interactions containing them. They are essential to an assortment of biological processes, ranging from gene regulation, signalling, biosynthesis and metabolism.[31] Consequently, designing compounds that mimic the phosphate containing groups is a significant focus in drug development. However, phosphate groups **1.06 – 1.08** invariably confer low permeability and low stability to the associated structure. Thus, a range of bioisosteric analogues have been devised to overcome these issues, as shown in Figure 1.7.
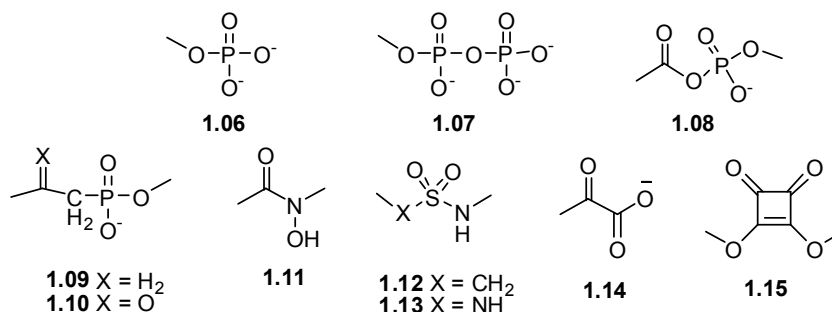
Figure 1.7: Phosphate groups found in nature (phosphodiester **1.06**, pyrophosphate **1.07** and phosphoroanhydride **1.08**) and examples of phosphate bioisosteres **1.09-1.15**.[30,32]

1.3.2 Bioisosterism in ligase inhibitors

BPL and ligases, such as aminoacyl synthetase, have commonality in the biochemical reaction that they catalyse with the reaction intermediate **1.17** being formed during the catalysed reaction (Figure 1.8).[33,34] Using **1.17** as a starting point for developing ligase inhibitors is problematic as it contains a hydrolytically and enzymatically unstable

phosphoroanhydride linkage.[35] Much work has thus gone into the synthesis and development of non-hydrolysable reaction intermediate mimics (phosphoryl bioisosteres) such as sulfonmyl, phosphodiester, hydroxylamine and di-keto-ester have been developed (Figure 1.8 and Table 1.1).
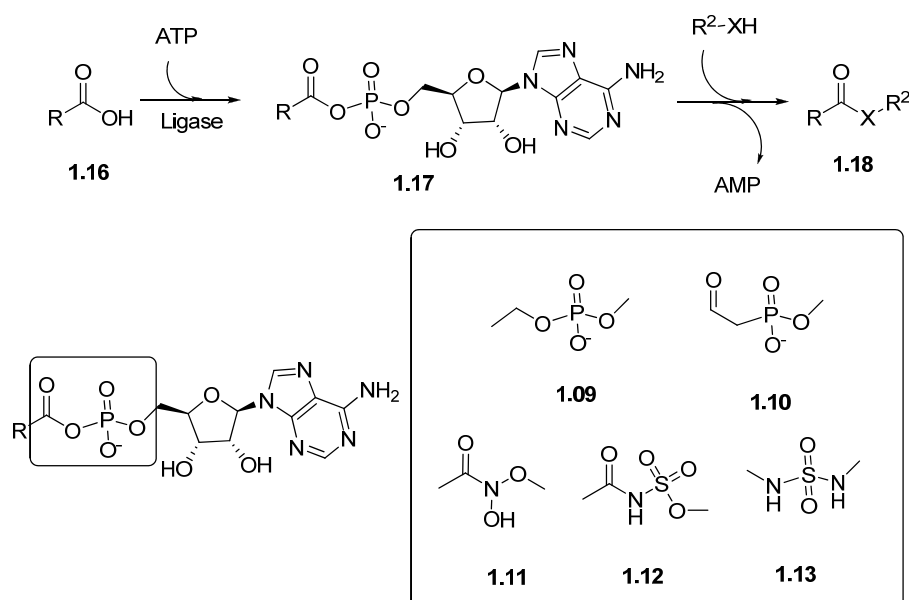
Figure 1.8: A general reaction scheme for ligases (top). A selection of phosphoroanhydride bioisosteres reported for ligase inhibitors (bottom).

Table 1.1: A selection of ligase targets, corresponding inhibitors and inhibition and whether the reported inhibitors were selective compared to human ligases

Enzyme	Linker	Inhibition	selectivity	Ref
LeuRS	**1.12**	$K_i = 1.6$ nM	N	Yu[36]
ArgRS	**1.12**	$K_i = 7.5$ nM	N	Forrest[37]
AspRS	**1.10**	$K_i = 15$ nM	N	Bernier[38]
MetRS	**1.11**	$K_i = 10.9$ μM	N	Lee[39]
o-Succinylbenzoyl-CoA Synthetase	**1.12**	$K_i = 5.6$ μM	N	Tian[40]
Bi-functional salicyl-AMP ligase	**1.13**	$K_i = 3.8$ nM	N[b]	Somu[41]
Pantothenate synthetase	**1.12**	$K_i = 0.22$ μM	N[b]	Tuck[42]
Phosphopantothenoylcysteine synthetase	**1.09**	$Ic_{50} = 10$ nM	Y[a]	Patrone[43]

[a] Modified adenylate analogues through rational design. [b] No human homologue equivalent enzyme.

Studies with reaction intermediate mimics as antibacterial agents highlight the most pressing issue to be limited selectivity, particularly when host ligase equivalents are present, as shown in Table 1.1. It is suggested that this issue will also affect biotinol-5'-AMP **1.05**. One reason for the limited success in developing selective reaction intermediate mimics is the low yielding and multiple synthetic steps required to form the bioisosteric linker such as **1.09** and **1.12** (also in biotinol-5'-AMP **1.05**). This results in limited ability to perform SAR studies and consequently limits the capabilities to delivery an inhibitor with the required selectivity. A new bioisostere is therefore required for the development of reaction intermediate mimics. To this end, we propose the 1,2,3-triazole ring as a suitable bioisostere of the phosphoroanhydride linker.

1.4 1,2,3-Triazole chemistry in bioisosterism

The 1,2,3-triazole motif is a versatile heterocycle with a number of desirable attributes that make it a good candidate as a bioisostere. It is stable to acid/base hydrolysis, reductive and oxidative conditions and typical physiologically conditions making it resistant to metabolic degradation. A 1,2,3-triazole ring has three potential hydrogen bond acceptor sites (nitrogens), a polarised proton and can also participate in π-π interactions (see Figure 1.9). These properties mean that 1,2,3-triazole has found wide applicability as a bioisosteric analogues for amides[44,45], olefins[46], disulphides[47,48], phosphomonoesters[49], pyrophosphate[50], phosphodiester linkers of oligonucleotide[51] and phosphoroanhydride[41].
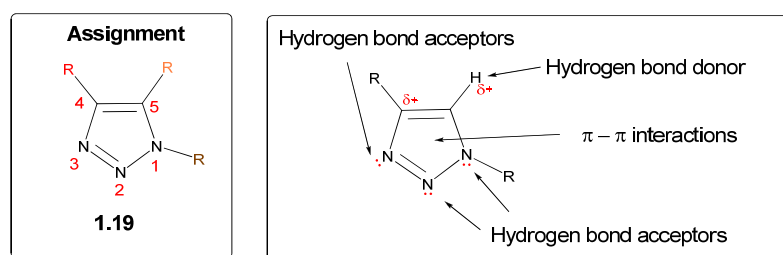
Figure 1.9: The assignment of 1,2,3-triazole (left); the potential intermolecular interaction sites of 1,2,3-triazole (right).

The facile and selective synthesis of 1,2,3-triazole from alkyne and azide reactants has also provided significant impetus for the use of the 1,2,3-triazole in many applications included its use as a bioisostere. The 1,2,3-triazole is typically prepared by reacting an alkyne and an azide via either a thermally mediated 1,3-cycloaddition (Huisgen), copper alkyne-azide cycloaddition (CuAAC), or ruthenium alkyne-azide cycloaddition (RuAAC). In some limited cases a triazole has also been prepared using an *in situ* click approach (see Scheme 1.2).
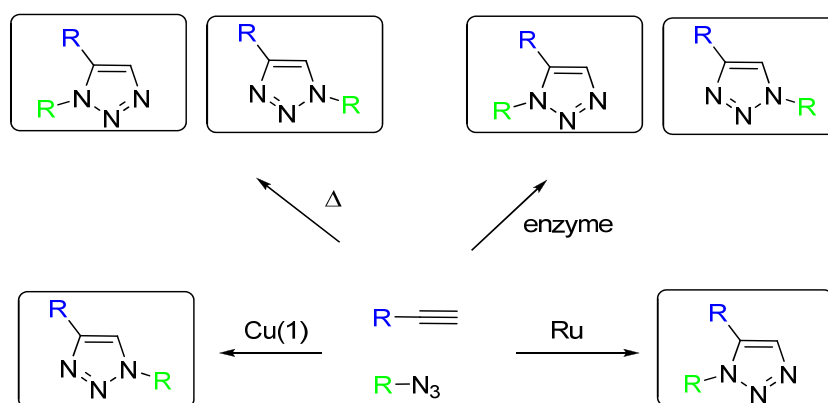
Scheme 1.2: Four possible synthetic routes to 1,2,3-triazole. Clockwise from top left: 1,3-dipolar cycloaddition, *in situ* click chemistry, ruthenium alkyne azide cycloaddition (RuAAC), copper alkyne azide cycloaddition (CuAAC).

1,3-Dipolar cycloaddition (Huisgen Cycloaddition)

The work by Rolf Huisgen and others during the early 1960's identified the 1,3-dipolar cycloaddition between dipolarophiles (nitrones, azides, and diazoalkanes) and alkyne/alkene reactants as a convenient method for the preparation of 5 membered heterocycles[52]. This approach, when applied to alkyne and azides, yields both 1,4 and 1,5-triazole as shown in scheme 3. Few reactions rival the 1,3-dipolar reactions in terms of its ability to combine fragments, with high atom economy and multiple bonds undergoing transformation to form products that are significantly more complex than the starting reactants. However, the 1,3-dipolar cycloaddition between alkyne and azide has a high energy of activation (requiring heating[53] or constraints (intramolecular reactions)[54] to yield the 5 membered ring) with the reaction being non-selective producing both 1,4 and 1,5-triazole.
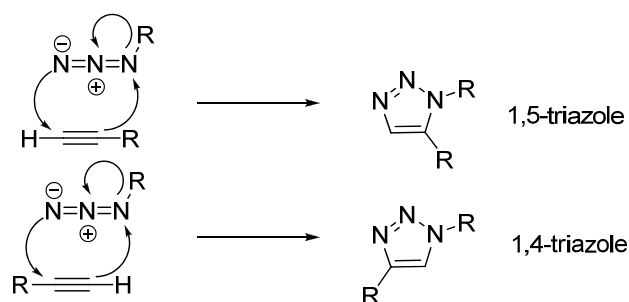
Scheme 1.3: 1,3-dipolar cycloaddition reaction between alkyne and terminal azide. A simplified mechanism is shown highlighting routes towards the 1,4 and 1,5-triazole configuration.

Copper alkyne azide cycloaddition reaction(CUAAC)

In 2002, two groups independently reported Cu(I) as a catalyst for the 1,3 dipolar cycloaddition reaction between terminal alkyne and azide.[55,56] The highlights of the copper mediated alkyne azide cycloaddition reaction (CuAAC) are a 10 million fold acceleration in the rate of reaction compared with the Husigen cycloaddition and the selective formation of the 1,4-triazole configuration over the 1,5-triazole (see Scheme 1.2).[57,58] Additionally, the CuAAC conditions described by Sharpless[56], epitomises the principle and attributes of Click Chemistry.[59] The most pertinent of these attributes that CuAAC fulfils are a facile reaction, high selectivity (1,4-triazole over the 1,5-triazole), reaction with high yields, limited by-products, insensitivity to a wide range of functional groups, and simple product isolation (crystallization, distillation or silica gel chromatography). The reliability and facile nature of CuAAC has underpinned the use of 1,2,3-triazole in many applications including macrocyclisation[60], bioconjugation[61], and bioisosterism.

Rutheniun alkyne azide cycloaddition reaction(RUAAC)

The 1,5-triazole configuration is reported as an effective bioisosteric fragment of disulphide[47] and cis-amides.[62] However, a problem facing 1,5-triazoles as bioisosteres (amongst other applications using 1,5-triazole) is a lack of accessibility to this configuration. A number of solutions have been reported including constrained 1,3-dipolar cycloaddition[63] and magnesium mediated 1,3-dipolar cycloaddition[64], but these proved to

be unsatisfactory as a general solution. In 2005, Zhang and co workers reported the selective synthesis of 1,5-triazole over the 1,4-triazole using the ruthenium catalyst **1.20**.[65] While the RuAAC does not rival CuAAC, a systematic study of the reaction of a terminal alkyne and azide, in the presence of ruthenium catalysts **1.20**, gives selectivity for the 1,5-triazole, with minimal by-products and high tolerance for a range of functional groups.[66]
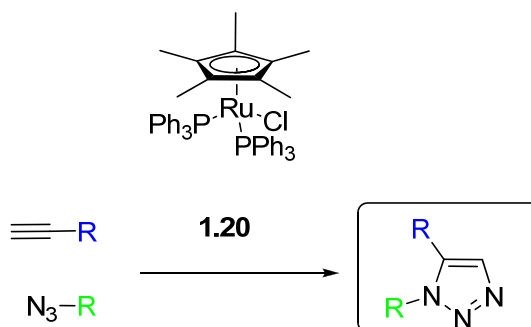
Scheme 1.4: RuAAC reaction with ruthenium catalyst Cp*(PPh$_3$)$_2$RuCl **1.20**

In situ click chemistry

The *in situ* click reaction is the latest development in target-guided synthesis.[67] This approach uses an enzyme to synthesise and screen 1,2,3-triazole compounds in the one process. Starting with a library of alkyne and azide fragments, the enzyme will select those fragments that are able to binding in the active site. Once an azide and corresponding alkyne fragment is bound and with both functional groups in close proximity, a 1,3-dipolar cycloaddition will occur to form the 1,2,3-triazole product. Studies have shown that the resultant 1,2,3-triazole are potent inhibitors, with increase potency compared to the alkyne and azide precursors and more potent than the possible 1,2,3-triazole analogues that were not produced by the enzyme.[68-71] Thus, using this approach it is possible to circumvent the need to synthesize all possible triazole analogues and thus remove a time consuming step in a drug design and discovery program.

In 2006, Brik and co workers reported the strategic use of 1,2,3-triazole as a bioisosteric analogue of amide for the purpose of an *in situ* click experiment.[45,70] Here, compound **1.22** was designed as an analogue of the reported HIV-1 protease inhibitor amprenavir **1.21** with a 1,2,3-triazole bioisostere in place of an amide bond (Figure 1.10). Using 1,2,3-triazole **1.22** as a template, a small library of four azide and one alkyne fragment was developed and the alkyne was screened against each azide in an *in situ* click experiment. Through

this approach the HIV-1 protease enzyme selectively synthesized compound **1.23**, which was found to be a novel and potent inhibitor of HIV-1 protease.[70] This study highlights the motivation for developing 1,2,3-triazole bioisosteric analogues and their utility in fragment-based approaches such as *in situ* click chemistry.

1.21

1.22

1.23
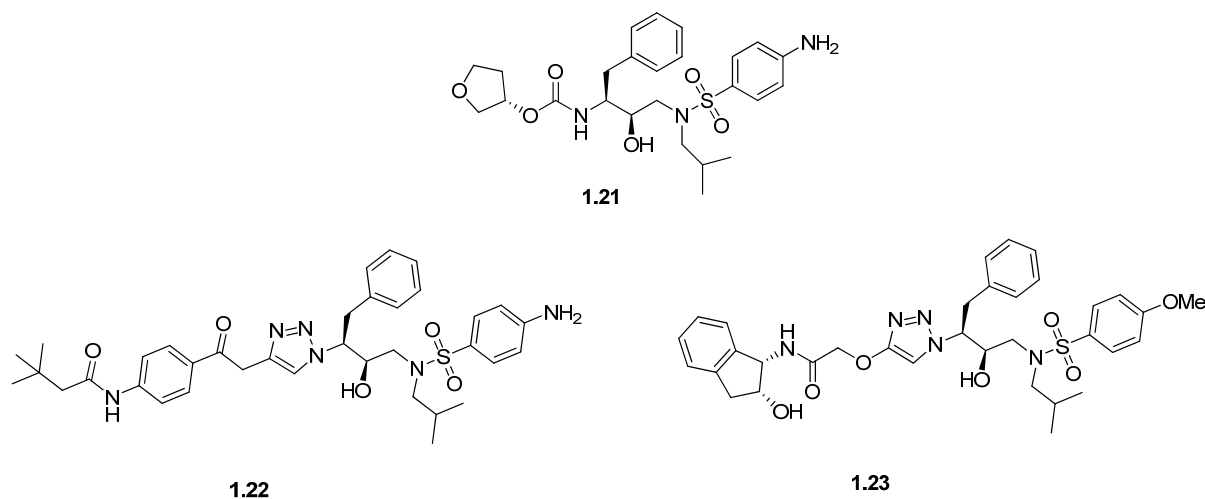
Figure 1.10: Amprenavir **1.21** and HIV-1 protease inhibitors **1.22** (synthesized via CuAAC) and **1.23** (synthesized via HIV-1 protease).

1.5 Research described in this thesis

Overall, this thesis describes the design of reaction intermediate analogues based on the X-ray crystal structure of SaBPL, with the first reported class of BPL inhibitors that are both potent and selective towards *S. aureus* BPL.

Chapter 1 described the structure and catalytic mechanism of *S. aureus* biotin protein ligase (SaBPL) and the medicinal chemistry approaches that are used in this thesis. Chapter 2 investigates biotinol-5'-AMP **1.05** as a potential inhibitor of SaBPL and examines synthetic approaches towards biotinol-5'-AMP **1.05** that are amenable for its large scaled up synthesis. The utility of 1,2,3-triazole as a bioisostere was described in Section 1.4. Consequently, Chapter 3 focuses on the design of 1,2,3-triazole as a bioisosteric analogue of the phosphoroanhydride linker of biotinyl-5'-AMP **1.03** and addresses both CuAAC and RuAAC techniques. Chapters 4 and 6 elaborate upon the 1,2,3-triazole analogues developed in Chapter 3 with both chapters investigating ATP and biotin binding components of 1,2,3-triazole inhibitors and developing a general structure for this novel

class of inhibitors. Chapter 4 also investigates an *in situ* click approach as a novel approach towards the synthesis and screening of 1,2,3-triazole analogues. Finally, Chapter 5 examines novel and potent biotin based inhibitors of SaBPL that were initially discovered and discussed in Chapter 4.

1.6 References for Chapter One

(1)   Kallen, A. J.; Mu, Y.; Bulens, S.; Reingold, A.; Petit, S.; Gershman, K.; Ray, S. M.; Harrison, L. H.; Lynfield, R.; Dumyati, G.; Townes, J. M.; Schaffner, W.; Patel, P. R.; Fridkin, S. K. *JAMA: The Journal of the American Medical Association* **2010**, *304*, 641.

(2)   Pearson, A.; Chronias, A.; Murray, M. *Journal of Antimicrobial Chemotherapy* **2009**, *64*, i11.

(3)   Ferguson, J. *Healthcare Infection* **2007**, *12*, 60.

(4)   Klein, E.; Smith, D.; Laxminarayan, R. Hospitalizations and deaths caused by methicillin-resistant Staphylococcus aureus, United States. *Emerg Infect Dis.* [Online Early Access]. DOI: 10.3201/eid1312.070629. Published Online: 2007 (accessed 16 Oct 2011).

(5)   Samols, D.; Thornton, C. G.; Murtif, V. L.; Kumar, G. K.; Haase, F. C.; Wood, H. G. *Journal of Biological Chemistry* **1988**, *263*, 6461.

(6)   Nenortas, E.; Beckett, D. *Journal of Biological Chemistry* **1996**, *271*, 7559.

(7)   Paul V, A. *The International Journal of Biochemistry & Cell Biology* **1995**, *27*, 231.

(8)   Bloch, K.; Vance, D. *Annual Review of Biochemistry* **1977**, *46*, 263.

(9)   Wallace, J. C.; Jitrapakdee, S.; Chapman-Smith, A. *The International Journal of Biochemistry & Cell Biology* **1998**, *30*, 1.

(10)   Abbott, J.; Beckett, D. *Biochemistry* **1993**, *32*, 9649.

(11)   Rodionov, D. A.; Mironov, A. A.; Gelfand, M. S. *Genome Research* **2002**, *12*, 1507.

(12)   Wood, Z. A.; Weaver, L. H.; Brown, P. H.; Beckett, D.; Matthews, B. W. *Journal of Molecular Biology* **2006**, *357*, 509.

(13)   Bagautdinov, B.; Kuroishi, C.; Sugahara, M.; Kunishima, N. *Journal of Molecular Biology* **2005**, *353*, 322.

(14)   Chapman-Smith, A.; Cronan Jr, J. E. *Biomolecular Engineering* **1999**, *16*, 119.

(15)   Reche, P. A. *Protein Science* **2000**, *9*, 1922.

(16)   Kim, D. J.; Kim, K. H.; Lee, H. H.; Lee, S. J.; Ha, J. Y.; Yoon, H. J.; Suh, S. W. *Journal of Biological Chemistry* **2005**, *280*, 38081.

(17) Polyak, S. W.; Chapman-Smith, A.; Brautigan, P. J.; Wallace, J. C. *Journal of Biological Chemistry* **1999**, *274*, 32847.

(18) Kwon, K.; Beckett, D. *Protein Science* **2000**, *9*, 1530.

(19) Tron, C. M.; McNae, I. W.; Nutley, M.; Clarke, D. J.; Cooper, A.; Walkinshaw, M. D.; Baxter, R. L.; Campopiano, D. J. *Journal of Molecular Biology* **2009**, *387*, 129.

(20) Bagautdinov, B.; Matsuura, Y.; Bagautdinova, S.; Kunishima, N. *Journal of Biological Chemistry* **2008**, *283*, 14739.

(21) Purushothaman, S.; Gupta, G.; Srivastava, R.; Ramu, V. G.; Surolia, A. *PLoS ONE* **2008**, *3*, e2320.

(22) Naganathan, S.; Beckett, D. *Journal of Molecular Biology* **2007**, *373*, 96.

(23) Rozwarski, D. A.; Vilchèze, C.; Sugantino, M.; Bittman, R.; Sacchettini, J. C. *Journal of Biological Chemistry* **1999**, *274*, 15582.

(24) Payne, D. J.; Gwynn, M. N.; Holmes, D. J.; Pompliano, D. L. *Nat Rev Drug Discov* **2007**, *6*, 29.

(25) Brown, P. H.; Cronan, J. E.; Grøtli, M.; Beckett, D. *Journal of Molecular Biology* **2004**, *337*, 857.

(26) Slavoff, S. A.; Chen, I.; Choi, Y.-A.; Ting, A. Y. *Journal of the American Chemical Society* **2008**, *130*, 1160.

(27) Floersheim, P.; Pombo-Villar, E.; Shapiro, G. *CHIMIA International Journal for Chemistry* **1992**, *46*, 323.

(28) Patani, G. A.; LaVoie, E. J. *Chemical Reviews* **1996**, *96*, 3147.

(29) Lima, L. M.; Barreiro, E. J. *Current Medicinal Chemistry* **2005**, *12*, 23.

(30) Meanwell, N. A. *Journal of Medicinal Chemistry* **2011**, *54*, 2529.

(31) Hirsch, A. K. H.; Fischer, F. R.; Diederich, F. *Angewandte Chemie International Edition* **2007**, *46*, 338.

(32) Rye, C. S.; Baell, J. B. *Current Medicinal Chemistry* **2005**, *12*, 3127.

(33) Artymiuk, P. J.; Rice, D. W.; Poirrette, A. R.; Willet, P. *Nat Struct Mol Biol* **1994**, *1*, 758.

(34) Ataide, S. F.; Ibba, M. *ACS Chemical Biology* **2006**, *1*, 285.

(35) Hurdle, J. G.; O'Neill, A. J.; Chopra, I. *Antimicrob. Agents Chemother.* **2005**, *49*, 4821.

(36) Yu, X. Y.; Hill, J. M.; Yu, G.; Wang, W.; Kluge, A. F.; Wendler, P.; Gallant, P. *Bioorganic & Medicinal Chemistry Letters* **1999**, *9*, 375.

(37)   Forrest, A. K.; Jarvest, R. L.; Mensah, L. M.; O'Hanlon, P. J.; Pope, A. J.; Sheppard, R. J. *Bioorganic & Medicinal Chemistry Letters* **2000**, *10*, 1871.

(38)   Bernier, S.; Akochy, P.-M.; Lapointe, J.; Chênevert, R. *Bioorganic & Medicinal Chemistry* **2005**, *13*, 69.

(39)   Lee, J.; Kang, S. U.; Kang, M. K.; Chun, M. W.; Jo, Y. J.; Kkwak, J. H.; Kim, S. *Bioorganic & Medicinal Chemistry Letters* **1999**, *9*, 1365.

(40)   Tian, Y.; Suk, D.-H.; Cai, F.; Crich, D.; Mesecar, A. D. *Biochemistry* **2008**, *47*, 12434.

(41)   Somu, R. V.; Boshoff, H.; Qiao, C.; Bennett, E. M.; Barry, C. E.; Aldrich, C. C. *Journal of Medicinal Chemistry* **2005**, *49*, 31.

(42)   Tuck, K. L.; Saldanha, S. A.; Birch, L. M.; Smith, A. G.; Abell, C. *Organic & Biomolecular Chemistry* **2006**, *4*, 3598.

(43)   Patrone, J. D.; Yao, J.; Scott, N. E.; Dotson, G. D. *Journal of the American Chemical Society* **2009**, *131*, 16340.

(44)   Monceaux, C. J.; Hirata-Fukae, C.; Lam, P. C. H.; Totrov, M. M.; Matsuoka, Y.; Carlier, P. R. *Bioorganic & Medicinal Chemistry Letters* **2011**, *21*, 3992.

(45)   Brik, A.; Alexandratos, J.; Lin, Y.-C.; Elder, J. H.; Olson, A. J.; Wlodawer, A.; Goodsell, D. S.; Wong, C.-H. *ChemBioChem* **2005**, *6*, 1167.

(46)   Mesenzani, O.; Massarotti, A.; Giustiniano, M.; Pirali, T.; Bevilacqua, V.; Caldarelli, A.; Canonico, P.; Sorba, G.; Novellino, E.; Genazzani, A. A.; Tron, G. C. *Bioorganic & Medicinal Chemistry Letters* **2011**, *21*, 764.

(47)   Empting, M.; Avrutina, O.; Meusinger, R.; Fabritz, S.; Reinwarth, M.; Biesalski, M.; Voigt, S.; Buntkowsky, G.; Kolmar, H. *Angewandte Chemie International Edition* **2011**, *50*, 5207.

(48)   Holland-Nell, K.; Meldal, M. *Angewandte Chemie International Edition* **2011**, *50*, 5204.

(49)   Byun, Y.; Vogel, S. R.; Phipps, A. J.; Carnrot, C.; Eriksson, S.; Tiwari, R.; Tjarks, W. *Nucleosides, Nucleotides and Nucleic Acids* **2008**, *27*, 244.

(50)   Chen, L.; Wilson, D. J.; Xu, Y.; Aldrich, C. C.; Felczak, K.; Sham, Y. Y.; Pankiewicz, K. W. *Journal of Medicinal Chemistry* **2010**, *53*, 4768.

(51)   El-Sagheer, A. H.; Brown, T. *Chemical Society Reviews* **2010**, *39*, 1388.

(52)   Hassner, A. *Synthesis of heterocycles via cycloadditions*; Springer, 2008.

(53)   Hlasta, D. J.; Ackerman, J. H. *The Journal of Organic Chemistry* **1994**, *59*, 6184.

(54)   Li, R.; Jansen, D. J.; Datta, A. *Organic & Biomolecular Chemistry* **2009**, *7*, 1921.

(55)   Tornøe, C. W.; Christensen, C.; Meldal, M. *The Journal of Organic Chemistry* **2002**, *67*, 3057.

(56)   Rostovtsev, V. V.; Green, L. G.; Fokin, V. V.; Sharpless, K. B. *Angewandte Chemie* **2002**, *114*, 2708.

(57)   Tron, G. C.; Pirali, T.; Billington, R. A.; Canonico, P. L.; Sorba, G.; Genazzani, A. A. *Medicinal Research Reviews* **2008**, *28*, 278.

(58)   Pedersen, D. S.; Abell, A. *European Journal of Organic Chemistry* **2011**, *2011*, 2399.

(59)   Kolb, H. C.; Finn, M. G.; Sharpless, K. B. *Angewandte Chemie International Edition* **2001**, *40*, 2004.

(60)   White, C. J.; Yudin, A. K. *Nat Chem* **2011**, *3*, 509.

(61)   Moses, J. E.; Moorhouse, A. D. *Chemical Society Reviews* **2007**, *36*, 1249.

(62)   Tam, A.; Arnold, U.; Soellner, M. B.; Raines, R. T. *Journal of the American Chemical Society* **2007**, *129*, 12670.

(63)   Baskin, J. M.; Prescher, J. A.; Laughlin, S. T.; Agard, N. J.; Chang, P. V.; Miller, I. A.; Lo, A.; Codelli, J. A.; Bertozzi, C. R. *Proceedings of the National Academy of Sciences* **2007**, *104*, 16793.

(64)   Krasiński, A.; Fokin, V. V.; Sharpless, K. B. *Organic Letters* **2004**, *6*, 1237.

(65)   Zhang, L.; Chen, X.; Xue, P.; Sun, H. H. Y.; Williams, I. D.; Sharpless, K. B.; Fokin, V. V.; Jia, G. *Journal of the American Chemical Society* **2005**, *127*, 15998.

(66)   Boren, B. C.; Narayan, S.; Rasmussen, L. K.; Zhang, L.; Zhao, H.; Lin, Z.; Jia, G.; Fokin, V. V. *Journal of the American Chemical Society* **2008**, *130*, 8923.

(67)   Mamidyala, S. K.; Finn, M. G. *Chemical Society Reviews* **2010**, *39*, 1252.

(68)   Krasiński, A.; Radić, Z.; Manetsch, R.; Raushel, J.; Taylor, P.; Sharpless, K. B.; Kolb, H. C. *Journal of the American Chemical Society* **2005**, *127*, 6686.

(69)   Mocharla, V. P.; Colasson, B.; Lee, L. V.; Röper, S.; Sharpless, K. B.; Wong, C.-H.; Kolb, H. C. *Angewandte Chemie International Edition* **2005**, *44*, 116.

(70)   Whiting, M.; Muldoon, J.; Lin, Y.-C.; Silverman, S. M.; Lindstrom, W.; Olson, A. J.; Kolb, H. C.; Finn, M. G.; Sharpless, K. B.; Elder, J. H.; Fokin, V. V. *Angewandte Chemie International Edition* **2006**, *45*, 1435.

(71)   Hirose, T.; Sunazuka, T.; Sugawara, A.; Endo, A.; Iguchi, K.; Yamamoto, T.; Ui, H.; Shiomi, K.; Watanabe, T.; Sharpless, K. B.; Omura, S. *J Antibiot* **2009**, *62*, 277.

Chapter Two

2.1 Introduction

A number of studies have highlighted the importance of inhibiting biotin protein ligases for species such as *Escherichia coli*[1]*, Staphylococcus aureus*[1] and *Mycobacterium tuberculosis*[2]. In particular, allelic replacement mutagenesis of individual bacterial genes have shown that BPL is indispensible for the normal functioning of *E. coli*[1]. However, to date, there has been limited success in developing inhibitors of biotin protein ligase (see Section 1.2.3 for further discussion). Nevertheless, Brown and co-workers[3,4] described preliminary work on two reaction intermediate mimics of natural reaction intermediate **1.03**, biotinol-5'-AMP **1.05** and BtnSA **2.01**, as shown in Figure 2.1. These two mimics are the only reported inhibitors of BPL, with biotinol-5'-AMP **1.05** being more effective and hence a good candidate for further investigation.
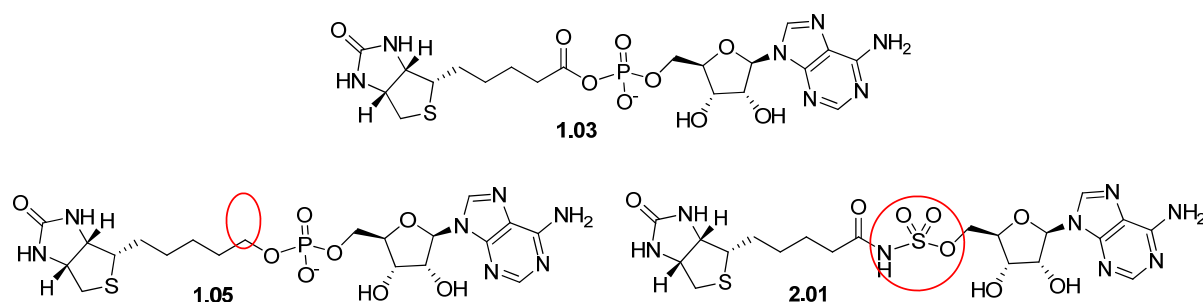
Figure 2.1: natural reaction intermediate biotinyl-5'-monophosphate adenosine **1.03**, reduced natural reaction intermediate mimic biotinol-5'-monophospahte adenosine, **1.05,** reaction intermediate mimic biotinyl-5'-sulphonmyl adenosine (BtnSA) **2.01**. Red circles denotes the differences.

Recent studies at Adelaide[5] have conclusively shown that biotinol-5'-AMP **1.05** is a potent competitive inhibitor of *S. aureus* biotin protein ligase (SaBPL), with an $IC_{50} = 0.23 \pm 0.06$ μM. By comparison, it has an $IC_{50} = 2.5 \pm 0.2$ μM against *E. coli* biotin protein ligase (EcBPL) and an $IC_{50} = 1.25 \pm 0.1$ μM against *Homo Sapien.* biotin protein ligases (*HsBPL*). These studies have also shown that biotinol-5'-AMP **1.05** has antimicrobial activity against *S. aureus* (MIC = 8 - 32 ug/L).

Given these encouraging and significant results, there is a need to develop an effective synthesis for biotinol-5'-AMP **1.05** that is amenable to large scale to allow further

biological characterisation. Work described in this chapter investigates two such synthetic approaches (the phosphodiester and phosphoramidite approach) and the biological characterisation undertaken using the prepared material.

2.2 Phosphodiester strategy for synthesis of biotinol-5'-monophosphate adenosine 1.05

The reported synthesis of biotinol-5'-AMP **1.05** utilises a phosphodiester synthetic strategy, as depicted in Scheme 2.1.[3,6] This approach involves the phosphorylation of 2',3' isopropylidene adenosine **2.02,** with 2-cyanoethyl phosphate and DCC, followed by deprotection of 2-cyanoethyl group with ammonia to give **2.03**.[7] This was followed by purification by sephadex A25 DEAE ion exchange chromatography and conversion of the resulting triethylamine salt to the pyridinium salt **2.04**. Subsequent coupling with biotinol **2.05** in the presence of DCC, followed by *in situ* acid deprotection of isopropylidene protecting group gave biotinol-5'-AMP **1.05**.[3]
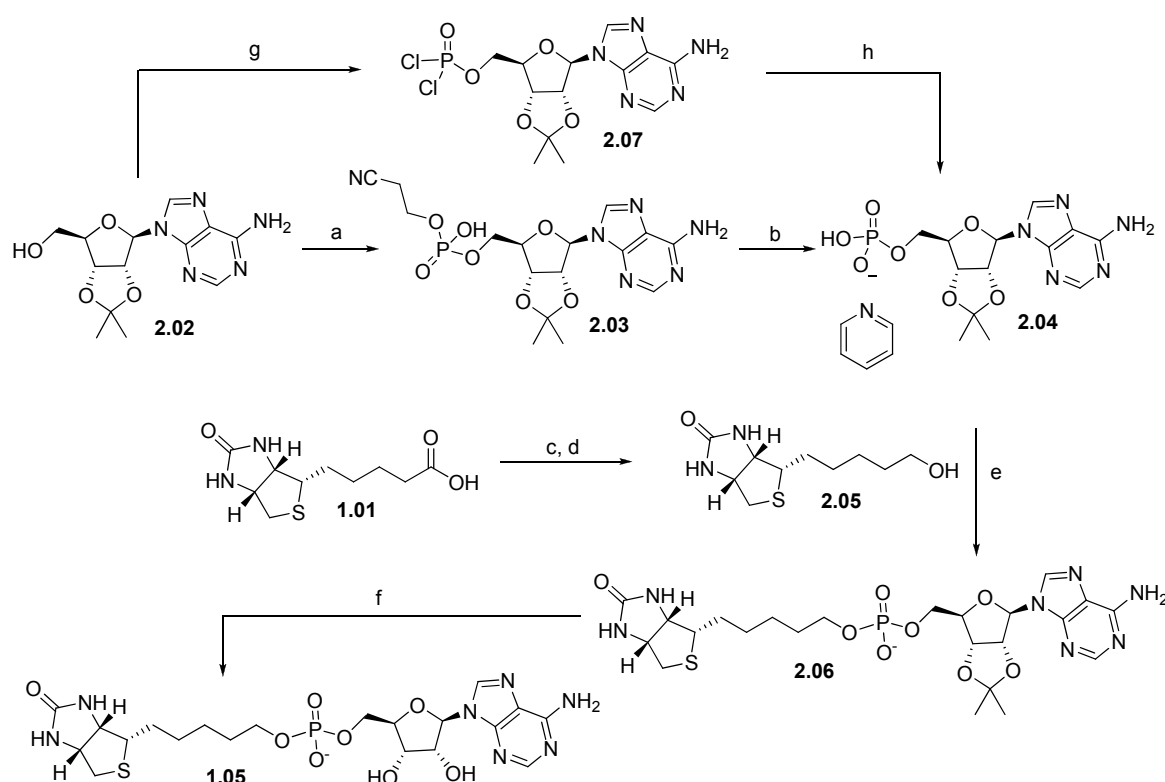
Scheme 2.1: a) P(OH)$_2$(OCH$_2$CH$_2$CN)Cl, DCC, Py b) i) NH$_3$; ii) Dowex x8 pyridinium form; c) SOCl$_2$, MeOH; d) DIBAL-H, THF; e) DCC, py; f) AcOH g) POCl$_3$, PO(OEt)$_3$ h) i) TEAB buffer; ii) Dowex x8 pyridinium form.

Our initial synthetic strategy for **1.05** was based on the phosphodiester synthetic approach described above. However, for multi-gram synthesis we proposed an alternative and facile Yoshikawa phosphorylation[8,9], as shown in steps g and h in Scheme 2.1. The use of phosphorous oxychloride (POCl$_3$) as the phosphorylating regent in the Yoshikawa phosphorylation provides a more cost effective and readily available reagent compared to 2-cyanoethyl phosphate. The synthesis thus required the preparation of the key building blocks **2.04** and **2.05** which is described below.

2.2.1 Synthesis of key building blocks, 2.04 and 2.05
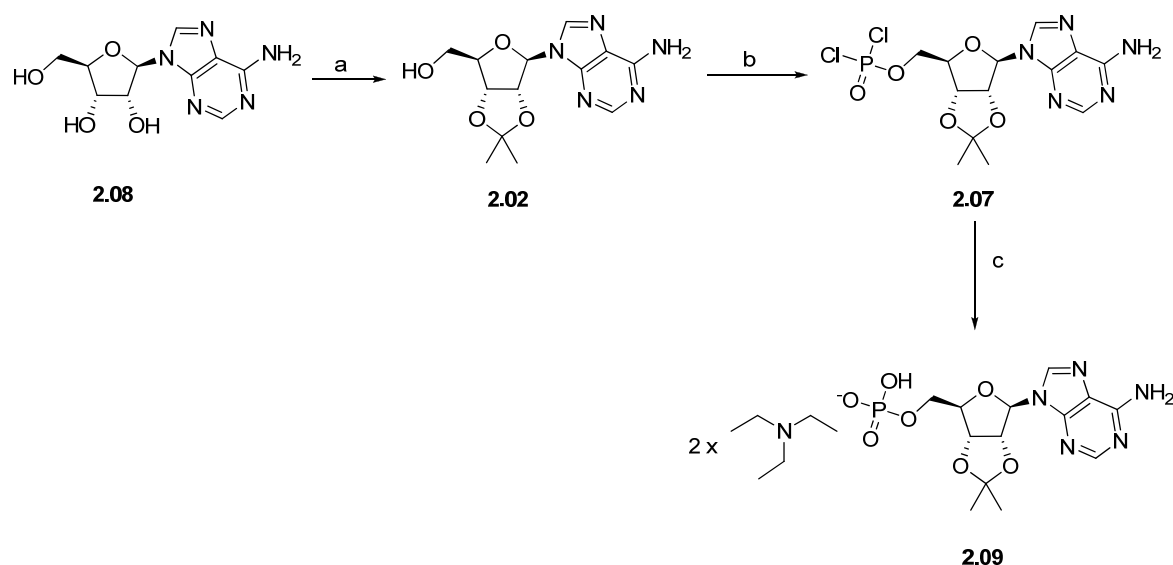
Scheme 2.2: a) (CH$_3$)$_2$C(OCH$_3$)$_2$, cat. *p*-TsOH, acetone; b) i) POCl$_3$, PO(OEt)$_3$, 5 ^{o}C; c) i) 0.05M TEAB, ii) Sephadex DEAE A25;

The synthesis of adenosine **2.09** was achieved, as shown in Scheme 2.2. The protection of 2',3'- diol of adenosine **2.02** was required to avoid undesired phosphorylation at these hydroxyl groups. An isopropylidene group was attached to **2.08** by reacting with 2,2-dimethoxypropane and *p*-toluene-sulphonic acid to give **2.02** in a 78% yield. The synthesis of adenosine **2.09**, was then achieved by reaction with 2 equivalents of phosphorous oxychloride, triethylphosphate as the solvent, (optimised conditions, see Table 2.1 and below for further discussion) and 0.05 M triethylamine bicarbonate to hydrolyse the

phosphorodichloridate intermediate **2.07**. The resulting material was purified by Sephadex DEAE A25 anion exchange chromatography, using a linear gradient (0.05 M to 0.6 M) of triethylamine bicarbonate buffer (TEAB) solution at pH 7.5 at ambient temperature. The required derivative **2.09** was eluted at 0.3 - 0.4 M of triethylamine bicarbonate in a yield of 65%, based on starting material **2.02**. A variety of conditions were investigated for the Yoshikawa phosphorylation of **2.02** to **2.09**, as outlined in Table 2.1.

Table 2.1: Conditions for Yoshikawa phosphorylation of **2.02** to **2.09**
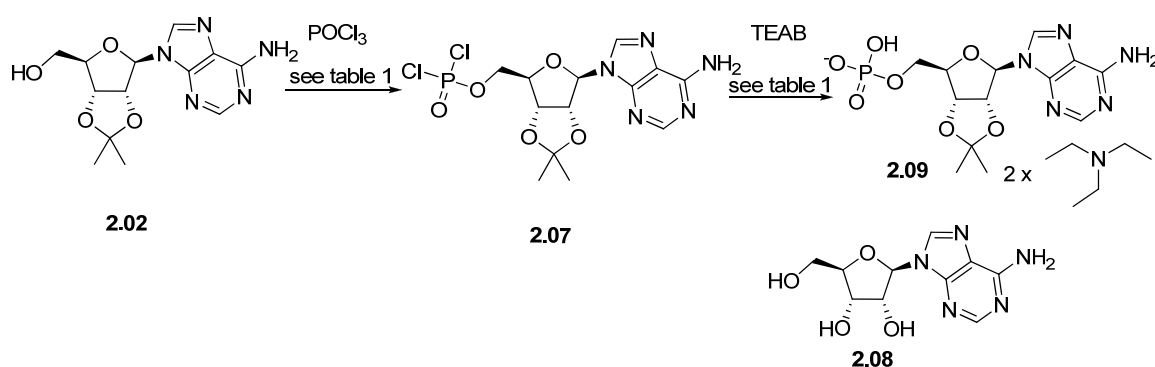
Entry	Quant of POCl₃[a]	Solvent	0.05M TEAB (L)[c]	Yield[d] (%)
1	4 equiv.	50 mL PO(OEt)$_3$	1	trace
2	4 equiv.	50 mL PO(OEt)$_3$	3	25%
3	2 equiv.	25 mL PO(OEt)$_3$	1	41%
4	1.2 equiv.	25 mL PO(OEt)$_3$	0.75	38%
5	2 equiv.	25 mL PO(OMe)$_3$	1	38%
6	2equiv[b]	25 mL PO(OEt)$_3$	1	65%

[a] All reactions were done with 5 mmol scale of adenosine **2.02** at 5 °C (fridge), over 48 h and monitored by TLC (2:1 iPrOH: 16% NH$_{3(aq)}$) [b] addition of 20 µL of water. [c]quantity of TEAB used for hydrolysis after 48 h. [d] isolated yield of **2.09** after Sephadex purification.

The initial conditions described in entry 1 were attempted on a 5 mmol scale with the treatment of **2.02** with $POCl_3$, followed by the addition of 0.05M TEAB buffer and purification by Sephadex ion exchange chromatography to give **2.09** in trace amounts as judged by TLC. The major products isolated were adenosine **2.08** and starting material **2.02** in 7% and 15% respectively. Adenosine **2.08** results from acid catalysed removal of the isopropylidene protecting group of **2.02**.

The TEAB buffer added at the completion of the reaction in order to hydrolyse **2.07** and to neutralise the generated acid, was observed to give a pH of 2 to 4. This suggested that insufficient quantities of TEAB were added to neutralise the liberated acid,[10] which resulted in hydrolysis of isopropylidene protecting group of **2.09** to give **2.08**. To further investigate the role of TEAB, the Yoshikawa reaction was attempted as shown in entry 2. The conditions were essentially the same as in entry 1, except that an extra 2 M aqueous TEAB buffer solution was added to give a final pH >6. Phosphate **2.09** was obtained in 25% yield under these conditions. Importantly the by-products (**2.08** and **2.02**) were not observed by TLC. However, the resulting large volume made purification of **2.09** by Sephadex A25 DEAE ion exchange problematic and time consuming.

In an attempt to overcome these problems the equivalents of $POCl_3$ were decreased from 4 to 2 and the quantity of triethylphosphate solvent decreased to 25 mL. This gave phosphate **2.09** in a much improved yield of 41% after purification by Spehadex chromatography (entry 3). The use of 1.2 equivalents of $POCl_3$, as described in entry 4, gave a 38% yield of phosphate **2.09**.

The use of trimethylphosphate, in place of triethylphosphate, as solvent was also investigated as in entry 5. In particular, treatment of adenosine **2.02** in $PO(OMe)_3$ with 2 equivalents of $POCl_3$ gave phosphate **2.09** in 38% yield after sephadex purification. Thus the use of trimethylphosphate, offers no advantage, which is consistent with literature reports. [8]

A synthesis of adenosine **2.09** from **2.02** under Yoshikawa phosphorylation conditions with the addition of a catalytic amount of water was reported to give a 90% yield[9]. However, the addition of water is counter-intuitive and would be expected to hydrolyse both $POCl_3$ and possibly the hemiacetal protecting group of **2.02**.[10,11] Nevertheless, the

reaction of **2.02** with POCl$_3$ under the conditions reported by Zatorski[9] (as shown in entry 6**)**, gave phosphate **2.09** in a good yield of 65% .

^{1}H NMR, ^{31}P and ^{13}C NMR spectra of phosphate **2.09** confirmed the attachment of a phosphate group to the 5'-hydroxyl group. The presence of a phosphate group was confirmed by a ^{31}P NMR resonance at 1.21 ppm and ^{1}H NMR chemical shift of 3.91 ppm was indicative of the 5'-methylene group. The ^{1}H NMR spectrum indicated the presence of triethylamine as can be seen in Figure 2.2 with resonances at 3.04 and 1.13 ppm. The molar ratio of triethylamine relative to **2.09** was confirmed to be 2:1 by ^{1}H NMR spectroscopy, as shown in Figure 2.2.
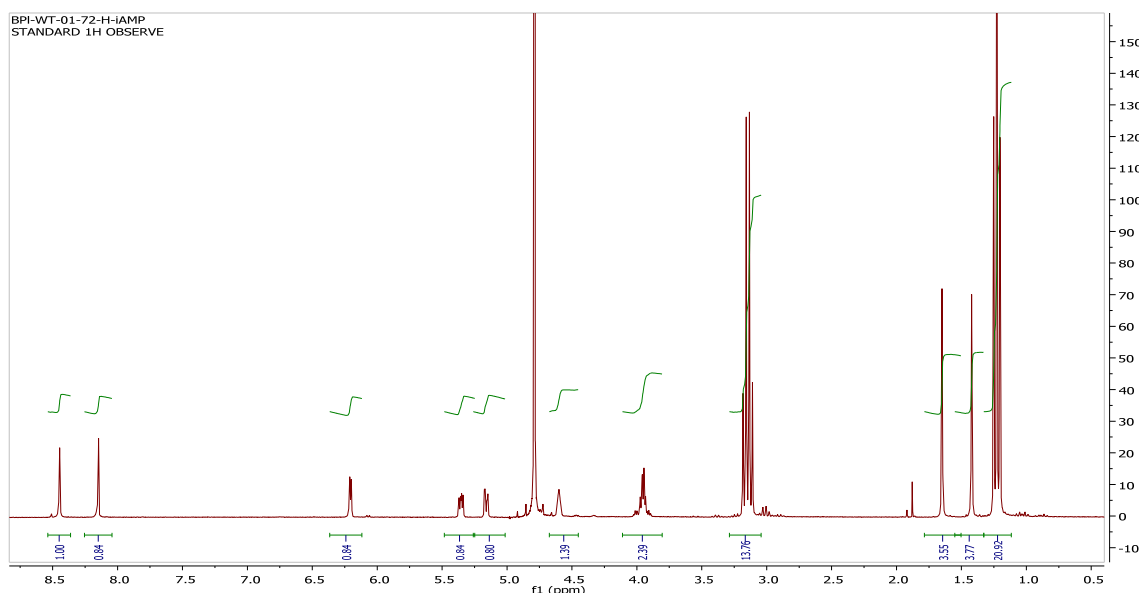
Figure 2.2: 300MHz NMR spectra of **2.09** as triethylamine salt.

Phosphate **2.09** was converted to the pyridinium salt by running the product through a cation exchange resin Dowex 50 x8 pyridium form, at pH = 7 to give **2.04** in 89% yield. The complete removal of triethylamine was confirmed by ^{1}H NMR which showed the lack of a characteristic resonance at 3.04 and 1.13 ppm due to triethylamine and the appearance of new resonances 8.47, 8.14 and 7.65 ppm due to the pyridinium salt.
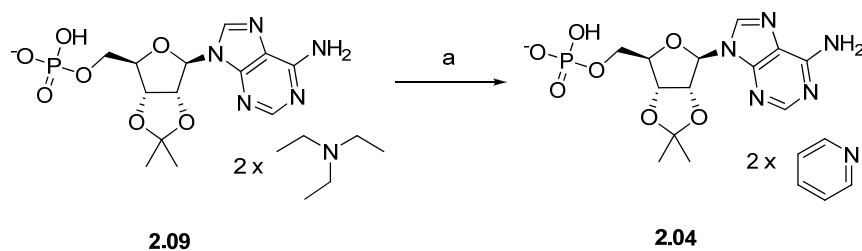
Scheme 2.3: a) Dowex 50X8 pyridinium form.

The second key building block, biotinol **2.05,** was prepared using a modified literature synthesis[12], as shown in Scheme 2.4.
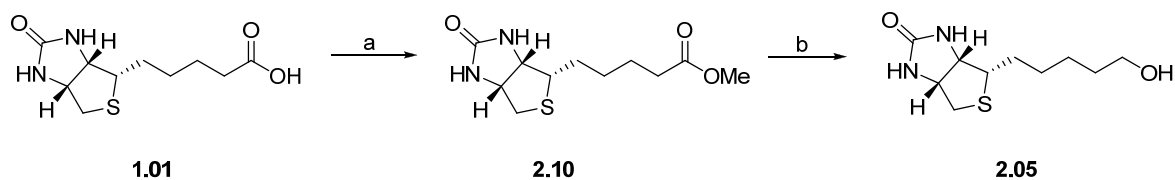
Scheme 2.4: a) $SOCl_2$, MeOH or $C(OCl)_2$, DMF, MeOH; b) $LiAlH_4$, THF

Biotin **1.01** was first esterified with the addition of thionyl chloride in methanol to give the methyl ester **2.10** in quantitative yields. Esterification was also achieved in quantitative yield on treatment with oxalyl chloride in methanol with a catalytic amount of DMF with either method being acceptable. The methyl ester **2.10** was then reduced with $LiAlH_4$ to give biotinol **2.05** in 84%. Importantly for larger scale reactions, the use of flash chromatography was not required in the purification. Biotinol **2.05** was obtained in >95% purity by simply adding saturated $Na_2SO_{4(aq)}$ and isolating the resulting solid by vacuum filtration.

2.2.2 Synthesis of biotinol-5'-AMP 1.05 from 2.04 and 2.05

Biotinol-5'-AMP **1.05** was synthesized from the building blocks biotinol **2.05** and adenosine **2.04**, as shown in Scheme 2.5.
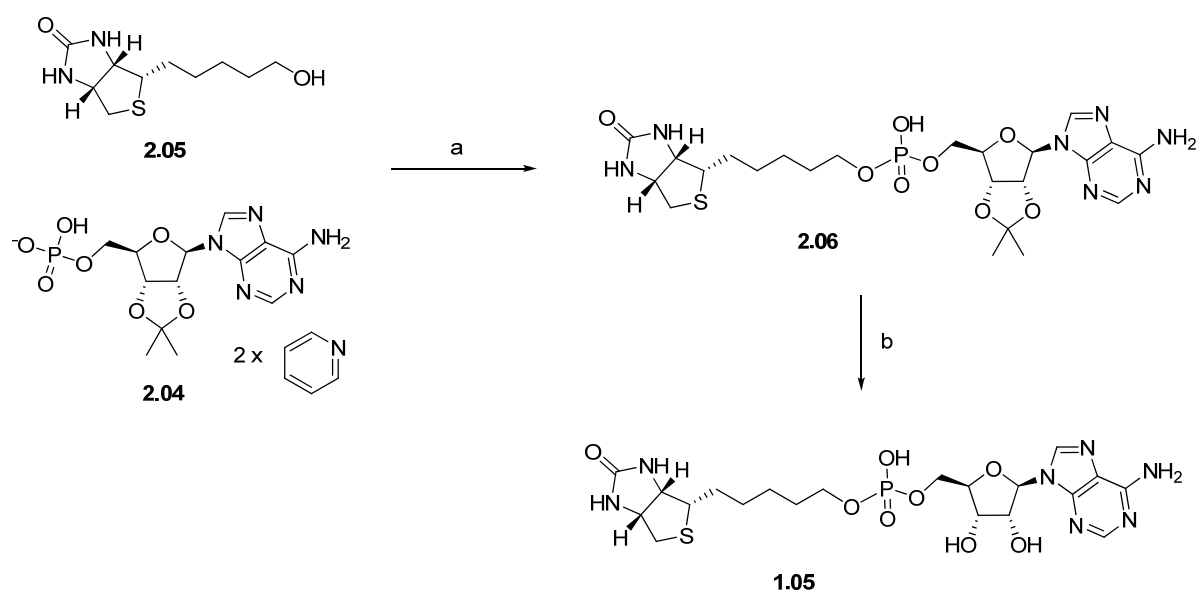
Scheme 2.5: a) DCC, py; b) AcOH 60% w/w, 80 °C (18% over two steps)

The monophosphate pyridinium salt of **2.04** and biotinol **2.05** were first reacted with DCC in pyridine to give a solution presumed to contain **2.06**, which was not purified. A solution of 60% w/w acetic acid was then added to this and the mixture heated to 80 °C, to remove the isopropylidene protecting group. The mixture was filtered to remove DCC by-product (dicyclohexylurea), concentrated *in vacuo* and the residue purified by Sephadex DEAE A25 chromatography. A liner gradient of 0.05 M to 0.6 M triethylamine bicarbonate buffer solution was created with buffer solution at pH 7.5 and at 25°C, biotinol-5'-AMP **1.05** was collected at 0.20-0.26 M, whilst isopropylidene derivative **2.06** was collected earlier at 0.15-0.20 M. The solvent was removed *in vacuo* to give biotinol-5'-AMP **1.05** in an overall yield of 18% (as triethylamine salt).

A ^{1}H NMR spectra of biotinol-5'-AMP **1.05** indicated a large excess of triethylamine, in a molar ratio of 6:1 with respect to biotinol-5'-AMP **1.05**, as shown in Figure 2.3 (above). Thus biotinol-5'-AMP **1.05** was further purified by reverse phase HPLC, eluting with a mixture of buffer A (90% acetonitrile with 0.1% acetic acid) and buffer B (99.9% milliQ water and 0.1% acetic) and gradient of buffer A to B 0-90% to give **1.05** in 11% yield over 2 steps and starting from phosphate **2.04**. The structure of biotinol-5'-AMP **1.05** was verified by a single ^{31}P NMR resonance at -22.23 ppm (reference against 85% H_3PO_4 in H_2O) and by ^{1}H NMR as shown in Figure 2.3 with resonance at 3.78 ppm indicative of alkyl phosphate[3]. The use of HPLC is clearly less than ideal for larger scale preparations.
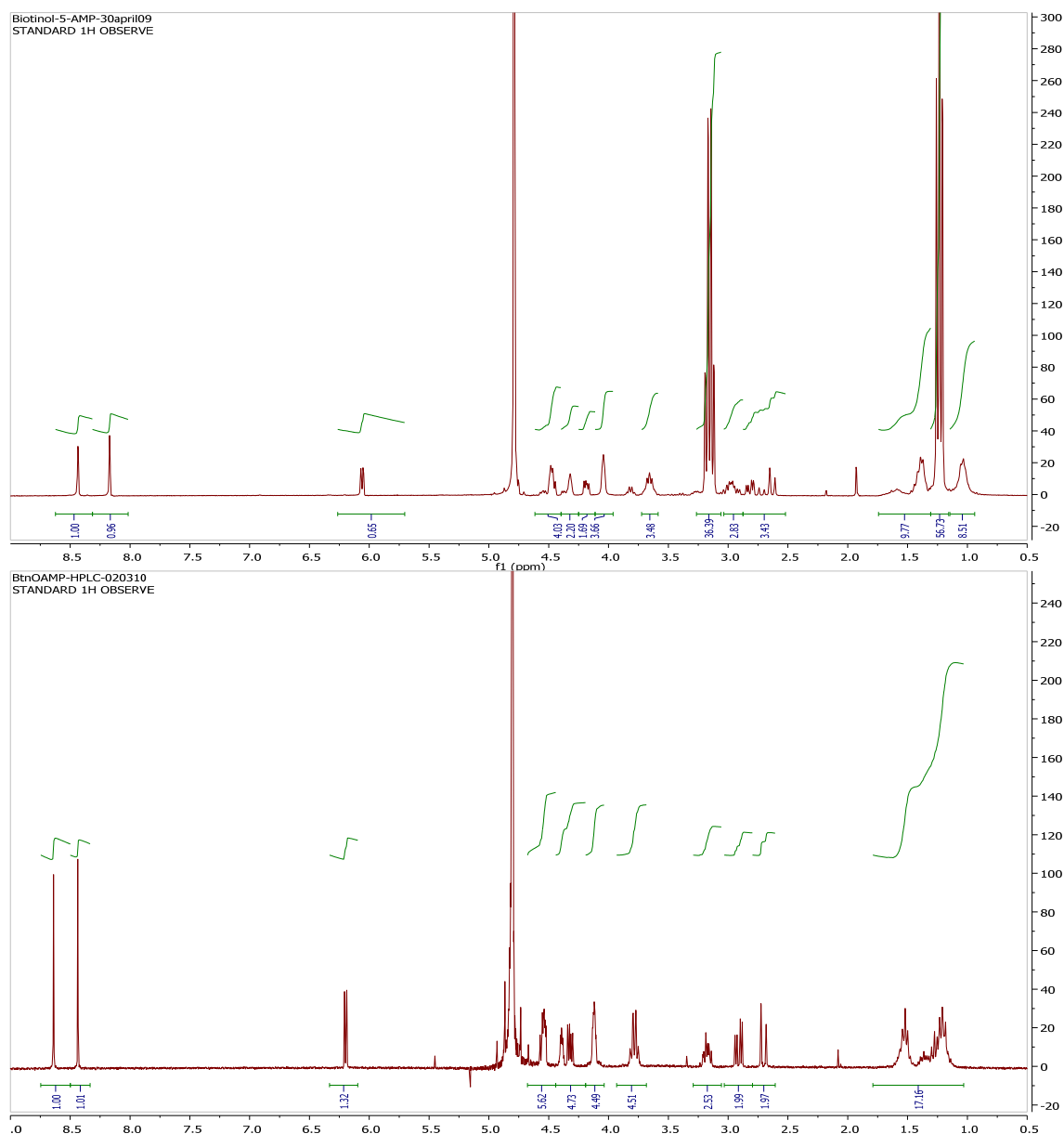
Figure 2.3: ^{1}H NMR (300 MHz, D$_2$O) spectra of crude sample of biotinol-5'-AMP **1.05** containing triethylamine (above) and a sample of biotinol-5'-AMP **1.05** after HPLC purification containing no triethylamine (below).

The DCC mediated coupling of **2.04** and **2.05** and subsequent acetic acid deprotection of the isopropylidene group described above and shown in Scheme 2.5, gave a low yield of 18% yield of **1.05** over two steps and after purification by sephadex chromatograhphy (see Section 2.2.2 and entry 1). An optimisation of this reaction was attempted under the conditions outlined in Table 2.2.
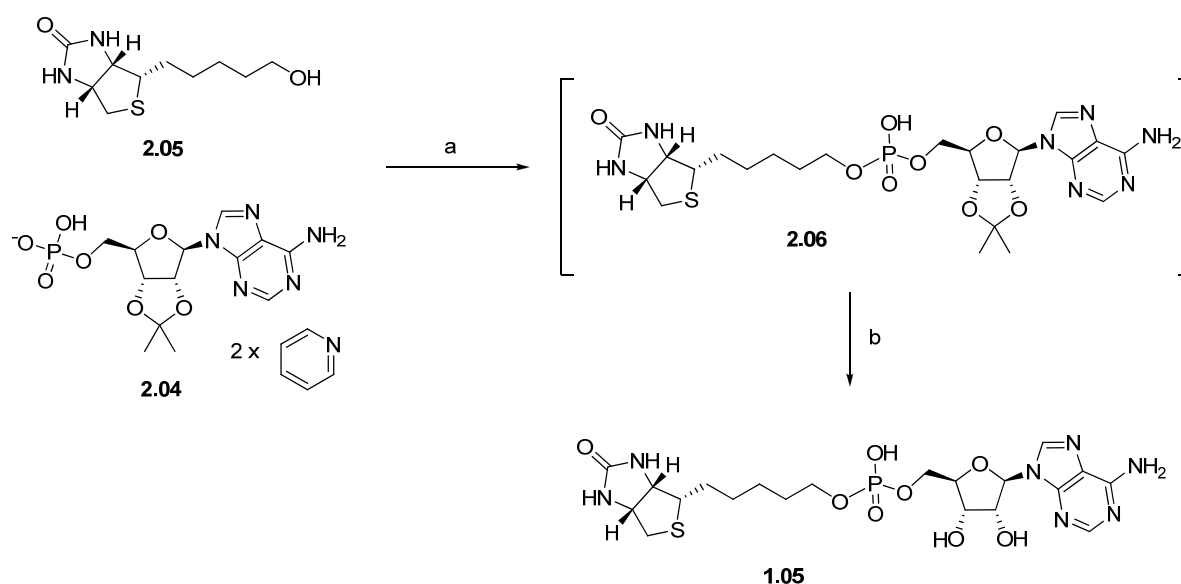
Scheme 2.6: a) DCC, Py; b) AcOH (see table 2 and 3)

Table 2.2[a]: Optimisation of DCC coupling between 2.05 and 2.04 and hydrolysis of 2.06.

entry	DCC (equiv)	Time (h)	Acetic acid w/v %[b]	Yield of 1.05 %[c, d]
1	1.5	24	60	18
2	3	24	60	26
3	5	24	60	31
4	3	12	60	15
5	3	48	60	17

[a] All reactions were carried out at ambient temperature. [b]acetic acid was added to the reaction mixture after prescribed timed and the resultant reaction mixture containing acetic acid was stirred for 6 h under reflux. [c]isolated yield of **1.05** after Sephadex purification. [d] **1.05** was isolated as a mixture containing triethylamine, thus yields were determined based on ^{1}H NMR spectroscopy.

Coupling of biotinol **2.05** and phosphate **2.04** in the presence of 1.5 equivalents of DCC under the original conditions (entry 1, Table 1) for 24 h, followed by reaction with acetic acid and purification by Sephadex, gave **1.05** in 18%. Increasing the amount of DCC from 1.5 to 3 equivalents and also 5 equivalents gave an improved yield of **1.05**, 26% (entry 2)

and 31% (entry 3). Increasing the reaction time from 12 h (entry 4) to 48 h (entry 5) had little effect.

Given the limited improvements in yields of **1.05** obtained under the conditions described in table 2, the use of DCC to mediate coupling of **2.05** and **2.04** to give **2.06**, and its subsequent deprotection to give **1.05**, were not investigated further**.** It is suggested that this approach is limited by the low reactivity of the monophosphate **2.04** with DCC, and the instability of the phosphodiester **2.06** during acid deprotection of the isopropylidene group. As such, an alternative synthetic approach was devised and is described in Section 2.3. The use of other potential coupling agents was not investigated.

## 2.3 Alternative phosphoramidite -based synthesis of biotinol-5'-AMP 1.05

An alternative synthetic approach was proposed for biotinol-5'-AMP **1.05**, as shown in Scheme 2.7. This approach involves a) generating the reactive phosphoramidite such as **2.11**; b) coupling of **2.11** with the alcohol **2.12** and oxidation of the subsequent phosphite **2.13** to phosphotriester **2.14** and c) deprotection of phosphotriester to give biotinol-5'-AMP **1.05**. Such an approach would allow purification of **2.11** - **2.14** by flash chromatography, since the negatively charged phosphodiester is masked until the final step. This would also avoid the use of triethylamine bicarbonate buffer, which proved problematic in the synthesis of biotinol-5'-AMP **1.05** using the phosphodiester strategy (see Section 2.2.2). The addition of protecting groups on both the adenosine **2.12** and biotin **2.11** building blocks was deemed necessary to prevent side reactions and to increase solubility for the coupling of **2.12** and **2.11**.[13] Protection of biotinol **2.05** with dimethoxytrityl group has the added advantages of improving solubility in common solvents (DCM, EtOAc, AcCN and DMF), as experienced in the Abell research group and as reported by other groups.[14] The benzoyl protection on adenosine **2.12** was suggested to prevent depurination during acid treatment.[15] The synthesis of biotinol-5'-AMP **1.05** via phosphoramidite approach is detailed below and required access to the key precursors **2.11** and **2.12**.
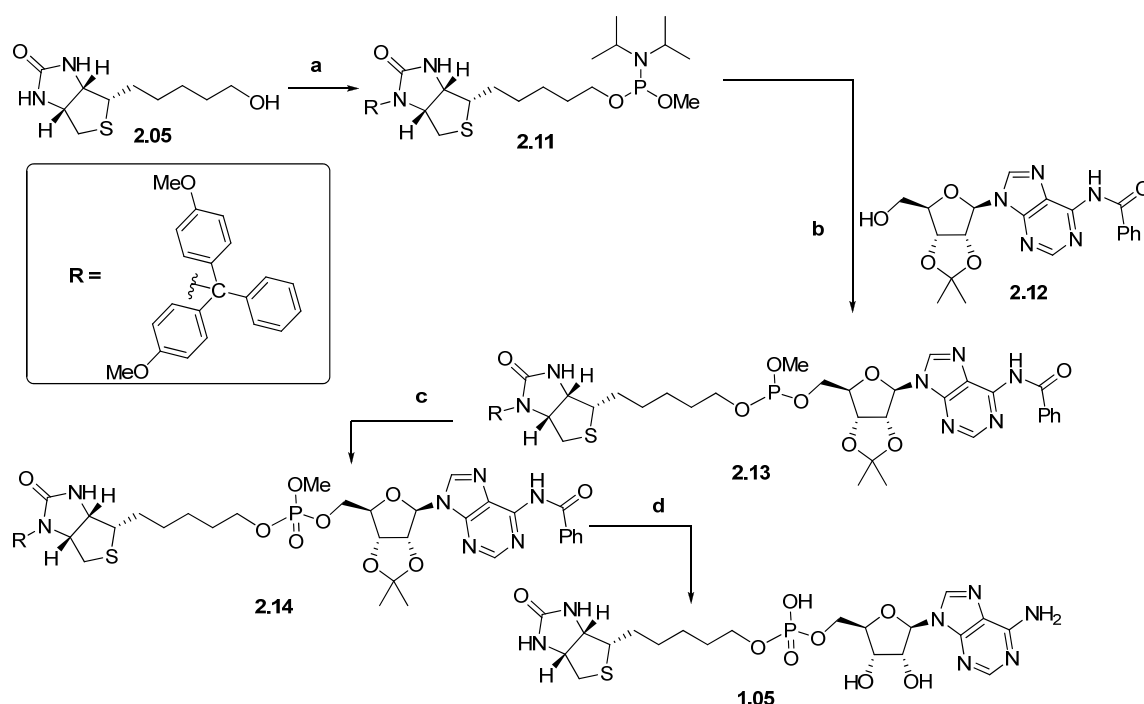
Scheme 2.7: a) phosphitylation; b) coupling; c) oxidation; d) deprotection.

2.3.1 Attempted synthesis of biotin 2.11 and synthesis of adenosine 2.18 precursors

The synthesis of the key precursor biotin phosphoramidite **2.11** was attempted as shown in Scheme 2.8. Biotin methyl ester **2.10** was treated with dimethoxytrityl chloride (DMTr-Cl) in dichloromethane under modified literature conditions[12] to give DMTr-biotin **2.15** in 35% yield. The treatment of **2.10** with DMtr-Cl, triethylamine and 4-DMAP increased the yield of **2.15** to 51%. Reduction of the methyl ester of DMTr-biotin **2.15** was achieved on treatment with lithium aluminium hydride in THF to give DMTr-biotinol **2.16** in 89% yield. However, treatment of **2.16** with *N,N*-diisopropyl-methoxyphosphonamidic and triethylamine in dichloromethane failed to give **2.11**. Whilst the consumption of starting material **2.16** was observed by TLC, any formed **2.11** was found to decompose on flash chromatography and it could thus not be isolated.
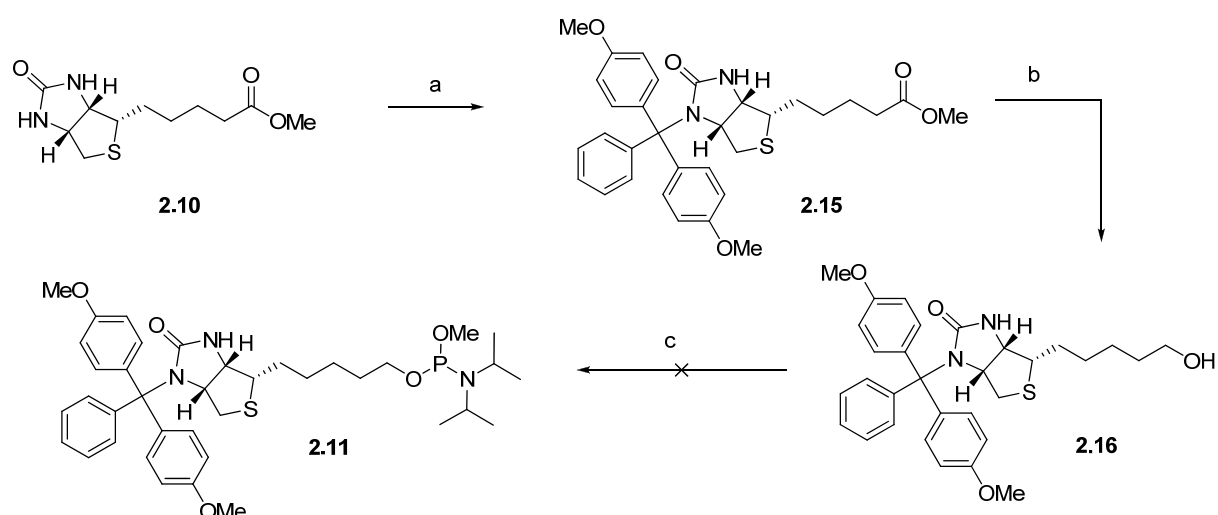
Scheme 2.8: a) DMTr-Cl, Et$_3$N, DMAP, DCM; b) LiAlH$_4$, THF; c) *N,N*-Diisopropyl-methoxyphosphonamidic, Et$_3$N, DCM;

Given biotin phosphoramidite **2.11** (Scheme 2.8) was found to readily decompose upon flash chromatography and thus could not be isolated, an alternative phosphoramidite analogue was proposed. The literature reported compound **2.17** was synthesized, as depicted in Scheme 2.9.[16] The 2',3'-diol was protected with a isopropylidene group to prevent undesirable formation of 2' and 3' phosphodiesters[13], whilst the *N*-benzoyl group is reported to prevent depurination (particularly under acidic conditions that is required to remove the isopropylidene group).[13,17]
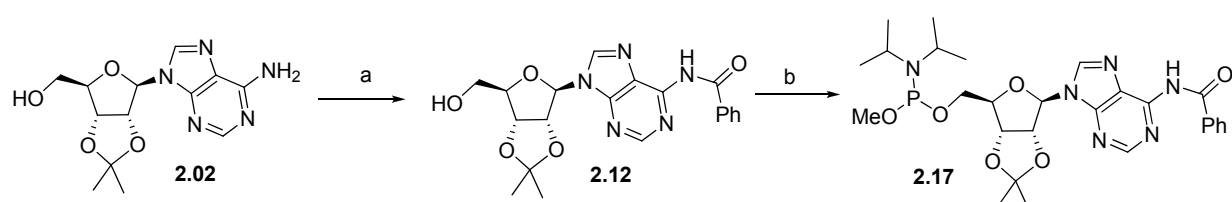
Scheme 2.9: a) TMS-Cl, pyridine; b) i) Bz-Cl, pyridine, ii) 32% NH$_{3(aq)}$; iii) *N,N*-Diisopropyl-methoxyphosphonamidic, Et$_3$N, DCM.

Trimethylsilyl (TMS) was used as a transient protecting group for the 5'-hydroxyl of adenosine **2.02** in order to allow for selective benzoylation of the excocyclic amine. Thus trimethylsilyl chloride was added to **2.02** in pyridine, followed by addition of benzoyl chloride was then added to the mixture and deprotection of TMS group with 32% aqueous

ammonia solution to give **2.12** in 77% yield. The synthesis of adenosine **2.17** was achieved by adding *N,N*-diisopropyl-methoxyphosphonamidic and triethylamine in dichloromethane to **2.12**. Purification of the crude material by flash chromatography gave **2.17** in 67% yield. ^{1}H NMR analysis indicated that **2.17** existed as a mixture of diastereomers with phosphorus as the centre of chirality. The phosphorous methoxy protons of **2.17** were observed to possess two distinct resonance at 3.34 and 3.30 ppm in the ^{1}H NMR spectrum, as was reported in literature.[16]

2.3.2 Preparation of biotinol-5'-AMP 1.05 from biotinol 2.16 and adenosine 2.17

The synthesis of biotinol-5'-AMP **1.05** was accomplished from the protected building blocks **2.16** and **2.17**, as shown in Scheme 10. The key to this approach is the use of standard flash chromatography techniques and short reaction times that were lacking in the phosphodiester approach in Section 2.2.
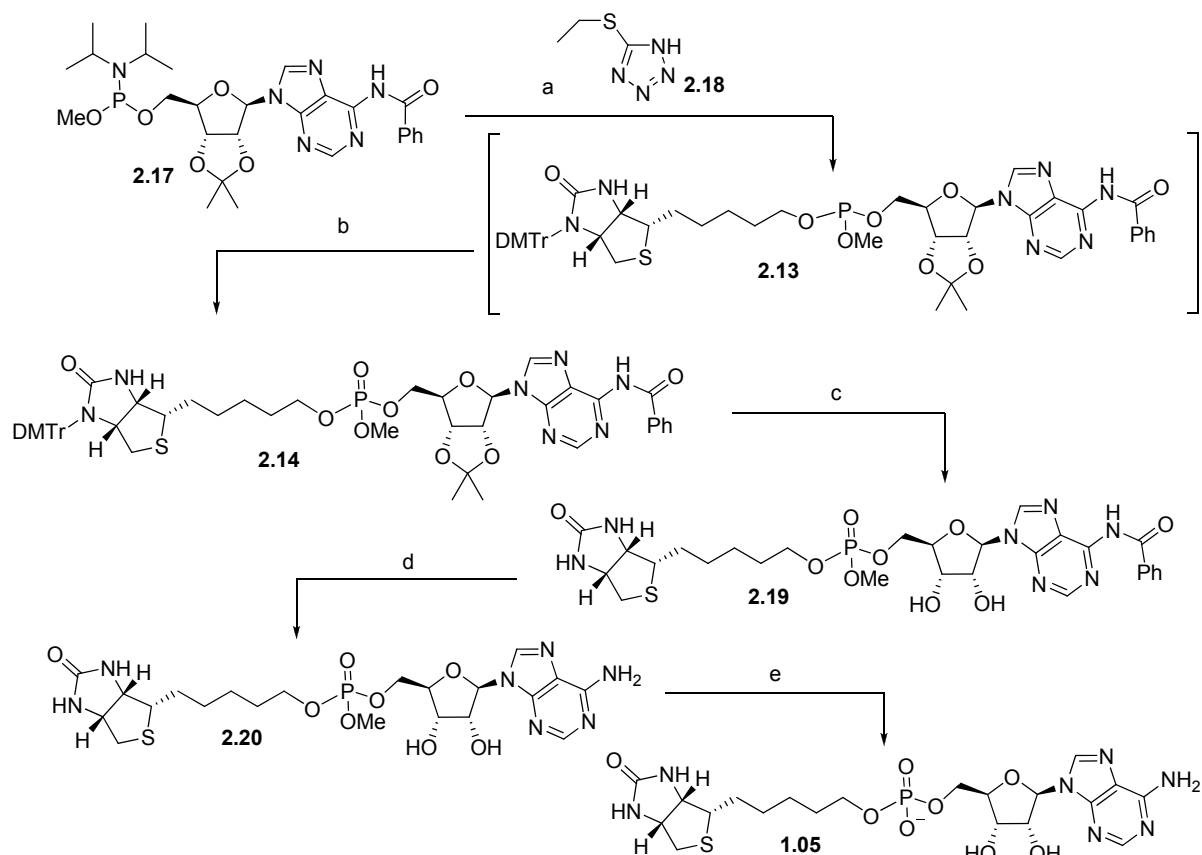
Scheme 2.10: a) **2.16,** CH₃CN; b) 5M TBHP; c) 1:1 TFA: DCM; d) NH₃, MeOH, THF; e) NaI, Acetone, reflux;

Compound **2.17** was reacted with **2.16** in the presence of 2-ethylthio-tetrazole **2.18**, which was freshly synthesized as reported.[18] The consumption of adenosine **2.17** and thereby generation of **2.13** was monitored by TLC, with the reaction complete after 30 min. The intermediate phosphite **2.13** was oxidised, with 10 equivalents of 5 M *tert*-butyl hydrogen peroxide (TBHP) in decane, to give phosphotriester **2.14** in 59% yield after flash chromatography. Possible sulphoxide and sulphone analogues, formed as a result of oxidation of the thiophene ring of biotin as reported in literature[19], were not apparent in the crude reaction mixture of **2.14** as determined based on mass spectrometry.

Removal of the trityl and the isopropylidene protecting groups of **2.14** was accomplished in a single step with the addition of 10% TFA in DCM. This gave **2.19** in 81% yield after purification by flash chromatography. The benzoyl group of **2.19** was removed on treatment with 32% aqueous ammonia to give **2.20** in 88% yield after purification by flash chromatography. Finally, de-protection of methoxy phosphate of **2.20** was achieved on treatment with NaI in refluxing acetone for 6 hours to give biotinol-5'-AMP **1.05** in 85% yield. Purification was achieved by HPLC with eluting mixture of buffer A (90% acetonitrile with 0.1% acetic acid) and buffer B (99.9% milliQ water and 0.1% acetic) and gradient of buffer A to B 0-90%.

Two such approaches to the synthesis of biotinol-5'-AMP **1.05** were examined as discussed in this chapter. A phosphodiester approach gave biotinol-5'-AMP **1.05** in an overall yield of 18% from adenosine **2.02**. The introduction of the negatively charged phosphate group early in the synthesis necessitated the use of a time consuming Sephadex-based purification. An alternative phosphoramidite approach gave biotinol-5'-AMP **1.05** in a comparable overall yield of 16% starting from adenosine **2.02**. This approach required an additional 5 steps. However, the use of the reactive adenosine **2.17**, facile coupling of biotinol **2.16** and adenosine **2.17**, and the use of standard purification by flash chromatography made it amenable to a multi-gram synthesis of biotinol-5'-AMP **1.05**. Optimisation of the phosphoramidite approach was not examined further due to the unfavourable drug profile of biotinol-5'-AMP **1.05**. Nevertheless, sufficient quantities of biotinol-5'-AMP **1.05** were obtained and its biological characterisation was undertaken as discussed below.

2.4 Enzyme and microbial assay of biotinol-5'-AMP 1.05 and compound 2.06

Compounds **1.05** and **2.06** were assayed against *S. aureus* biotin protein ligase (SaBPL), *E. coli* biotin protein ligase (EcBPL) and *H. Sapiens* biotin protein ligase (HsBPL) by collaborators at Molecular Life Science, University of Adelaide, using an assay method described by Chapman-Smith and co-workers.[20] The results are shown in Table 2.3. IC_{50} values were determined for each compound from a concentration-response curve by varying the concentration of the inhibitor under the same enzyme concentration.

Table 2.3: Enzyme assay and microbial assay of phosphate analogues
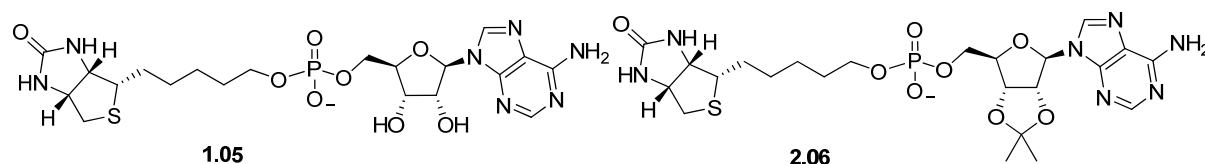
	SaBPL[a]	EcBPL[b]	HsBPL[c]
	IC_{50} (µM)	IC_{50} (µM)	IC_{50} (µM)
1.05	0.12 ± 0.01	2.5 ± 0.2	1.25 ± 0.1
2.06	0.15 ± 0.02	-	-

[a] *S aureus* biotin protein ligae [b] *E. Coli* biotin protein ligase [c] *Homo sapiens* biotin protein ligase.

Biotinol-5'-AMP **1.05** was a potent inhibitor of SaBPL (IC_{50} = 0.23 ± 0.06 µM) and a weaker micromolar inhibitor of HsBPL (1.25 ± 0.1) and EcBPL (2.5 ± 0.2). As shown in Table 2.3, biotinol-5'-AMP **1.05** was a moderately selective inhibitor of SaBPL over EcBPL (20 fold less potent) and HsBPL (10 fold less potent).

The isopropylidene protected derivative **2.06** had comparable potency to biotinol-5'-AMP **1.05** against SaBPL (IC_{50} = 0.15 ± 0.06 µM). This was expected as both the 2' and 3' hydroxyl group of biotinol-5'-AMP **1.05** are observed to lie in a solvent-exposed region of SaBPL in the X-ray crystal structure of biotinol-5'-AMP **1.05** (see discussions below).

Antimicrobial Minimal Inhibitory Concentrations (MICs) were determined for biotinol-5'-AMP against *S. aureus* by a microdilution broth method with cation-adjusted Mueller-Hinton broth. Biotinol-5'-AMP **1.05** was found to have anti-*Staphylococcus* activity with an MIC value of 8-32 μg/mL with bacteriostatic mode of action as shown in time kill experiments. Finally, the toxicity of biotinol-5'AMP **1.05** was examined against a mammalian cell culture model using HepG2 cells. No toxicity, as measured by metabolic activity, was observed when cells were treated with 64 μg/mL of biotinol-5'-AMP **1.05**.

A detailed discussion of the hydrogen bonding (summarised in Table 2.4) and the electrostatic interactions between biotinol-5'-AMP **1.05** and SaBPL is outlined below. This discussion is simplified by dividing the active site of SaBPL into four distinct regions based on the binding of the discrete components of biotinol-5'-AMP **1.05**, that is, the biotin, phosphate, pentose and adenine components (see Table 2.4). All four regions are discussed in turn below.
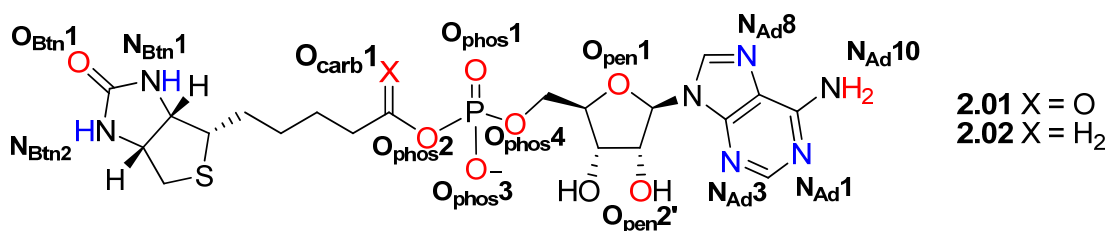
2.5 Analysis of X-ray structure of biotinol-5'-AMP 1.05 bound to SaBPL

The X-ray crystallography data of biotinol-5'-AMP **1.05** bound to SaBPL was solved[21] with a resolution of 2.50 Å by our collaborators at Monash University, Melbourne in order to elucidate the binding mode in SaBPL. The structure reveals that biotinol-5'-AMP **1.05** binds to SaBPL in a U-shaped conformation, as shown in Figure 2.4. This conformation allows both the biotin and adenine components of the inhibitor to bind in their respective pockets. A total of 15 hydrogen bonds are observed between biotinol-5'-AMP **1.05** and SaBPL**.** This compares to 13 for both biotinol-5'-AMP **1.05** bound to EcBPL and also biotinyl-5'-AMP **1.03** bound to SaBPL, as shown in Table 2.4 below. A summary of the hydrogen bonding interactions between biotinol-5'-AMP **1.05** and SaBPL, biotinol-5'-AMP **1.05** and EcBPL and biotinyl-5'-AMP **1.03** and SaBPL is shown in Table 2.4 below.
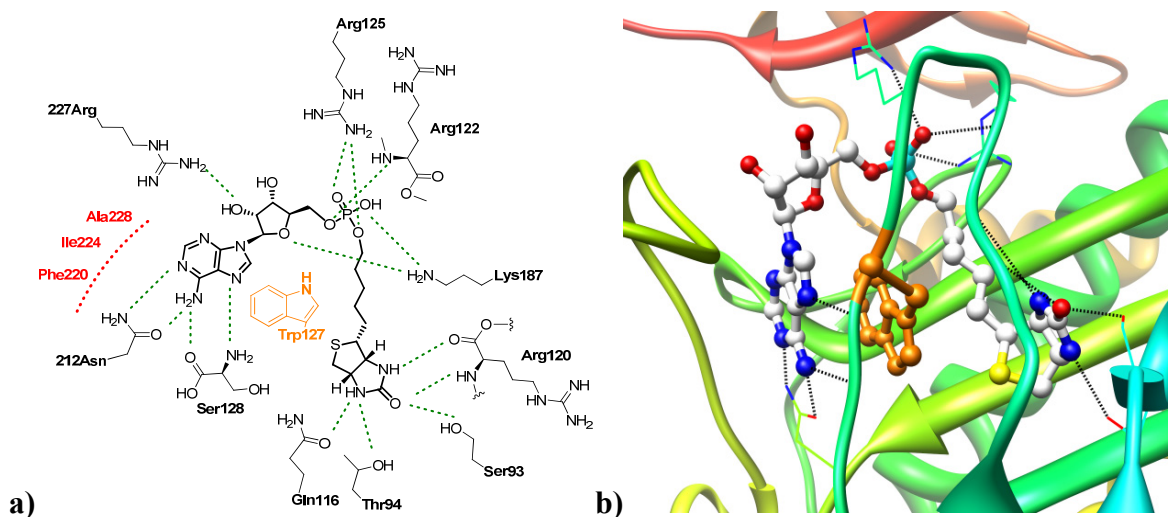
Figure 2.4: a) A 2D depiction of biotinol-5'-AMP **1.05** bound to SaBPL with hydrogen bonding interactions shown in green dashes. cut-off hydrogen bonding distance and angle determined using parameters set by Mills.[22] **b)** The corresponding 3D depiction obtained through Chimera[23] with black dash indicating the hydrogen bonding interactions.

Table 2.4[a]: Hydrogen bonding interactions and distances of biotinol-5'-AMP **1.05** bound to SaBPL and EcBPL and biotinyl-5'-AMP **1.03** bound to SaBPL

|	atom	SaBPL Biotinol-5'-AMP **1.05**	SaBPL Biotinyl-5'-AMP **1.03**[d]	EcBPL[b] Biotinol-5'-AMP **1.05**[b]
Biotin	$O_{Btn}1$	Arg120[c] NH (3.01) Ser93 OH (2.69)	Arg120[c] NH (2.94) Ser93 OH (2.73)	Arg116[c] NH (2.98) Ser89 OH (2.52)
	$N_{Btn}1$	Arg120[c] O (2.73)	Arg120[c] O (2.87)	Arg116[c] O (2.92)
	$N_{Btn}2$	Thr94 O (3.24) Gln116 O (2.99)	Thr94 O (3.25) Gln116 O (2.75)	Thr90 O (2.92) Gln122 O (2.89)
	$O_{carb}1$	-	Lys187 NH (3.12)	-
Phosphate	$O_{phos}1$	Lys187 NH (3.11- H_2O-3.28) Arg122 NH (2.62- H_2O-2.73) Asp180 O (3.20- H_2O-2.73)	Arg125 NH (3.08)	Lys183 NH (3.00) Arg121 NH (3.23)
	$O_{phos}2$	-	Arg122[c] NH (2.56)	-
	$O_{phos}4$	-	-	-
	$O_{phos}3$	Arg122[c] NH (2.59) Arg125 NH (3.06)	Arg122[c] NH (2.75) Arg125 NH (2.85)	Arg121 NH (2.84) Arg118[c] NH (2.77)
Pentose	$O_{pen}2'$	Arg227 NH (2.98)	-	Asn220 O (3.15) Val218 O[c] (3.17)
	$O_{pen}1$	Lys187 NH (3.13)	-	-
Adenine	$N_{Ad}1$	-	-	Asn208 NH (2.69)[c]
	$N_{Ad}3$	Arg227[c] O (2.82- H_2O-2.93)	-	Gly 222 O[c] (3.07- H_2O-2.89)
	$N_{Ad}8$	Ser128[c] NH (2.96)	Ser128[c] NH (3.42)	Phe124[c] NH (3.21)
	$N_{Ad}10$	Asn212 NH (3.04) Ser128[c] O (3.12)	Asn212 NH (3.06) Ser128[c] O (3.48)	Asn208 O (3.18) Phe124[c] O (3.21)

[a]Distances reported in angstroms [b]EcBPL obtained from PDB: 2EWN, [c] Interactions with backbone of corresponding residue as opposed to side chain., [d] X-ray crystal structure of biotinyl-5'-AMP bound to SaBPL were resolved and discussed in Section 1.2.2).

Biotin binding region

The ureido ring of the biotin of **1.05** was found to hydrogen bonds with residues Gln116, Thr94, Ser93 and Arg120 of SaBPL, as shown in Figure 2.4a. These residues are located at the base of the biotin binding pocket. The hydrogen bond lengths are summarised in Table 2.4. The biotin binding region is also characterised by a hydrophobic narrow shaft comprising of 3 beta sheets and the backbone of biotin binding loop, which accommodates the hydrophobic valeric tail of biotinol-5'-AMP **1.05** (Figure 2.4b).

Phosphate binding region

The phosphate binding region of SaBPL is dominated by the positively charged residues Arg125, Arg122 and Lys187. The phosphodiester group of biotinol-5'-AMP **1.05** is involved in an intricate hydrogen bonding network, as shown in Figure 2.5. The peptidic amino group of Arg122 and guanidinium group of Arg125 are hydrogen bonding with O1, whilst Lys187, Asp180, Arg122 and two water molecules are involved in a hydrogen bonding network with O2 (see Figure 2.5).
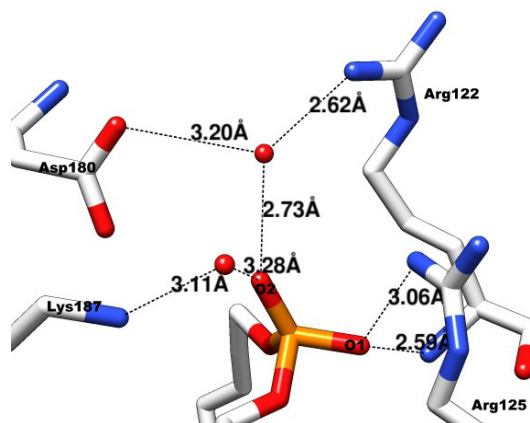
Figure 2.5: A 3D depiction of the phosphodiester linker of biotinol-5'-AMP **1.05** generated with Chimera. The hydrogen bonding interactions are shown in yellow dashes, the distances for hydrogen bonding interactions are described in table 4 below.

Pentose binding region

The region of ATP binding pocket responsible for hydrogen bonding with the pentose component of biotinol-5'-AMP **1.05** is characterised by a shallow pocket defined by

Trp127 at the bottom of this region and Arg227 and Lys187 at the top of a largely solvent exposed region (see Figure 2.6). Lys187 forms a hydrogen bond with the ether bridge of the pentose ring of **1.05**, whilst Arg227 and 2' hydroxyl group of biotinol-5'-AMP **1.05** are linked by a hydrogen bond.
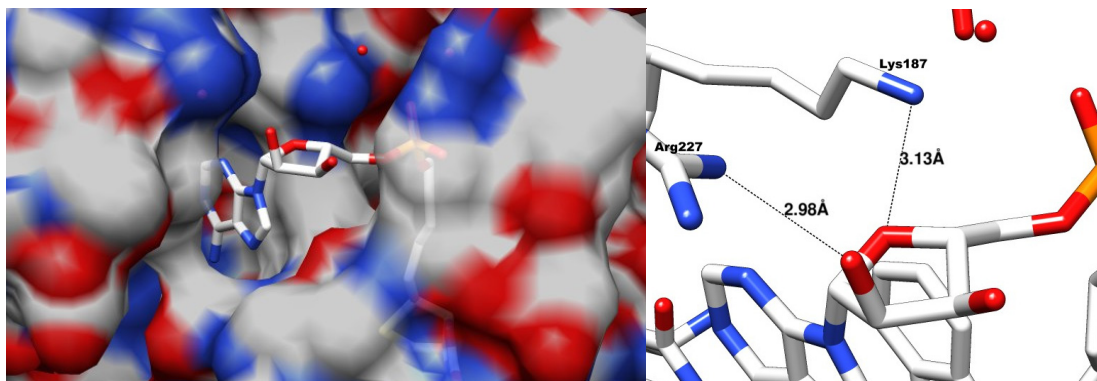

Figure 2.6: A 3D depiction of SaBPL surface with biotinol-5'-AMP **1.05** bound. The pentose ring was found to be sit at the opening of the active site (left). The hydrogen bonding interactions between SaBPL and the pentose ring are shown with black dashes (right), the distances of the hydrogen bonding interactions are shown in Table 2.4.

There is little difference in the potency of **2.06** (IC_{50} = 0.15 µM) and biotinol-5'-AMP **2.06** (IC_{50} = 0.12 µM). This suggests that the large opening of the pentose binding region, as shown in Figure 2.6, is capable of accommodating the isopropylidene group of compound **2.06**.

Adenine binding region

The adenine binding domain is defined by an ATP binding loop (dominated by Phe220, Ile224, Ala228) that encloses the adenine ring upon binding of biotinol-5'-AMP **1.05**.[24] This region is further defined by hydrogen bonding residues at the bottom of the pocket Asn212 and Ser128 in SaBPL and aromatic residue Trp127, as shown in Figure 2.7. The adenine ring of biotinol-5'-AMP **1.05** forms multiple hydrogen bonds with Asn212 and the backbones of Ser128 and Arg227, as shown in Figure 2.7. Moreover the adenine NH_2 forms a hydrogen bond with Asn212 of SaBPL. Finally, the parallel displaced π-stacking between the adenine rings of biotinol-5'-AMP **1.05** and Trp127 is shown in figure7. The

distance and displacement angles between centroids of Trp127 and biotinol-5'-AMP **1.05**, as shown in Figure 2.7 were observed to be 3.8 Å and 19°. These values are within the ranges suggested by McGaughey.[25]
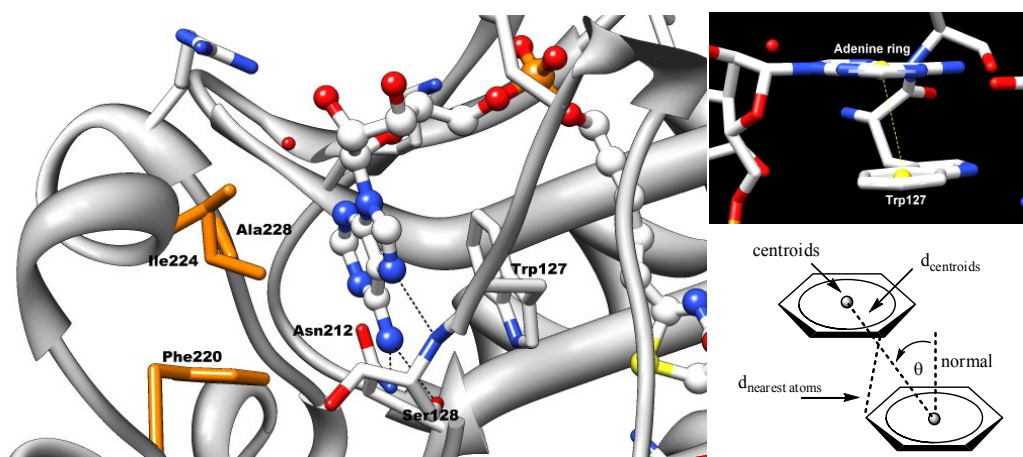

Figure 2.7: 3D depiction of adenine ring of biotinol-5'-AMP **1.05** with hydrophobic residues (Ile224, Ala228 and Phe220) shown in orange and hydrogen bonding between the adenine ring and Asn212 and Ser128 shown with black dashes (distances in table 4) (left). A side view of adenine ring and Trp127 highlighting the displaced parallel interaction, centroids of both aromatic ring are shown with yellow spheres (top right). The distance and angles measured determine degree of displacement of aromatic rings (bottom left).

Comparison of the X-ray crystal structures of biotinyl-5'-AMP and biotinol-5'-AMP bound to SaBPL

An overlay of the structures of biotinol-5'-AMP **1.05** and biotinyl-5'-AMP **1.03** bound to SaBPL was accomplished using Chimera[23] (Figure 2.8). As observed, the conformation of biotinol-5'-AMP **1.05** and biotinyl-5'-AMP **1.03** are superimposed, with 10 hydrogen bond interactions in common, as detailed in Table 2.4. Nevertheless, the lack of an α-carbonyl found in biotinol-5'-AMP **1.05**, compared to biotinyl-5'-AMP **1.03**, means the hydrogen bonding interaction with Lys187 is not formed. Rather when biotinol-5'-AMP **1.05** is bound, Lys187 is shifted towards the ATP binding pocket to form hydrogen bonding interaction with the phosphodiester and pentose ether bridge (see Figure 2.8). In addition, there is a marginal difference between the two SaBPL structure's ATP binding loop (ABL) between residues Arg220 – Ser128. This difference allows the guanidium group of Arg227 and the 2' hydroxyl of the pentose ring of biotinol-5'-AMP **1.05** to form a hydrogen

bonding interaction that is not present when biotinyl-5'-AMP **1.03** is bound (see Figure 2.8).
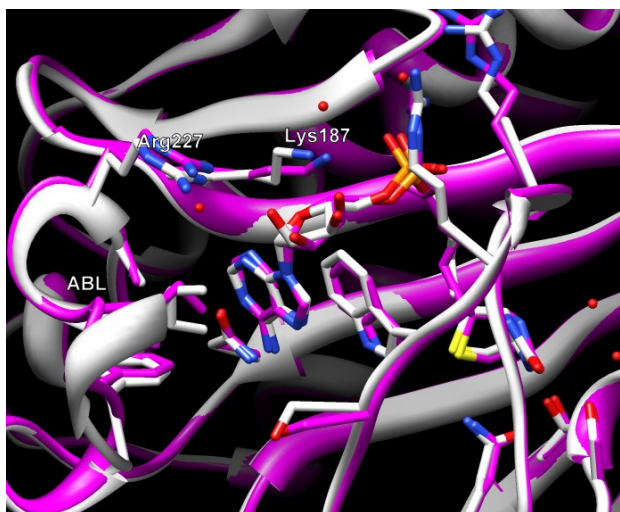
Figure 2.8: An 3D overlay of biotinyl-5'-AMP **1.03** bound to SaBPL (magenta) and biotinol-5'-AMP **1.05** bound to SaBPL (white) generated using Chimera. Marginal shifts with ABL, Arg227, Lys187 and Arg125 were observed.

A comparison of the structures of biotinol-5'-AMP bound to EcBPL and SaBPL

A superimposition of the structures between biotinol-5'-AMP **1.05** bound to both EcBPL (PDB: 2EWN) and SaBPL was accomplished using Chimera[23] with Needleman-Wunsch algorithm and BLOSUM62 matrix and is shown in Figure 2.9. For both structures, biotinol-5'-AMP **1.05** adopts a U-shaped conformation (Figure 2.9), with the biotin component maintaining identical hydrogen bonding interactions and adenine component adopting similar interactions (see Table 2.4). There are, however, differences in the way biotinol-5'-AMP **1.05** binds to SaBPL and EcBPL. Namely, a) the hydrogen bonding network between the phosphodiester and SaBPL is not conserved in EcBPL (see Table 2.4) and b) the ATP binding loop of both EcBPL and SaBPL (within EcBPL these residues involve Val214, Val218, Val219 and Trp223, whilst SaBPL the corresponding residues are Phe220, Ile224, Ala228). These differences form the basis for our rationally designed selective inhibitors discussed ahead in chapters 3, 4 and 6.
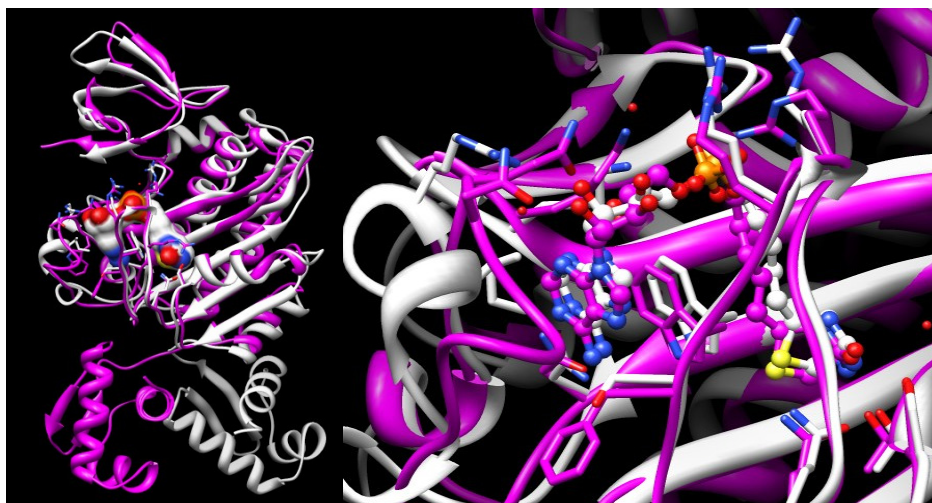
Figure 2.9: Alignment of biotinol-5'-AMP **1.05** bound to SaBPL (white) and EcBPL (PDB: 2EWN) (magenta) using Chimera. (RMSD = 1.163 Å).

2.6 Conclusion

Biotinol-5'-AMP **1.05** is a non-hydrolysable reaction intermediate mimic that has been used in mechanistic and kinetic studies of MtBPL, EcBPL, SaBPL and PhBPL (see Chapter 1 for discussion). Further work is required to understand the intricate allosteric interactions of BPL (discussed in Chapter 1) and the conformational changes that occur within the BPL active site. Thus an efficient and simple phosphoramidite protocol for the synthesis of biotinol-5'-AMP **1.05** is of great utility to provide further understanding of BPLs.

Two such approaches to the synthesis of biotinol-5'-AMP **1.05** were examined, as discussed in this chapter. A phosphodiester approach gave biotinol-5'-AMP **1.05** in an overall yield of 14% from adenosine **2.02** and after HPLC purification. The introduction of the negatively charged phosphate group early in the synthesis necessitated the use of time consuming Sephadex-based purification. An alternative phosphoramidite approach gave biotinol-5'-AMP **1.05** in a comparable overall yield of 16% starting from adenosine **2.02** and after HPLC purification. This approach required an additional 5 steps. However, the use of the reactive phosphite **2.17**, facile coupling of biotinol **2.16** and adenosine **2.17**, and the use of standard purification by flash chromatography makes it amenable to a multi-gram synthesis of biotinol-5'-AMP **1.05**.

Two key issues with developing reaction intermediate mimics of ligases were evident with biotinol-5'-AMP **1.05** as an inhibitor of SaBPL: a) a lack of synthetic ease for the phosphodiester linker (low yields, problematic product isolation and multiple synthetic steps) and b) limited selectivity between homologues (HsBPL, SaBPL and EcBPL). The X-ray crystal structure of biotinol-5'-AMP **1.05** bound to SaBPL and EcBPL supports the lack of selectivity observed in *in vitro* studies. Both enzymes adopt similar binding modes with biotinol-5'-AMP **1.05**. However, the adenylate and phosphoroanhydride binding domains were found to be varied and are the focus of our investigation in chapters 3 and 4. These structures provide important structural information for the design and synthesis of subsequent inhibitors of SaBPL, as described in the following chapters.

2.7 References for Chapter Two

(1)   Payne, D. J.; Gwynn, M. N.; Holmes, D. J.; Pompliano, D. L. *Nat Rev Drug Discov* **2007**, *6*, 29.

(2)   Purushothaman, S. G., Garima.; Srivastava, Richa.; Ramu, Vasanthakumar, Ganga. Ramu.; Surolia, Avadhesha.; *PloS ONE* **2008**, *3*, 12.

(3)   Brown, P. H.; Cronan, J. E.; Grøtli, M.; Beckett, D. *Journal of Molecular Biology* **2004**, *337*, 857.

(4)   Brown, P. H.; Beckett, D. *Biochemistry* **2005**, *44*, 3112.

(5)   Unpublished.

(6)   Purushothaman, S.; Gupta, G.; Srivastava, R.; Ramu, V. G.; Surolia, A. *PloS ONE* **2008**, *3*, e2320.

(7)   Tener, G. M. *Journal of the American Chemical Society* **1961**, *83*, 159.

(8)   Yoshikawa, M. K., Tetsuya.; Takenishi, Tadao.; *Bulletin of the Chemical Society of Japan* **1969**, *42*, 3.

(9)   Zatorski, A.; Watanabe, K. A.; Carr, S. F.; Goldstein, B. M.; Pankiewicz, K. W. *Journal of Medicinal Chemistry* **1996**, *39*, 2422.

(10)   Jansen, R. S.; Rosing, H.; Schellens, J. H. M.; Beijnen, J. H. *Nucleosides, Nucleotides & Nucleic Acids* **2010**, *29*, 14.

(11)   *Organophosphorus Reagents: A Practical Approach in Chemistry*; 1 ed.; Williams, D. M. H., V. H.;, Ed.; Oxford University Press: Oxford, 2004; Vol. 1.

(12)   Alves, A. M.; Holland, D.; Edge, M. D. *Tetrahedron Letters* **1989**, *30*, 3089.

(13)   Fisher, E. F.; Caruthers, M. H. *Nucleic Acids Research* **1983**, *11*, 1589.

(14)   Schirrmacher, E.; Beck, C.; Brueckner, B.; Schmitges, F.; Siedlecki, P.; Bartenstein, P.; Lyko, F.; Schirrmacher, R. *Bioconjugate Chemistry* **2006**, *17*, 261.

(15)   Froehler, B. C.; Matteucci, M. D. *Nucleic Acids Research* **1983**, *11*, 8031.

(16)   Desjardins, M.; Garneau, S.; Desgagnés, J.; Lacoste, L.; Yang, F.; Lapointe, J.; Chênevert, R. *Bioorganic Chemistry* **1998**, *26*, 1.

(17)   van der Heden van Noort, G. J.; Overkleeft, H. S.; van der Marel, G. A.; Filippov, D. V. *Organic Letters* **2011**, *13*, 2920.

(18)   LeBlanc, B. W.; Jursic, B. S. *Synthetic Communications: An International Journal for Rapid Communication of Synthetic Organic Chemistry* **1998**, *28*, 3591

(19)   Upadhya, K.; Khattak, I. K.; Mullah, B. *Nucleosides, Nucleotides & Nucleic Acids* **2005**, *24*, 919.

(20)   Chapman-Smith, A.; Cronan, J. E. *Trends in biochemical sciences* **1999**, *24*, 359.

(21)   Pendini, N. R.; Polyak, S. W.; Booker, G. W.; Wallace, J. C.; Wilce, M. C. J. *Acta Crystallographica Section F* **2008**, *64*, 520.

(22)   Mills, J. E. J.; Dean, P. M. *Journal of Computer-Aided Molecular Design* **1996**, *10*, 607.

(23)   Pettersen, E. F.; Goddard, T. D.; Huang, C. C.; Couch, G. S.; Greenblatt, D. M.; Meng, E. C.; Ferrin, T. E. *Journal of Computational Chemistry* **2004**, *25*, 1605.

(24)   Naganathan, S.; Beckett, D. *Journal of Molecular Biology* **2007**, *373*, 96.

(25)   McGaughey, G. B.; Gagné, M.; Rappé, A. K. *Journal of Biological Chemistry* **1998**, *273*, 15458.

Chapter Three

3.1 Introduction

As discussed in Chapter 2, biotinol-5'-AMP **1.05** is an important lead for the development of a new class of antibacterial agent against *S. aureus*. Nevertheless, it does present a number of issues that require attention if it is to be developed into an antibiotic. These are 1) The synthesis of biotinol-5'-AMP **1.05** is somewhat problematic (see Section 2.2) and 2) Biotinol-5'-AMP **1.05** has a relatively poor drug profile with regards to stability and a lack of enzyme selectivity (see Section 2.4). The phosphodiester of **1.05** is central to both of these issues and its replacement is the subject of this chapter. An overview on each of these two key issues follows:

Synthesis of biotinol-5'-AMP 1.05: The key step that contributed to the problematic synthesis of biotinol-5'-AMP **1.05** involved a phosphate esterification of adenosine **2.04** and biotinol **2.05** with DCC (Scheme 3.1), which occurred in only 31% after significant optimisation (Section 2.2). This reaction is central to the synthesis in that it introduces the negatively charged phosphodiester linker, however it does so early in the synthesis and thereby requires extensive purification by cation and anion exchange chromatography and HPLC. An alternative approach, utilising the more reactive phosphorus(III) reagent, resulted in ligation of both biotin and adenosine groups in 59% yield (see Section 2.3 for further detail). Briefly, the negatively charged phosphodiester is concealed until the final synthetic step. As such the immediate precursors (**2.14** and **2.19**) can be purified by normal phase silica gel chromatography to greatly facilitate isolation. Nevertheless this approach still required 5 steps and gave a modest increase in overall yield to 18% .
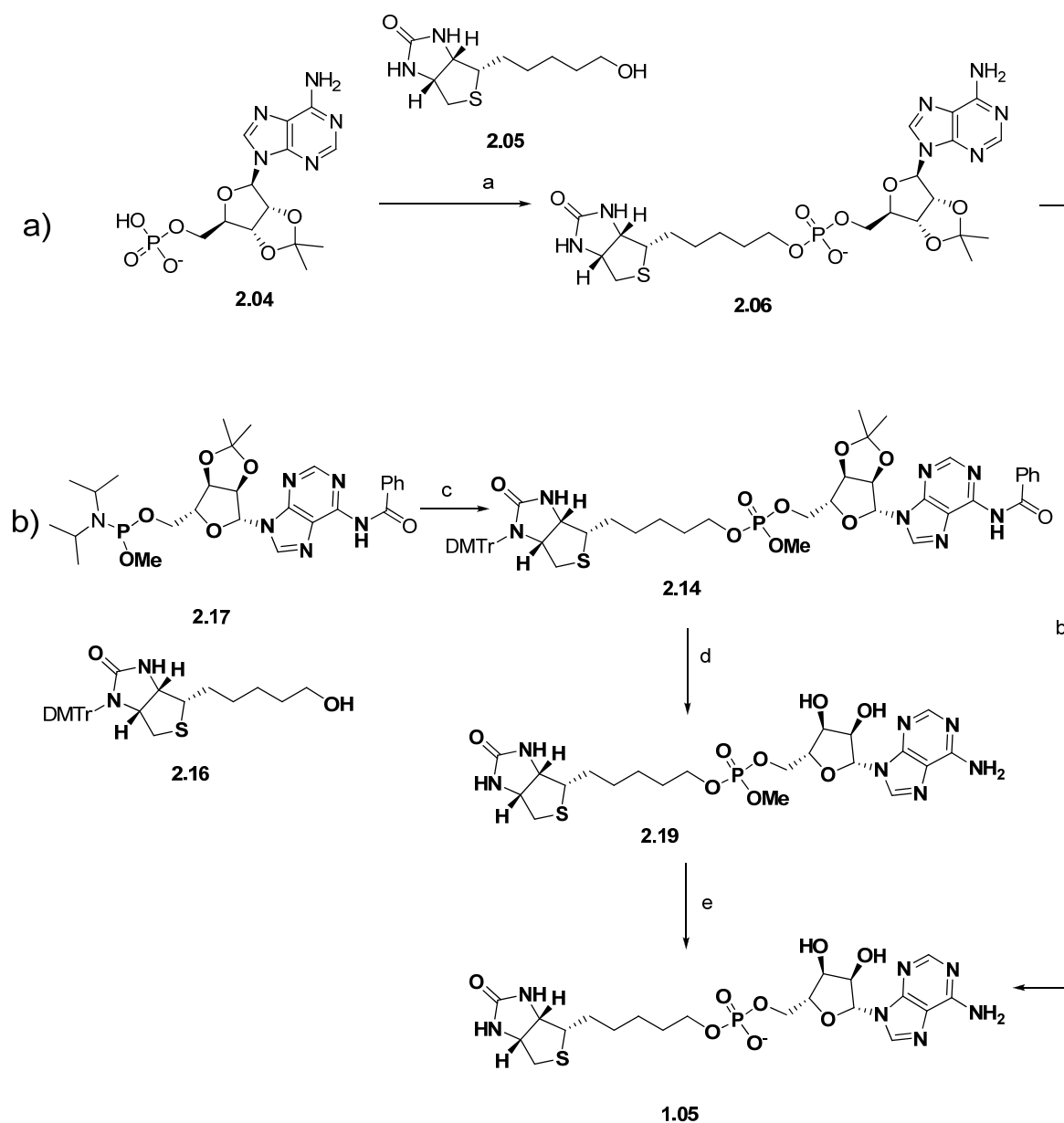
Scheme 3.1: a) DCC, py; b) i) AcOH, 80 $^{\circ}$C; ii) Sephadex DEAE A25; iii) HPLC; c) i) ETT, AcCN; ii) 6M TBHP in decane; d) i) 10% TFA, DCM; ii) 32% NH$_3$, 1:1 THF:MeOH; iii) NaI, Acetone, Δ; iv) HPLC;

Selectivity of biotinol-5'-AMP 1.05 and its drug profile: The key *in vitro* issue with regards biotinol-5'-AMP **1.05**, is that it displays poor selectivity for BPLs among different species (e.g. SaBPL IC$_{50}$ = 0.23 $\pm$ 0.06 μM, EcBPL IC$_{50}$ = 2.5 $\pm$ 0.01 μM, and HCS IC$_{50}$ = 1.25 $\pm$ 0.01 μM, see Section 2.4 for further discussion). This limited selectivity is a result of a high degree of homology between BPL species, in particular within the active site

residues that are responsible for hydrogen bonding to the key metabolic intermediate, biotinyl-5'-AMP **1.03** (discussed in Section 1.2.2) and biotinol-5'-AMP **1.05** (discussed in Section 2.5). To overcome this limited selectivity for different SaBPL, we required a new structural class of inhibitor. Replacement of the phosphate based linkage of **1.03** and **1.05** was identified as a key requirement for the design and synthesis of such a new class of inhibitor. To this end, we sort a replacement that would provide improved stability and ease of synthesis compared to the phosphodiester linker in our lead structure biotinol-5'-AMP **1.05**. The main goal was to develop an approach that would allow the rapid synthesis of a diverse structural range of compounds that would enable us to obtain high selectivity for SaBPL compared to human BPL. This is important because the main obstacle to developing inhibitors of ligases such as BPL, is the limited selectivity (see Section 1.3.2).

3.1.1 Phosphoroanhydride bioisosteres

Given the issues stated above, we investigated the alternative phosphate linkage, as outlined in Section 1.3 and 1.4 and detailed in this chapter. A number of key features were required for our desired bioisosteric phosphoroanhydride linkage:

Molecular recognition: The bioisostere must maintain molecular recognition through the formation of key hydrogen bonds between the phosphodiester linkage of **1.05** and Lys187, Arg122 and Arg125 of SaBPL observed in co-crystal structures (see Section 2.5 for further discussion).

Conformation: More critically, the bioisostere must allow a 'U-shaped conformation' that is exhibited by biotinol-5'-AMP **1.05** and biotinyl-5'-AMP **1.03** on binding to SaBPL. This conformation places both the biotin and adenine groups of **1.05** and **1.03** into their respective binding pockets in order to facilitate overall binding. Indeed 9 out of the 15 hydrogen bonding interactions are found between BPL and adenine and biotin groups with residues Ser93, Thr94, Gln116, Arg120 adopting hydrogen bonding interactions with biotin ring and Asn212 and Ser127 adopting hydrogen bonding interactions with adenine (see Section 2.5 for further discussion).

Synthetic ease: The bioisostere must be able to be introduced in only a few synthetic steps and in high yields, using chemistry that is compatible with range functional groups, thus avoiding the need for extensive protection and deprotection steps. Ideally the bioisostere

would not be negatively charged as is the phosphodiester of **1.05**. This would greatly facilitate purification, with the use of simple silica gel-based chromatography, and also enables its preparation on a large scale. Ultimately, the chemistry used to prepare the bioisostere should allow the facile coupling of biotin and adenosine based analogues in a combinatorial or in vitro way to facilitate both lead generation and optimisation of potential SaBPL inhibitors.

As discussed in Chapters 1 and 2, the biotinol-5'-AMP **1.05** provides an enzymatically stable reaction intermediate mimic of biotinyl-5'-AMP **1.05**. This same approach has been applied to pathogenic ligases, such as amino-acyl tRNA synthethases[2-4], bi-functional salicyl-AMP ligase[5,6] and pantothenate synthetase[7,8] utilising sulphamoyl linker **3.02**; D-alanine-D-alanine ligase[9] utilising phosphonate linker **3.04** and phosphopantothenoylcysteine synthetase[10] utilising phosphodiester linker **3.03**.
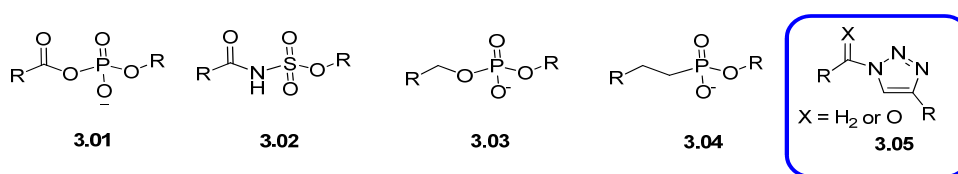

Figure 3.1: Common bioisosteres of the phosphoryl-anhydride linker found in reported ligase inhibitors.

Whilst the approach of utilising sulphamoyl, phosphodiester and phosphonates for the development of reaction intermediate mimics of ligase invariably leads to potent inhibitors, as discussed in Section 1.3.2, it is apparent that there is limited selectivity when host homologue (such as *H. sapiens*) are present, as was observed with biotinol-5'-AMP **1.05**. Moreover, the synthesis of these common bioisosteres, particularly in a combinatorial way, is difficult and requires several steps and difficult purification (see Section 1.3.2). Thus, the development of a new synthetically efficient phosphoroanhydride mimic is needed to assist in developing selective and potent inhibitors against ligases, such as SaBPL. To this end, we propose the 1,2,3-triazole **3.05** as an alternative to overcome the synthetic problems associated with these bioisosteres (**3.02 – 3.04**).

3.2 1,2,3-Triazole-based phosphate bioisosteres

The 1,2,3 - triazole derivative **3.05** (triazole) meets the criteria outlined in Section **3.1.3**, with a number of structural and electronic characteristics that are favourable for binding to target enzymes (see Figure 3.2). The key features of the triazole derivative include:

Molecular recognition: The phosphate binding domain of SaBPL is dominated by positively charged and flexible residues of Arg122, Arg125 and Lys187 which converge into the domain. It is proposed the three electronegative nitrogens of the triazole ring (see Figure 3.2) would be able to mimic the interactions between residues Arg122, Arg125 and Lys187 and the phosphodiester of biotinol-5'-AMP **1.05**. Moreover the close proximity of Trp126 to the phosphodiester binding domain would allow an edge-to-face interaction with the aromatic triazole ring. The centroid of the aromatic Trp126, as shown in Figure 3.3 is 5.2 Å away from the phosphorous atom of biotinol-5'-AMP **1.05**. The optimal distance for edge-to-face interactions of two aryl system is 4.96 Å between their ring centres.[11]
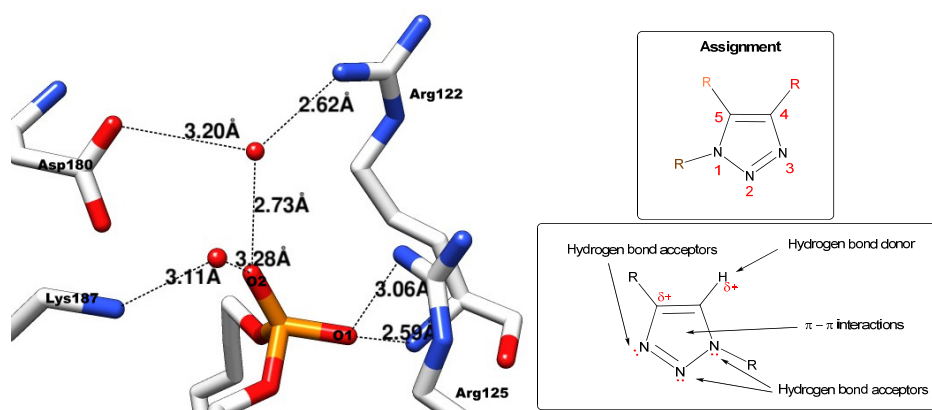
Figure 3.2: *Left:* 3D depiction of X-ray crystal structure of biotinol-5'-AMP **1.05** bound to SaBPL with hydrogen bonding interactions shown in black dashes. *Right Top*: nomenclature for 1,2,3-triazole. *Right bottom:* The reported potential interactions with 1,2,3-triazole based on X-ray crystallography.[12,13]

Conformation*: The U-shaped conformation adopted by biotinol-5'-AMP **1.05** on binding to SaBPL, as shown in Figure 3.3A is defined by binding of the biotin and adenosine groups into their two respective pockets. Both the 1,4- and 1,5-triazole regioisomers, see **3.06** and **3.07** in Figure 3.3B, are obtainable by reaction of the synthetic precursor alkyne and azides (discussed in Section 1.4). The 1,4-disubstituted triazole ring provides a linear

conformational constraint[13,14], while 1,5-disubstituted triazole is proposed to provide the requisite U-shaped conformation.[13,15] It is noteworthy that a 1,5-triazole has been used to mimic U-shaped conformations of cis-amide bonds[13,16] and cis-alkenes[17]. The appropriate linkage length between biotin and adenosine of approximately 4 Å is required if both groups are able to bind in the respective pockets of SaBPL. The X-ray crystal structure of SaBPL reveals that the separation of the carbon at 5 position of adenosine from the valeric tail of biotin of biotinol-5'-AMP **1.05** and biotinyl-5'-AMP **1.03** to be 4.5 Å and 4.1 Å, respectively, as shown in Figure 3.3A. X-ray crystal structures of triazole ligands bound to HIV-1 protease and acetylcholine esterase have shown the 1,4-disbustitution and 1,5-disubstituted triazole groups to provide linkage lengths of 4.9 Å and 3.2 Å respectively, as shown in Figure 3.3C.[12,18] The data in Figure 3.3B and 3.3C reveals a compromise, with the 1,4-disubstituted triazole providing an appropriate linkage length, but a linear constraint; whilst the 1,5-disubstituted triazole provides the required U-shaped conformation, but a significantly shorter linkage, approximately 1 Å shorter than phosphodiester or phosphoryl anhydride linkage
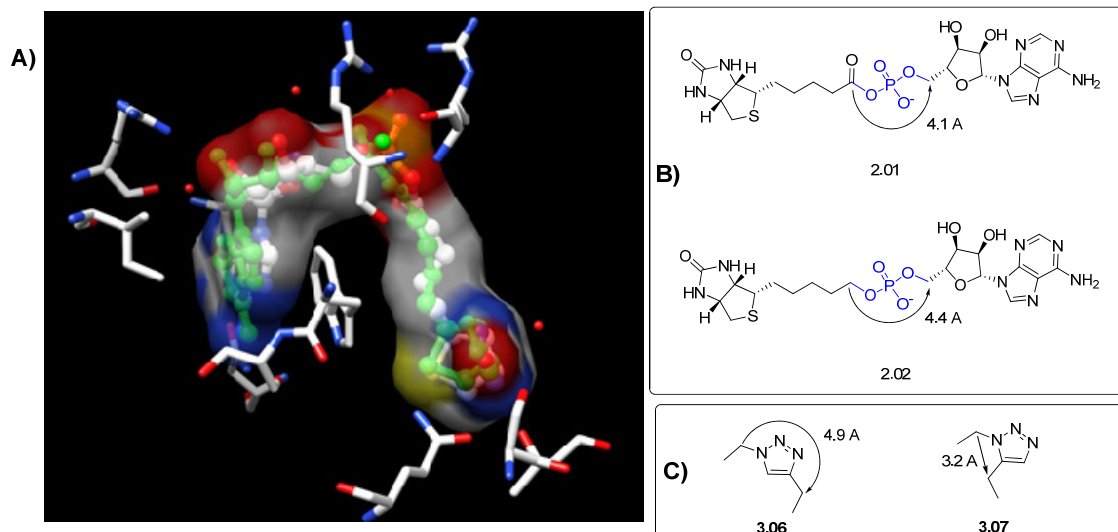
Figure 3.3: **A)** a superposition of biotinyl-5'-AMP **1.03** (white) and biotinol-5'-AMP **1.05** (green) bound to SaBPL with key residues shown. **B)** linkage length of phosphoryl anhydride of biotinyl-5'-AMP **1.03** and phosphodiester of biotinol-5'-AMP **1.05** determined through UCSF Chimera 1.5.2. **C)** linkage length of 1,4-triazole **3.06** and 1,5-triazole **3.07** determined through PDB structures.[13,18]

Synthetic ease: The key attribute of a triazole linkage is the reliable and efficient formation of the ring, such as through copper catalysed azide alkyne cycloaddition (CuAAC) and to a lesser extent ruthenium catalysed azide alkyne cycloaddition (RuAAC), as depicted in Figure 3.4. CuAAC can 'click' a range of azides and alkynes together in a facile, selective and high yielding manner that is compatible with a range of functional groups. By establishing the triazole as a viable linker between the biotin and adenylate components, we have the potential to undertake a combinatorial and fragment-based approach in developing inhibitors (see Chapter 1 for general discussion).
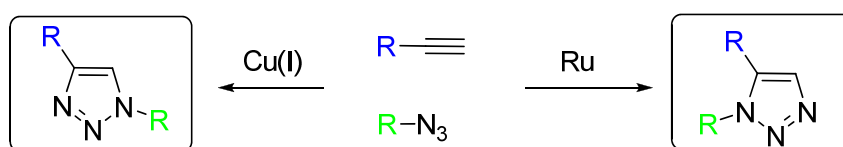
Figure 3.4: Routes to 1,4-triazole (CUAAC) and 1,5-triazole (RuAAC) from alkyne and azide.

Proposed 1,4-triazole inhibitors

As discussed above, 1,4- and 1,5-triazoles offer different structural constraints and linkage lengths, with each mimicking different aspects of the structure of biotinol-5'-AMP **1.05**. Thus, four analogues of biotinyl-5'-AMP **1.03** and biotinol-5'-AMP **1.05** were initially proposed based on the attributes discussed above and shown in Figure 3.5 below. Triazoles **3.08** and **3.09** are direct bioisosteric analogues of biotinol-5'-AMP **1.05**, with the di-substituted triazole replacing the phosphodiester. Triazole **3.10** and **3.11** retained the carbonyl group of the reactive intermediate biotinyl-5'-AMP **1.03**.

The proposed synthetic strategy for the preparation of triazole **3.08 – 3.11** utilised the reported alkyne precursors **3.12 - 3.14**[19] and azide precursors **3.15**[20], **3.16**[21] **3.17**[22](Figure 3.6). The acetylene **3.13** has its two ureido nitrogens protected in order to improve solubility.

2.02   **2.01**

3.08   **3.10**

3.09   **3.11**
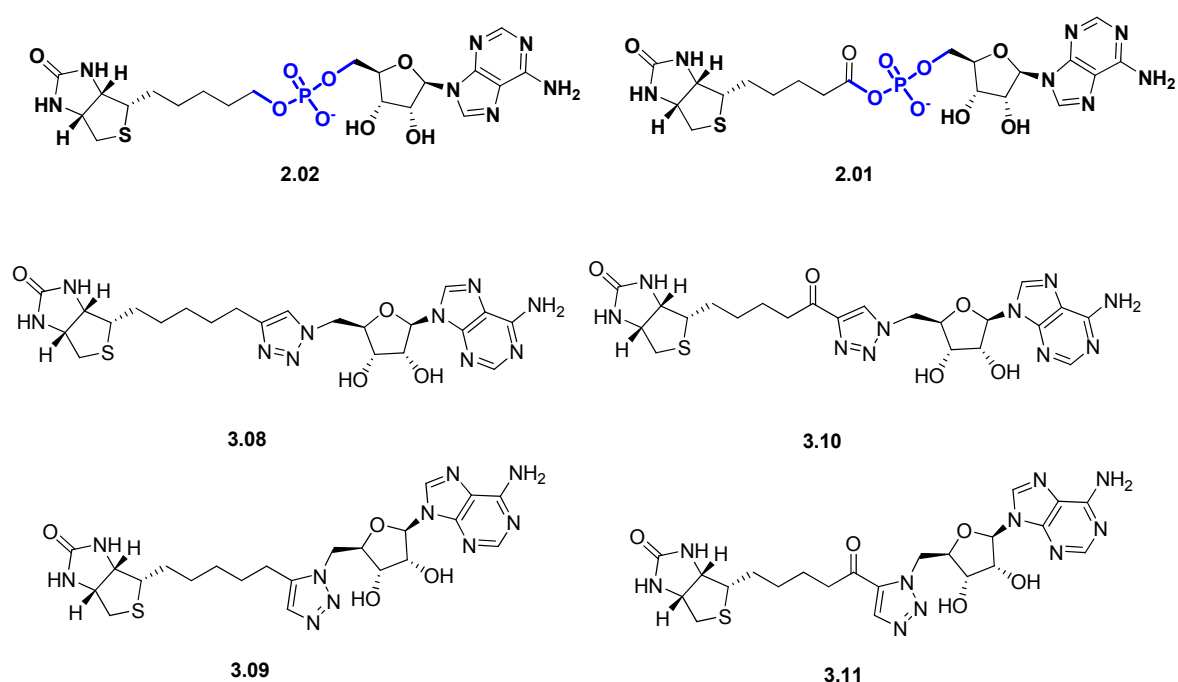
Figure 3.5: Proposed triazoles analogues of biotinyl-5'-AMP **1.03** and biotinol-5'-AMP **1.05**

3.12   **3.13**   **3.14**

3.15   **3.16**   **3.17**
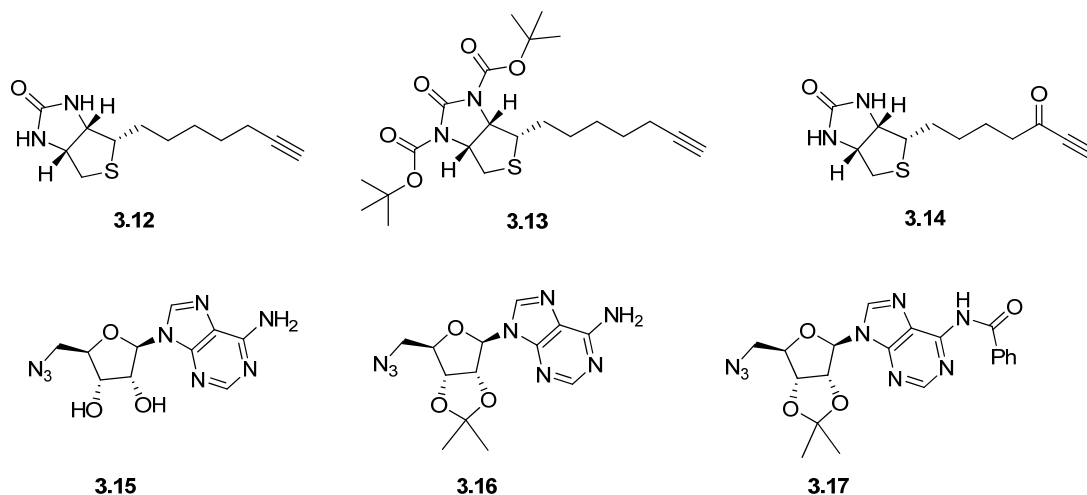
Figure 3.6: Proposed precursors **3.12 – 3.17** for the synthesis of triazole **3.08 – 3.11.**

The synthetic approach to the triazole **3.08 – 3.11** is shown in Scheme 3.2. The synthesis of 1,4-substituted triazoles (**3.08** and **3.10**) involves the *in situ* generation of Cu(I) catalysis from Cu_2SO_4 or Cu(0) to facilitate CuAAC of alkyne **3.12 – 3.14** with azide **3.15 – 3.17**. The synthesis of the alternative 1,5-substituted triazoles **3.09** and **3.11** involves RuAAC of
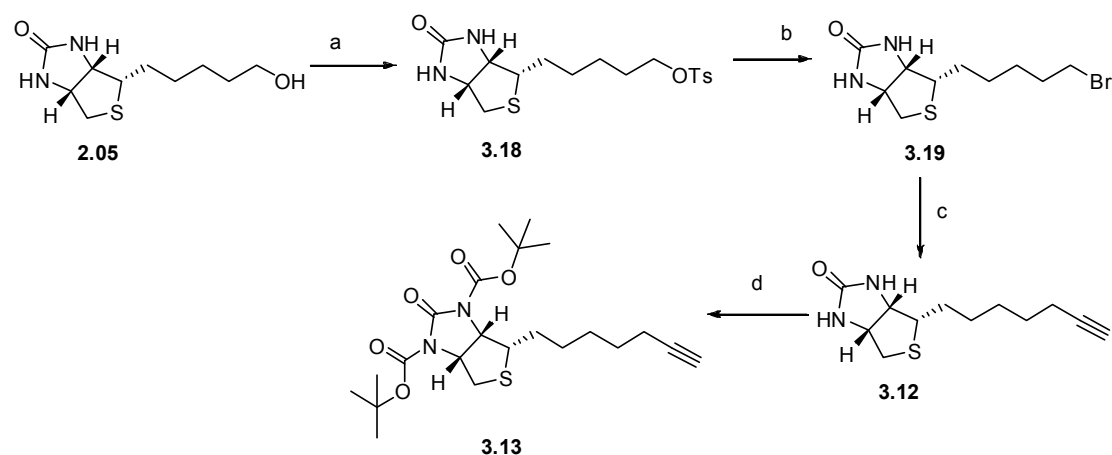
alkyne **3.12 – 3.14** with azide **3.15 – 3.17**and using the ruthenium catalyst Cp*Ru(PPh$_3$)$_2$Cl **1.20**.[23]
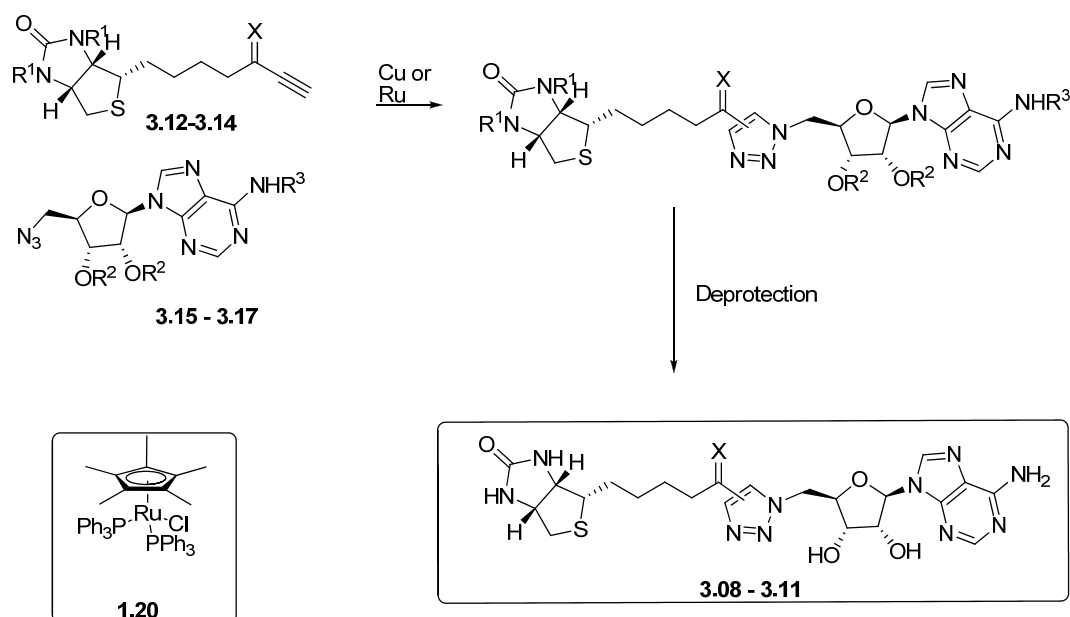
Scheme 3.2: proposed synthesis of triazole **3.08 – 3.11**

## 3.2.1 Synthesis of Biotin and Adenosine Precursors

The synthesis of the key biotin alkynes (**3.12** and **3.13**) and the attempted synthesis of alkyne **3.14** are outlined in Schemes **3.3** and **3.4,** respectively.

Scheme 3.3: a) TsCl, Py; b) LiBr, MEK; c) Li-acetylide EDA complex, DMSO, 15 ^{o}C;

Biotin alkyne **3.13** was prepared in seven steps, in 16% overall yield from biotin, according to the method described by Corona *et al.*[19] Biotinol **2.05** was prepared as previously described in chapter 2. Tosylation of this, with tosyl chloride, in dry pyridine, at 5 °C, gave tosylate **3.18** as a crude product. The tosylate underwent some decomposition on silica gel chromatography and was thus used in the next synthetic step without purification. The crude tosylate **3.18** was treated with lithium bromide in 2-butanone (MEK) under reflux, to give biotin bromide **3.19** in 51% yield over two steps. Treatment of **3.19** with lithium acetylide ethylene diamine complex (EDA), in DMSO at ambient temperature, gave biotin alkyne **3.12** in a yield of 71%. Some decomposition of the commercial and hydroscopic lithium acetylide EDA complex was observed within a month of opening the bottle, regardless of the method of storage. Reactions of biotin **3.19** with an 'older' sample (more than 1 month) of lithium acetylide EDA complex required the use of increased equivalents of the reagent. Even with this modification lower yields of **3.12** were obtained, ranging from 41 % to 55 %. The outcome was further complicated by increased levels of impurities and thus it is recommended to use 'fresh' reagent. Biotin alkyne **3.12** was next reacted with BOC anhydride, triethylamine, 4-DMAP in DCM to give the BOC-protected biotin alkyne **3.13** in 54% yield. This derivative was prepared in order to increase the solubility of biotin alkyne **3.12** in preparation for CuAAC (discussed below).

The synthetic strategy for preparing alkyne **3.14**, involved Grignard reaction between weinreb amine **3.22** with magnesium[24] or lithium acetylide.[25] The reaction of aldehyde **3.20** with magnesium[26] or lithium acetylide[27] followed by oxidation of the α-hydroxyl group was considered as an alternative route.
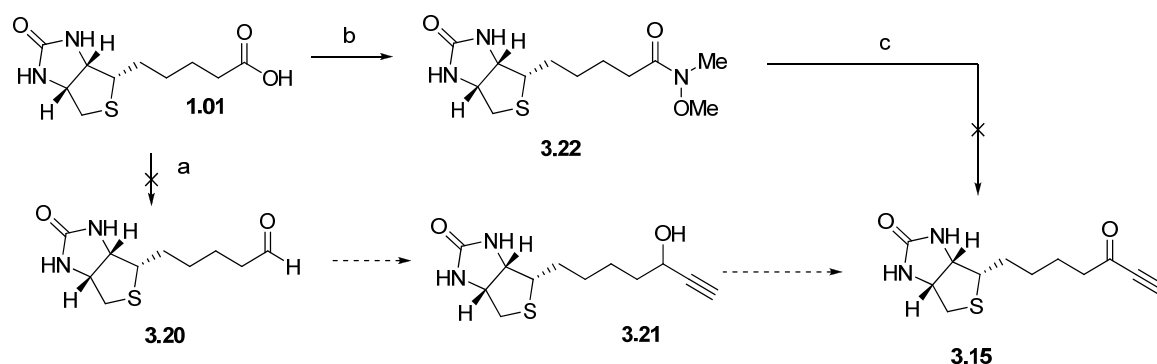

Scheme 3.4: a) Dess-martin periodinane, DMSO b) MeNH(OMe), EDCI, DIPEA, DCM c) Li-acetylide EDA, THF or MgBr acetylide, THF.

Oxidation of biotin **1.01** with Dess Martin periodinane in 9:1 DCM and DMSO gave a product consistent with aldehyde **3.20**, with a characteristic aldehyde resonance at 9.3 ppm in the ^{1}H NMR spectrum of the crude material. However, the aldehyde **3.20** could not be isolated from the complex mixture by chromatography. Therefore an alternate route towards enynone **3.15** was examined. Weinreb amide **3.22** was prepared by treatment of biotin **1.01** with EDCI, N,O-dimethylhydroxyamide, DIPEA in DCM, in 43% yield. However, subsequent treatment of **3.22** with magnesium ethynyl bromide, or lithium acetylide EDA complex in THF, resulted in complex mixtures, with only starting material being isolated after flash chromatography. The synthesis of enynone **3.14** and the subsequent triazoles **3.10** and **3.11** was therefore not examined further.

As shown in Scheme 3.5, the adenosine-containing azides **3.15–3.17** were prepared according to literature procedures, with some modification and improvements given the limited information available.[20,21]
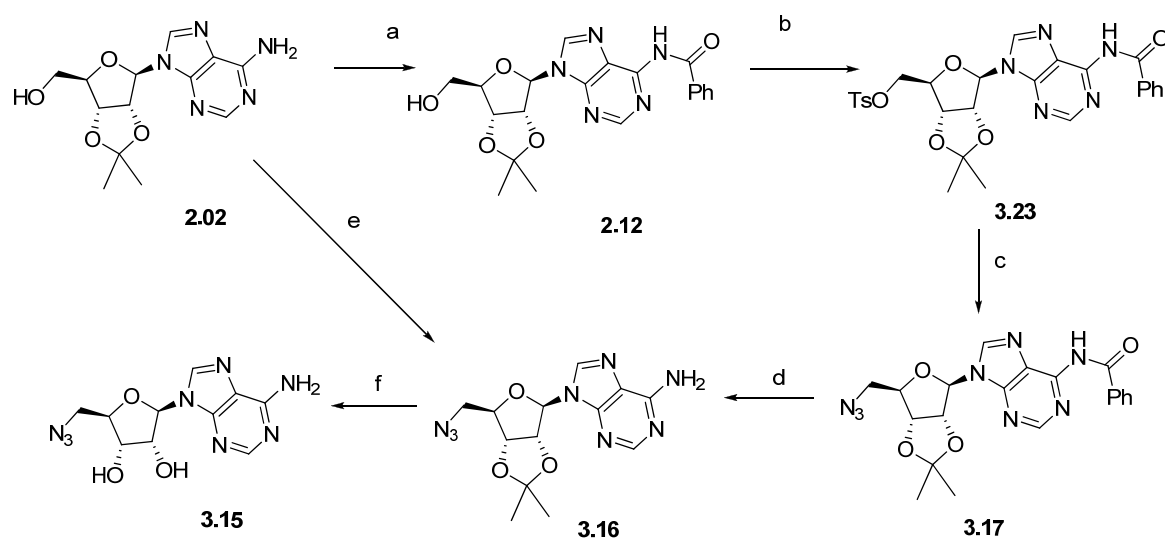

Scheme 3.5: a) i) TMSCl, acetone; ii) BzCl, acetone; iii) NH$_{3(aq)}$; b) TsCl, Py, 5 ^{o}C; c) NaN$_3$, DMF; d) LiOH, 1:1:1 MeOH/THF/H$_2$O; e) DPPA, DEAD, DCM; f) 1:5 TFA, DCM.

The *N*-benzoyl-2',3'-isopropylidiene adenosine **2.12** was prepared as described in Section 2.3.1. Tosylation of adenosine **2.12** on treatment with tosyl chloride in pyridine, gave **3.23** in 75% yield. Subsequent addition of sodium azide to tosylate **3.23** gave azide **3.17** in 79%

yield after flash chromatography. De-protection of the benzoyl group of **3.17**, on treatment with lithium hydroxide in 1:1:1 MeOH/H$_2$O/THF gave **3.16** in 64% yield. This was followed by hydrolysis of the isopropylidene, with TFA in DCM, to give the key azide **3.15** in 78% yield. Alternatively, the key precursor **3.16** was prepared in an improved 78% overall yield by Mitsunobu reaction of adenosine **2.02** with diphenylphosphorylazide (DPPA), diethyl azo dicarboxylate (DEAD) in DCM.

3.2.2 Synthesis of 1,4-triazoles 3.08, 3.25 and 3.26 using CuAAC reaction

A wide variety of conditions have been reported for selective formation of a 1,4-triazole over the 1,5-triazole, by CuAAC. This reaction can be performed in a variety of solvents, at different temperatures and using various additives.[28] However, the key to the CuAAC reaction is the generation of the catalytically active Cu(I) species with sources of Cu(0), Cu(I) and Cu(II) reported. A comprehensive review of CuAAC by Meldal[28] noted that an obvious trend between the method and source of Cu(I) catalyst used and the yield obtained, is not apparent. Rather and as noted by Meldal, studies tend to involve a case-by-case optimization processes. In light of this a series of conditions were examined for CuAAC between alkyne **3.12** and **3.13** and azide **3.15 – 3.17**, as shown in Scheme 3.6, and with conditions using Cu(I) and Cu(II) shown in Table 3.1 and conditions using Cu(O) Shown in Table 3.2.
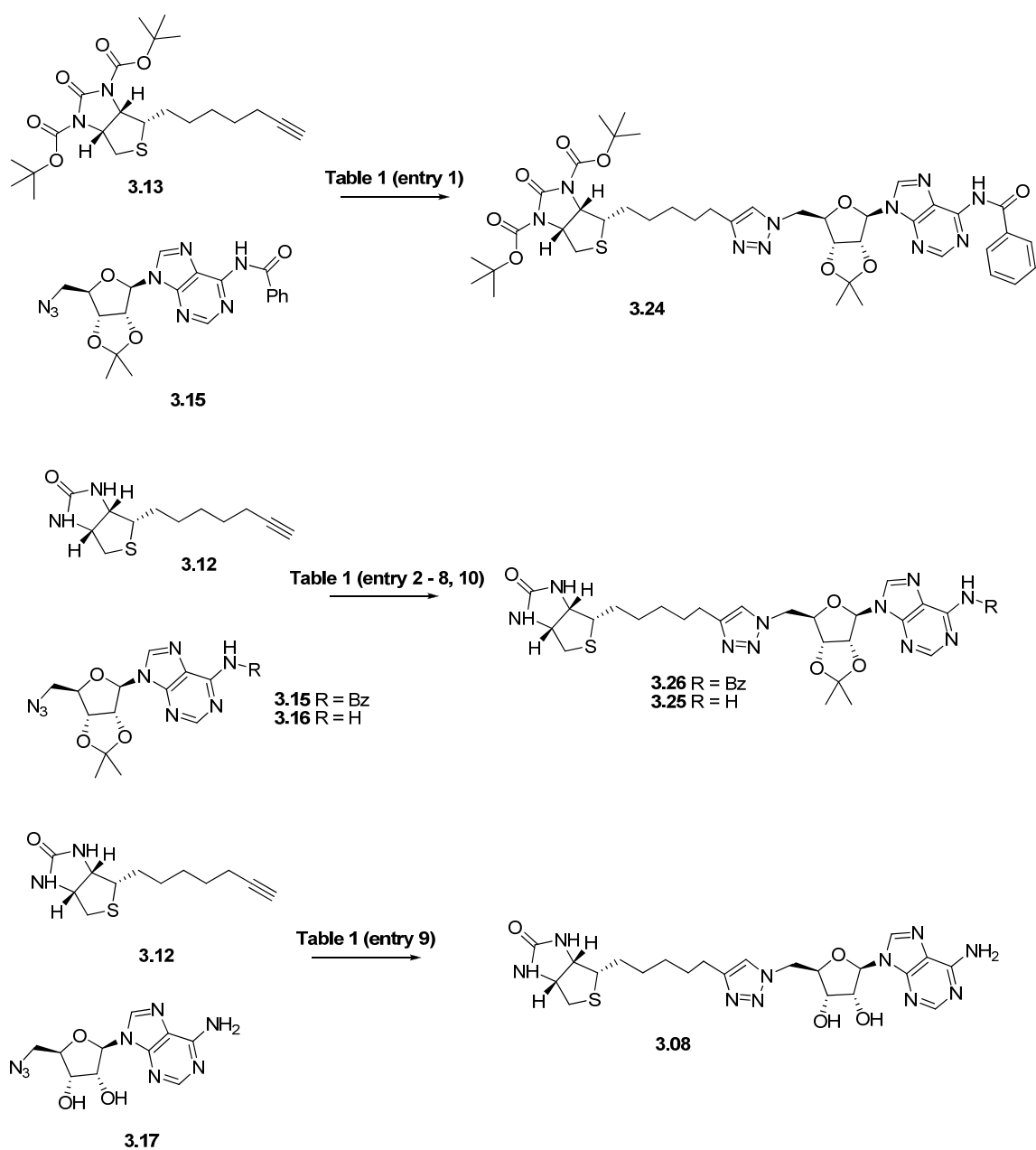
Scheme 3.6: The synthesis of triazole **3.24-3.26** and **3.08** were investigated with various conditions as described in Table 3.1.

Table 3.1[a]: Synthesis of triazole **3.08 – 3.27** using Cu(II) and Cu(I) salt**.**

Entry	Alkyne	Azide	$CuSO_4.H_2O$ (mol%)	Sodium ascorbate (mol%)	Solvent	Product	Isolated yield (%)[b]
1	**3.13**	**3.17**	5	15	1:1 t-BuOH: H_2O	**3.24**	0[c]
2	**3.12**	**3.17**	5	15	1:1 t-BuOH: H_2O	**3.26**	0[d]
3	**3.12**	**3.17**	10	20	1:1 t-BuOH: H_2O	**3.26**	4
4	**3.12**	**3.17**	10	20	1:1 AcCN: H_2O	**3.26**	11
5	**3.12**	**3.17**	10	20	1:1 DCM: H_2O	**3.26**	9
6	**3.12**	**3.16**	10	20	1:1 AcCN: H_2O	**3.25**	10
7	**3.12**	**3.16**	10	20	1:1 DCM: H_2O	**3.25**	14
8	**3.12**	**3.15**	10	20	1:1 DMSO: H_2O	**3.08**	0[e]
9	**3.12**	**3.16**	CuI 5 mol%[f]	-	AcCN[f]	**3.25**	0[d]

[a] All reactions were carried out at room temperature over 3 h. [b]Isolated yield after flash chromatography, [c] complex mixture was obtained and thus not purified. [d]trace amount of target product detected by TLC. [e] insoluble product, hence not isolated. [f] Attempted CuAAC with Cu(I) salt in dry acetonitrile.

Conditions for CuAAC established by Rostovstev[29], using $CuSO_4$ as the Cu(II) source and sodium ascorbic as the reducing agent in a 1:1 *tert*-butanol/water mixture, were initially investigated. The desired triazole product **3.24** was not observed or isolated on reaction of the biotin alkyne **3.13** and azide **3.17** under these conditions (entry 1). Rather a mixture, with TLC and ^{1}H NMR of the crude product suggesting that the acid labile Boc protecting group of **3.13** or product derived from it is not retained during the CuAAC reaction and its workup.

Our attentions thus turned to CuAAC reaction between the biotin alkyne **3.12** and adenosine **3.15 – 3.17** (entry 2 – 9) in order to avoid the labile Boc group. CuAAC reaction of azide **3.12** and alkyne **3.17**, in the presence of 5 mol% Cu_2SO_4 and 10 mol% sodium ascorbic, resulted in only traces of triazole **3.26** as detected by TLC. In this case the reaction returned starting material rather than giving a complex mixture due to the labile Boc group as in entry 1. A change in colour from cloudy yellow to white to blue over the 45 min reaction was observed under the conditions described in entry 2. This rapid change in colour suggests the limited capacity of 10 mol% of ascorbic acid to generate the short-lived Cu(I) active species. An increase in catalysis load to 10 mol% Cu_2SO_4 coupled with an increase of reductant (sodium ascorbate 25 mol%) resulted in a little increase to 4% yield of **3.26** after purification by flash chromatography (entry 3).

The 0 to 4 % yield obtained for triazole **3.26** under the conditions of entries **1 - 3** is possibly also the result of low solubility of alkyne **3.12**. Indeed, Lee and co workers report that the use of more polar solvents, such as DCM and DMSO in CuAAC reactions, to solubilise both the alkyne and azide, results in improved yields of the triazole.[30] Thus, an investigation into the preparation of triazole **3.26** under similar conditions, using 10 mol% Cu_2SO_4 and 25 mol% sodium ascorbate and both acetonitrile and DCM separately, was investigated to give triazole **3.26** in 11% (entry 4) and 9% (entry 5), respectively. Interestingly, reaction of azide **3.16**, which lacks the benzoyl protecting group of **3.17**, in AcCN (10 %, entry 6) and DCM (14 %, entry 7) gave **3.25** in comparable yields compared to the synthesis of triazole **3.26** (entry 4 and 5). The CuAAC reaction of the unprotected azide **3.15** and alkyne **3.12** gave **3.08** based on TLC. However, we were unable to isolated the highly insoluble triazole **3.08** from the copper salt using flash chromatography (entry 8).

A brief investigation into the Cu(I) catalyst for the CuAAC reaction between azide **3.16** and alkyne **3.12** was made. However using 5 mol% CuI with DIPEA in dry AcCN gave only trace amounts of **3.25** as shown in entry 9. The use of Cu(I) salts was not investigated further.

Given the limited success in obtaining good yields of **3.25** using both Cu(I) and Cu(II) salts our attention turned to Cu(O) as the catalytic source for CuAAC. The catalysis of CuAAC reactions using Cu(O) in the form of wire, turnings, powder or nanopowder (with or

without the addition of a Cu(II) source) has been reported with varying success.[28] The main advantage of using elemental copper in CuAAC reaction is that it facilitates product isolated, with standard filtration being possible to remove solid and insoluble copper at the completion of the reaction. Thus, the preparation of **3.25** from **3.12** and **3.16** was investigated using copper wire, copper turning and copper nano-powder, as summarised in Scheme 3.7 and Table 3.2
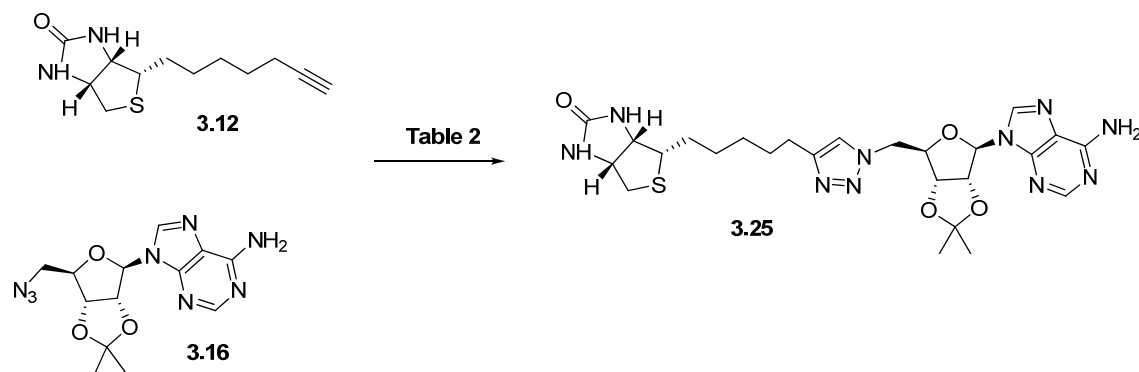
Scheme 3.7: see Table 3.2

Table 3.2[a]: Synthesis of triazole **3.25** using Cu(O).

Entry	Catalyst	Solvent	Temp[h]	Yield[g]
1	Cu wire[b]	2:1 DCM:H_2O	rt	23%
2	Cu wire[b]	2:1 AcCN:H_2O	rt	27%
3	Cu turning[c]	2:1 AcCN:H_2O	rt	35%
4	Cu nano powder[d]	2:1 AcCN:H_2O	rt	47%
5	Cu nano powder[d]	2:1 DCM:H_2O	rt	23%
6	Cu nano powder[d]	2:1 AcCN:H_2O	35 °C	67%
7	Cu nano powder[e]	2:1 AcCN:H_2O	35 °C	67%
8	Cu nano powder[d, f]	2:1 AcCN:H_2O	35 son[f]	73%

[a] All reaction times were 6 h. [b] catalyst loading was 2 cm copper wire per 0.01 mmol of alkyne 3.12 [c] 2 pieces of 0.5 cm copper turnings per 0.01 mmol of alkyne. [d] 20 mol% of Cu nano powder. [e] 15 mol% of triethylamine hydrochloride salt was added. [f] sonication for 15 min, [g] isolated yields after flash chromatography (9:1 DCM/MeOH). [h] rt = ambient temperature (approximately 22 °C).

Treatment of a mixture of alkyne **3.12** and azide **3.16** with copper wire gave triazole **3.25** using 2:1 DCM/H_2O (23%, entry 1) and 2:1 acetonitrile/H_2O (27%, entry 2). Thus, the use

of copper wire was found to give improved yields between 23 – 27% when compared to the copper salt catalysts discussed above in Table 3.1 with yields of 10 – 14% using the same building blocks of azide **3.15** and alkyne **3.12**.

Treatment with 20% w/w copper turnings, with its greater surface area, gave further improved yields of triazole **3.25** in 2:1 AcCN/water (35%, entry 3). Finally, treating alkyne **3.12** and azide **3.16** with 20 mol% of Cu nanopowder gave further improved yields of **3.25** when using 2:1 AcCN/water (47%, entry 4) and 2:1 DCM/water (23%, entry 5) at ambient temperature.

Following the markedly improved yields obtained in entry 4, we investigated factors such as temperature, sonication or additives (such as triethylamine hydrochloride) used in conjunction with Cu nano powder catalyst and 2:1 acetonitrile/water solvent system. Here, alkyne **3.12** and azide **3.16** were treated with 20 mol% Cu nanopowder in 2:1 acetonitrile/water mixture and stirred at 35 ^{o}C over 6 h to give triazole **3.25** in a 65 % yield (entry 6). Alternatively, sonication[31] of the reaction mixture of **3.12** and **3.16** and with 20 mol% Cu nanopowder in 2:1 acetonitrile/water mixture for 15 mins, followed by stirring at 35 ^{o}C for 3 h gave triazole **3.25** in 73% yield (entry 8). It is suggested that sonication of the reaction mixture as in entry 8 results in the Cu nano-powder forming a fine suspension. This increases the surface area compared to the same reaction mixture without ultrasound, where it was observed the Cu nano-powder coagulated at the bottom of the reaction vessel (entry 4 and 6). Interestingly, treatment of alkyne **3.12** and azide **3.15** with 20 mol% Cu nano powder and triethylamine hydrochloride salt, which is reported[32] to increase the oxidative dissolution of Cu(I) from Cu nano-powder, gave similar yield (67%, entry 7) compared to the same conditions without triethylamine hydrochloride salt (67%, entry 6). The conditions described in entry 8 were applied to the preparation of 1,4-triazole inhibitors as described in chapter 4 and 6 and are discussed therein.

Although the synthesis of target triazole **3.08** was attempted as shown in Table 3.1, entry 8, it was achieved in limited yields. On the other hand triazole **3.25** and **3.26** were obtain in high yields (see Table 3.1 and 3.2). Thus in order to obtain triazole **3.08**, the deprotection of both **3.25** and **3.26** was investigated as shown in scheme 8.
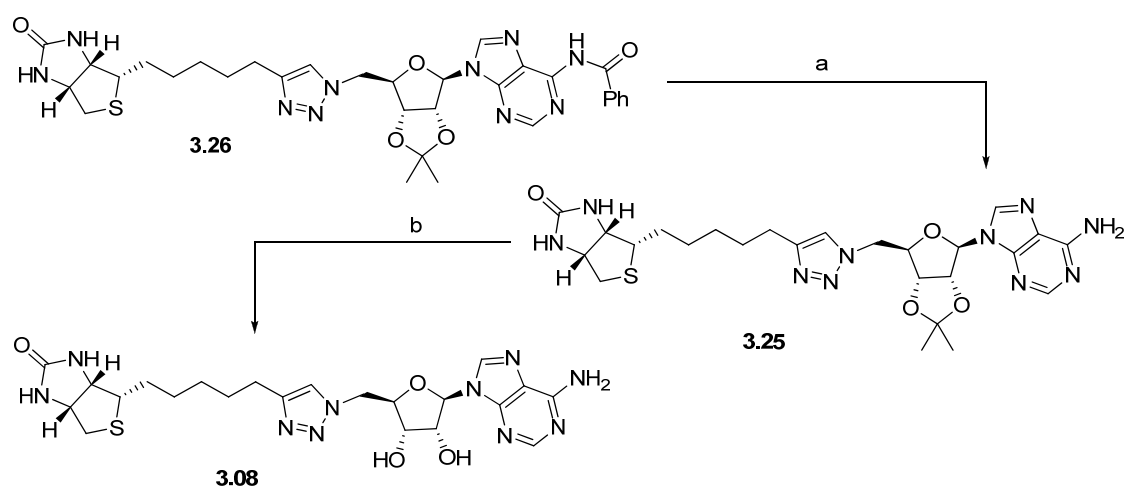
Scheme 3.8: a) LiOH 2:2:1 THF/H$_2$O/MeOH; b) 10% TFA in DCM

The benzoyl protecting group of triazole **3.26** was removed on treatment with lithium hydroxide in 1:1:1 THF:H$_2$O:MeOH mixture to give triazole **3.25** in 47% yield. The triazole **3.25** was also prepared by reacting **3.26** with 16% ammonia solution in 1:1 solvent mixture of methanol and water in a comparable 43% yield. The removal of the isopropylidene group of triazole **3.25** was treated with 20% TFA in DCM to give the target triazole **3.08** in 45% yield.

3.2.3 Synthesis of 1,5-triazole 3.32 by RuAAC reaction

The selective synthesis of a 1,5-triazole by reaction of alkyne with azide using a ruthenium catalyst such as **1.20** was first reported by Zhang and co-workers.[33] To obtain 1,5-triazole analogue **3.09** through the RuAAC of alkyne **3.12** and azide **3.16** (see Scheme 3.10), we required ruthenium **1.20** which was prepared as shown in Scheme 3.9.
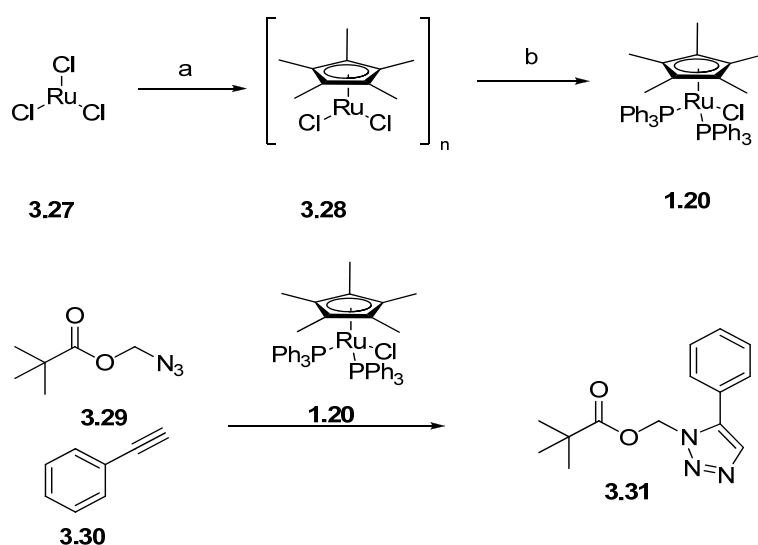
Scheme 3.9: a) Cp*, EtOH, reflux; b) PPh$_3$, EtOH; b) **1.20**, THF, Δ

RuCl$_3$ **3.27** was treated with cyclopentadiene in ethanol under reflux to give **3.28** in 58% yield. The ruthenium complex **3.28** was reacted with triphenylphosphine to give the required Cp*RuCl(PPh$_3$)$_2$ catalyst **1.20** in 51%. The catalytic activity of Cp*RuCl(PPh$_3$)$_2$ **1.20** was determined by reaction of azido-methyl pivalate and phenylacetylene and using 5 mol% of **1.20** under literature conditions to give **3.31** in a yield of 87%. This compares favourably to literature for structurally similar 1,5-triazoles.[23] With the suitable catalyst in hand, the reaction of alkyne **3.12** with azide **3.16** was investigated under a number of conditions, as shown in Scheme 3.10 and Table 3.3. The optimum conditions for 1,5-triazole **3.32** (a precursor of **3.09**) involved reacting alkyne **3.12** and azide **3.16** with 20 mol% of Cp*RuCl(PPh$_3$)$_2$ in 1:1 mixture of THF and DMF at 70 °C over 4 h, as shown in entry 7.
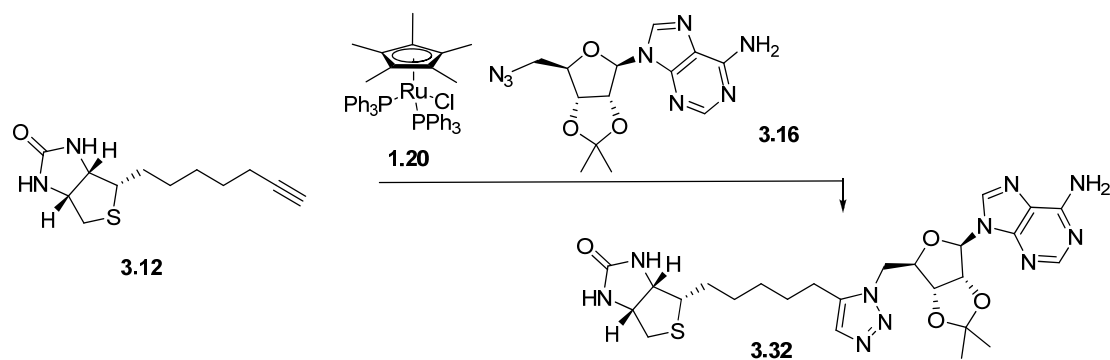
Scheme 3.10: see Table 3.3 for conditions.

Table 3.3: RuAAC synthesis of **3.32** from alkyne **3.12** and azide **3.16** using catalysis Me$_6$Cp*RuCl(PPh$_3$)$_2$.

Entry	Cp*RuCl(PPh$_3$)$_2$ mol%	Solvent	Temp	Time	Yield[a]
1	2	THF	Reflux	4 h	10%
2	5	THF	Reflux	4 h	23%
3	10	THF	Reflux	4 h	23%
4	20	THF	Reflux	4 h	25%
5	20	THF	Reflux	12 h	29%[b]
6	20	DMF	80	8 h	35%
7	20	1:1 THF:DMF	70	4 h	52%
8	10	1:1 THF:DMF	70	4 h	41%

[a] isolated yield after flash chromatography; [b] THF was found to have evaporated.

Initial attempts at this reaction involved the use of literature conditions reported by Boren and co-workers.[23] Alkyne **3.12** and azide **3.16** were treated with 2 mol% Ru catalyst **3.30** in anhydrous THF at reflux to give triazole **3.32** in 10% yield (entry 1). Moderate increases in yield of **3.32** were obtained by increasing catalyst **1.20** loading to 5 mol% (23% entry 2), 10 mol% (23%, entry 3) and 20 mol% (25% entry 4). Moreover, increased reaction time from 4h to 12h (29%, entry 5) only resulted in moderate increase of yield of **3.32**. Finally, using alternative solvent systems, such as DMF (35%, entry 6) and 1:1 THF/DMF (52%, entry 7), gave slight improvements in the yields. A combination of using 1:1 THF/DMF solvent system and a decreased catalyst loading (from 20 mol% to 10 mol%) gave a decreased yield of **3.32** (41%, entry 8).

No further optimisation was undertaken as triazole **3.32** was found to be inactive against SaBPL (see Section 3.2.2). The synthesis of triazole **3.09** was attempted in 20% TFA in DCM, as show in Scheme 3.11. Similar to triazole **3.08** (shown in Scheme 3.8), this compound was found to be insoluble and thus was not isolated.
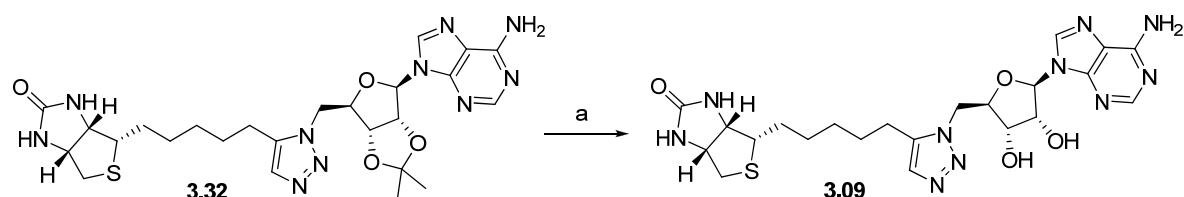

Scheme 3.11: a) 10% TFA, DCM.

3.2.4 Assignment of 1,4-triazole and 1,5-triazole isomers by ^{1}H NMR

The CuAAC and RuAAC reactions of alkyne **3.12** and azide **3.16** investigated in Section 3.2.2 and 3.2.3 provided two different regioisomer as shown in Figure 3.8. It is generally accepted that the CuAAC forms 1,4-triazole over the 1,5-triazole with limited reported instances of CuAAC generating 1,5-triazole.[28] Conversely, the proposed regioselectivity through RuAAC, is capable of producing both 1,4 and 1,5 - triazole.[23] Thus, it was imperative to determine and confirm the regioisomer of the purported 1,4 - triazole **3.25**, **2.08** and 1,5-triazole **3.32**. To this end, both 1D and 2D NMR spectra for 1,4-triazole **3.08** and **3.25** and 1,5-triazole **3.32** were obtained to confirm the regioisomer.

An ^{1}H NMR spectrum of the triazole **3.25** obtained by reaction of azide **3.16** with alkyne **3.12** in the presence of copper nano powder, indicated a single regioisomer was produced based on a single resonance in the aromatic region at 7.06 ppm (CDCl$_3$). 2D HMQC ^{1}H NMR confirmed this resonance to be due to the 5th position proton upon the triazole ring (H$_a$). Moreover 2D ROESY ^{1}H NMR indicated through space interactions with both methyl groups adjacent to the triazole ring (H$_B$ and H$_C$), as shown in Figure 3.7. These interactions were also observed for 1,4-triazole **3.08** and in particular the resonance at 7.67 ppm (DMSO-d6) attributed to the H$_a$. The same through space interactions were not observed for the 1,5 - triazole **3.32**, rather only a through space interaction between the methylene proton (H$_B$) and triazole proton (H$_A$) was observed (Figure 3.7). Finally, the 1,4-substitution pattern of 3.25 was confirmed in the X-ray crystal structure of **3.25** bound to SaBPL (see Section 3.4)
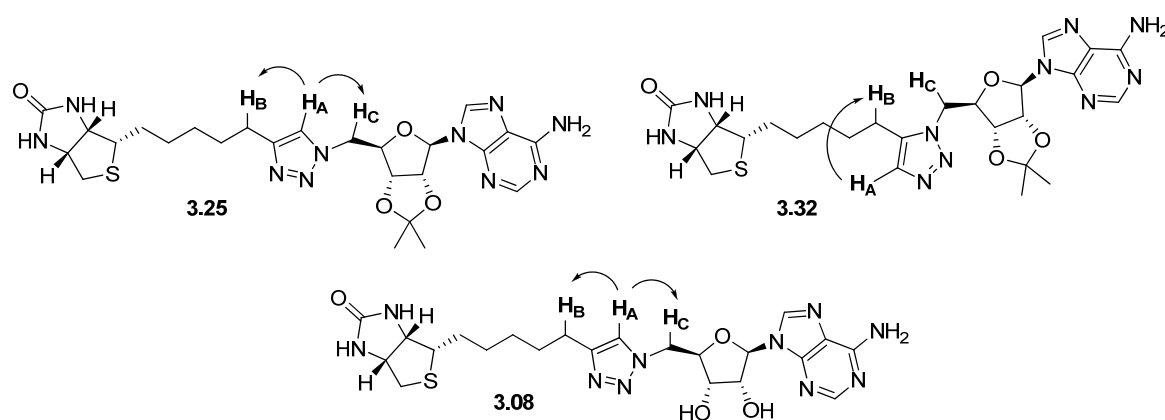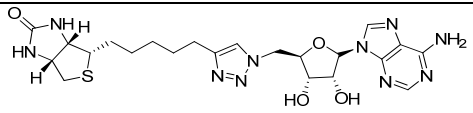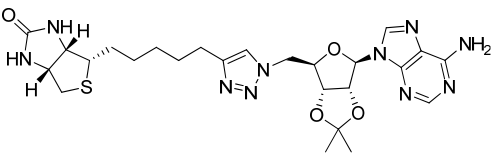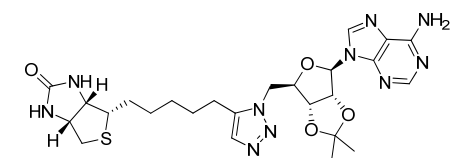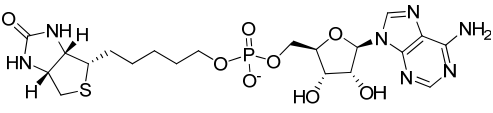

Figure 3.7: Depiction of the through-space interaction observed in ^{1}H NMR ROESY experiment for 1,4-triazole **3.08** and **3.25** and 1,5-triazole **3.33**. The arrows depict the correlation between the triazole proton and methylene groups in close proximity.

3.3 BPL inhibition and antimicrobial activity of triazole analogues

Triazoles **3.08**, **3.25** and **3.32** and the reference inhibitor biotinol-5'-AMP **1.05** were assayed against SaBPL, EcBPL and HCS and the results are shown in Table 4. The assay was performed by collaborators at Molecular Life Science, University of Adelaide, following method described by Chapman-Smith and co-workers.[34] The IC_{50} value for each compound was determined from a concentration-response curve by varying the concentration of the inhibitor under the same substrate and enzyme concentration.

Table 3.4[a]: Enzyme inhibitions of triazole analogues

Compound	SaBPL		EcBPL	HCS
	Ki (µM)	IC_{50} (µM)	IC_{50} (µM)	IC_{50} (µM)
3.08	1.7 ± 0.3	-	33 µM $(K_i)^b$	33 µM $(K_i)^b$
3.25	1.8 ± 0.33	11 ± 2.2	> 200	> 200
3.32	-	> 200	> 200	> 200
1.05	0.09 ± 0.01	0.12 ± 0.01	2.5 ± 0.2	1.25 ± 0.1

[a] see Chapter 7 for conditions; [b] values in K_i.

1,4-Triazole **3.08**, the direct triazole analogue of biotinol-5'-AMP **1.05**, was found to be 100 fold less active toward SaBPL (K_i = 1.8 ± 0.3 μM), compared to biotinol-5'-AMP **1.05**. Due to the limited solubility of 1,4-triazole **3.08** and the limited quantities of triazole **3.08** synthesized, we did not investigate 1,4-triazole **3.08** in further enzyme inhibition assays.

1,4-triazole **3.25**, the isopropylidene precursor of **3.08**, was remarkably found to possess the same level of inhibition as **3.08** against SaBPL (K_i = 1.83 ± 0.33 μM). Significantly and serendipitously, 1,4-triazole **3.25** was highly selective towards SaBPL, showing no inhibition against EcBPL and HsBPL at less than 200uM. This observation is the key obstacle in developing inhibitors of ligases such as BPL (see Section 1.3.2 for discussion on the problem of selectivity of ligases inhibitors). Moreover, antimicrobial minimal inhibitory concentrations (MICs) on triazole **3.25** against *S. aureus* through the microdilution broth method with cation-adjusted Mueller-Hinton broth indicated this compound possess antibacterial properties, albeit it was weakly bacteriostatic (no MIC value could be obtained). Thus, for triazole **3.25** we have addressed a number of desirable attributes required for developing a clinical drug candidate (selective inhibition, facile synthetic protocol and antibacterial activity).

1,5-triazole **3.32**, a regioisomeric analogue of **3.25**, was found to display no inhibition against SaBPL, HsBPL or EcBPL. Based on the X-ray crystal structure of **3.25** bound to SaBPL there is a structural conformation that **3.32** might not be capable of adopting (i.e. the U-shaped conformation). Analogues of 1,5-triazole **3.32** were further investigated in Chapter 4 and their implications are discussed therein.

3.4 X-ray crystal structure of 1,4-triazole 3.25 bound to SaBPL

The structure of the first reported selective inhibitor of BPL (triazole **3.25**) bound to SaBPL was solved by our collaborators at Monash University, Australia using the method proscribed by Pendini and co-workers (see Chapter 7 for conditions), to give a final resolution of 2.50 Å. Consistent with the proposed design (see Section 3.2), triazole **3.25** was found to bind in the requisite U-shaped conformation. This allowed for both biotin and adenine analogues to adopt hydrogen bonding interactions with residues Gln116, Thr94,

Ser93 and Arg120 for biotin and Asn212 and Ser127 for adenine ring (see Figure 3.8 and red dashes). These hydrogen bonding interactions are identical in the mode of binding as with reported structures of biotinyl-5'-AMP **1.03** and biotinol-5'-AMP **1.05** bound to SaBPL.
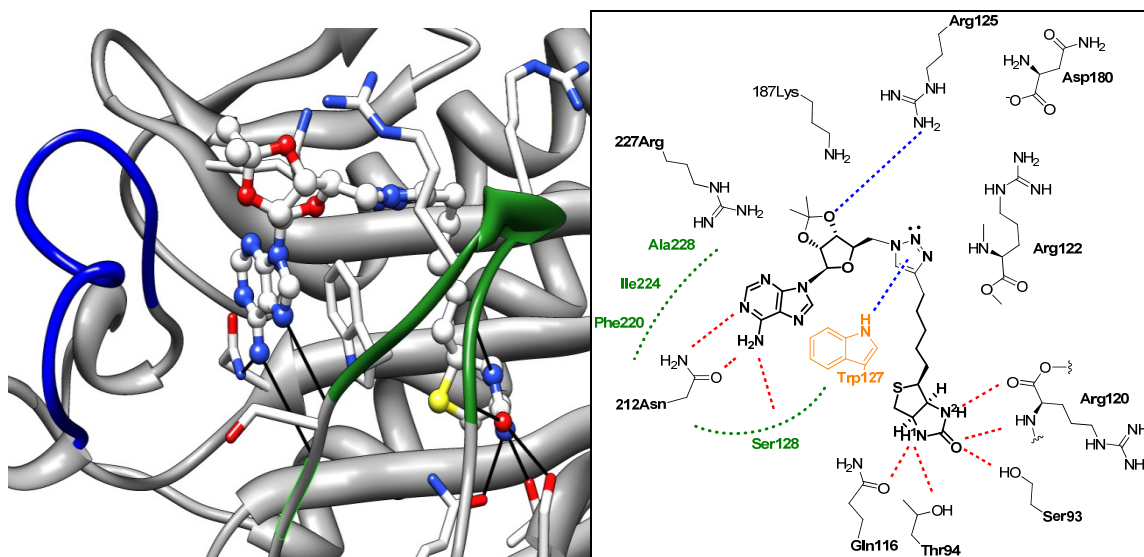
Figure 3.8: 3D depiction of triazole **3.25** bound to SaBPL. The green ribbon denotes the BBL and blue ribbon denotes the ABL (left). 2D depiction of triazole **3.25** bound to SaBPL with conserved hydrogen bonding interactions shown in red dashes and novel pi-pi interaction and hydrogen bonding interaction shown in blue. (right)

As designed, the triazole ring of **3.25** participates in an edge-tilted-T shape[35] interaction with Trp127. The 5.6 Å distance between the centroids of the triazole ring and phenyl ring of Trp127 and a displacement of 7° from the centroid of the phenyl ring of Trp127 to the normal of the triazole plane are in accordance with both observed ligand-protein and experimental results for protein ligand edge-to-face aryl-aryl interactions.[36]

Interestingly, there was no evident hydrogen bonding between the triazole ring and SaBPL. Arg122, Arg125 and Lys187, which form hydrogen bonding interactions with the phosphodiester of **1.05** (see Section 2.5), were found to have limited interactions with **3.25**. This suggests that the hydrogen bonding interactions with Arg122, Arg125 and Lys187 are not seminal for ligand binding, moreover, it also highlights the limited effects of these residues in conformationally ordering the biotin binding loop (both Arg122 and Arg125 are

contained within this loop). Nevertheless, the hydrogen bonding interactions from Arg122, Arg125 and Lys187 is suggested to be critical in binding affinity and is may be the key factor in the 100 fold difference in potency between **3.25** and **1.05**.

3.5 Conclusion

Triazole **3.08** and **3.09** were designed as bioisosteric analogues of biotinol-5'-AMP **1.05**. Key to the design were analogues which could mimic the U-shaped conformation of biotinol-5'-AMP **1.05** when bound to SaBPL, mimic the hydrogen bonding interactions and finally provide a facile synthetic protocol that could be scaled up and used for derivitization.

In this chapter, triazole **3.08** and its precursor **3.25** were prepared by CuAAC reaction with the optimal catalysis identified as Cu nano powder catalyst. Through this catalyst was obtained triazole **3.25** over 8 steps and with an overall yield of 27%, whilst triazole **3.08** was obtain yield in 13% over 9 steps. The regioisomer 1,5-triazole **3.32**, a precursor of **3.09**, was obtained through the optimised RuAAC reaction using Cp*Ru(PPh$_3$)$_2$Cl. Here, triazole **3.32** was obtain in 18% overall yield over 8 steps from biotin. The synthesis of triazole **3.09** was attempted from **3.33**, but resulted in an insoluble mixture and was not investigated further.

1,4-Triazole **3.08**, **3.25** and 1,5-triazole **3.32** were assayed for inhibitory potency against a library of BPLs (SaBPL, EcBPL and HsBPL). 1,4-Triazole **3.25** proved to be a moderate SaBPL inhibitor with an IC$_{50}$ of 1.8 ± 0.3 μM and importantly was selective towards SaBPL (*cf.* EcBPL (IC$_{50}$ >200 μM) and HCS (IC$_{50}$ >200 μM)). Additionally, 1,4-triazole **3.25** was found to possess antibacterial properties. These results are encouraging and validate 1,4-triazole **3.25** as a member of the first class of selective inhibitors against BPL. Further work was undertaken to investigate the positioning and orientation of the triazole ring (Chapter 4), the effect of positioning the pentose ring (Chapter 4) and of analogues of the adenine ring (Chapter 6).

The X-ray crystal structure of **3.25** bound to SaBPL validated the U-shaped conformation that was required for molecular recognition, within the active site of BPL. Through this conformation, both the biotin and adenine rings of **3.25** were found to provide extensive hydrogen bonding interactions with their respective pockets. Interestingly, the limited

hydrogen bonding interactions between the pentose and triazole ring of **3.25** suggests that these interactions are not involved in molecular recognition but may nevertheless explain the lower binding affinity of **3.25**. On this point, we investigated analogues of **3.25** which modified a pentose and triazole ring (see Chapter 4).

3.6 References for Chapter Three

(1)   Reese, C. B. *Organic & Biomolecular Chemistry* **2005**, *3*, 3851.

(2)   Hurdle, J. G.; O'Neill, A. J.; Chopra, I. *Antimicrobial Agents and Chemotherapy* **2005**, *49*, 4821.

(3)   Brown, M. J. B.; Mensah, L. M.; Doyle, M. L.; Broom, N. J. P.; Osbourne, N.; Forrest, A. K.; Richardson, C. M.; O'Hanlon, P. J.; Pope, A. J. *Biochemistry* **2000**, *39*, 6003.

(4)   Brown, P.; Richardson, C. M.; Mensah, L. M.; O'Hanlon, P. J.; Osborne, N. F.; Pope, A. J.; Walker, G. *Bioorganic & Medicinal Chemistry* **1999**, *7*, 2473.

(5)   Ferreras, J. A.; Ryu, J.-S.; Di Lello, F.; Tan, D. S.; Quadri, L. E. N. *Nat Chem Biol* **2005**, *1*, 29.

(6)   Somu, R. V.; Boshoff, H.; Qiao, C.; Bennett, E. M.; Barry, C. E.; Aldrich, C. C. *Journal of Medicinal Chemistry* **2005**, *49*, 31.

(7)   Tuck, K. L.; Saldanha, S. A.; Birch, L. M.; Smith, A. G.; Abell, C. *Organic & Biomolecular Chemistry* **2006**, *4*, 3598.

(8)   Ciulli, A.; Scott, D. E.; Ando, M.; Reyes, F.; Saldanha, S. A.; Tuck, K. L.; Chirgadze, D. Y.; Blundell, T. L.; Abell, C. *ChemBioChem* **2008**, *9*, 2606.

(9)   Fan, C.; Park, I.-S.; Walsh, C. T.; Knox, J. R. *Biochemistry* **1997**, *36*, 2531.

(10)   Patrone, J. D.; Yao, J.; Scott, N. E.; Dotson, G. D. *Journal of the American Chemical Society* **2009**, *131*, 16340.

(11)   Meyer, E. A.; Castellano, R. K.; Diederich, F. *Angewandte Chemie International Edition* **2003**, *42*, 1210.

(12)   Brik, A.; Alexandratos, J.; Lin, Y.-C.; Elder, J. H.; Olson, A. J.; Wlodawer, A.; Goodsell, D. S.; Wong, C.-H. *ChemBioChem* **2005**, *6*, 1167.

(13)   Horne, W. S.; Yadav, M. K.; Stout, C. D.; Ghadiri, M. R. *Journal of the American Chemical Society* **2004**, *126*, 15366.

(14)   Palmer, M. H.; Findlay, R. H.; Gaskell, A. J. *Journal of the Chemical Society, Perkin Transactions 2* **1974**, 420.

(15)   Pedersen, D. S.; Abell, A. *European Journal of Organic Chemistry* **2011**, *2011*, 2399.

(16)   Tam, A.; Arnold, U.; Soellner, M. B.; Raines, R. T. *Journal of the American Chemical Society* **2007**, *129*, 12670.

(17)   Pagliai, F.; Pirali, T.; Del Grosso, E.; Di Brisco, R.; Tron, G. C.; Sorba, G.; Genazzani, A. A. *Journal of Medicinal Chemistry* **2005**, *49*, 467.

(18)   Radic, Z.; Manetsch, R.; Fournier, D.; Sharpless, K. B.; Taylor, P. *Chemico-Biological Interactions* **2008**, *175*, 161.

(19)   Corona, C.; Bryant, B. K.; Arterburn, J. B. *Organic Letters* **2006**, *8*, 1883.

(20)   Wang, T.; Lee, H. J.; Tosh, D. K.; Kim, H. O.; Pal, S.; Choi, S.; Lee, Y.; Moon, H. R.; Zhao, L. X.; Lee, K. M.; Jeong, L. S. *Bioorganic & Medicinal Chemistry Letters* **2007**, *17*, 4456.

(21)   Comstock, L. R.; Rajski, S. R. *Tetrahedron* **2002**, *58*, 6019.

(22)   Chiesa, K.; Shvoryna, A.; Bernet, B.; Vasella, A. *Helvetica Chimica Acta* **2010**, *93*, 668.

(23)   Boren, B. C.; Narayan, S.; Rasmussen, L. K.; Zhang, L.; Zhao, H.; Lin, Z.; Jia, G.; Fokin, V. V. *Journal of the American Chemical Society* **2008**, *130*, 8923.

(24)   Turunen, B. J.; Georg, G. I. *Journal of the American Chemical Society* **2006**, *128*, 8702.

(25)   Nattrass, G. L.; Díez, E.; McLachlan, M. M.; Dixon, D. J.; Ley, S. V. *Angewandte Chemie International Edition* **2005**, *44*, 580.

(26)   Adamo, M. F. A.; Pergoli, R. *Organic Letters* **2007**, *9*, 4443.

(27)   Shibata, C.; Mori, K. *European Journal of Organic Chemistry* **2004**, *2004*, 1083.

(28)   Meldal, M.; Tornøe, C. W. *Chemical Reviews* **2008**, *108*, 2952.

(29)   Rostovtsev, V. V.; Green, L. G.; Fokin, V. V.; Sharpless, K. B. *Angewandte Chemie International Edition* **2002**, *41*, 2596.

(30)   Lee, B.-Y.; Park, S. R.; Jeon, H. B.; Kim, K. S. *Tetrahedron Letters* **2006**, *47*, 5105.

(31)   Sreedhar, B. R., P. S. *Synth. Commun.* **2007**, *37*, 7.

(32)   Orgueira, H. A.; Fokas, D.; Isome, Y.; Chan, P. C. M.; Baldino, C. M. *Tetrahedron Letters* **2005**, *46*, 2911.

(33)   Zhang, L.; Chen, X.; Xue, P.; Sun, H. H. Y.; Williams, I. D.; Sharpless, K. B.; Fokin, V. V.; Jia, G. *Journal of the American Chemical Society* **2005**, *127*, 15998.

(34)   Chapman-Smith, A.; Cronan, J. E. *Trends in Biochemical Sciences* **1999**, *24*, 359.

(35)   Jennings, W. B.; Farrell, B. M.; Malone, J. F. *Accounts of Chemical Research* **2001**, *34*, 885.

(36)   McGaughey, G. B.; Gagné, M.; Rappé, A. K. *Journal of Biological Chemistry*
        1998, *273*, 15458.

Chapter Four

4.1 Introduction

Chapter 2 introduced biotinol-5'-AMP **1.05** as a reaction intermediate mimic of biotinyl-5'-AMP **1.03**. Biotinol-5'-AMP **1.05** was found to be a potent inhibitor against SaBPL, but was limited by its inhibition of HsBPL (*H. sapiens*) and difficulties in its synthesis, as discussed in Chapter 2. To overcome the synthetic and biological issues of biotinol-5'-AMP **1.05**, Chapter 3 investigated the design, synthesis, and assay of triazole based analogues of biotinol-5'-AMP **1.05**. From the small library of triazole analogues, triazole **3.25** was found to be a low micromolar inhibitor of SaBPL. However, more importantly, this analogue was highly selective against SaBPL over HsBPL and possessed antibacterial properties against *S. aureus*. Additionally, the X-ray crystal structure of 1,4 - triazole **3.25** bound to SaBPL revealed: a) significant hydrogen bonding interactions between the biotin and adenine components and the active site, b) a U-shaped conformation as is required for binding and c) the triazole ring makes an edge-to-face π interaction with Trp127. Based on the selective SaBPL inhibition result, X-ray crystal structure results and the facile synthesis of triazole **3.25** by CuAAC reaction (as reported in Section 3.2.2), we proposed the general structure **4.01** .

This chapter builds on the results of the previous chapters with the rational design of triazole inhibitors, based on an analysis of the X-ray crystal structure of **3.25** bound to SaBPL, in an attempt to access more potent and selective inhibitors of SaBPL. To this end, two series of triazole analogues were designed, synthesized and assayed against SaBPL (shown in Scheme 4.1, triazole **4.01-4.17**). The proposed triazole analogues retain the biotin, adenine and triazole components which are suggested to be necessary for binding. The first series (see **4.01 – 4.08**) investigates the linker length between the key components (biotin, triazole and adenine), whilst the second (see **4.09 – 4.15**) examines the orientation and configuration of the triazole ring.
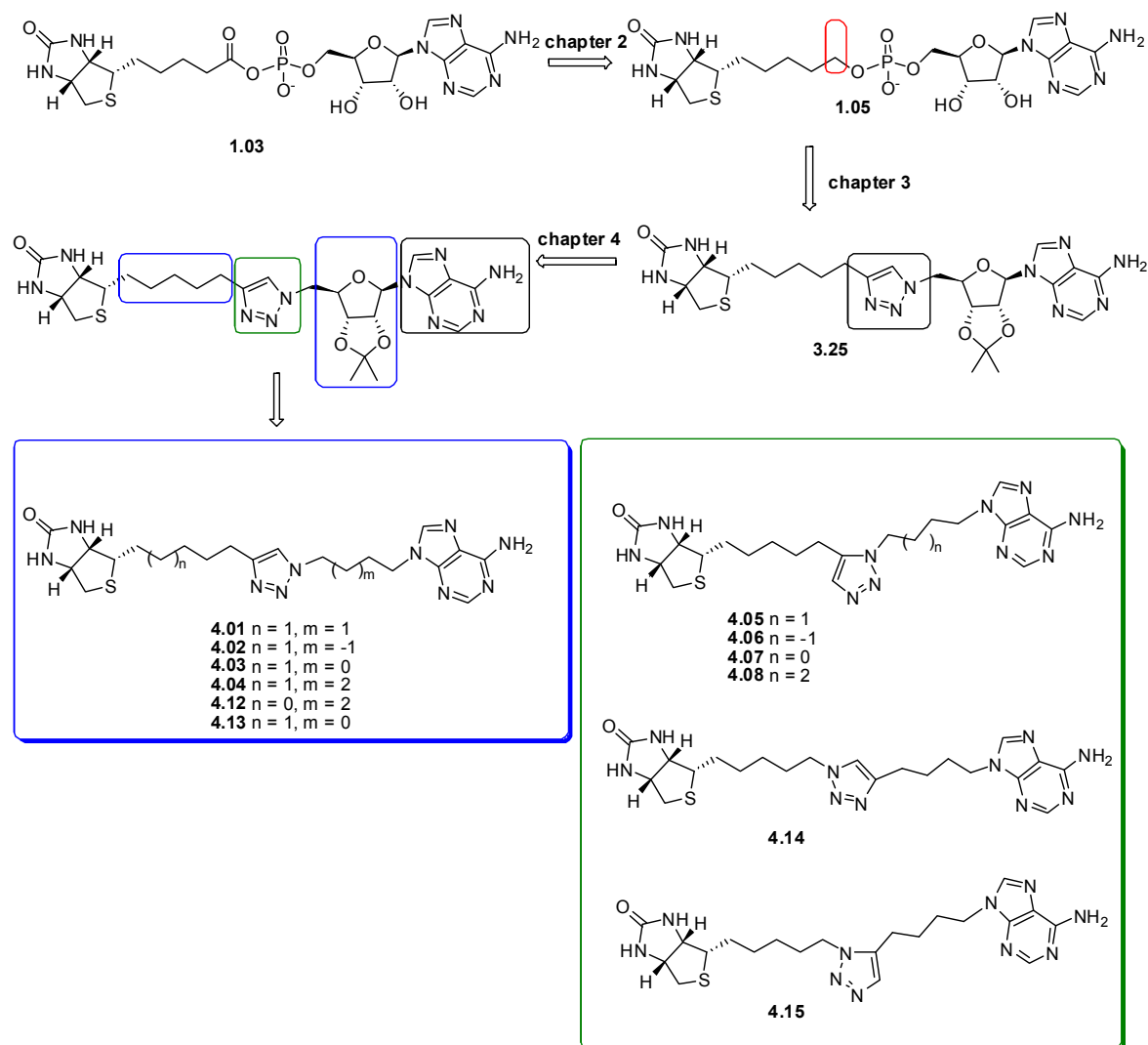
Scheme 4.1: An overview of chapter 2 and 3 (top). Proposed triazole analogues **4.01** – **4.15**. Triazole **4.14** and **4.15** were synthesized by Kelly Keeling (Abell group).

4.2 Design and synthesis of 4.01 and analogues 4.02– 4.13

The design of triazole **4.01** (scheme 4.1) was based on the X-ray crystal structure of triazole **3.25** bound to SaBPL (discussed in Section 3.4) and the mechanism by which substrates bind to BPL (such as biotinol-5'-AMP and biotinyl-5'-AMP) within SaBPL active site (see Section 3.4).

These features are summarised below:

1. The substrate biotinyl-5'-AMP **1.03** and the inhibitor biotinol-5'-AMP **1.05** bind to BPL via an induced fit mechanism.[1-3] This occurs with the sequential binding of biotin to the static residues Ser94, Thr93, followed by the biotin binding loop (residues 113-130) and ATP binding loop (residues 218-230) undergoing a conformational changes to form the active ATP binding site. Upon ATP binding, the ATP binding loop undergoes further conformational changes to bury the substrates within the active site and away from solvent. Based on this mechanism, it is suggested the biotin and adenine components, which make the initial contact with SaBPL, are critical for providing the necessary conformational changes to form the active site of SaBPL.

2. X-ray crystallography has shown that the adenine and biotin rings of triazole **3.25** and biotinol-5'-AMP **1.03** provide the majority of hydrogen bonding and electrostatic interactions with SaBPL. This observation emphasizes the importance of both adenine and biotin components for rationally designed inhibitor.

3. By comparison, the pentose ring of biotinyl-5'-AMP **1.03**, biotinol-5'-AMP **1.05** and triazole **3.25** forms limited interactions with the active site of SaBPL, with biotinol-5'-AMP **1.05** adopting only two hydrogen bonding interactions.

4. The replacement of a pentose ring with an acyclic chain is well documented in nucleic based antiretroviral drugs such as acyclovir, cidofovir, tenofovir and adefovir[4]. Such a modification removes the need for protection of 2', 3' diol with an isopropylidene group as in triazole **3.25 (**see Section 3.2.2).

5. Although the triazole ring of **3.25** provides only minimal interactions with SaBPL as compared to the phosphodiester of biotinol-5'-AMP **1.05** (i.e. the edge to face π interaction with Trp127, see Section 3.4), this ring was considered important. As discussed in Section 3.2.2, a 1,4-triazole can be introduced by facile and reliable CuAAC ligation. Moreover, the 1,4-triazole ring was considered to be the key feature that provided selective inhibition for SaBPL over EcBPL and HsBPL (this feature is discussed further in this chapter and Chapter. 5). Thus the triazole ring was retained in our designed inhibitor **4.01**.

The target triazole **4.01** also provides an opportunity to develop useful structure-activity relationship data with respect to the length of the tether between the triazole, biotin and adenine components. With this in mind, the triazoles **4.02** − **4.15** were identified as extended targets for synthesis and biological evaluation (see Scheme 4.1).

4.2.1 Building blocks for the synthesis of 4.01-4.13

The synthesis of triazoles **4.01 – 4.13** utilises the building blocks alkyne **4.16, 4.17** and **3.12** and azides **4.18 – 4.21** (shown in Figure 4.1A) and involves optimised CuAAC and RuAAC reaction conditions developed in chapter 3 for their coupling (shown in Figure 4.1B).
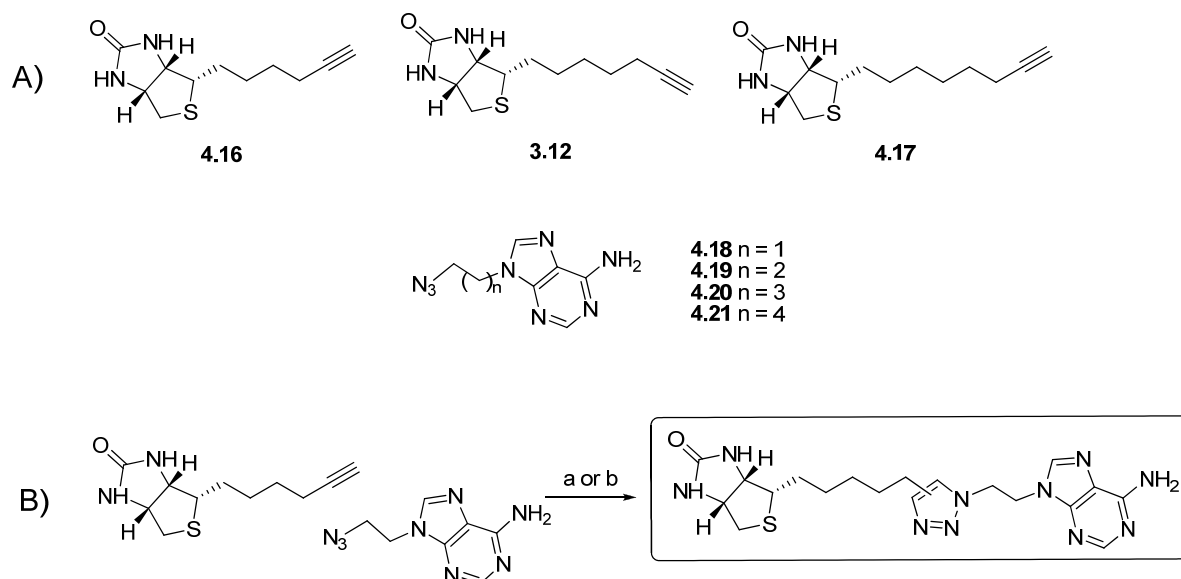
Figure 4.1: A) Precursors for the synthesis of triazole **4.01 – 4.13** (top) : B) a) 20 mol% Cu nano-powder, 2:1 AcCN/H$_2$O; b) Cp*RuCl(PPh$_3$)$_2$, 1:1 THF/DMF, 80 $^{\circ}$C (bottom).

Adenine 4.18 – 4.21 building blocks
The synthesis of azides **4.18 – 4.21** was accomplished from adeneine **4.22**, as shown in Scheme 4.2. Adenine **4.22** was treated with K$_2$CO$_3$ and then the appropriate dihalo-alkane **4.23 – 4.26** in DMF. The resulting halides **4.27 – 4.31** were then converted to azides **4.19 – 4.22** on treatment with NaN$_3$ in DMF, with the yields shown in Scheme 4.2.
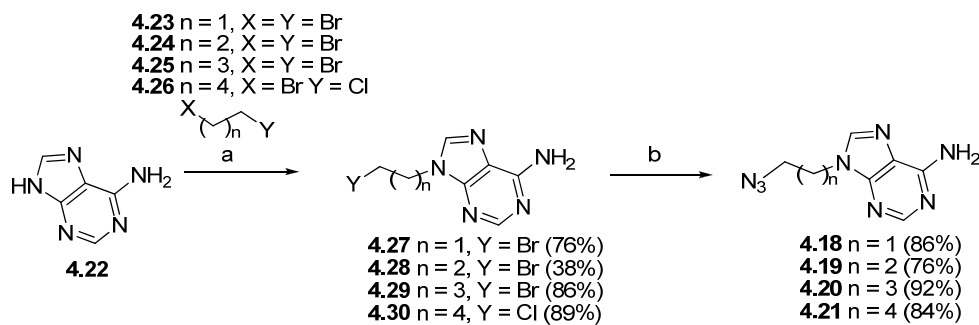
Scheme 4.2: a) alkyl dihalide **4.23 – 4.26**, K$_2$CO$_3$, DMF; b) NaN$_3$, DMF

Norbiotin alkyne 4.16

The first attempted synthesis of norbiotin alkyne **4.16** was inspired by the report a Curtius rearrangement of biotin to norbiotin amine **4.33**. Access to the norbiotin alkyne **4.16** required the conversion of the amine functionality of **4.33** to the alcohol of **4.34**. Here, two literature procedures for the diazotination of aliphatic amine were the subject of the first approach shown in scheme 3.
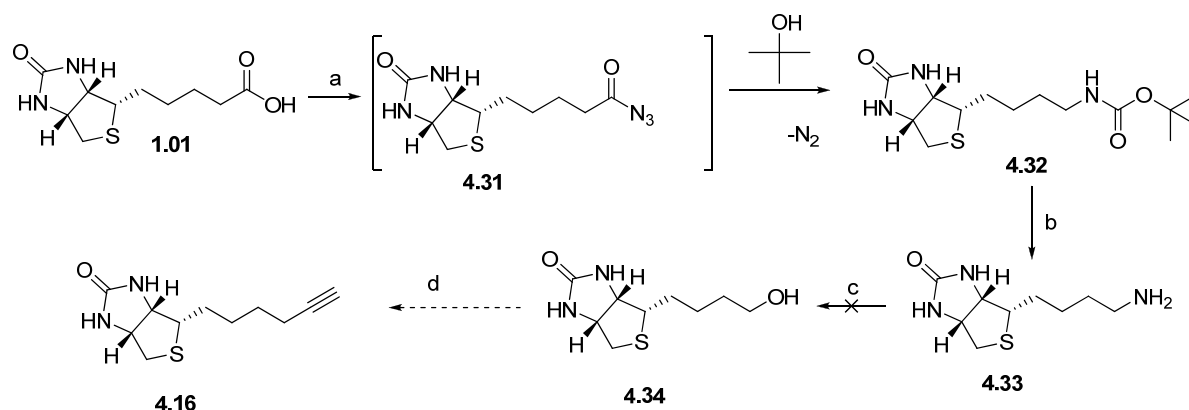
Scheme 4.3: a) DPPA, Et₃N, *t*-BuOH; b) 6N HCl, H₂O; c) NaNO₂, AcOH, 1:1 THF/H₂O or Na₂[Fe(CN)₅NO].2H₂O, NaOH, H₂O; d) i) TsCl, py; ii) LiBr, MEK, iii) Li-acetylide EDA, DMSO.

Biotin was treated with diphenylphosphoryl azide (DPPA) and triethylamine in tert-butanol under reflux to give acyl azide **4.31**, which underwent a Curitius rearrangement to give the Boc protected biotin amine **4.32** in 51% yield after purification by flash chromatography. Deprotection of the Boc group of **4.32** was achieved on treatment with 6N HCl to give **4.33** in 87% yield without the need for chromatography.

Following the protocol of Nevill and co-workers[5] for diazotination of lysine, the norbiotin amine **4.33** was treated with sodium nitrite in acetic acid in 1:1 THF/H₂O at both 0 °C and 50 °C, in separate experiments in an attempt to prepare **4.34**. However, both conditions returned starting material without evidence of the desired norbiotinol. An alternative protocol for diazotination reported by Glenn and co-workers[6] was also examined. Here biotin amine **4.33** was treated with sodium nitroprusside in 3M aqueous sodium hydroxide (until pH 10) at 60 °C, followed by acidification with 1 M aqueous HCl, but gave a complex intractable mixture as assessed by ^{1}H NMR.

Given this limited success and the dearth of reports on the diazonation of aliphatic amines[5,7,8], an alternative synthetic route to norbiotin alkyne **4.16** was devised. This approach involved the radical mediated Barton decarboxylation of biotin **1.01** to norbiotin bromide **4.38** and subsequent conversion of the bromide to norbiotin alkyne **4.16**, as shown in Scheme 4.4 and 4.5.
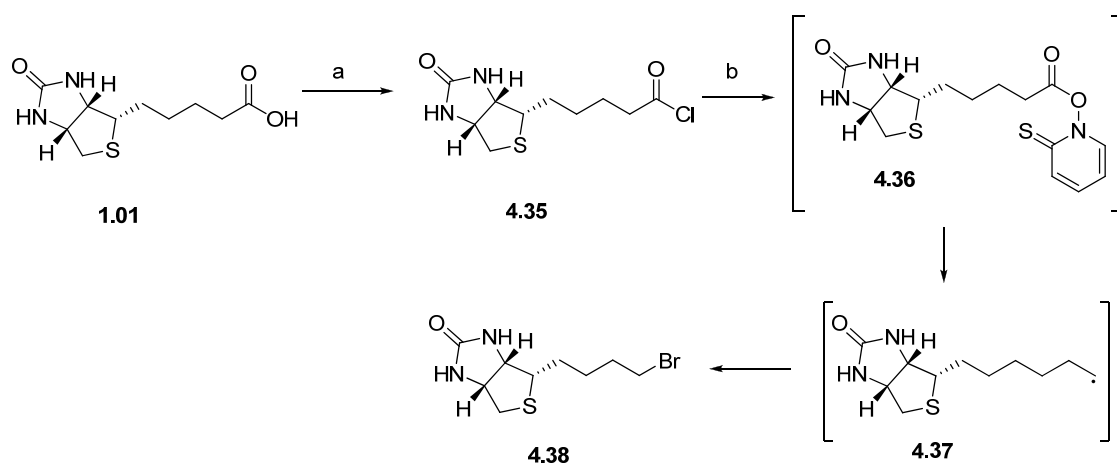
Scheme 4.4: a) SOCl$_2$, DMF, DCM; b) see Table 4.1 for conditions.

Biotin **1.01** was converted to the acid chloride **4.35** on treatment with thionyl chloride and DMF in DCM and directly used without further purification in the Barton decarboxylation reaction. A variety of conditions, such as activation sources (light, heat and AIBN) and solvent systems, were investigated for the Barton decarboxylation of **1.01** to **4.38** (see Table 4.1).

Following reported conditions described by Barton[9], biotin acid chloride **4.35** was treated with 2-pyrithione sodium salt in the solvent and trapping agent bromotrichloromethane at 80 ^{o}C, which gave norbiotin bromide **4.38** in 1% yield (entry 1). Alternatively, treating biotin acid chloride **4.35** with 2-pyrithione sodium salt in bromotrichloromethane and subjecting the reaction to light (from 2 x 250W sunlamps) at room temperature gave a complex mixture, as judged by TLC with only trace quantities of norbiotin bromide observed by ^{1}H NMR spectroscopy after flash chromatography (entry 2). Subjecting a reaction mixture of biotin acid chloride, 2-pyrithione sodium salt in bromotrichloromethane to a combination of heat and light gave norbiotin bromide **4.38** in 1% yield after purification by flash chromatography. Given the low yields obtained, it was

suggested that both the light and heat sources were insufficient to cause the radical cleavage of pyrithione ester **4.36** to form the alkyl radical **4.37**. Thus, to a reaction mixture of biotin acid chloride **4.35** and 2-pyrithione sodium salt in bromotrichloromethane was added the radical activating agent, AIBN. However, a negligible yield of norbiotin bromide was isolated after flash chromatography (3%, entry 4). Alternatively, addition of 4-DMAP had limited effect on the Barton decarboxylation reaction as shown in entry 5 (1%).

A key observation on the reactions carried out in entry 1 – 4 was the formation of a precipitate at the bottom of the reaction vessel during these reactions. Isolating this precipitate through filtration and/or flash chromatography gave a complex and unidentifiable mixtures based on ^{1}H NMR spectroscopy, presumably including the precipitate pyrithione ester **4.36**. On this basis, alternative solvents systems such as THF and DMF were investigated in a bid to solubilise pyrithione ester **4.36**. As described in entry 6-8, the Barton decarboxylation of **1.01** was undertaken with solvent mixtures containing 1:1 DMF/BrCCl$_3$ (7%, entry 6), 2:1 DMF/BrCCl$_3$ (15%, entry 7) and 8:1 DMF/BrCCl$_3$ (21%, entry 8). A 8:1 DMF/BrCCl$_3$ gave the greatest increase in yields of biotin **4.38**.

Table 4.1: Conditions investigated for the decarboxylation of biotin **4.35**, as shown in Scheme **4.4**.

Entry	Solvent	Activation source	Additives	Yield[a]
1	BrCCl$_3$	Heat (80 ^{o}C)	-	1 %
2	BrCCl$_3$	RT/Light[b]	-	0%[c]
3	BrCCl$_3$	Heat (80 ^{o}C)/Light[b]	-	1 %
4	BrCCl$_3$	Heat (80 ^{o}C)	AIBN	3%
5	BrCCl$_3$	Heat (80 ^{o}C)	4-DMAP	1%
6	1:1 DMF: BrCCl$_3$	Heat (80 ^{o}C)	-	7%
7	2:1 DMF: BrCCl$_3$	Heat (80 ^{o}C)	-	15%
8	8:1 DMF: BrCCl$_3$	Heat (80 ^{o}C)	-	21%

[a] Isolated yields after flash chromatography. [b] 250W lamps, [c] trace quantity as determined by TLC.

With sufficient norbiotin bromide **4.38** in hand, the synthesis of norbiotin alkyne **4.16** was undertaken (see Scheme 4.5). Norbiotin bromide **4.38** was treated with lithium acetylide EDA complex in DMSO to give norbiotin alkyne **4.16** in 41% yield after flash chromatography. Norbiotin alkyne **4.16** was utilised for the synthesis of triazole **4.09** and **4.11** described below.
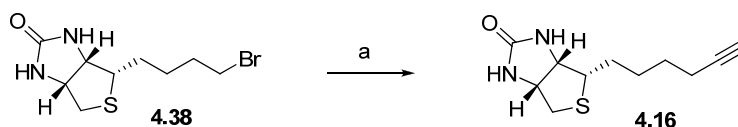
Scheme 4.5: a) Li-acetylide EDA complex, DMSO;

Homobiotin alkyne 4.18

The synthesis of homobiotin alkyne **4.18** is shown in Scheme 4.6. This synthetic approach involved access to the reported synthesis of homobiotin **4.40**[10], followed by functional group transformation to give homobiotin alkyne **4.18**.
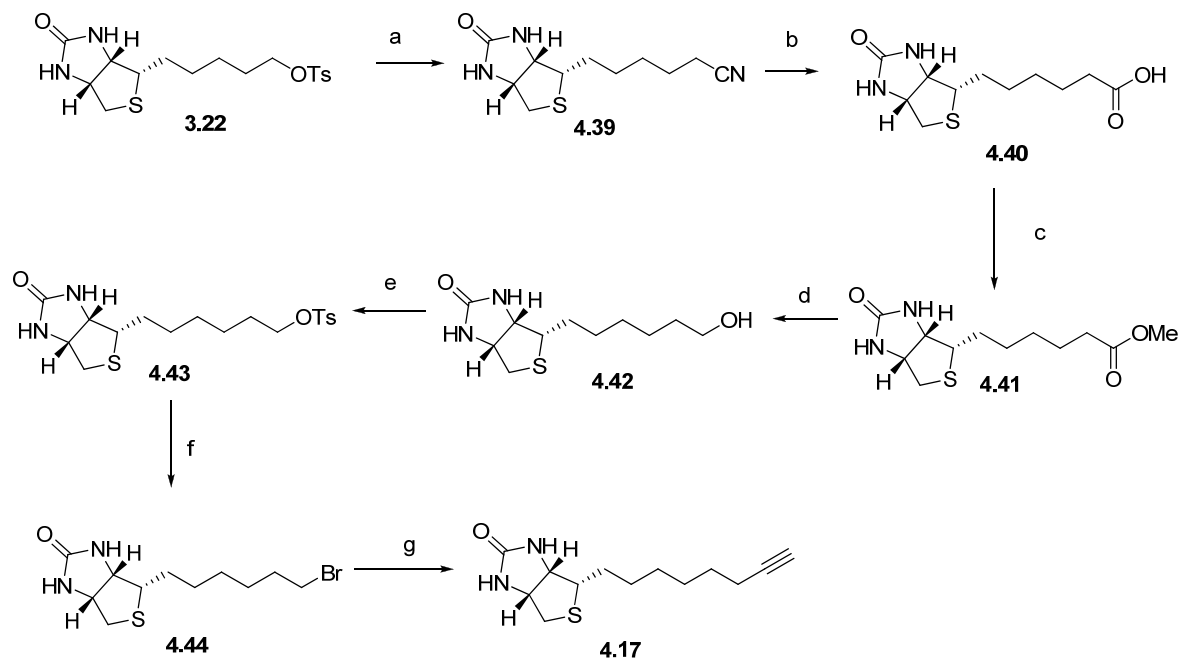
Scheme 4.6: a) KCN, DMF; b) NaOH, H_2O, reflux; c) $SOCl_2$, MeOH; d) $LiAlH_4$, THF; e) TsCl, py; f) LiBr, MEK, 79 °C; g) Li-acetylide EDA, DMSO.

Biotin tosylate **3.22** was treated with sodium cyanide in DMF at ambient temperature to give nitrile **4.39** in 72% yield. Hydrolysis of nitrile **4.39** with 4 N sodium hydroxide under reflux, followed by acidification with 6 N HCl gave homobiotin **4.40** in 96% yield after vacuum filtration and without further purification. Acid esterification with thionyl chloride gave methyl ester **4.41** in quantitative yields, which was reduced with LiAlH$_4$ to give homobiotinol **4.42** in 91% yield. Conversion of homobiotinol **4.42** to the tosylate **4.43** was achieved on reaction with tosyl chloride in pyridine. The crude tosylate **4.43** was treated with lithium bromide in 2-butanone under reflux to give homobiotin bromide **4.44** in 51% yield over two steps from homobiotinol **4.42** and after flash chromatography. Finally, addition of lithium acetylide EDA complex to homobiotin bromide **4.44** in DMSO at 15 $^{\circ}$C gave homobiotin acetylene **4.17** in 36% yield. The low yield obtained for **4.17** was suggested to be due to the decomposition of the hydroscopic lithium acetylide EDA complex. This was not investigated further as sufficient quantities of **4.17** were obtained for the CuAAC reactions described below.

4.2.3 Synthesis of triazole 4.01-4.13 *via* CuAAC and RuAAC reactions

The synthesis of triazole **4.01 – 4.04, 4.12** and **4.13** is shown in Scheme 4.7 with yields reported therein. The triazole analogues were synthesized according to optimised reaction conditions discussed in Section 3.2.2. The appropriate alkyne and azide were dissolved in 2:1 acetonitrile and water mixture treated with 20 mol% copper nano powder, sonicated for 15 min and stirred at 35 $^{\circ}$C for 4 h. Due to the low solubility of azide **4.19**, the CuAAC formation of **4.02** was accomplished in a solvent mixture of acetonitrile:water:DMSO (5:4:1). The 1,4-triazole regioisomer configuration of **4.01 – 4.04, 4.12** and **4.13** was confirmed by ^{1}H NMR ROESY and COSY experiments (see Section 4.2.4).
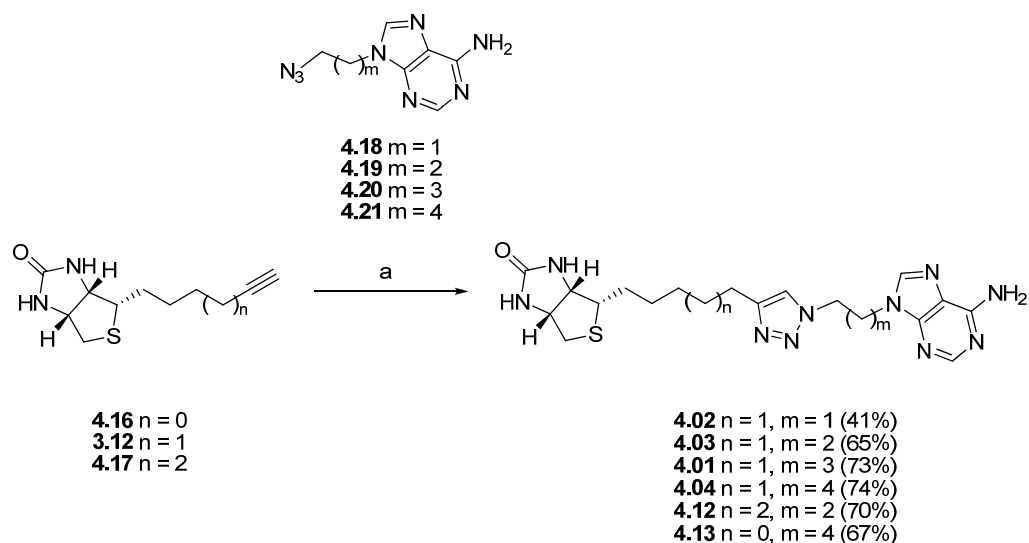
Scheme 4.7: a) Cu nano-powder, 2:1 acetonitrile/water, sonication, 35 °C.

The synthesis of triazole **4.09** and **4.10**, shown in scheme 8, retained the pentose ring as both triazole **4.09** and **4.10** were initially developed as analogues of triazole **3.25**. Thus alkynes **4.16** and **4.17** were treated separately with azide **3.16** in 2:1 acetonitrile and water mixture containing 20 mol% copper nano powder. Triazole **4.09** and **4.10** were purified with flash chromatography with isolated yields of 68% and 61% respectively.
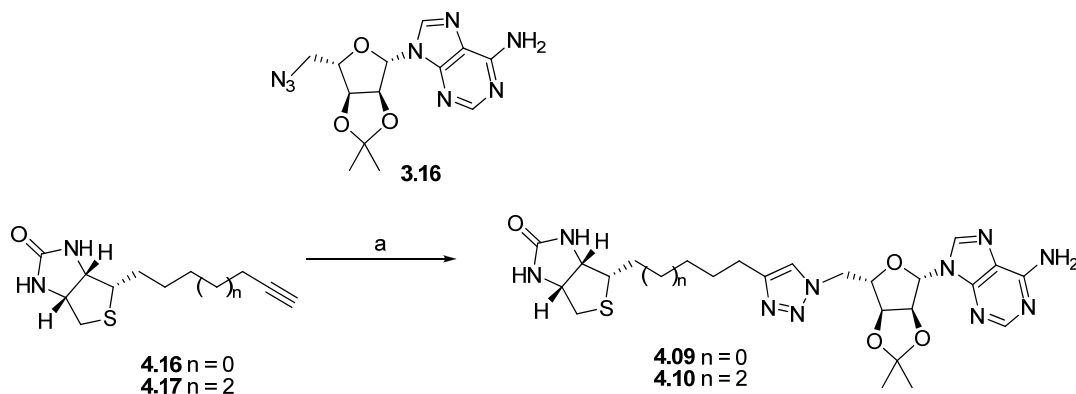
Scheme 4.8: a) Cu nano-powder, 2:1 acetonitrile/water, sonication, 35 °C.

Triazole **4.05 − 4.08**, shown in Scheme 4.9, were synthesized according to optimised conditions discussed in chapter 3. Azides **4.18 − 4.21** were treated with alkyne **3.12** and Cp*Ru(PPh₃)₂Cl in 1:1 DMF and THF solvent mixture at 80 °C. The resulting triazole **4.05 − 4.08** were isolated and purified by flash chromatography in yields reported in

scheme 10. The 1,5-triazole configurations of **4.05 – 4.08** were confirmed by ^{1}H NMR ROESY and COSY experiments (see Section 4.2.4).

4.18 m = 1
4.19 m = 2
4.20 m = 3
4.21 m = 4

4.05 m = 1 (41%)
4.06 m = 1 (52%)
4.07 m = 1 (55%)
4.08 m = 1 (48%)
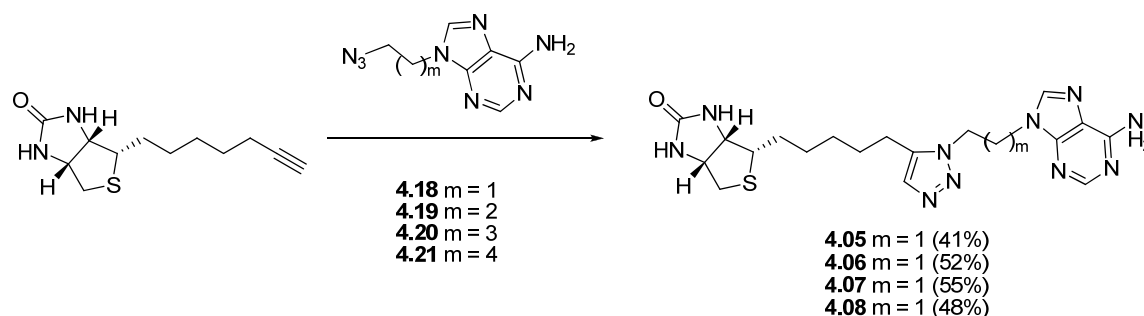
Scheme 4.**9**: Cp*Ru(PPh$_3$)$_2$Cl, 1:1 THF\DMF, 80 ^{o}C

4.2.4 Determination of 1,4 and 1,5 regioisomer of triazoles 4.01 – 4.13

1D ^{1}H NMR and 2D COSY spectra of triazoles **4.01 – 4.13** confirmed that a single regioisomer was present. 2D ROESY ^{1}H NMR experiments indicated that the 1,4-triazole and 1,5-triazole triazoles **4.01 – 4.12** possess distinguishable through space interactions with adjacent methylene protons (H$_A$ and H$_C$) and 5 position hydrogen upon the triazole ring (H$_B$). The 1,4-triazoles (**4.01 – 4.04, 4.09 – 4.12**) were found to provide the diagnostic through space interactions between the triazole proton H$_B$ and both adjacent methylene protons H$_A$ and H$_C$. Whilst the 1,5-triazole (**4.05 – 4.08**) only possessed through space interactions between methylene H$_B$ and triazole H$_A$. A representative depiction is shown in Figure 4.2.
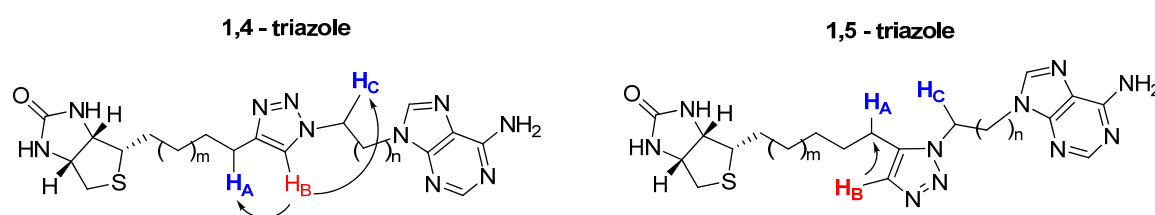
Figure 4.2: Depiction of ^{1}H NMR ROESY correlations for triazoles **4.01 – 4.12.**

4.2.5 The synthesis and screening of triazole analogues 4.01 – 4.08 via *in situ* click chemistry.

As discussed in Section 1.4, we anticipated that it would be possible to prepare triazole-based inhibitors of SaBPL via a target-guided synthesis of *in situ* click chemistry. The structural features of both the SaBPL active site and our designed triazole **3.25** inhibitor presented the ideal opportunity to investigate this approach. Moreover, the active site of SaBPL is characterised by two distinct pockets (ATP and biotin binding pocket), which are in close proximity to each other, as seen in X-ray crystal structures discussed in Section 3.4.

An initial *in situ* click experiment was performed on the two fragments of triazole **3.25** (biotin alkyne **3.12** and adenosine azide **3.16**), as shown in Scheme 10. As with reported *in situ* click chemistry experiments[11], it was paramount that at least one of these fragments was capable of binding within the active site of SaBPL. Importantly, the building block biotin alkyne **3.12** was shown by our collaborators at Biomedical Science at University of Adelaide to bind to SaBPL ($K_i = 0.33 \pm 0.05$ µM, a detailed discussion is made in chapter 5), however, adenosine azide **3.16** had limited binding affinity to SaBPL. Our collaborators at Biomedical Science at the University of Adelaide, conducted an *in situ* click experiment with adenosine **3.16** and biotin alkyne **3.12** using wild type SaBPL. It was observed that wild type SaBPL was ineffective at providing the *in situ* cycloaddition reaction at a high enough rate for detection by HPLC or LC-MS. Thus, Arg122, which is known to act as a gatekeeper for ligands bound to the homologous EcBPL[12], was selectively mutated to Gly122. This mutation was suggested to increase the dissociation rate of ligands compared to wild type SaBPL. Using SaBPL-R122G mutant, the cycloaddition reaction between **3.16** and **3.12** was accomplished (Scheme 4.10).
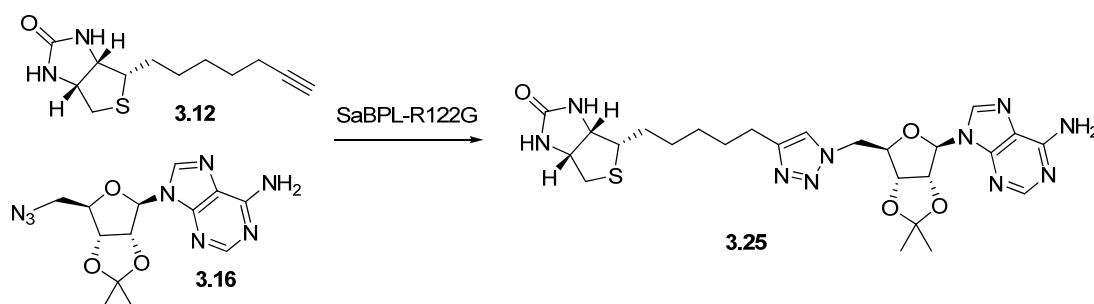
Scheme 4.10: *In situ* click experiment with alkyne **3.12** and azide **3.16** using mutant SaBPL-R122G to give triazole **3.25** (based on HPLC).

Based on the success with *in situ* click chemistry to form triazole **3.25,** we investigated the screening of triazole analogues **4.01 – 4.08** (see Scheme 4.11). It was proposed that only fragments with the appropriate tether length, and with their respective azide and alkyne functional groups in close proximity to each other,will undergo a 1,3-dipolar cycloaddition reaction. Fragments with their functional groups far removed from each other would not be expected to undergo the 1,3-dipolar cycloaddition reaction. In other words, SaBPL will only select and form the triazole analogues from those that are capable of binding within the active site.
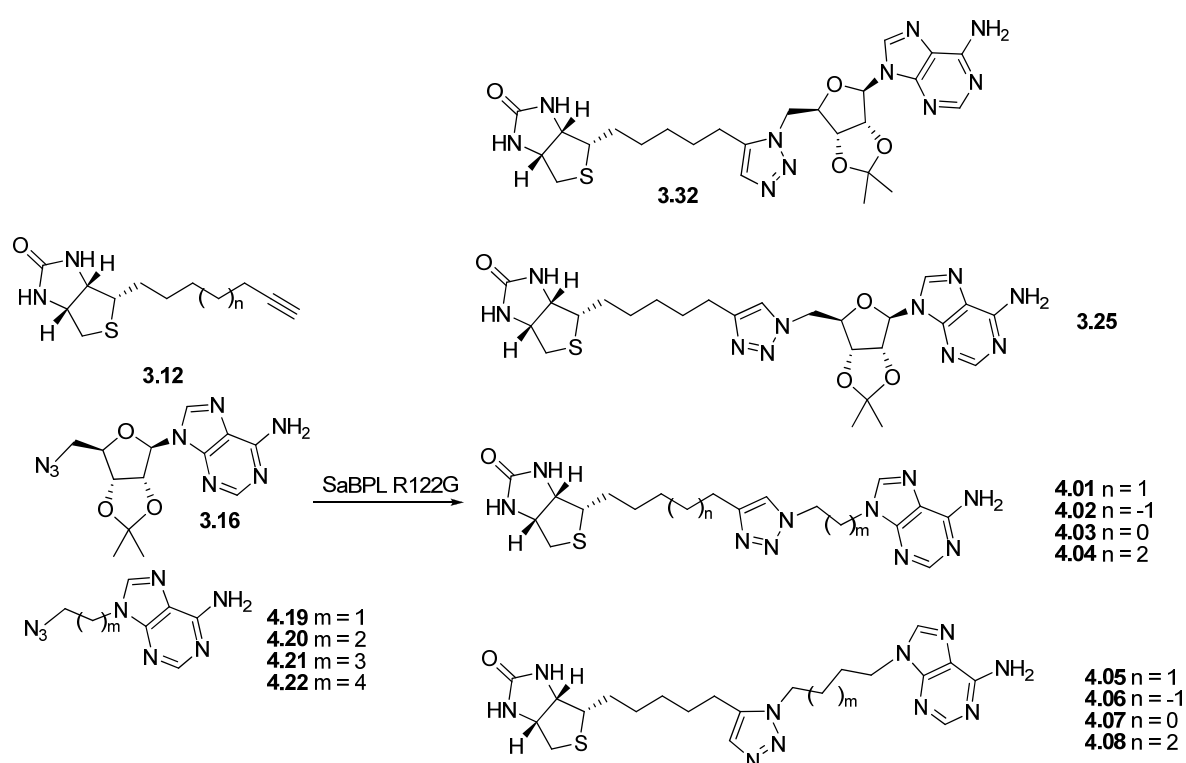
Scheme 4.**11:** *In situ* click experiment with alkyne **3.12** and azides **3.16**, **4.19-4.20** using SaBPL-R122G mutant to give the possible triazole combinations **4.01- 4.08.**

To validate the *in situ* click experiment, all possible triazole analogues (**4.01 – 4.08**) from the combination of adenine and alkyne fragments were required as reference samples. These analogues were synthesized through CuAAC and RuAAC reactions (Section 4.2.3) and their retention times on a C18 reverse phase HPLC column were determined (see Chapter 7: experimental). Enzyme inhibition assay was investigated for on triazole **4.01 – 4.08**, with only triazole **4.01** seen to inhibit SaBPL (K_i = 0.66 ± 0.15 μM, Section 4.6).

Based on these results, it was suggested that only triazole **4.01** would be obtained from the *in situ* click experiment.

The *in situ* click experiment and three control experiments (Table 4.2) were conducted by Kelly Keeling in the Abell research group and the results are shown in Table 4.2. The first experiment, an *in situ* click reaction, involved the addition of adenine fragments **4.19 – 4.22** and biotin alkyne **3.12** in the presence of SaBPL-R122G. The second experiment (control experiment) was conducted to confirm that the cycloaddition reaction from the first experiment occurred within the active site of SaBPL-R122G. Thus, the known inhibitor, biotinol-5'-AMP **1.05**, was added. In the third and fourth experiment, bovine serum albumin and buffer solution both in the absence of SaBPL-R122G, was performed to confirm that the rate of cycloaddition through non-specific peptidic catalysis and background cycloaddition, respectively. All four experiments were analysed by HPLC and mass spectrometry to determine the presences or not of triazoles **4.01 -4.08** (Figure 4.2).

Table 4.2

Experiment	Compounds	Protein	Hits[a]
1	Adenine **4.19 – 4.22**, Biotin **3.12**	SaBPL-R122G	Triazole **4.01**
2	Adenine **4.19 – 4.22**, Biotin **3.12**	Bovine serum albumin	None
3	Adenine **4.19 – 4.22**, Biotin **3.12**	Buffer (no enzyme)	None
4	Adenine **4.19 – 4.22**, Biotin **3.12** Biotinol-5'-AMP **1.05**	SaBPL-R122G	None

[a] obtained through HPLC and mass spectrometry.
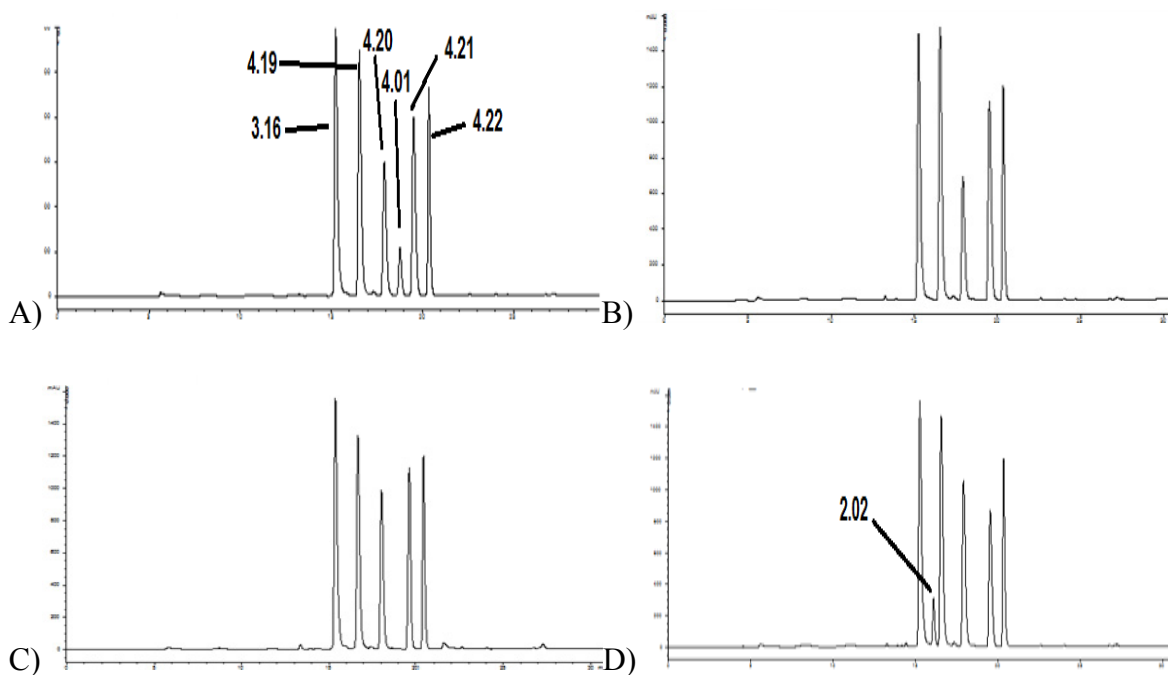
Figure 4.3: HPLC traces from experiments 1 – 4 (described in Table 4.2). A) experiment 1 contains SaBPL-R122G with adenine 4.19 – 4.22 indicated the formation of triazole 4.01. B) experiment 2 contains no SaBPL enzyme, but BSA and indicates no formation of triazole analogues C) experiment 3 contains buffer solution without SaBPL and indicates no formation of triazole analogues D) experiment 4 contains both SaBPL-R122G and biotinol-5'-AMP **1.05** and indicates no triazole formation by HPLC (courtesy of Ms Keeling).

Analysis by HPLC of experiment 1 (see Table 4.2) indicated that triazole **4.01** was formed, as evident by the extra peak corresponding to the same retention time as triazole **4.01** (Figure 3A). Whilst HRMS analysis of experiment 1 indicated the presence of of two species with molecular weight of 471.4 and 570.3 Da corresponding to triazole **4.01** and **3.25**. Both HPLC and HRMS analysis of experiments 2 – 4 showed that no triazole analogues (**4.01 – 4.08**) were formed.
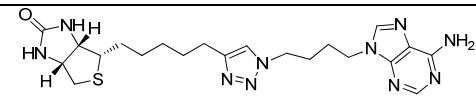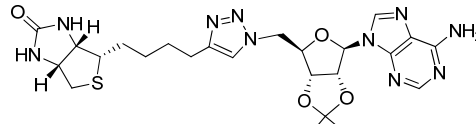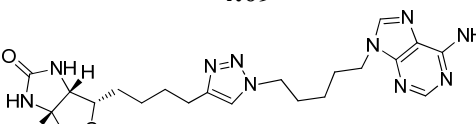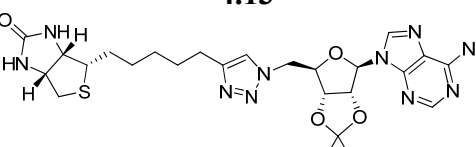
Based on these results, the *in situ* click experiments highlighted that the enzyme SaBPL R122G was able to select the precursors (**3.12**, **3.16**and **4.21**) of the two most potent inhibitors and synthesize the corresponding triazole analogue **3.25** and **4.01**. Importantly, the control experiments indicated that the formation of both triazole required the enzyme

SaBPL R122G (experiment 3) and the formation of the triazole occurred within the active site (experiment 4). Given these observations, it is suggested the *in situ* click approach is a viable alternative route to CuAAC/RuAAC for screening triazole analogues.

4.3 Enzyme inhibition results

Triazole **4.01 – 4.15** were assayed for inhibitory potency against SaBPL, EcBPL and HsBPL. Triazole **4.01, 4.09** and **4.13** exhibiting nanomolar inhibition against SaBPL, as shown in Table 4.3. The assay was performed by collaborators at Molecular Life Science, University of Adelaide, following a method described by Chapman-Smith and co-workers.[13] The IC_{50} values for each compound were determined from a concentration-response curve by varying the concentration of the inhibitor under the same substrate and enzyme concentrations.

Table 4.3: Inhibition of triazole **4.01, 4.09, 4.13** and **3.25** against SaBPL, HsBPL and EcBPL.

Compound	SaBPL K_i (µM)	EcBPL K_i (µM)	HsBPL K_i (µM)
4.01	0.66 ± 0.15	>90	>90
4.09	7.53 ± 1.90	>10	>10
4.13	2.86 ± 0.75	>10	>10
3.25	1.83 ± 0.33	>90	>90

[a]Enzyme inhibition assay conditions are detailed in Chapter 7

As shown in Table 4.3, three triazole analogues were potent and selective inhibitors against SaBPL (**4.01, 4.09** and **4.13**). Triazole **4.01** was the most potent ($K_i = 0.66 \pm 0.15$ µM, IC$_{50}$ = 4.0 ± 0.9) and was threefold more potent than the lead triazole **3.25** ($K_i = 1.8 \pm 0.33$ uM). Similar to **3.25**, triazole **4.01** was found to be at least 400 fold selective towards SaBPL over EcBPL (>200µM) and HsBPL (>200µM).

The tether between the triazole and biotin groups of triazole **4.09**, which is one carbon shorter than that for triazole **3.25**. This analogue was found to inhibit SaBPL with a K_i = 7.53 ± 1.90 µM, which is 4 fold less potent compared to triazole **3.25** ($K_i = 1.83 \pm 0.33$ µM).

Finally, triazole **4.13,** which possesses the same linker length between the adenine and biotin rings as triazole **4.01**, but with the triazole ring 'shunted' towards the biotin ring was found to inhibit SaBPL with a $K_i = 2.9 \pm 0.75$ µM. This is 4 fold less potent than triazole **4.01 (**$K_i = 0.66 \pm 0.15$ µM). Similar to triazole **4.01**, triazole **4.13** exhibited some selectivity towards SaBPL ($K_i = 2.86 \pm 0.75$ µM) over HsBPL (K_i >10 µM) and EcBPL (K_i >10 µM). Based on these enzyme inhibition results a number of SAR features were elucidated (Section 4.3.1).

No antimicrobial minimal inhibitory concentration (MICs) was elucidated for triazole **4.01** against *S. aureus* through the microdilution broth method with cation-adjusted Mueller-Hinton broth. This result is remarkable given that triazole **4.01,** though more potent compared to triazole **3.25** in enzyme assays, did not retain antibacterial activity against *S. aureus* in time kill experiments.

4.3.1 Summary of structure activity relationship

The enzyme inhibition assay results of triazole **4.01** – **4.15** revealed a structural activity relationship. It is suggested the ideal features for this class of triazole inhibitors of SaBPL are:

1. <u>The pentose ring was detrimental to binding affinity of triazole inhibitors</u>. Triazole **4.01** (containing the acyclic butyl linker) was found to be 4-fold more potent than triazole **3.25** and **3.08** (contains a pentose sugar).

2. <u>The optimal linker length between the biotin to the triazole rings is 5 carbons.</u> This observation is based on the inhibition results of triazole **3.25**, **3.26, 3.08** and **4.01** which possess the 5 atom distance between the biotin and triazole ring. Whilst, triazole **4.09** and **4.13** possess a 4 atom distance between the biotin and triazole ring, both inhibitors were 4 to 12 fold less potent than triazole **4.01**.

3. <u>The optimal linker length between the adenine and triazole ring is 4 atoms</u>, with triazoles **3.25**, **4.01** and **4.09** maintaining this attribute. Although triazole **4.13** with a 5 carbon tether length was potent against SaBPL, albeit with a 4 fold decrease in potency compared to triazole **4.01**.

4. <u>A 1,4-triazole substitution pattern is favoured over 1,5-triazole </u>(see Figure 4.4). The only potent triazole based analogues (triazole **4.01**, **4.13**, **4.09** and **3.25**) examined thus far contained the 1,4-substitution pattern. Triazole **4.07** and **4.08**, which retains the same tether lengths mention in points 2 and 3 but has the 1,5-substitution pattern was observed to have limited inhibition against SaBPL at $K_i > 10$ µM.

5. <u>The optimal position and configuration of the triazole ring is depicted in Figure 4.4.</u> Changing the configuration of the triazole ring from **4.01** to the configuration depicted in triazole **4.14** and **4.15** resulted in inactive inhibitors against SaBPL. Changing the position of triazole ring from **4.01** to **4.12** (i.e. shunting the triazole ring towards the adenine component) and **4.13** (i.e. shunting the triazole ring towards the biotin component) resulted in limited inhibition against SaBPL.
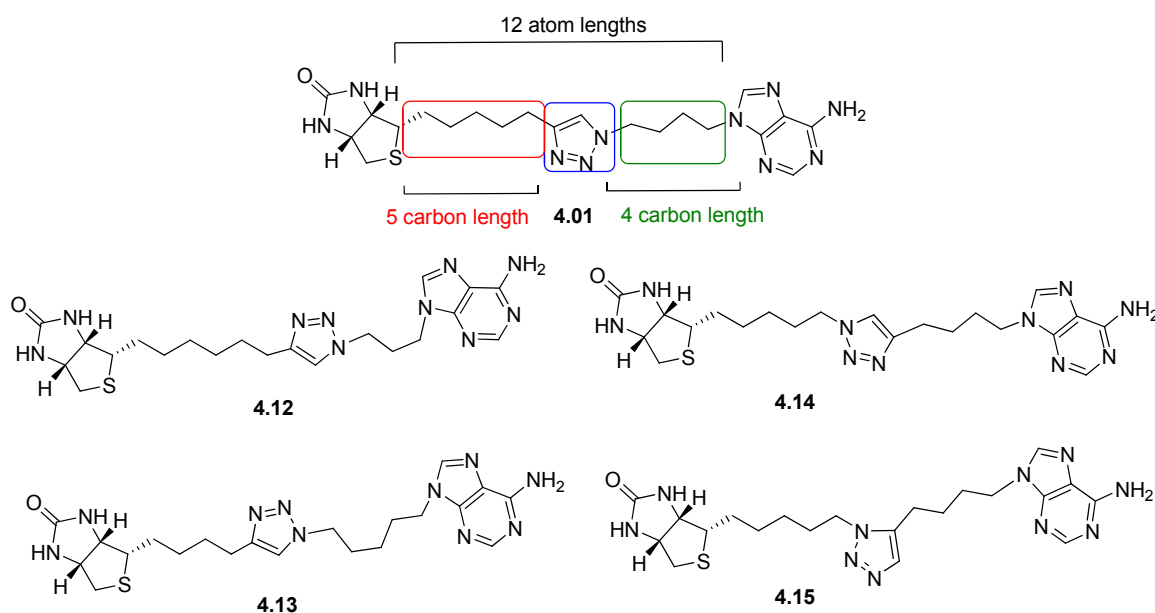
Figure 4.4: A cartoon depiction based on the SAR features for **4.12 – 5.15**. The red denotes the optimal tether length between the triazole and biotin ring (5 carbon lengths), the green denotes the optimal tether length between the triazole and adenine ring (4 carbon lengths) and the blue denotes the optimal position and configuration for the triazole ring.

4.4 Discussion of X-ray crystal structure of triazoles 4.01 bound to SaBPL

The structure of triazole **4.01** bound to SaBPL was solved with resolution of 2.61 Å by collaborators at Monash University, Australia using the method prescribed by Pendini and co-workers (see Chapter 7 for conditions). Overall, triazole **4.01**, triazole **3.25**, biotinyl-5'-AMP **2.01** and biotinol-5'-AMP **1.05** all bind to SaBPL in a U-shaped conformation as shown in Figure 4.5. This conformation allows the adenine and biotin groups of triazole **4.01** to bind in the same orientation and position as found for triazole **3.25** and biotinol-5'-AMP **1.05** bound to SaBPL (see Sections 2.5 and 3.4 for details of **1.05** and **3.25**). Consequently, the interactions of triazole **4.01** bound to SaBPLretains a number of the hydrogen bonding interactions as found with **1.05** and **3.25** (red dashes, Figure 4.5). Nevertheless, three novel hydrogen bonding interactions were also found between the triazole of **4.01** and SaBPL, shown in blue. A focus on these novel interactions is discussed below.
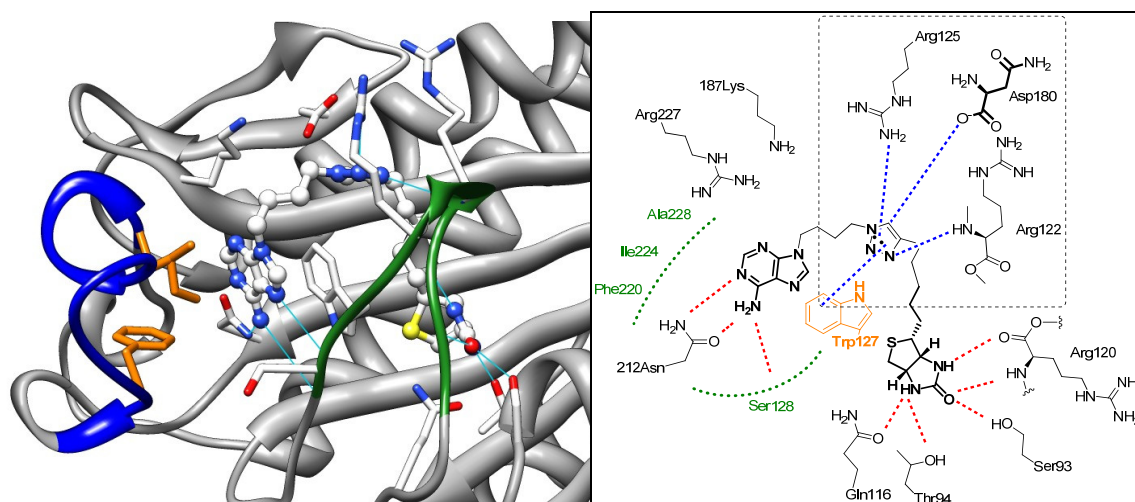
Figure 4.5: A 3D depiction of triazole **4.01** bound to SaBPL (left). 2D depiction of triazole **4.01** bound to SaBPL with hydrogen bonding interactions shown in colour dashes (right). The red dashes denotes the hydrogen bonding interactions in common with biotinol-5'-AMP **1.05** bound to SaBPL. The blue dashes denotes novel hydrogen bonding interactions not observed in X-ray crystal structures of biotinol-5'-AMP **1.05**, biotinyl-5'-AMP **1.03** and triazole **3.25.**

Phosphate binding domain

The interactions between the triazole ring of **4.01** and phosphate binding domain are summarised as followed:

1. The amino group of Arg122 was seen to hydrogen bond with N3 of the triazole ring at 3.00 Å (N_{Arg}-N_3) apart. (see Figure 4.6)

2. Arg125 makes a hydrogen bond with N2 of the triazole ring at 2.92 Å (N_{Arg}-N_2) away. (see Figure 4.6)

3. The proton on the fifth position of the triazole ring was found to form a hydrogen bonding interaction with side chain carboxylate of Asp180 at 3.43 Å (Figure 4.6). This type of hydrogen bonding interaction has been reported by Brik and co-workers between a fifth positioned proton of a triazole ligand and HIV-1 protease was 3.8 Å apart.[14]

4. The triazole ring of **4.01** was found to be in an edge-to-face interaction with Trp127. Here, the centroid of phenyl ring of Trp127 is 5.6 Å away from the centroid of the

triazole ring and the centroid of the phenyl ring of Trp127 has a displacement of 6 $^{\circ}$ from the normal of the triazole plane. (see Figure 4.6).
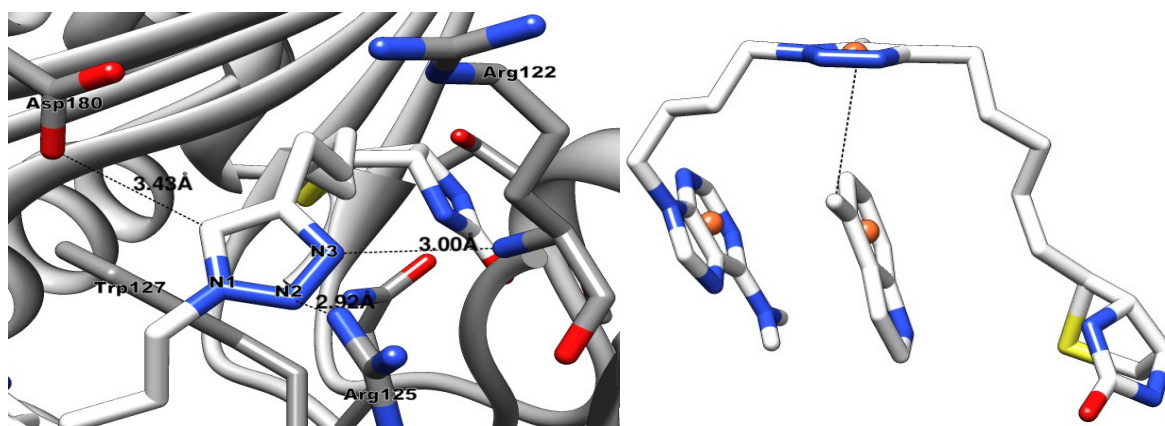
Figure 4.6: A 3D depiction of triazole **4.01** looking down into the pocket (left). The hydrogen bonding interactions are depicted with black dashes. A 3D depiction of triazole **4.01** bound to SaBPL with only Trp127 shown (Right). As highlighted Trp127 forms an edge to face π interaction with the triazole ring, whilst also forming a displaced parallel π interaction with the adenine ring.
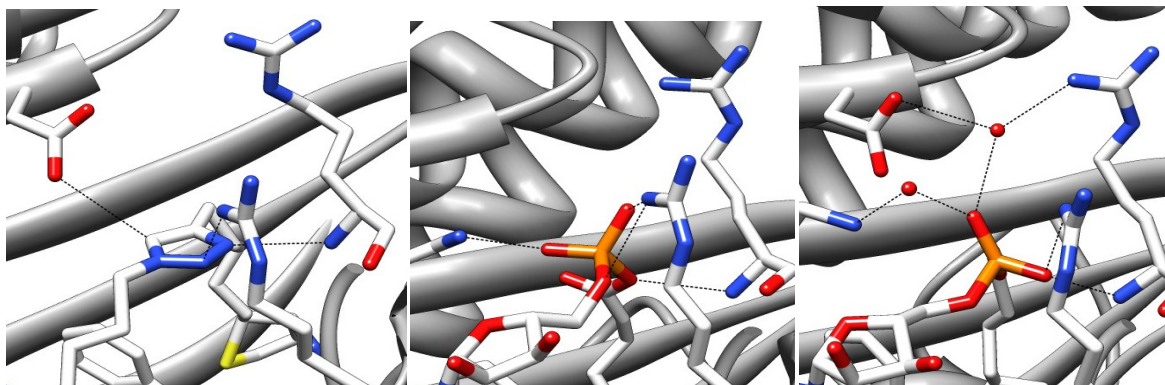
Figure 4.7: 3D depiction of triazole **4.01**, biotinyl-5'-AMP **1.03** and biotinol-5'-AMP **1.05** bound to SaBPL (left to right). The black dashes denote the hydrogen bonding interaction between their respective linkers and Arg122, Arg125, Asp180 and Lys187 of SaBPL.

Compared to biotinyl-5'-AMP **1.02**, the triazole ring for **4.01**, retains all hydrogen bonds except that to Lys187 (see Section 2.4). The triazole ring, however, makes two additional and novel interactions with Asp180 and edge to face interaction with Trp127. Compared with the phosphodiester of biotinol-5'-AMP **1.05**, the triazole ring again lacks the hydrogen bonding interaction with Lys187. Based on these results, it is suggested that for

4.01 and its triazole ring is a bioisosteric analogue of both the phosphodiester and phosphoroanhydride linkers, (Figure 4.7 above).

4.5 Conclusion

A library of acyclic adenine azide analogues **4.19** – **4.22**, with varying tether lengths between adenine ring and azide functional group, were synthesized. Synthesis of the required building block, norbiotin alkyne, was achieved by Barton decarboxylation of biotin over 3 steps in 12 % yield. The synthesis of the other key building block, homobiotin alkyne **4.17,** was achieved in 10 steps with an overall yield of 8% from biotin **1.01**. The synthesis of triazole analogues **4.01** – **4.12** was then achieved using these building blocks by CuAAC and RuAAC reactions, with the regiochemistry of the triazole rings being determined by 2D ROESY ^{1}H NMR spectroscopy.

An alternative approach, to the synthesis and screening of triazole **4.01** – **4.08** as inhibitors against SaBPL, was undertaken. These triazole analogues were synthesized and screened through an *in situ* click experiment between adenine fragments **4.19** – **4.22** with biotin alkyne **3.12**. It was found that a mutant enzyme (SaBPL R122G) was able to select the adenine fragment **4.21** and subsequently catalyse its cycloaddition with alkyne **3.12** to give triazole **4.01**. The *in situ* click approach provides a facile and expedient method for screening libraries of triazole analogues from analogues of adenine-based and biotin-base fragments.

Triazoles **4.01** – **4.12** were assayed against SaBPL, EcBPL and HCS. Triazole **4.01**, **4.09** and **4.13** were found to be active inhibitors and selective against SaBPL. Triazole **4.01** was the most potent triazole inhibitor prepared thus far (K_i = 0.66 ± 0.15 μM). Interestingly, triazole **4.01** lacked antimicrobial activity against *S. aureus*. Preliminary SAR (**4.01** – **4.12**) indicated that triazole **4.01** is the optimal scaffold for binding to SaBPL.

The X-ray crystal structure was solved for triazole **4.01** bound to SaBPL. The key hydrogen bonding interactions between the triazole ring of **4.01** and Arg122, Arg125 and Asp180, and the edge to face interaction with Trp127, suggested that the triazole ring is a suitable mimic of the phosphoroanhydride linker of biotinyl-5'-AMP **1.03**.

Applying the key attributes from the SAR study of triazole **4.01 – 4.15** and the X-ray crystal structure of triazole **4.01** bound to SaBPL, the rational design and synthesis of potent triazole inhibitors was investigated in Chapter 6.

4.6 References for Chapter Four

(1)   Brown, P. H.; Cronan, J. E.; Grøtli, M.; Beckett, D. *Journal of Molecular Biology* **2004**, *337*, 857.

(2)   Wood, Z. A.; Weaver, L. H.; Brown, P. H.; Beckett, D.; Matthews, B. W. *Journal of Molecular Biology* **2006**, *357*, 509.

(3)   Bagautdinov, B.; Kuroishi, C.; Sugahara, M.; Kunishima, N. *Journal of Molecular Biology* **2005**, *353*, 322.

(4)   De Clercq, E. *Clinical Microbiology Review* **2003**, *16*, 569.

(5)   Nevill, C. R.; Angell, P. T. *Tetrahedron Letters* **1998**, *39*, 5671.

(6)   Glenn, M. P.; Pattenden, L. K.; Reid, R. C.; Tyssen, D. P.; Tyndall, J. D. A.; Birch, C. J.; Fairlie, D. P. *Journal of Medicinal Chemistry* **2001**, *45*, 371.

(7)   Hegarty, A. F. In *Diazonium and Diazo Groups (1978)*; John Wiley & Sons, Ltd.: 2010, p 511.

(8)   March, J. *Advance Organic Chemistry*; 3 ed.; John Wiley & Sons: New York, 1985.

(9)   Barton, D. H. R.; Crich, D.; Motherwell, W. B. *Journal of the Chemical Society, Chemical Communications* **1983**, 939.

(10)   Wilbur, D. S.; Hamlin, D. K.; Chyan, M.-K.; Kegley, B. B.; Pathare, P. M. *Bioconjugate Chemistry* **2001**, *12*, 616.

(11)   Whiting, M.; Muldoon, J.; Lin, Y.-C.; Silverman, S. M.; Lindstrom, W.; Olson, A. J.; Kolb, H. C.; Finn, M. G.; Sharpless, K. B.; Elder, J. H.; Fokin, V. V. *Angewandte Chemie International Edition* **2006**, *45*, 1435.

(12)   Choi-Rhee, E.; Schulman, H.; Cronan, J. E. *Protein Science* **2004**, *13*, 3043.

(13)   Chapman-Smith, A.; Cronan, J. E. *Trends in Biochemical Sciences* **1999**, *24*, 359.

(14)   Brik, A.; Alexandratos, J.; Lin, Y.-C.; Elder, J. H.; Olson, A. J.; Wlodawer, A.; Goodsell, D. S.; Wong, C.-H. *ChemBioChem* **2005**, *6*, 1167.

Chapter Five

5.1 Design, synthesis and biological assays of biotin analogues

Chapter 4 revealed biotin alkyne **3.12**, a key precursor for the synthesis of potent inhibitors triazole **3.25** and **4.01**, as a potent inhibitor of SaBPL (K_i = 0.30 ± 0.05 μM) and interestingly also of EcBPL (K_i = 3.50 ± 0.5 μM). Further investigations revealed that the precursors of 1,4-triazole discussed in Chapter 4, norbiotin alkyne **4.16** (ki = 0.08 ± 0.01 μM), homobiotin alkyne **4.17** (K_i = 2.40 ± 0.2 μM) and biotinol **2.07** (K_i = 3.37 ± 0.25 μM), were potent inhibitors of SaBPL, whilst norbiotin amine **4.33** and biotin bromides **4.38**, **3.19** and **4.44** were limited inhibitors of SaBPL (K_i > 10 μM). Biotin analogue inhibitors synthesized in previous chapters are shown in Figure 5.1.
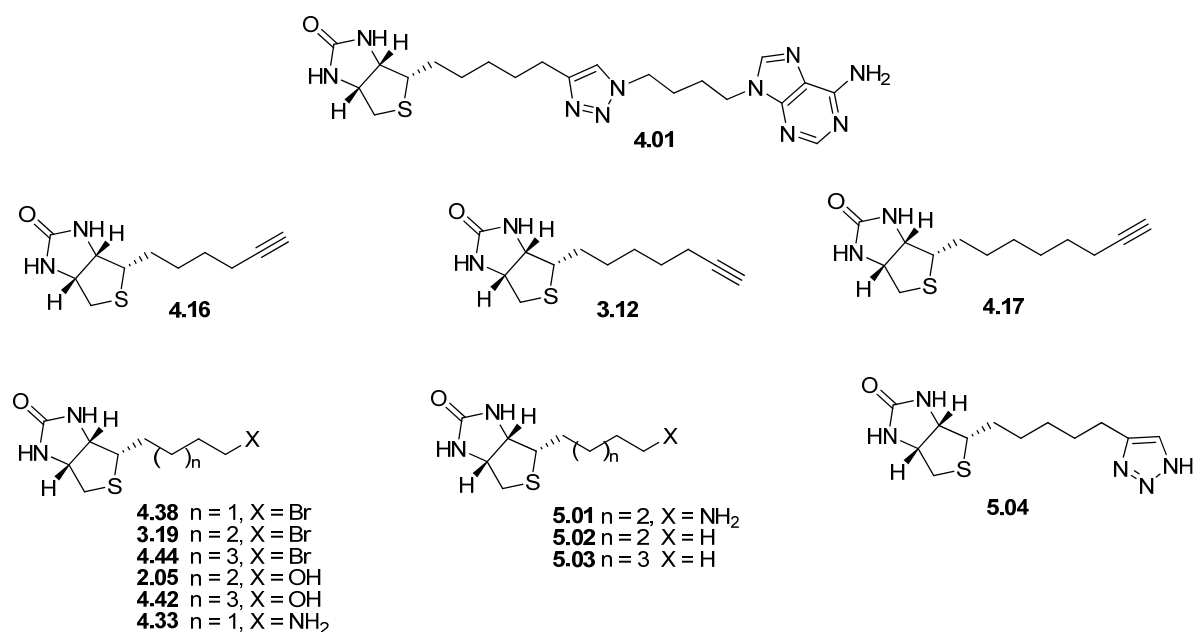
Figure 5.1: Biotin analogues synthesised in chapter 2 – 5 and assayed against BPL (**4.16**, **4.17**, **4.38**, **3.19**, **4.44**, **2.05**, **4.42** and **4.33**). Proposed biotin analogues synthesized in this chapter (**5.01 – 5.04**).

The enzyme inhibition results of these biotin analogues against SaBPL suggested that only certain functional groups are accommodated within the biotin binding pocket, with hydrophobic functional groups such as alkyne providing the most potent inhibitors (e.g. structures **4.16** and **3.12**). To investigate this further, a series of analogues were proposed, as shown in Figure 5.1. Thus, biotin amine **5.01**, biotin alkyl **5.02** and homobiotin alkyl

5.03 were designed to probe the nature of the biotin binding pocket of SaBPL. In addition, biotin triazole **5.04** was designed to investigate the role of the triazole ring in binding to SaBPL and consequently shed light on the role of the triazole ring in the selective inhibition of SaBPL, as found in triazole **3.25** and **4.01** (see Section 4.4 for details on selective inhibition).

A second series of analogues, shown in Figure 5.2, was proposed on the basis of literature reports on orthogonal labelling between biotin and streptavidin. It has been suggested by Kwon and co-worker that the binding mode of biotin with BPL is analogous to the binding mode of between biotin to both avidin and streptavidin.[1] The main commonality between avidin active site and BPL are: their tight binding to biotin, both contain a disordered biotin binding loop that envelopes substrates upon biotin binding and the hydrogen bonding interactions that are formed between the substrate and protein are comparable. Both biotin sulphone **5.05a**[2] and desthiobiotin **5.06a**[3] are reported biotin analogues that have been used in conjunction to avidin and streptavidin binding and are of interest in the current study. As biotin alkyne **3.12** was a potent inhibitor of SaBPL, this analogue was used as a reference inhibitor. To this end, we investigated analogues **5.05** and **5.06** as potential inhibitors of BPL (see Figure 5.2).
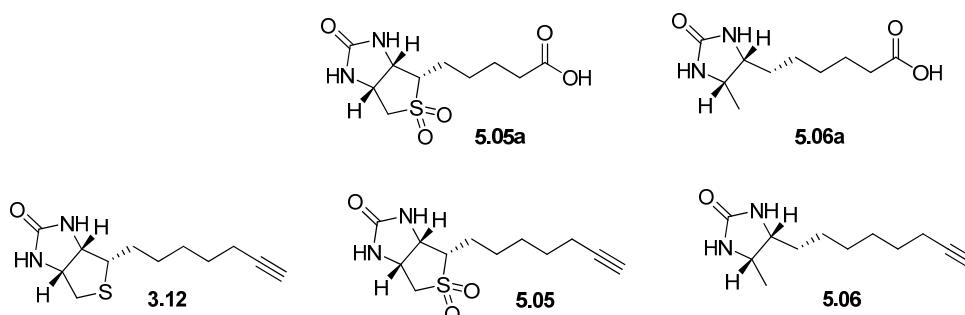
Figure 5.2: Proposed biotin analogues of **3.12**: biotin sulphoxide **5.05** and desthiobiotin **5.06** and literature reported biotin analogues **5.05a**[2] and **5.06a**[3].

5.1.1 Synthesis of biotin 5.01 – 5.04

The synthesis of biotin amine **5.01** was accomplished by the conversion of biotin tosylate **3.18** to biotin azide **5.07** in 86% yield, followed by Staudinger hydrolysis with triphenylphosphine to give biotin amine **5.01** in 18% yield (see Scheme 5.1). The synthesis of biotin alkyl **5.02** and **5.03** followed the modified reported synthesis of **5.02**[4]. Biotin

tosylate **3.18** and **4.43** were separately treated with lithium aluminium hydride in THF to give biotin alkyl **5.02** (56%) and **5.03** (43%), respectively.
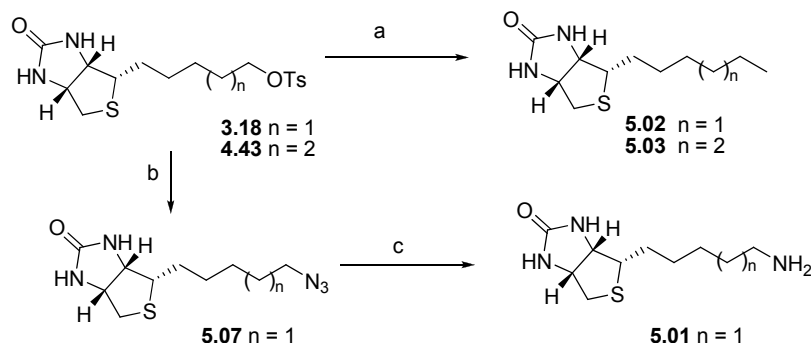
Scheme 5.1: a) LiAlH$_4$, THF, reflux; b) NaN$_3$, DMF; c) i) PPh$_3$, THF; ii) 1:1 H$_2$O/THF.

The synthesis of triazole **5.04** is shown in Scheme 5.2. Following the literature report[5], chloromethylpivalate **5.08** was treated with sodium azide in water to give azidomethylpivalate **5.09** in 72% yield without flash chromatography. A CuAAC reaction of biotin alkyne **3.12** and azidomethylpivalate **5.09** was accomplished using 20 mol% copper nanopowder in 2:1 acetonitrile and water mixture to give triazole **5.10** in 48% yield after flash chromatography. Following a literature procedure for the removal of the pivaloyloxymethyl (POM) group[5-7], triazole **5.10** was treated with 32% ammonia solution in THF to give triazole **5.04** in 43% yield.
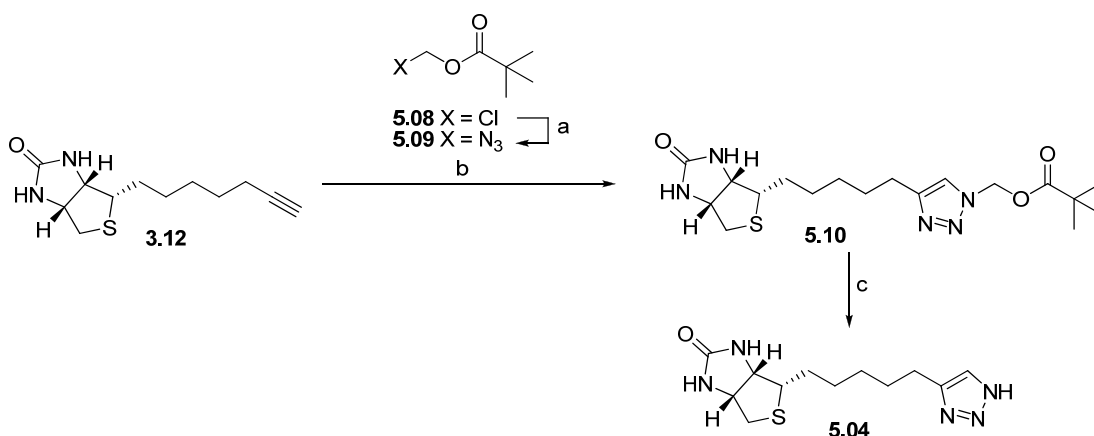
Scheme 5.2: a) NaN$_3$, H$_2$O, reflux; b) 20 mol% Cu nanopowder, 2:1 AcCN/H$_2$O; c) 1:1 32% NH$_{3(aq)}$/THF.

5.1.2 Synthesis of biotin analogues 5.05 and 5.06

The synthesis of biotin sulphone **5.05** was accomplished with treatment of biotin alkyne **3.12** with m-CPBA (Scheme 5.3). High resolution mass spectrometry confirmed the sulphone analogue was formed with M^+H of 271.3558 obtained (as opposed to the sulphoxide).
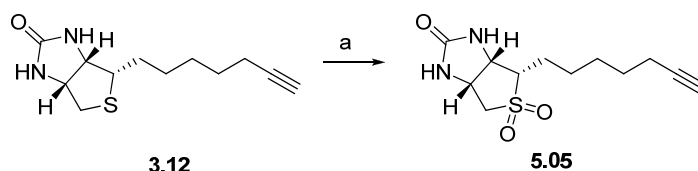
Scheme 5.3: a) *m*-CPBA, 9:1 DMF/DCM.

The synthesis of desthiobiotin **5.06** was accomplished as shown in Scheme 5.4. Commercially available desthiobiotin **5.11** was treated with thionyl chloride to give the methyl ester **5.12** (in quantitative yield), which was subsequently reduced with lithium aluminium hydride to give desthiobiotinol **5.13** in 82% yield. Conversion of the alcohol **5.13** to bromide **5.14** was achieved on treatment with DDQ in DCM (89%). Subsequent reaction with lithium acetylide EDA complex gave desthiobiotin alkyne **5.06** in 50% yield.
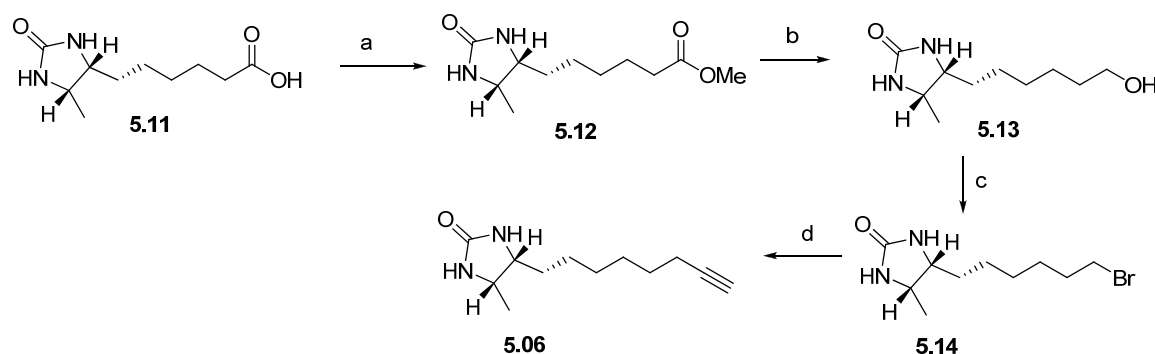
Scheme 5.4: a) $SOCl_2$, MeOH; b) $LiAlH_4$, THF c) DDQ, DCM; d) Li acetylide EDA complex, DMSO.

5.1.3 Enzyme inhibition assay results

The biotin analogues (Figures 5.3 and 5.4) were assayed against SaBPL, EcBPL and HsBPL and the results are shown in Tables 5.1 and 5.2. The assay was performed by collaborators at Molecular Life Science, University of Adelaide, following methodology described by Chapman-Smith and co-workers.[8]
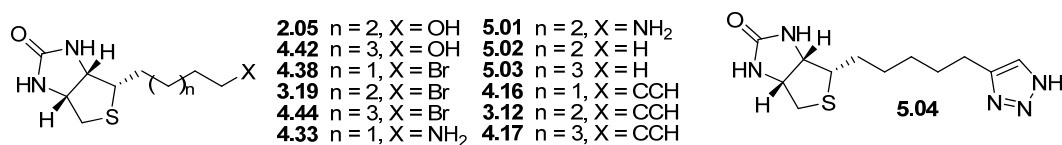
Figure 5.3: Biotin analogues assayed against SaBPL, EcBPL and HsBPL

Table 5.1^a: Enzyme inhibition assay (K_i) for biotin analogues against SaBPL, EcBPL and HsBPL.

Compound	n	R	SaBPL K_i (μM)	*EcBPL* K_i (μM)	*HsBPL* K_i (μM)
2.05	2	OH	3.3 ± 0.25	4.0 ± 0.37	3.9 ± 0.3
4.42	3	OH	>10	>10	>10
4.38	1	Br	>10	>10	>10
3.19	2	Br	>10	>10	>10
4.44	3	Br	>10	>10	>10
4.33	1	NH$_2$	>10	>10	>10
5.01	2	NH$_2$	>10	>10	>10
5.02	1	CH$_3$	0.05 ± 0.01	1.1 ± 0.12	0.14 ± 0.02
5.03	2	CH$_3$	0.52 ± 0.06	7.3 ± 1.9	6.4 ± 1.4
4.16	1	C≡CH	0.08 ± 0.01	0.90 ± 0.08	0.20 ± 0.03
3.12	2	C≡CH	0.30 ± 0.05	7.3 ± 1.0	3.5 ± 0.5
4.17	3	C≡CH	2.4 ± 0.2	20.0 ± 0.3	12.0 ± 1.8
5.04	2	triazole	30 ± 5	N/A	N/A

^{a}Conditions for inhibition assay are described in Chapter 7.

The biotin analogues containing bromine (**4.38**, **3.19** and **4.44**) and amine groups (**4.33** and **5.01**) were inactive against all BPL species with a K_i >10 μM. Interestingly, biotinol **2.07** gave a modest K_i 3-4 μM across all three BPL species assayed, whilst homobiotinol **4.42**, with its extended aliphatic lengths, was inactive against all three BPL. The X-ray crystal structure of biotinol **2.07** bound to SaBPL was solved and this is discussed in Section **5.2**

The biotin alkyne analogues of norbiotin alkyne **4.16**, biotin alkyne **3.12** and homobiotin alkyne **4.17** provided some interesting findings. Decreasing the aliphatic lengths from 8 to 7 and 6 atoms resulting in an increase in potency against SaBPL. Here, homobiotin alkyne **4.17** with the extended aliphatic tail was found to be a moderately potent inhibitor of SaBPL (K_i = 2.4 ± 0.2 μM), whilst shorter aliphatic tails of biotin alkyne **3.12** (K_i = 0.3 ± 0.05 μM) and norbiotin **4.16** (K_i = 0.08 ± 0.01 μM) produced greater potency against SaBPL. Interestingly, all three alkyne analogues were found to be selective for SaBPL. Homobiotin alkyne **4.17**, biotin alkyne **3.12** and norbiotin alkyne **4.16** showed 5, 11 and 2 fold respectively for SaBPL over HsBPL. An X-ray crystal structure of biotin alkyne **3.12** bound to SaBPL was solved and is discussed in Section 5.2.

As eluded to in Section 5.1, the observed potency of biotin alkyne **3.12** toward SaBPL prompted the synthesis of the hydrophobic biotin alkyl **5.02** and homobiotin alkyl **5.03**. Homobiotin alkyl **5.03** proved to be a potent inhibitor of SaBPL (K_i = 0.52 ± 0.06 μM) with 12 and 14 fold selectivity over both HsBPL and EcBPL, respectively. Interestingly, homobiotin alkyl **5.03** was 6 fold less potent against SaBPL than norbiotin alkyne **4.16**, which has the same number of carbons (six) in its aliphatic tail. This suggests that hydrophobic interactions with the carbon chain are also important in the binding of these biotin analogues to SaBPL. As for the biotin alkyne series (**see 3.12**, **4.16**, and **4.17**, Figure 5.3), a shorten aliphatic tail such as biotin alkyl **5.02** results in higher potency against SaBPL (K_i = 0.05 ± 0.01 μM). Interestingly, the 2 fold selectivity towards SaBPL over HsBPL observed for biotin alkyl **5.02** is less significant that that observed for homobiotin alkyl **5.03** which displayed X-fold selectivity. Finally, biotin triazole **5.04** is only a moderately potent inhibitor of SaBPL (K_i = 30 ± 5 μM), but nevertheless suggests that the triazole ring had an additive effect upon binding to SaBPL and thus is important for binding as in triazole **4.01** (see Chapter 4).

A number of conclusions can be drawn based on the inhibition obtained for the biotin analogues shown in Table 5.1. Firstly, it is clear that the design and development of inhibitors of BPL does not necessarily need to focus on both the ATP and biotin binding pocket as was presumed in Chapter 2 – 4 (cf. biotinol-5'-AMP IC_{50} = 0.12 ± 0.01 μM , triazole **4.01** K_i = 0.66 ± 0.15 μM**,** norbiotin alkyne **4.16** K_i = 0.08 ± 0.01 μM). Secondly, whilst it was presumed that the biotin binding pocket is generally conserved between different species (i.e. SaBPL, EcBPL and HsBPL, see chapter 1), the fact that biotin alkyne **3.12** and biotin alkyl **5.03** show some selectivity for SaBPL suggests some differences in the biotin binding pocket of BPLs across different species, that might be exploited to improve selectivity. It seems likely that hydrophobic residues in SaBPL are key to defining further selectivity towards this enzyme.
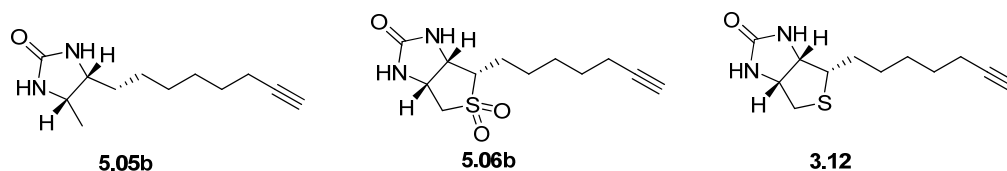
Figure 5.4: Desthiobiotin **5.05b**, biotin sulphone **5.06b** and biotin alkyne **3.12**

The bicyclic analogues **5.05b** and **5.06b** (Figure 5.4) were inactive against BPL from all species (K_i >10 μM, Table 5.2). The limited inhibition observed for biotin analogue **5.05b** and **5.06b** suggests that modification of the bicyclic core of biotin provides limited scope for improving binding affinity.

Table 5.2[a]

Compound	SaBPL K_i (μM)	*EcBPL* K_i (μM)	*HsBPL* K_i (μM)
3.12	3.4 ± 0.25	4.0 ± 0.37	3.9 ± 0.3
5.05b	>10	>10	>10
5.06b	>10	>10	>10

[a]Assay conditions are described in Chapter 7.

5.1.4 Antimicrobial assay results

Norbiotin alkyne **4.16** provided the most potent antibacterial activity, of the derivatives discussed in this section, against clinical isolates of *S. aureus* with MICs of 4 - 16 μg/ml, including methicillin susceptible and resistant strains. Interestingly, biotin alkyl **5.02** whilst not possessing antibacterial properties against the MSSA and MRSA, was active against vancomycin-resistant *Enterococci* (MIC 32 μg/ml). Finally, the toxicity of compounds **2.05**, **4.16**, **3.12** and **5.02** was assessed in a mammalian cell culture model using HepG2 cells. No toxicity was observed when cells were treated with 64 μg/ml of biotinol **2.05**, norbiotin alkyne **4.16**, biotin alkyne **3.12** and biotin alkyl **5.02**.

Table 5.3[a]: Antibacterial activity of norbiotin alkyne **4.16**. MICs are shown for a library of *S. aureus* clinical isolates of coagulase negative and positive strains, including methicillin sensitive (MSSA) and resistant (MRSA) subtypes.

	MIC_{50} (μg/mL)	MIC_{50} (μg/mL)
MSSA (n = 7)	8	16
MRSA (n = 7)	8	16
Coagulase negative Staphylococci (n = 7)	4	8

[a] Antibacterial assay conditions are described in Chapter 7.

5.4 X-ray crystal structure of biotinol 2.05 and biotin alkyne 3.12 bound to SaBPL

The structures of biotin analogues **2.05** and **3.12** bound to SaBPL were solved with resolution of 2.75 Å and 2.65 Å by collaborators at Monash University, Australia using the method prescribed by Pendini and co-workers[9] (see Chapter 7 for crystallisation conditions), as depicted in Figure 5.5. Biotinol and biotin alkyne bind to the biotin binding pocket of SaBPL in a similar fashion, with residues Gln116, Ser93, Thr94 and Arg120 making contact with the ureido ring of both analogues. The same type of interactions was observed in the structures of SaBPL and biotinol-5'-AMP **1.05**, triazole **4.01** and **3.25** (see Section 4.4 for description). The only exception with respect to biotinol **2.05** involved the

hydroxyl group of **2.05** hydrogen bonding with Arg122 (Figure 5.5). Interestingly, biotin alkyne **3.12** appears to show the interaction between its alkyne moiety and biotin binding pocket. Rather the region which the alkyne moiety occupies is largely hydrophobic, consisting of Trp127, β sheets and Leu192.
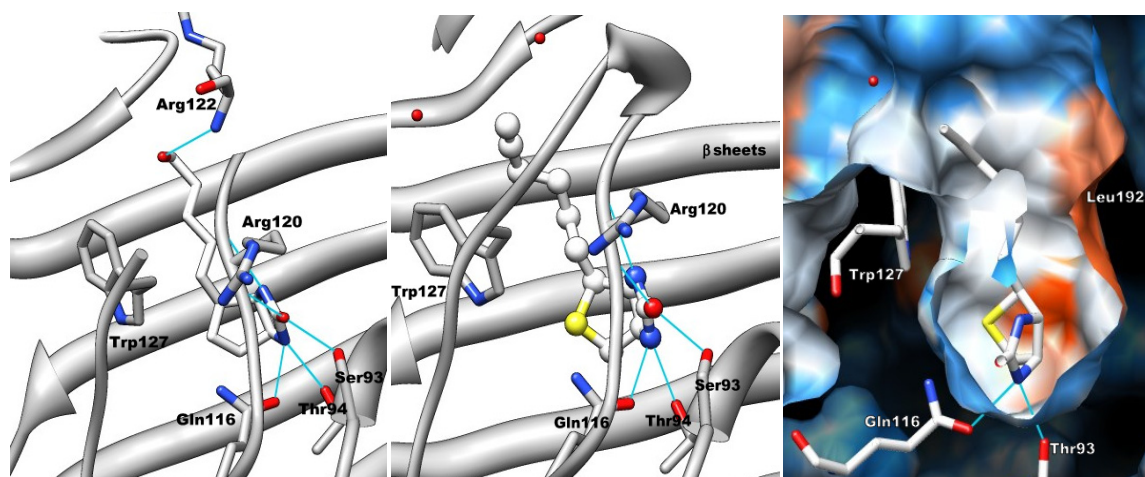
Figure 5.5: 3D depiction of biotinol **2.05**(left) and biotin alkyne **3.12** (centre) bound to SaBPL. The biotin binding loop between Trp127 and Arg120 is hidden to provide clarity for the ligand-enzyme binding. 3D surface depiction of biotin alkyne **3.12** bound to SaBPL with hydrophobic regions highlighted in orange, neutral regions highlighted in white and hydrophilic regions highlighted in blue (right).

5.5 Conclusion

Biotin analogues synthesized in chapters 2 – 4 (**4.16**, **4.17**, **4.38**, **3.19**, **4.44**, **2.05**, **4.42** and **4.33**) and in this chapter (**5.01 – 5.03**), were assayed for inhibitor potency against SaBPL, EcBPL and HsBPL. Norbiotin alkyne **4.16** and biotin alkyl **5.02** proved to be potent inhibitors of SaBPL at nanomolar range with some selectivity (3-fold) over human BPL. A number of the derivatives were potent against clinically significant strains of bacteria. Norbiotin alkyne **4.16** was found to be potent against MRSA, whilst biotin alkyl **5.02** was potent against VRE. The assay results against SaBPL revealed a number of significant trends. It was found that derivatives with hydrophobic functional groups attached to the valeric tail of biotin (see **4.16**, **3.12**, **4.17**, **5.02** and **5.03**) are the most potent against

SaBPL, whilst decreasing the valeric tail of biotin alkyne (see **4.16**, **3.12** and **4.17**) or biotin alkyl (see **5.02** and **5.03**) provided increased potency of SaBPL.

Biotin analogues with modifications upon the thiophene ring (**5.05** and **5.06**) were found to found to have limited activity against SaBPL, EcBPL and HsBPL, thus suggesting there is a limited scope for modifying the bicyclic core of biotin. No further investigation examining modifications upon the biotin ring was undertaken.

5.6 References for Chapter Five

(1)   Kwon, K.; Streaker, E. D.; Beckett, D. *Protein Science* **2002**, *11*, 558.

(2)   Collot, M.; Sendid, B.; Fievez, A. l.; Savaux, C.; Standaert-Vitse, A.; Tabouret, M.; Drucbert, A. S.; Marie Danzé, P.; Poulain, D.; Mallet, J.-M. *Journal of Medicinal Chemistry* **2008**, *51*, 6201.

(3)   Hirsch, J. D.; Eslamizar, L.; Filanoski, B. J.; Malekzadeh, N.; Haugland, R. P.; Beechem, J. M.; Haugland, R. P. *Analytical Biochemistry* **2002**, *308*, 343.

(4)   Liu, F.-T.; Leonard, N. J. *Journal of the American Chemical Society* **1979**, *101*, 996.

(5)   Loren, J. C.; Krasiński, A.; Fokin, V. V.; Sharpless, K. B. *Synlett* **2005**, *2005*, 2847.

(6)   Yang, L.; Xu, W.; Chen, F.; Liu-Chen, L.-Y.; Ma, Z.; Lee, D. Y. W. *Bioorganic & Medicinal Chemistry Letters* **2009**, *19*, 1301.

(7)   Kočalka, P.; Andersen, N. K.; Jensen, F.; Nielsen, P. *ChemBioChem* **2007**, *8*, 2106.

(8)   Chapman-Smith, A.; Cronan, J. E. *Trends in Biochemical Sciences* **1999**, *24*, 359.

(9)   Pendini, N. R.; Polyak, S. W.; Booker, G. W.; Wallace, J. C.; Wilce, M. C. J. *Acta Crystallographica Section F* **2008**, *64*, 520.

Chapter Six

6.1 Introduction

The design and development of SaBPL inhibitors described in Chapters 3 and 4 highlighted a novel class, as shown in Scheme 6.1. This class of inhibitor was found to be synthetically attractive compared to that for the non-selective BPL inhibitor biotinol-5'-AMP **1.05**. The synthesis utilising accessible alkyne and azide building blocks that were conjugated by a facile and reliable CuAAC reaction to form the 1,4-triazole linker. Importantly, from this work the triazole **4.01** was identified as a potent and selective inhibitor of SaBPL with a $K_i = 0.66 \pm 0.05$ µM and >180-fold selectivity over human BPL. The X-ray crystal structure of **4.01** bound to SaBPL was solved as discussed in section 4.4. This structure revealed that **4.01** adopted the requisite conformation on binding to present both the adenine and biotin components to their respective pockets in SaBPL. The 1,4-triazole linker of **4.01** provided hydrogen bonding interactions with residues Arg122, Arg125 and Trp127 (see Section 4.4 for detail).
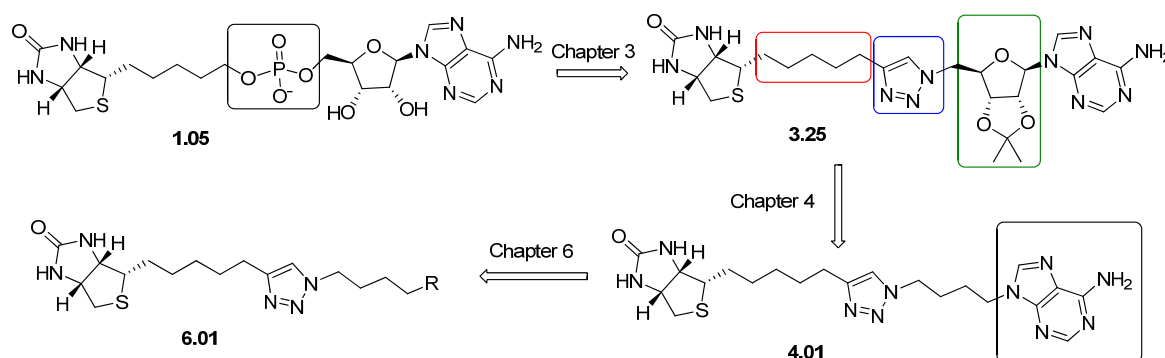
Scheme 6.1: A schematic summary of potent and selective triazole inhibitors developed in Chapters 3 - 6. The boxes highlighted indicate the components that were examined.

This next chapter builds on this result with the design, synthesis, and assay of further triazole-based inhibitors of SaBPL based on the general structure **6.01** (see Scheme 6.1). The proposed triazole analogues **6.02-6.10** (Figure 6.1), discussed herein, retain the biotin and triazole components of earlier examples, whilst modifying the adenine component with aromatic scaffolds such as phenyl and naphthyl and a privileged 2-benzoxazolone scaffold.[1,2] These groups were chosen as possible adenine analogues. The most potent triazole inhibitor **6.10** of SaBPL was further investigated by replacing the triazole linker of

6.10 with a phosphodiester linker, as is found in biotinol-5'-AMP **1.05**, see analogue **6.34** and Chapter 2 for discussion on phosphodiester inhibitors of SaBPL.
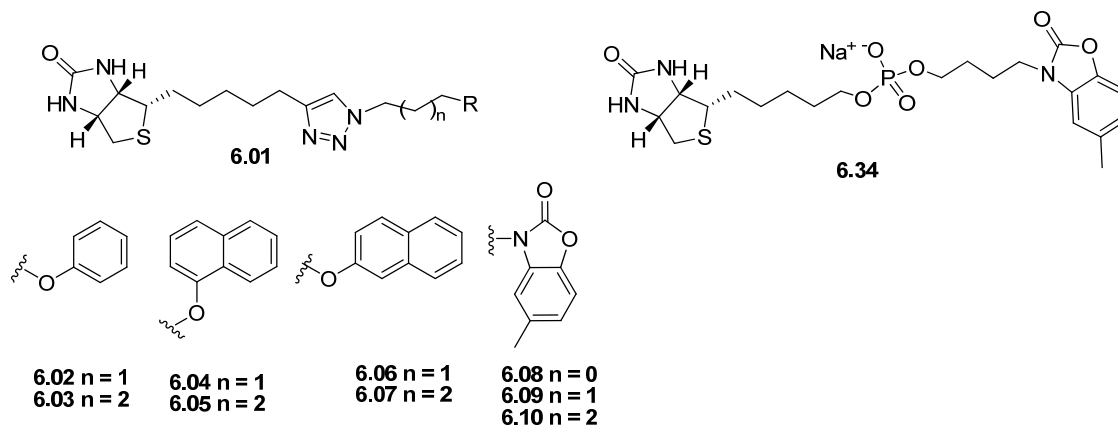
Figure 6.1: The proposed triazole analogues **6.02 – 6.10** and phosphodiester **6.34**.

6.2 Design and synthesis of 1,4-triazole 6.02 – 6.10

The design of triazole inhibitors **6.02 – 6.10**, from Figure 6.1 was based on the SAR data presented in Chapters 3, 4 and 5 as summarised in Figure 6.2.
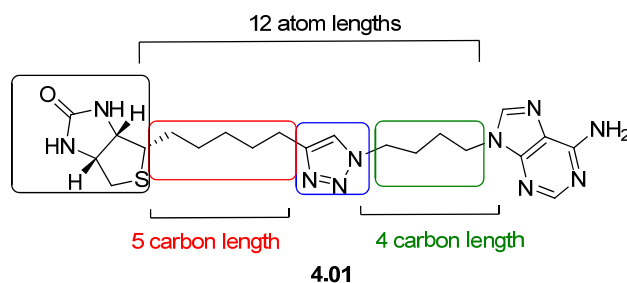
Figure 6.2: Lead inhibitor, triazole **4.01** with the boxes highlighting the components investigated in Chapters 4 and 5.

1. Replacement of the pentose group of triazole **3.25** with the acyclic chain of triazole **4.01** resulted in increased potency, discussed in Chapter 3.

2. Modification of the biotin bicyclic core resulted in a loss of potency against SaBPL (see Chapter 5). In particular, it was found that replacement of the thiophene ring of biotin alkyne **3.12** with biotin sulphoxide **5.06** or desthiobiotin **5.05** resulted in significant reduction in potency toward SaBPL.

3. The appropriate orientation and configuration of the triazole linker for inhibition is presented in Figure 6.2. The key observations are: a 1,4-triazole (as found in triazole **4.01)** gives more potent inhibitors compared to a 1,5-triazole (see Section 4.3.1) and the optimal tether lengths between the biotin and triazole is 5 carbons and that between the triazole and adenine is 4 carbons as in triazole **4.01** (see Figure 6.2).

Based on this SAR data it was concluded that a 1,4-triazole is central to this class of inhibitor and that little modification to the biotin group is accommodated. Thus it was considered that the most fruitful approach to improving potency was to focus on analogues of the adenine group. This is epitomised with the general structure **6.01** (Figure 6.2).

The choice of adenine analogues (phenyl **6.02** and **6.03**, naphthyl **6.04** – **6.07** and 2-benzoxazolone **6.08 – 6.10**) was guided by an examination of the ATP binding pocket in X-ray crystal structures of SaBPL. This reveals two key characteristics relevant to design:

1) The ATP binding pocket is dominated by hydrophobic residues found within the ATP binding loop (see Figure 6.3). Ile224, Ala228 and Phe220 define a hydrophobic region within the ATP binding loop that presents to the plane of the adenine ring, as seen with triazole **4.01** and biotinol-5'-AMP **1.05** bound to SaBPL (see Figure 6.2 and Chapters 2 and 4 for discussion).

2) The ATP binding pocket is also dominated by Trp127. Based on the X-ray crystal structures of triazole **4.01** and biotinol-5'-AMP **1.05** bound to SaBPL, Trp127 is clearly involved in a displaced parallel π interaction with the adenine ring.
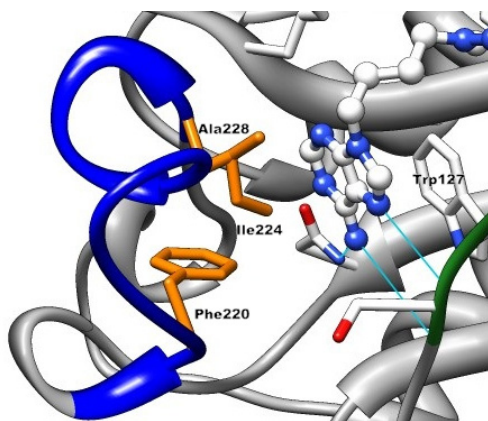
Figure 6.3: The ATP binding pocket of SaBPL with triazole **4.01** bound (see Chapter 4 for further discussion). Hydrophobic residues Phe220, Ile224 and Ala228 are highlighted in orange and Trp127 is shown in green. The ATP binding loop is depicted with blue ribbon.

6.2.1 Synthesis of azide building blocks 6.16, 6.17, 6.22 – 6.25 and 6.31 – 6.33

A retrosynthetic analysis of these triazole structures (**6.02 – 6.10**) suggests that they would be prepared by coupling the azides **616**, **6.17**, **6.22 – 6.25** and **6.31 – 6.33** (see Section 6.2.2) to alkyne **3.12**. The azides were prepared as shown in Schemes 6.2 and 6.3.

Phenol was treated with potassium carbonate and the resulting phenoxide separately alkylated with alkyl dihalide **6.12** and **6.13** to give **6.14** and **6.15** respectively, see Scheme 6.2. The halides **6.14** and **6.15** were then reacted with sodium azide in DMF to give the azide **6.15** and **6.16.** The 1-naphthyl (**6.22** and **6.23**) and 2-naphthyl (**6.24** and **6.25**) examples were prepared from 1-naphthol and 2-naphthol respectively using the same conditions to those used to prepare **6.15** and **6.16**. Formation of the azides was confirmed by FT-IR spectroscopy with azide absorptions between 2093 – 2098 cm^{-1}.
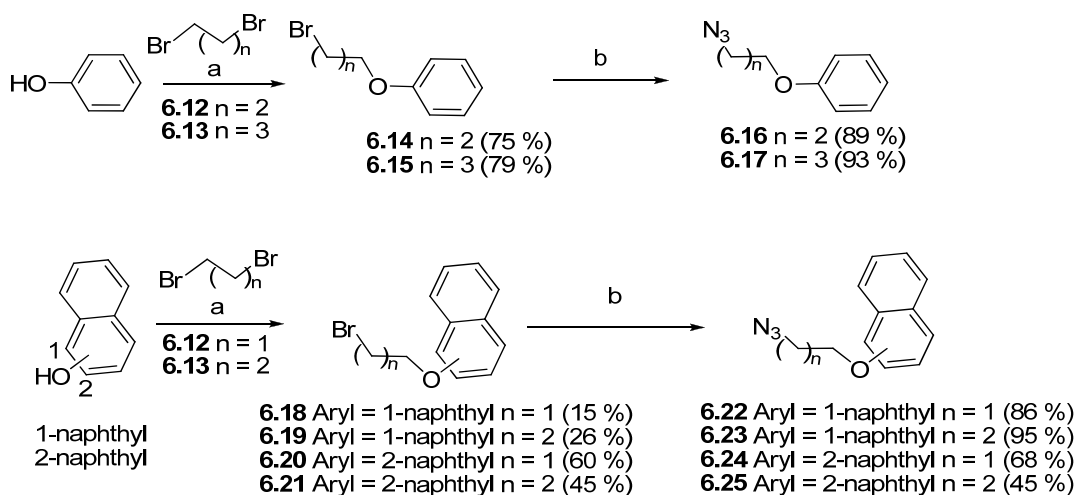
Scheme 6.2: a) Br(CH$_2$)$_n$Br, K$_2$CO$_3$, DMF; b) NaN$_3$, DMF.

2-Benzoxazolone **6.27** was obtained by cyclising 2-amino-cresol with CDI as shown in Scheme 6.3. This material was treated with potassium carbonate, followed by separate reactions with alkyl dihalide **6.26, 6.12** and **6.13** in DMF, to give halide **6.28 – 6.30** respectively. These halides were converted to the corresponding azides **6.31 – 6.33** on reaction with sodium azide in DMF, as shown in Scheme 6.3.
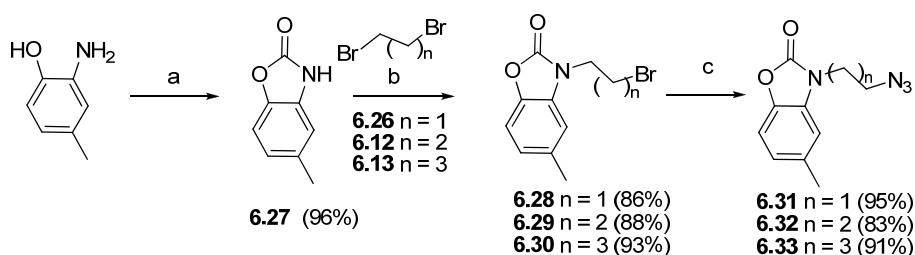
Scheme 6.3: a) CDI, DCM; b) $Br(CH_2)_nBr$, K_2CO_3, DMF; c) NaN_3, DMF

6.2.2 Synthesis of 1,4-triazole 6.02 – 6.10 via CuAAC Reaction

The synthesis of triazoles **6.02 – 6.10** was accomplished by separate treatment of azides **6.16**, **6.17**, **6.22 - 6.25** and **6.31 – 6.33** with biotin acetylene **3.12** in the presence of copper nano powder (20 mol%) in 2:1 acetonitrile/water (see Table 6.1, next page). All CuAAC reactions in Table 6.1 were obtained in good yields.

2D ROESY NMR spectra of **6.03, 6.07** and **6.10** indicated through-space correlations between protons H_A and H_B with H_A and H_C, which is consistent with a 1,4-disubstution rather than 1,5-disubstitution pattern (Figure 6.4). This is the expected result based on the CuAAC reaction used in their preparation. A crystal structure of triazole **6.10** bound to SaBPL confirmed the 1,4-disubstitution pattern for that particular compound (see Section 6.5 for discussion).
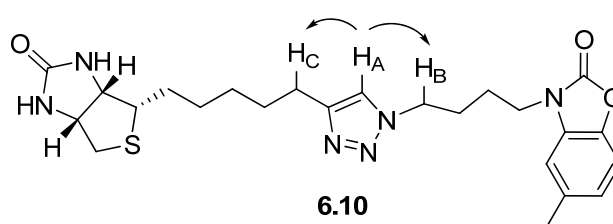
Figure 6.4: A depiction of through-space correlations (arrows) observed in ROESY 2D ^{1}H NMR experiment. Triazole **6.10** is shown as a representative example.

Table 6.1[a]: CuAAC between alkyne **3.12** and azides **6.16**, **6.17**, **6.22 – 6.25**, **6.31** and **6.32**
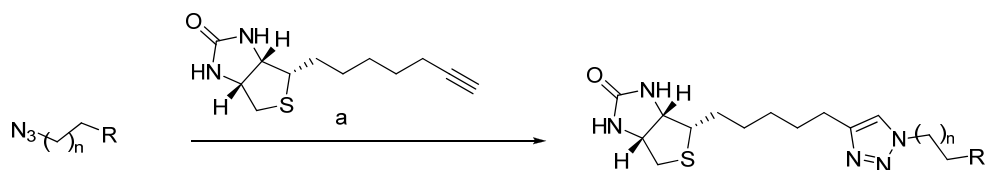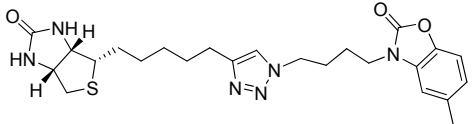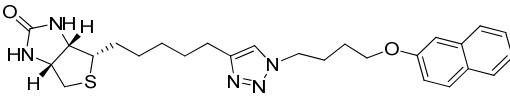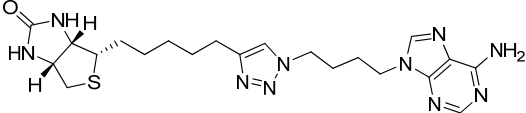
Reactant	R (product)	n =	Yield[a]	Reactant	R (product)	n =	Yield[a]
6.16	**6.02**	2	56%	**6.24**	**6.06**	2	51%
6.17	**6.03**	3	64%	**6.25**	**6.07**	3	74%
6.22	**6.04**	2	34%	**6.31**	**6.08**	1	65%
6.23	**6.05**	3	41%	**6.32**	**6.09**	2	64%
				6.33	**6.10**	3	69%

[a] Conditions: Cu nanopowder, 2:1 AcCN/H$_2$O, 4 h, sonication, 35 $^{\circ}$C; [b] Isolated yields after flash chromatography

6.3 BPL inhibition and antimicrobial results

1,4-Triazole **6.02 – 6.10** were assayed for inhibitor potency against SaBPL, EcBPL and HsBPL and the results are shown in Table 6.2. The assays were performed by collaborators at Molecular Life Science, University of Adelaide, following method described by Chapman-Smith and co-workers, (see Chapter 7 for assay conditions).[3]

Table 6.2[a,b]: Inhibition by select triazole analogues of enzymatic activity against SaBPL, EcBPL and HsBPL

Compound	SaBPL		EcBPL	HsBPL
	K_i (µM)	IC_{50}(µM)	IC_{50}(µM)	IC_{50}(µM)
6.10	0.09 ± 0.02	0.53 ± 0.01	>200	>200
6.07	1.17 ± 0.17	7.0 ± 1.0	>200	>200
4.01	$0.66 + 0.05$	4.0 ± 0.9	>200	>200

[a] Assay conditions are described in Chapter 7, [b] Triazoles 6.02 – 6.06, 6.08 and 6.09 were found to have a K_i > 10 µM.

2-Naphthyl **6.07** was found to be potent inhibitor of SaBPL with $IC_{50} = 7.0 \pm 1.0$ µM with at least an 28-fold selectivity over EcBPL and HsBPL. While the 2-naphthyl **6.07** was less potent than the parent lead structure **4.01** (7 fold decrease), the retained selectivity towards SaBPL highlights the importance of the 1,2,3-triazole ring for selectivity. Moreover, this result validated the general scaffold structure **6.01** as an ideal starting point for future structure based drug design. Interestingly, the 2-naphthyl ring of **6.07** had limited potential for hydrogen bonding with SaBPL as compared to the parent lead adenine structure **4.01**. This suggests that hydrogen bonding interactions within the ATP binding pocket may have

a limited role in binding affinity and that electrostatic interactions may dominate the ATP binding pocket. The significance of the electrostatic interactions is consistent with the observed limited activity of the sterically smaller phenyl analogue **6.02** (K_i >10 µM) and **6.03** (K_i >10 µM). However, further investigation is required to accurately determine the extent of the electrostatic interactions of 2-naphthyl **6.07**.

2-Benzoxazolone **6.10** was found to be highly potent and selective towards SaBPL with K_i = 0.09 ± 0.02 µM (IC_{50} = 0.53 ± 0.01 µM). Significantly, this inhibitor was 2 fold more potent toward SaBPL compared to the lead adenine structure **4.01**, while retaining or perhaps improving selectivity over HsBPL and EcBPL (400 fold, IC_{50} >200 µM). This derivative was only 5 fold less potent compared to biotinol-5'-AMP **1.05**, which is devoid of selectivity. Further investigation of **6.10** was undertaken by solving its crystal structure when bound to SaBPL (see Section 6.5 below) and antimicrobial assays against a library of gram negative and gram positive microbes. The antimicrobial assay results revealed 2-benzoxazolone **6.10** prevented cell growth of *S. aureus* ATCC 49775 by 80% at 8µg/ml. However, no inhibition of growth was observed for other gram negative microbes such as *Enterococcus faecalis* or *Enterococcus faecium*. Given the limited inhibition 2-benzoxazolone **6.10** against EcBPL, this compound also proved to have limited effect against the gram negative *E. coli*. Finally, 2-benzoxazolone **6.10** exhibited no toxicity in a human HepG2 cell culture model. This concurs with the limited activity of triazole **6.10** against HsBPL (IC_{50} > 200 µM).

6.4 X-ray crystal structure of 1,4-triazole 6.10 bound to SaBPL

The structure of triazole **6.10** bound to SaBPL was solved with a resolution of 3.10 Å by collaborators at Monash University, Australia using the method prescribed by Pendini and co-workers[4] (see Figure 6.5 and Chapter 7 for crystallisation conditions). 2-Benzoxazolone **6.10** was found to retain the characteristic binding features found in other SaBPL inhibitors presented in this thesis (see Section 2.5, 4.4 and 3.4). In particular, 2-benzoxazolone **6.10** adopts a U-shaped conformation with the biotin and 2-benzoxazolone components binding directed into their respective pockets. This U-shaped conformation placed the ureido ring of biotin in the vicinity of residues Ser93, Thr94, Gln116 and Arg120 and subsequently provided the characteristic hydrogen bonding interactions as shown in Figure 6.5.
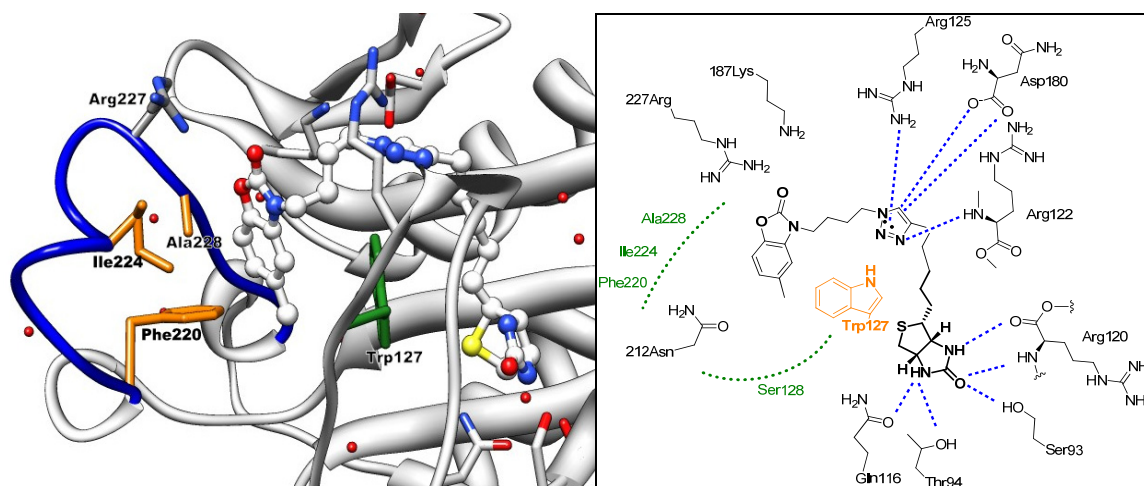
Figure 6.5: A 3D depiction of triazole **6.10** bound to SaBPL (left); a 2D depiction of the hydrogen bonding interactions (shown in blue dashes) between triazole **6.10** and SaBPL (right).

The placement of the triazole ring of **6.10** dictates hydrogen bonding interactions with residue Arg122, Arg125 and Asp180 and edge-to-face π interaction with Trp127 of SaBPL (Figure 6.5). These interactions are similar to those observed for triazole **4.01**, albeit with an additional hydrogen bond between **6.10** and Asp180 (Figure 6.6). The commonality of hydrogen bonds observed for the triazole rings of **4.01** and **6.10** highlights this as a critical interaction for this class of inhibitor.
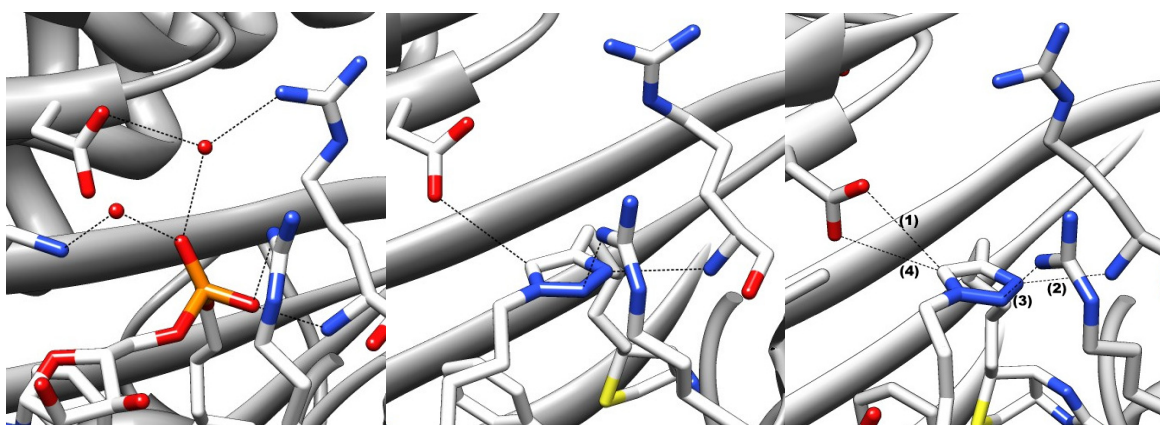
Figure 6.6: Close up of phosphate binding domain and biotinol-5'-AMP **1.05** (left), triazole **4.01** (centre) and triazole **6.10** (right). (Hydrogen bonding distances for **6.10** [(1) = 3.59 Å, (2) = 2.96 Å, (3) = 2.71 Å, (4) = 3.44 Å]. See Section 2.5 and 4.4 for hydrogen bonding distances for **1.05** and **4.01**)

The crystal structure of 2-benzoxazolone **6.10** further reveals that the 2-benzoxazolone ring maintains a displaced π interaction with Trp127 as observed with the adenine ring of triazole **4.01** when bound to SaBPL. As shown in Figure 6.7, the angle placement of the 2-benzoxazolone is accommodated by the grooved hydrophobic region created by Ile224 Ala228 and Phe220 and highlighted in orange. Finally, the hydrophilic region of the ATP binding pocket, containing residue Arg227, does not appear to provide any hydrogen bonding interactions with the carbamate of **6.10** (3.60 Å between guanidium group of Arg227 and carbamate ring).
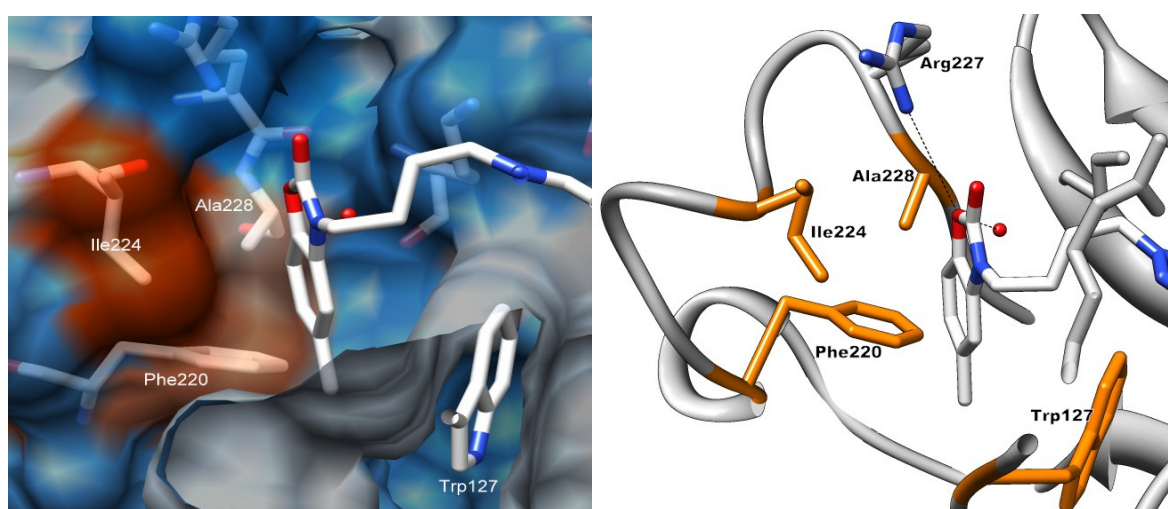
Figure 6.7: A 3D depiction of the ATP binding pocket of SaBPL with 2-benzoxazolone **6.10** bound (left). The orange surface signifies the hydrophobic region of the ATP pocket, whilst the blue signifies the hydrophilic regions of the ATP pocket. The 3D depiction of the ATP binding pocket with hydrophobic residues highlighted in orange (right).

6.5 Design and synthesis of phosphodiester 6.34

Biotinol-5'-AMP **1.05**, discussed in chapter 2, was reported to contain an intricate network of hydrogen bonding interactions between its phosphodiester linker and SaBPL (Figure 6.8). As discussed above, 1,4-triazole **6.10** and **4.01** lacks this extensive hydrogen bonding network, albeit containing three hydrogen bonds between its triazole ring and SaBPL (Figure 6.8). It is thus suggested that the presence of the phosphodiester group and its' the intricate network of hydrogen bonds was a contributory factor for biotinol-5'-AMP **1.05** potency against SaBPL ($IC_{50} = 0.12 \pm 0.01$).

Conversely, the presence of the 2-benzoxazolone in **6.10** was suggested to be favourable for binding in the ATP pocket of SaBPL, with its electrostatic interactions, compared with the adenine ring of **4.01** (see discussed above). It is noteworthy that the adenine ring of **4.01** and biotinol-5'-AMP **1.05** bind in same orientation and adopting the same interactions.

Thus we postulated that combining both the phosphodiester linker and 2-benzoxazolone component in the one structure would take advantage of both hydrogen bonding and electrostatic interactions within SaBPL. To this end, the replacement of 1,4-triazole linker of **6.10** with a phosphodiester linker to give **6.34** was investigated and is described below.
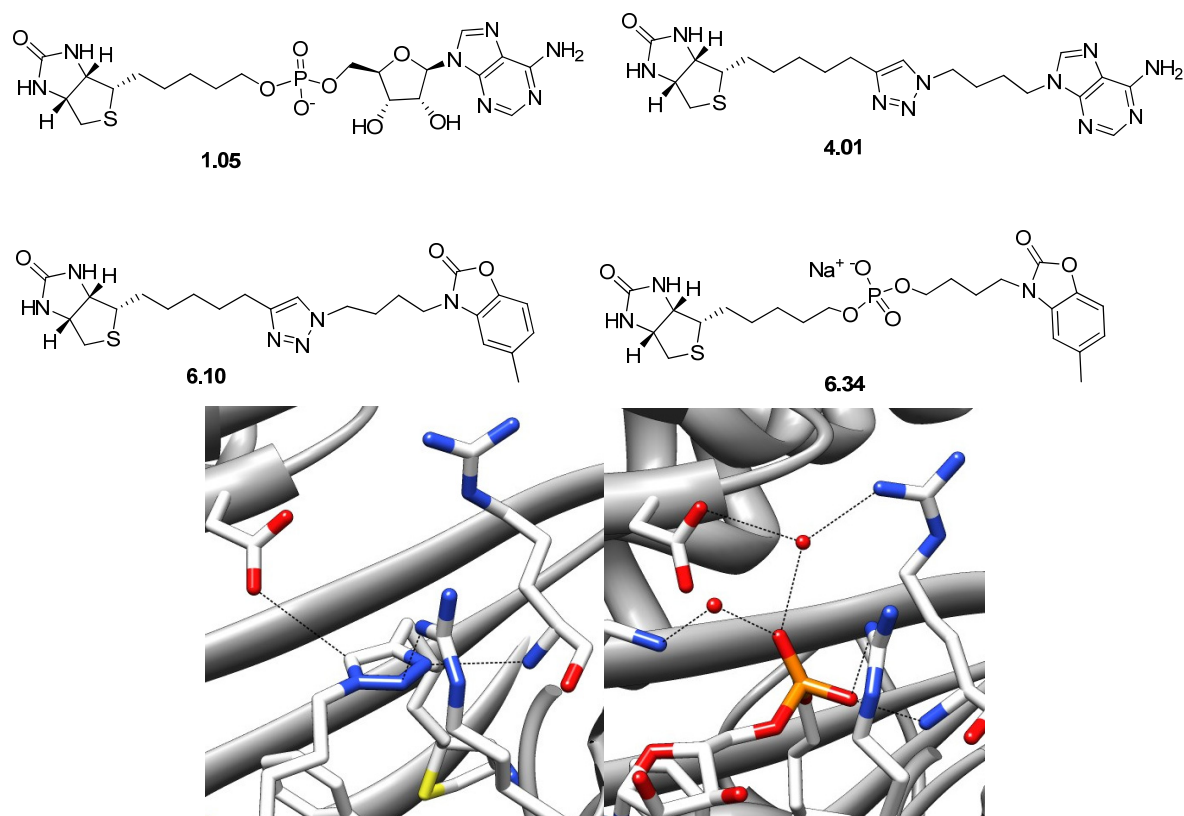
Figure 6.8: Potent inhibitors of SaBPL (**1.05**, **4.01**, **6.10**). X-ray crystal structure of triazole **4.01** and biotinol-5'-AMP **1.05** bound to SaBPL, focusing on the phosphate binding domain (bottom). As shown, the triazole ring of **4.01** was found to provide three hydrogen bonding interactions (not shown is the edge to face π interaction). Biotinol-5'-AMP **1.05** provided four hydrogen bonding interactions.

Synthesis of phosphodiester 6.34

The synthetic strategy to obtain **6.34** was inspired by the approach developed for the preparation of biotinol-5'-AMP (see Section 2.3). The overall synthesis of benzoxazolone **6.34** is shown in Scheme 6.4.
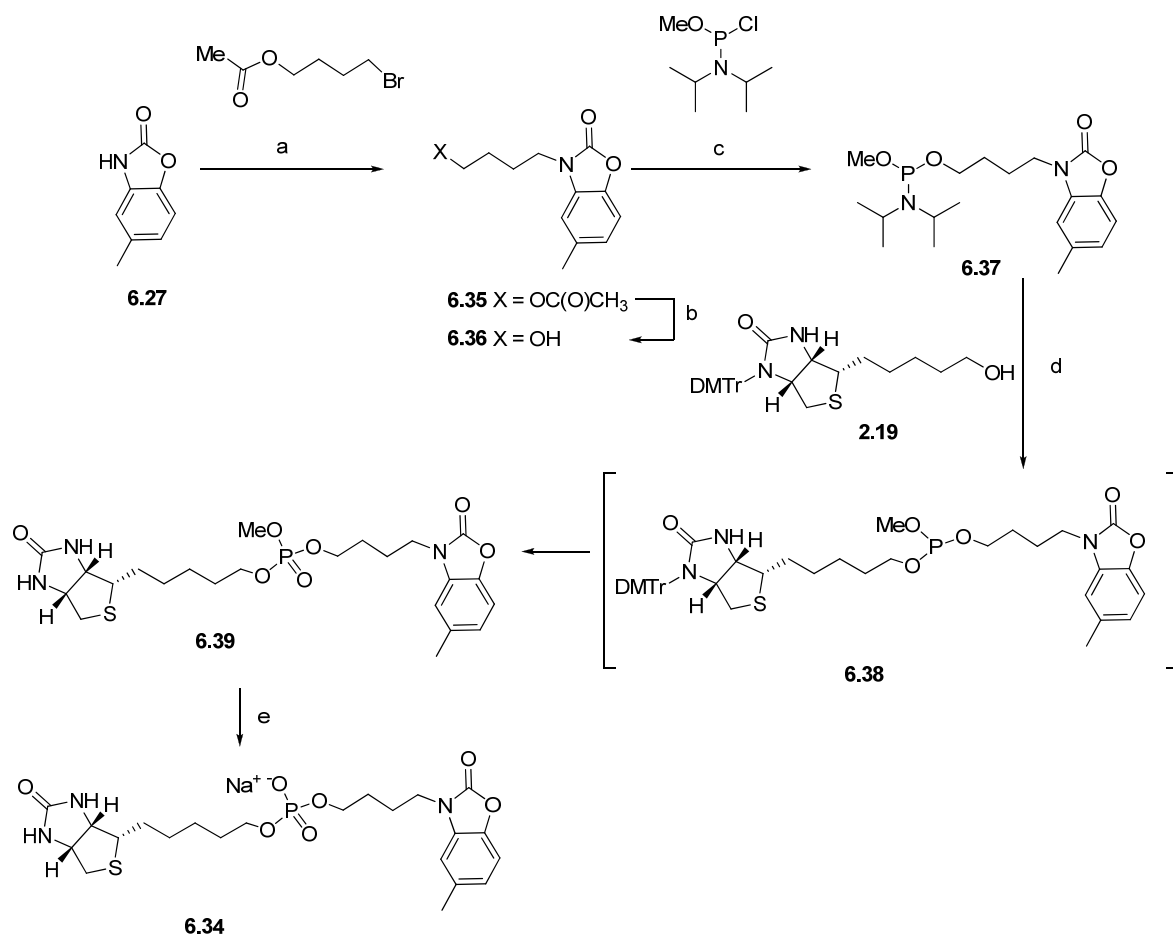
Scheme 6.4: a) K_2CO_3, TBAI, DMF; b) LiOH, 1:1 THF/H_2O c) Et_3N, DCM; d) i) 5-ETT, AcCN; ii) TBHP; iii) 5% TFA, DCM; f) NaI, acetone, 60 ^{o}C.

The synthesis of phosphodiester **6.34** required access to the phosphite precursor **6.37** as shown in Scheme 6.4. Alkylation of 2-benzoxazolone with 4-bromo-butyoxylacetate gave **6.35** in 78% yield. Hydrolysis of the acetate with lithium hydroxide then gave **6.35** in 78% yield. Phosphitylation of **6.36** with *N,N*-diisopropyl-methoxyphosphonamidic chloride gave the crude phosphite **6.37** The crude phosphoramidite **6.37** was subsequently treated with 5-ethylthio-tetrazole and DMTr-biotinol **2.19** in acetonitrile to give **6.38**, the phosphite of which was oxidised with *tert*-butoxyl hydrogen peroxide followed by

acidification with 5% TFA to give phosphotriester **6.39** in 39% yield from **6.36**. Finally, **6.39** was demethylated on reaction with NaI in acetone, under reflux, to give **6.34** in 67% yield after purification by reversed phase HPLC.

Phosphodiester **6.34** was assayed for inhibitor potency against SaBPL. The assays were performed by collaborators at Molecular Life Science, University of Adelaide, following method described by Chapman-Smith and co-workers.[3] Interestingly, this analogue was found to have limited potency compared to its triazole counterpart (K_i >50 μM). This unexpected result requires further investigation.

6.6 Conclusion

1,4-Triazole analogues **6.02 – 6.10** were successfully synthesized using CuAAC reactions in yields of 34 – 74%. Enzyme inhibition against SaBPL, EcBPL and HsBPL revealed that both triazole **6.07** and **6.10** were selective and potent inhibitors of SaBPL. Triazole **6.10** was the most active triazole inhibitor against SaBPL (IC_{50} = 0.53 ± 0.01 μM). X-ray crystallography of triazole **6.10** bound to SaBPL was undertaken. This revealed that triazole **6.10** bound to SaBPL in the characteristic U-shaped conformation and adopted the characteristic hydrogen bonding interactions between the biotin component and biotin binding pocket and between the 1,4-triazole linker and the phosphate binding domain. Furthermore, the binding mode of the 2-benzoxazolone ring of **6.10** within the ATP binding pocket revealed limited hydrogen bonding interactions but rather electrostatic interactions were observed.

The phosphodiester analogue of the most potent triazole inhibitor was synthesized, phosphodiester **6.34**. This analogue retained the biotin and 2-benzoxazolone component of **6.10**, but with a phosphodiester linker in place of the 1,4-triazole. Whilst it was suggested the phosphodiester linker would provide additional hydrogen bonding interactions, the inhibition assay results for phosphodiester **6.34** (>50 μM) against SaBPL did not support this assertion. Rather, the inhibition results suggested that other underlying factors may be involved. Further work is required to understand and potentially exploit this finding.

Future work in developing potent SaBPL inhibitors might involve extending and expanding upon the general scaffold of **6.01** and the most potent triazole inhibitor **6.10**. Analogue **6.10** was a potent ((IC_{50} = 0.53 ± 0.01 μM) and selective inhibitor of SaBPL,

with corresponding antibacterial activity and no toxicity to human cells examined. The 2-benzoxazolone motif is a privileged scaffold and as such can be chemically manipulated and elaborated upon to further improve potency, selectivity and solubility for *in vivo* studies.

6.7 Reference for Chapter Six

(1)   Poupaert, J.; Carato, P.; Colacino, E. *Current Medicinal Chemistry* **2005**, *12*, 877.

(2)   Costantino, L.; Barlocco, D. *Current Medicinal Chemistry* **2006**, *13*, 65.

(3)   Chapman-Smith, A.; Cronan, J. E. *Trends in Biochemical Sciences* **1999**, *24*, 359.

(4)   Pendini, N. R.; Polyak, S. W.; Booker, G. W.; Wallace, J. C.; Wilce, M. C. J. *Acta Crystallographica Section F* **2008**, *64*, 520.

Chapter Seven

7.1 General methods

All reagents were from standard commercial sources and of reagent grade or as specified. Solvents were from standard commercial sources, except for anhydrous THF, anhydrous methanol, anhydrous dichloromethane and anhydrous acetonitrile which were dried and distilled according to literature procedures[1]. Reactions were monitored by ascending TLC using precoated plates (silica gel 60 F_{254}, 250 μm, Merck, Darmstadt, Germany), spots were visualised under ultraviolet light at 254 nm and with either sulphuric acid-vanillin spray, potassium permanganate dip or Hanessian's stain. Column chromatography was performed with silica gel (40-63 μm 60 Å, Davisil, Grace, Germany). HPLC was performed on HP Series 1100 with Phenomenex Gemini C18 5 μM (250 x 4.60 mm) for Analytical HPLC and Phenomenex Luna C18 10 μM (50 x 10.00 mm) for Semi-preparative HPLC. Samples were dissolved in water, acetonitrile or dimethylformamide. Melting points were recorded uncorrected on a Reichert Thermovar Kofler microscope. ^{1}H and ^{13}C NMR spectra were recorded on Varian Gemini model (200 MHz), Varian Gemini 2000 (300 MHz) or a Varian Inova 600 MHz. Chemical shifts are given in ppm (δ) relative to the residue signals, which in the case of DMSO-d_6 were 2.55 ppm for ^{1}H and 39.55 ppm for ^{13}C, $CDCl_3$ were 7.26 ppm for ^{1}H and 77.23 ppm for ^{13}C and D_2O was 4.79 for [1]H. ^{31}P NMR spectra were recorded on a Varian Gemini 2000 (32 MHz), with chemical shifts given in ppm (δ) and referenced against external standard of 85% H_3PO_4 in H_2O. Structural assignment was confirmed with COSY, ROESY, HMQC and HMBC. Nomenclature describing proton assignment for biotin and triazole containing compounds are shown in Figure 1. High-resolution mass spectra (HRMS) were recorded on a Thermo Fisher Scientific LTQ orbitrap FT MS equipment (Δ < 2 ppm) at Adelaide Proteomics, University of Adelaide and Brucker micrO TOF-Q at The Australia Wine Research Institute. Low resolution mass spectra (LRMS) were recorded on Finnigan MAT LCQ spectrometer. Infrared spectra were recorded on an ATI Mattson Genesis Series FTIR spectrophotometer as nujol mulls or neat as denoted or recorded on PerkinElmer Spectrum 100 FTIR with a Universal Zinc Selenide crystal ATR attachment.
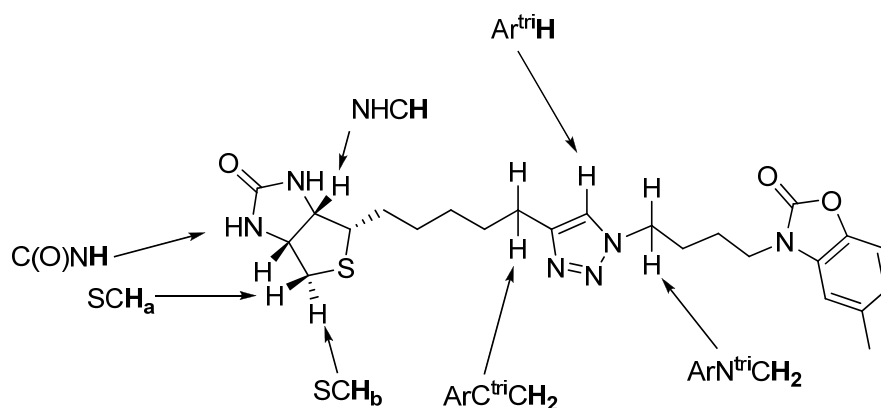
Figure 7.1: Nomenclature describing proton assignment (bold atoms highlighted). 1,4-Triazole **6.10** is shown as a representative example.

7.2 Biological Methods

In vitro biotinylation assays:

Quantitation of BPL catalysed ^{3}H-biotin incorporation into the biotin domain substrate was performed as previously described [2,3]. The IC_{50} value of each compound was determined from a dose-response curve by varying the concentration of the inhibitor under the same enzyme concentration. The data was analysed with GraphPad Prism using a non-linear fit of $\log_{10}$ (inhibitor) vs. normalized response. The K_i, the absolute inhibition constant for a compound, was determined using Eq1 [4]:

$$Eq1. \quad K_i = \frac{IC_{50}}{1 + \dfrac{[S]}{K_m}}$$

where K_m is the affinity of the substrate for the enzyme ([biotin] =1 µM) and [S] is the substrate concentration ([biotin] =5 µM).

The mode of inhibition was investigated by varying the concentrations of inhibitor alongside varying the concentrations of ^{3}H-biotin. The data was plotted as double reciprocal plots and assessed using Lineweaver-Burk analysis.

Antibacterial Activity Evaluation:

Antimicrobial activity of the compounds was determined by a microdilution broth method as recommended by the CLSI (Clinical and Laboratory Standards Institute, Document

M07-A8, 2009, Wayne, Pa.) with cation-adjusted Mueller-Hinton broth (Trek Diagnostics Systems, U.K.). Compounds were dissolved using DMSO. Serial two-fold dilutions of each compound were made using DMSO as the diluent. Trays were inoculated with 5 x 10^4 CFU of each strain in a volume of 100 μL (final concentration of DMSO was 3.2 % (v/v)), and incubated at 35° C for 16-20 hours. Growth of the bacterium was quantitated by measuring the absorbance at 620 nm.

Assay of cytotoxicity:

HepG2 cells were suspended in Dulbecco-modified Eagle's medium containing 10% fetal bovine serum, and then seeded in 96-well tissue culture plates at either 5 000, 10 000 or 20 000 cells per well. After 24 hours, cells were treated with varying concentrations of compound, such that the DMSO concentration was consistent at 4% (v/v) in all wells. After treatment for 24 or 48 hours, WST-1 cell proliferation reagent (Roche) was added to each well and incubated for 0.5 hours at 37° C. The WST-1 assay quantitatively monitors the metabolic activity of cells by measuring the hydrolysis of the WST-1 reagent, the products of which are detectable at absorbance 450 nm.

X-ray crystallography:

Apo-*Sa*BPL was buffer exchanged into 50 mM Tris HCl pH 7.5, 50 mM NaCl, 1 mM DTT and 5% (v/v) glycerol, and concentrated to 5 mg/mL. Each compound was then added to BPL in a 10:1 molar ratio. The complex was crystallized using the hanging drop method at 4°C in 8 – 12% Peg 8000 in 0.1 M Tris pH 7.5 or 8.0, and 10% (v/v) glycerol as the reservoir. A single crystal was picked using a Hampton silicon loop and streaked through cryoprotectant containing 25% (v/v) glycerol in the reservoir buffer prior to data collection. X-ray diffraction data was collected at the macromolecular crystallography beamline at the Australian Synchrotron using an ADSC Quantum 210r Detector. 90 images were collected for 1 second each at an oscillation angle of 1° for each frame. Data was integrated using HKL, and refined using the CCP4 suite of programs. PDB and cif files for the compounds were obtained using the PRODRG web interface. The models were built using cycles of manual modelling using COOT and refinement with REFMAC. The quality of the final models was evaluated using MOLPROBITY.

7.3 General Procedures

General procedure A1: Methylation of carboxylic acid:

To a suspension of carboxylic acid (1 eq) in methanol (5 mL) per 100 mg of carboxylic acid was added drop-wise thionyl chloride (3 eq) and the mixture was stirred for 90 min with a calcium chloride drying tube. The reaction mixture was concentrated *in vacuo*, diluted with dichloromethane, concentrated *in vacuo* and the residue was purified by silica gel chromatography. See individual experiments for details.

General procedure B1: Reduction of methyl ester to alcohol

To a suspension of methyl ester (1 eq) in freshly distilled THF (7.5 mL per 100 mg of methyl ester) was added portion-wise lithium aluminium hydride (1.5 eq) and the mixture stirred overnight under a nitrogen atmosphere. The reaction mixture was quenched with methanol and water. To the mixture was added saturated sodium sulphate, stirred for 20 min and concentrated *in vacuo*. The residue was dissolved in 1:4 methanol and dichloromethane, stirred for 30 min, filtered, washed with 1:4 methanol and dichloromethane. The filtrate was concentrated *in vacuo* and purified by silica gel. See individual experiments for details.

General procedure C1: Phosphitylation of alcohols

To a suspension of alcohol (1 eq) in dry dichloromethane (1 mL per 100 mg of alcohol) were added *N,N*-diisopropylmethoxyphosphonamidic (1.5 eq) and DIPEA (4 eq) and the mixture was stirred for 45 min under nitrogen atmosphere. The reaction mixture was diluted with ethylacetate and washed with brine, dried over Na_2SO_4, filtered, concentrated *in vacuo*. See individual experiments for details.

General procedure D1: Tosylation of alcohol

To a suspension of alcohol (1 eq) in dry pyridine (1 mL per 100 mg of alcohol) was added dropwise a solution of tosyl chloride (1.1 eq) in dry pyridine (0.25 mL per 100 mg of tosyl chloride), and the solution was stirred with an ice bath for 1 h and left for 5 h in a 4 °C fridge. The reaction mixture was diluted with dichloromethane and washed with 0.5 M aqueous HCl, aqueous saturated sodium bicarbonate, water and brine. The organic layer was dried over Na_2SO_4, filtered and concentrated *in vacuo*. See individual experiments for details.

General procedure E1: Bromination of tosylate

To a suspension of tosylate (1 eq) in methyl ethyl ketone (1 mL per 100 mg of tosylate) was added lithium bromide (2 eq) and stirred at 80 °C for 3 h. The reaction mixture was cool, diluted with dichloromethane and washed with water and brine. The organic layer was dried over Na_2SO_4, filtered and concentrated *in vacuo* and purified by silica gel chromatography. See individual experiments for details.

General procedure F1: Alkynation of Bromide

To a suspension of 90% lithium acetylide ethylene diamine complex (1.5 eq) in dry DMSO (0.25 mL per 100 mg) cooled at 15 °C was added dropwise a solution of bromide (1 eq) in dry DMSO (0.25 mL per 100 mg) and stirred at ambient temperature for 3 h. The reaction mixture was poured into ice-water and extracted with dichloromethane. The organic layer was collected and washed with water and brine, dried over Na_2SO_4, filtered, concentrated *in vacuo* and purified by silica gel flash chromatography. See individual experiments for details.

General procedure G1: CuAAC

To solution of the azide (1.0 eq) and alkyne (1.0 eq) in acetonitrile (1 mL per 100 mg of alkyne) were de-ionised water (0.5 mL per 100 mg of alkyne) added copper nano powder (0.2 eq), sonicated for 15 min followed by stirring for 4 h. The reaction mixture was concentrated *in vacuo* and purified by silica gel column chromatography. See individual experiments for details.

General procedure H1: RuAAC

To solution of the azide (1.0 eq) and alkyne (1.0 eq) in 1:1 dry THF/DMF (1 mL per 100 mg of alkyne) was added Cp*Ru(PPh$_3$)$_2$Cl (0.1 eq) and stirred at 80 °C under nitrogen atmosphere for 4 h. The reaction mixture was concentrated *in vacuo* and purified by silica gel column chromatography. See individual experiments for details.

General procedure I1: Alkylation of aryl amines and aryl alcohols:

To a solution of the alcohol or amine (1 eq) in dry DMF (1 mL per 100 mg of alcohol/amine) was added potassium carbonate (1.5 eq) and stirred at 50 °C for 30 min. Followed by addition of the alkyl dihalide (1.5 eq) and stirred at 50 °C overnight under nitrogen atmosphere. The reaction mixture was diluted with dichloromethane and washed

with 0.5 M aqueous HCl, aqueous saturated Na$_2$SO$_4$, water and brine, dried over NaSO$_4$, filtered, concentrated *in vacuo* and purified by silica gel column chromatography. See individual experiments for details.

General procedure for alkylation I2: Conversion of alkyl bromide to alkyl azide

To a solution of the bromide (1 eq) in dry DMF (1 mL per 100 mg of bromide) was added sodium azide (1.2 eq) and stirred overnight under nitrogen atmosphere. The reaction mixture was diluted with dichloromethane and washed with water and brine, dried over NaSO$_4$, filtered, concentrated *in vacuo* and purified by silica gel column chromatography. See individual experiments for details.

7.3 Experimental work as described in Chapter 2

5-[(3a*S*,6a*R*)-2-Oxo-1,3,3a,4,6,6a-hexahydrothieno[3,4-*d*]imidazol-4-yl]pentyl [(3*S*,4*R*,5*R*)-5-(6-aminopurin-9-yl)-3,4-dihydroxy-tetrahydrofuran-2-yl]methyl hydrogen phosphate (1.05)[5]
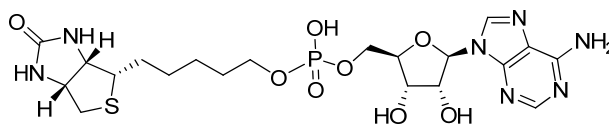

1.05

Method 1a (Chapter 2, table 2, entry 1)

To a suspension of biotinol **2.05** (168 mg, 0.73 mmol) and adenosine 5'-monophosphate **2.04** (375 mg, 0.80 mmol) in dry pyridine (10 mL) was added DCC (226 mg, 1.10 mmol) and stirred under nitrogen atmosphere for 24 h. Acetic acid (15 mL) was added to the reaction mixture and stirred at 80 ^{o}C for 2 h. The reaction mixture was concentrated *in vacuo* and purified by Sephadex A25 DEAE eluting with a gradient of 0.05 − 0.35 M triethylamine bicarbonate solution at pH 7-8. As judged by TLC, fractions containing the biotinol-5'-AMP **1.05** (between 0.20 − 0.26 M) were pooled and concentrated *in vacuo* to give a clear gum (73 mg, 18% [yield based on ^{1}H NMR see section 2.2.2 for discussion]) Preparative HPLC was performed using solvent A (0.1% AcOH in H_2O) and solvent B (0.08% AcOH in 90% AcCN) and gradient of solvent B (0% − 90%) over 30 minutes to give a white solid. ^{1}H NMR was consistent with literature.[5]

^{1}H NMR (300 MHz, D_2O): δ 8.62 (1H, s, ArH), 8.42 (1H, s, ArH), 6.18 (1H, d, *J* = 5.4 Hz, 1' CH), 4.78-84 (1H, m (with D_2O peak), 2' CH), 4.52-4.57 (2H, m, 2 x NHCH), 4.39-4.41 (1H, m, 4' CH), 4.31 (1H, dd, *J* = 4.5, 8.1 Hz, 3' CH), 4.11-4.14 (2H, m. 5' CH_2), 3.78 (2H, quart (apparent), *J* = 7.5 Hz, $POCH_2$), 3.14-3.20 (1H, m, SCH), 2.90 (1H, dd, *J* = 5.1, 12.9 Hz, SCH_a), 2.69 (1H, d, *J* = 12.9 Hz, SCH_b), 1.44-1.62 (2H, m, CH_2), 1.11-1.41 (6H, m, 3 x CH_2); **^{13}C NMR** (75 MHz, DMSO-d_6): δ 163.6, 156.7, 153.3, 150.3, 140.1, 119.6, 87.7, 84.5, 74.4, 71.6, 64.8, 61.8, 59.9, 56.3, 30.9, 30.8, 29.1, 26.2; **^{13}C NMR** (75 MHz, D_2O): δ 165.3, 155.3, 152.7, 149.1, 139.9, 118.6, 87.1, 84.1, 74.1, 70.5, 66.3, 64.9, 62.1, 60.3, 55.5, 39.8, 29.6, 28.1, 27.9, 24.8.

Method 1b (Chapter 2, table 2, entry 2)

Following method 1a. To a suspension of biotinol **2.05** (168 mg, 0.73 mmol) and adenosine 5'-monophosphate **2.04** (375 mg, 0.80 mmol) in dry pyridine (10 mL) was added DCC (452 mg, 2.20 mmol) and stirred under nitrogen atmosphere for 24 h. Acetic acid (15 mL) was added to the reaction mixture and stirred at 80 °C for 2 h. The reaction mixture was concentrated *in vacuo* and purified by Sephadex A25 DEAE using a gradient of 0.05 – 0.35 M triethylamine bicarbonate solution at pH 7-8 (as judge by universal pH indicator paper). Compound **1.05** was eluted between gradient 0.20 – 0.26 M TEAB (106 mg, 26% [yield based on NMR see section 2.2.2 for discussion]). ^{1}H NMR was consistent with method 1a.[5]

Method 1c (Chapter 2, table 2, entry 3)

To a suspension of biotinol **2.05** (168 mg, 0.73 mmol) and adenosine 5'-monophosphate **2.04** (375 mg, 0.80 mmol) in dry pyridine (10 mL) was added DCC (414 mg, 1.83 mmol) and the mixture was stirred under nitrogen atmosphere for 24 h. Acetic acid (15 mL) was added to the reaction mixture and stirred at 80 °C for 2 h. The reaction mixture was worked up according to method 1b. (127 mg, 31% [yield based on NMR spectroscopy, see section 2.2.2 for discussion]). ^{1}H NMR spectra was consistent with literature.[5]

Method 1d (Chapter 2, table 2, entry 4)

To a suspension of biotinol **2.05** (168 mg, 0.73 mmol) and adenosine 5'-monophosphate **2.04** (375 mg, 0.80 mmol) in dry pyridine (10 mL) was added DCC (452 mg, 2.20 mmol) and the mixture was stirred under nitrogen for 12 h. Acetic acid (15 mL) was added to the reaction mixture and stirred at 80 °C for 2 h. The reaction mixture was worked up according to method 1b. (61 mg, 15% % [yield based on NMR spectroscopy, see section 2.2.2 for discussion]). ^{1}H NMR spectra was consistent with literature.[5]

Method 1e (Chapter 2, table 2, entry 5)

To a suspension of biotinol **2.05** (168 mg, 0.73 mmol) and adenosine 5'-monophosphate **2.04** (375 mg, 0.80 mmol) in dry pyridine (10 mL) was added DCC (452 mg, 2.20 mmol) and the mixture was stirred under nitrogen atmosphere for 48 h. Acetic acid (15 mL) was added to the reaction mixture and stirred at 80 °C for 2 h. The reaction mixture was worked up according to method 1b. 69 mg, 17% % [yield based on NMR spectroscopy, see section 2.2.2 for discussion]). ^{1}H NMR spectra was consistent with literature.[5]

Method 2 (see section 2.3)

To a suspension of compound **2.20** (8 mg, 0.02 mmol) in dry acetone (1 mL) was added sodium iodide (6 mg, 0.04 mmol) and stirred under reflux for 6 h. The reaction mixture was cooled and concentrated *in vacuo* and purified by HPLC using solvent A (0.1% TFA in water) and solvent B (0.08% TFA, 90% acetonitrile) with gradient of 0 - 0% of solvent B for 5 min, 0%-65% of solvent B for 25 min and 65-90% 10 min of solvent B to give a white solid (6 mg, 77%). ^{1}H NMR spectra was consistent with literature.[5]

[(3a*R*,4*R*,6a*R*)-4-(6-Aminopurin-9-yl)-2,2-dimethyl-3a,4,6,6a-tetrahydrofuro[3,4-*d*][1,3]dioxol-6-yl]methanol (2.02)[6]
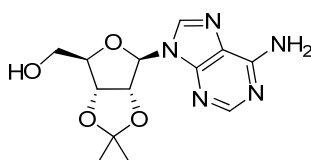
To a stirring solution of adenosine (1.00 g, 3.75 mmol) in anhydrous DMF (50 mL) were added 2,2-dimethoxylpropane (0.780 g, 7.49 mmol) and *p*-TsOH (0.19 g, 1.12 mmol) and the solution stirred overnight at 60 $^{\circ}$C under a nitrogen atmosphere. The reaction mixture was quenched with saturated aqueous sodium bicarbonate (50 mL) and extracted with ethyl acetate (3 x 75 mL). The combined organic layer was washed with water (150 mL) and brine (150 mL), dried over Na_2SO_4, filtered and concentrated *in vacuo*. The residue was purified by silica gel chromatography 5% methanol in dichloromethane to give a white solid (0.897 mg, 78%).^{1}H NMR spectra was consistent with literature[6]

[(3a*R*,4*R*,6a*R*)-4-(6-Aminopurin-9-yl)-2,2-dimethyl-3a,4,6,6a-tetrahydrofuro[3,4-*d*][1,3]dioxol-6-yl]methyl hydrogen phosphate (2.04)
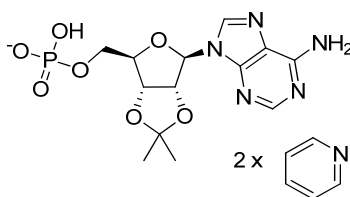
30% pyridine in water was passed through a 10 cm Dowex 50W X8 H$^+$ form column until pH>7 (as judge by universal indicator paper). This was washed with de-ionised water (100 mL) and a solution of adenosine 5'-monophosphate triethylamine salt (1.51 g) in de-ionised water (10 mL) was loaded onto the Dowex 50W X8 pyridinium form column and eluted with de-ionised water (100 mL). Fractions containing UV active spots as judge by TLC were pooled and concentrated *in vacuo* to give a light yellow oil (1.27 g, 89%).

^{1}H NMR (300 MHz, D$_2$O): δ 8.47 (4H, d, J = 5.1 Hz, Ar**H**), 8.12-8.16 (3H, m, Ar**H**), 7.90 (1H, s, Ar**H**), 7.62-7.67 (4H, m, Ar**H**), 5.97 (1H, d, J = 3.3 Hz, 1' **CH**), 5.16 (1H, dd, J = 3.3, 6.0 Hz, 2' **CH**), 5.00 (1H, dd, J = 2.1, 6.0 Hz, 3' **CH**), 4.44-4.49 (1H, m, 4' **CH**), 3.90-3.93 (2H, m, 5' **CH₂**), 1.50 (3H, s, CC**H₃**), 1.28 (3H, s, CC**H₃**); **^{13}C NMR** (75 MHz, D$_2$O): 150.6, 148.2, 147.3, 145.6, 142.3, 141.3, 127.6, 118.7, 114.9, 91.7, 85.9, 84.6, 81.8, 74.9, 65.4, 26.3, 24.5.

(3a*S*,4*S*,6a*R*)-4-(5-Hydroxypentyl)-1,3,3a,4,6,6a-hexahydrothieno[3,4-*d*]imidazol-2-one (2.05)[7]
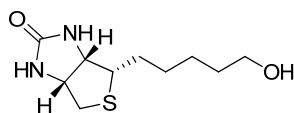
Biotin methyl ester **2.10** (3.00 g, 11.6 mmol) was selectively reduced according to general procedure **B1** and without column chromatography purification to give a white solid (2.25 g, 84%). >95% purity as judge by ^{1}H NMR spectroscopy.

^{1}H NMR (300 MHz, DMSO-d$_6$): δ 6.44 (1H, bs, C(O)N**H**), 6.36 (1H, bs, C(O)N**H**), 4.28-4.37 (2H, m, C**H₂**OH, NHC**H**), 4.10-4.15 (1H, NHC**H**), 3.38 (2H, t, J = 6.0 Hz, C**H₂**OH), 3.07-3.13 (1H, m, SC**H**), 2.81 (1H, dd, J = 5.1, 12.6 Hz, SC**Hₐ**), 2.57 (1H, d, J = 12.6 Hz, SC**H_b**), 1.25-1.67 (8H, m, C**H₂**); **^{13}C NMR** (75 MHz, CDCl$_3$): δ 166.2, 63.4, 62.8, 61.6, 57.2, 41.0, 33.4, 33.4, 30.2, 29.8, 26.9.

[(3a*R*,4*R*,6a*R*)-4-(6-Aminopurin-9-yl)-2,2-dimethyl-3a,4,6,6a-tetrahydrofuro[3,4-*d*][1,3]dioxol-6-yl]methyl   5-[(3a*S*,6a*R*)-2-oxo-1,3,3a,4,6,6a-hexahydrothieno[3,4-*d*]imidazol-4-yl]pentyl hydrogen phosphate (2.06)
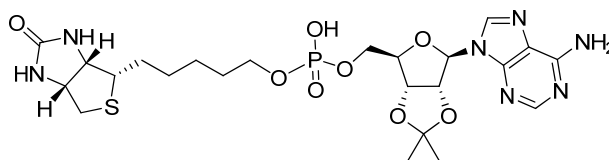
Compound **2.06** was obtained as a by-product from the synthesis of **1.05** following method **1c**. Compound **2.06** was eluted on Sephadex DEAE column using TEAB and obtained between gradient 0.15 – 0.20 M TEAB (22 mg, 5%) [yield based on ^{1}H NMR spectroscopy, see section 2.2.2 for discussion]).

^{1}H NMR (300 MHz, D$_2$O): δ 8.37 (1H, s, Ar**H**), 8.20 (1H, s, Ar**H**), 6.22 (1H, d, *J* = 3.0 Hz, 1' C**H**), 5.41 (1H, dd, *J* = 3.0, 6.0 Hz, 2' C**H**), 5.16-5.19 (1H, m, 3' C**H**), 4.59-4.65 (1H, m, 4' C**H**), 4.49-4.53 (1H, m, NHC**H**), 4.24-4.28 (1H, m, NHC**H**), 3.98-4.01 (2H, m, 5' C**H**), 3.49-3.54 (2H, m, POC**H$_2$**), 3.16 (12H, quart, *J* = 7.5 Hz, NC**H$_2$**) 3.04-3.09 (1H, m, SC**H**), 2.88 (1H, dd, *J* = 5.1, 13.2 Hz, SC**H$_a$**), 2.67 (1H, d, *J* = 13.2 Hz, SC**H$_b$**), 1.63 (3H, s, CC**H$_3$**), 1.42 (3H, s, CC**H$_3$**) 1.20-1.31 (26H, m, C**H$_2$**, C**H$_2$**CH$_3$); **^{13}C NMR** (300 MHz, DMSO-d$_6$): δ 163.0, 156.1, 152.8, 149.0, 140.0, 119.0, 113.2, 89.3, 85.2, 83.5, 81.7, 64.6, 61.2, 59.4, 55.6, 33.4, 30.2, 28.4, 27.1, 25.5, 25.3, 24.5; **^{31}P NMR** (32 MHz, DMSO-d$_6$): δ -22.73; **HRMS** calcd. for (M+ H) C$_{23}$H$_{35}$N$_7$O$_8$PS: requires 600.2005, found 600.1996.

[(3a*R*,4*R*,6a*R*)-4-(6-Aminopurin-9-yl)-2,2-dimethyl-3a,4,6,6a-tetrahydrofuro[3,4-*d*][1,3]dioxol-6-yl]methyl hydrogen phosphate bis-triethylamine salt (2.09)[8]
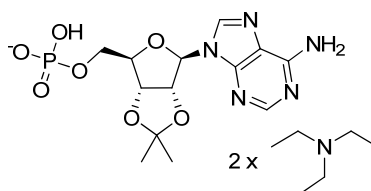
Preparation of triethylamine bicarbonate buffer solution[9]

Triethylamine (278 ml, 202 g, 2 mol) was added portion-wise to de-ionised water (500 mL). To the stirring solution was added portion-wise dry ice until pH >8 (as judged by universal indicator paper). The buffer was diluted with water (500 mL), sealed and stored at 4 °C fridge. The triethylamine bicarbonate buffer was diluted with de-ionised water to the specified concentrations, dry ice was added to adjust the pH >7 (as judged by universal indicator paper) and the buffer was degassed *in vacuo* and used as eluting solvent for Sephadex DEAE A25 ion exchange purification.

Method 1a (see table chapter 2, table 1 entry 1)

A solution of adenosine **2.02** (600 mg, 1.96 mmol) in triethyl phosphate (10 mL) was cooled in a sodium chloride ice bath and stirred under nitrogen atmosphere. A ice cooled solution of phosphorous oxychloride (590 mg, 7.92 mmol) in triethyl phosphate (10 mL) at 0 °C was added drop-wise to the first solution. The reaction mixture was stirred for 2 h under nitrogen atmosphere, then sealed and placed in a 4 °C fridge overnight. The reaction mixture was poured into 0.05 M triethylamine bicarbonate buffer solution (1 L), stirred for 20 min and purified by Sephadex A25 DEAE column using a step-wise gradient of 0.05 to 0.5 M TEAB solution. Fractions containing the target compound were pooled (as judge by TLC) and concentrated *in vacuo* to give a trace quantity of the target compound was determined by ^{1}H NMR (300 MHz, D_2O) and consistent with literature.[8]

Method 1b (see table chapter 2, table 1 entry 2)

The reaction mixture was prepared according to method 1. However, after placing the reaction mixture in a 4 °C fridge, the reaction mixture was poured into 2 M triethylamine bicarbonate buffer solution (50 mL), stirred for 20 min. Additional triethylamine bicarbonate buffer solution was added until pH >7 (as judge by universal indicator paper) and the solution was diluted with de-ionised water to give a TEAB concentration of 0.05 M (total volume 3 L). The solution was purified by Sephadex A25 DEAE column using a step-wise gradient of 0.05 to 0.5 M TEAB solution. Fractions containing the target compound were pooled and concentrated *in vacuo* to give a clear oil (238 mg, 25%). ^{1}H NMR (300 MHz, D_2O) indicated a ratio of 3:1 of triethylamine to target compound.

Method 1c (see table chapter 2, table 1 entry 3)

To a solution of adenosine **2.02** (600 mg, 1.96 mmol) in triethyl phosphate (10 mL) was added drop-wise a solution of phosphorous oxychloride (590 mg, 3.91 mmol) in triethyl phosphate (10 mL). Hydrolysis and purification of the reaction mixture followed method 1a to give a clear gum (390 mg, 41%). ^{1}H NMR (300 MHz, D_2O) indicated a ratio of 2:1 of triethylamine to target compound.

^{1}H NMR (300 MHz, D_2O): δ 8.40 (1H, s, Ar**H**), 8.09 (1H, s, Ar**H**), 6.11 (1H, d, J = 3.6 Hz, 1' **CH**), 5.26 (1H, dd, J = 3.6, 6.0 Hz, 2' **CH**), 5.06 (1H, dd, J = 1.8, 6.0 Hz, 3' **CH**), 4.55-4.47 (1H, m, 4' **CH**), 3.84-3.88 (2H, m, 5' **CH₂**), 3.04 (12H, quart, J = 7.2 Hz, N**CH₂**CH₃[2 x Et₃N]), 1.55 (3H, s, C**CH₃**), 1.32 (3H, s, C**CH₃**), 1.13 (18H, t, J = 7.2 Hz, NCH₂**CH₃** [2 x Et₃N]); **^{13}C NMR** (75 MHz, D_2O): δ 154.4, 151.9, 139.4, 117.5, 114.2, 99.1, 89.1, 84.4, 84.2, 83.2, 80.8, 63.7, 45.8, 25.6, 23.8, 7.5.

Method 1d (see table chapter 2, table 1 entry 4)

To a solution of adenosine **2.02** (600 mg, 1.96 mmol) in triethyl phosphate (10 mL) was added drop-wise a solution of phosphorous oxychloride (324 mg, 2.14 mmol) in triethyl phosphate (10 mL). Hydrolysis and purification of the reaction mixture followed method 1a to give a clear gum (361 mg, 38%). ^{1}H NMR (300 MHz, D_2O) consistent with method 3 and literature.[8]

Method 5 (see table chapter 2, table 1 entry 5)

To a solution of adenosine **2.02** (600 mg, 1.96 mmol) in trimethyl phosphate (10 mL) was added drop-wise a solution of phosphorous oxychloride (590 mg, 3.91 mmol) in trimethyl phosphate (10 mL). The hydrolysis and purification of the reaction mixture followed method 2 to give a clear gum (361 mg, 38%). ^{1}H NMR (300 MHz, D_2O) consistent with method 3 and literature.[8]

Method 6 (see table chapter 2, table 1 entry 6)

To a solution of adenosine **2.02** (600 mg, 1.96 mmol) and water (20 μL) in triethyl phosphate (10 mL) was added drop-wise a solution of phosphorous oxychloride (324 mg, 2.14 mmol) and in triethyl phosphate (10 mL). The hydrolysis and purification of the reaction mixture followed method 1a to give a clear gum (619 mg, 65%). ^{1}H NMR (300 MHz, D_2O) consistent with method 3 and literature.[8]

**Methyl   5-[(3a*S*,4*S*,6a*R*)-2-oxo-1,3,3a,4,6,6a-hexahydrothieno[3,4-*d*]imidazol-4-yl]
pentanoate (2.10)[10]**
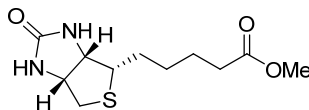
Method 1

Biotin (4.00 g, 16.4 mmol) was esterified using general procedure **A1** and the crude material was purified by silica gel chromatography eluting with 10% methanol in dichloromethane to give a white solid (4.23 g, 100%). >95% purity as judge by NMR spectroscopy.

^{1}H NMR (300 MHz, CDCl$_3$): δ 6.01 (1H, bs, C(O)N**H**), 5.59 (1H, bs, C(O)N**H**), 4.47-4.52 (1H, m, NHC**H**), 4.30 (1H, ddd, *J* = 1.5, 4.5, 7.8 Hz, NHC**H**), 3.65 (3H, s, COOC**H$_3$**), 3.11-3.18 (1H, m, SC**H**), 2.90 (1H, dd, *J* = 5.1, 12.6 Hz, SC**H$_a$**), 2.73 (1H, d, *J* = 12.6 Hz, SC**H$_b$**), 2.33 (2H, t, *J* = 7.8 Hz, C**H$_2$**COO), 1.61-1.74 (4H, m, 2 x C**H$_2$**), 1.40-1.48 (2H, m, C**H$_2$**); **^{13}C NMR** (75 MHz, CDCl$_3$): δ 174.3, 163.8, 62.1, 60.3, 55.6, 51.8, 40.8, 33.9, 28.5, 28.4, 25.0.

Method 2

To a suspension of biotin (2 g, 8.20 mmol) and DMF (0.1 mL) in dry methanol (40 mL) was added drop-wise oxalyl chloride (3.07 g, 24.6 mmol) and stirred for 90 min with a calcium chloride filled drying tube attached. The reaction mixture was concentrated *in vacuo*, diluted with dichloromethane and concentrated *in vacuo* to give a white solid (2.11 g, 100%).^{1}H NMR spectra consistent with method 1, >95% purity as judge by NMR spectroscopy.

Attempted synthesis of (3a*R*,6*S*,6a*S*)-3-[bis(4-methoxyphenyl)-phenyl-methyl]-6-[5-[(diisopropylamino)-methoxy-phosphanyl]oxypentyl]-3a,4,6,6a-tetrahydro-1*H*-thieno[3,4-*d*]imidazol-2-one (2.11)
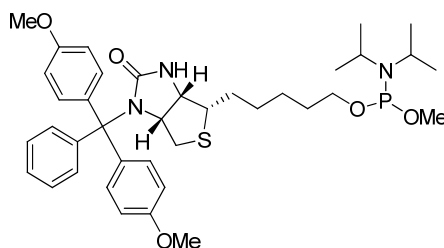
DMTr-biotinol **2.16** (200 mg, 0.357 mmol) was treated according to general procedure **C1** and purification by silica gel chromatography eluting with 1% triethylamine in dichloromethane to give a complex mixture.

_N_-[9-[(3a*R*,4*R*,6*R*,6a*R*)-6-(Hydroxymethyl)-2,2-dimethyl-3a,4,6,6a-tetrahydrofuro[3,4-*d*][1,3]dioxol-4-yl]purin-6-yl]benzamide (2.12)[11]
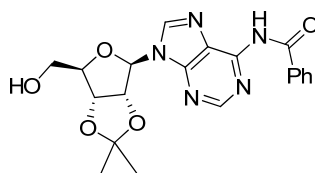
To a solution of adenosine **2.02** (400 mg, 1.30 mmol) in dry pyridine (10 mL) was added TMS-Cl (562 mg, 5.21 mmol) and the solution stirred for 45 min, followed by dropwise addition benzoyl chloride (200 mg, 1.43 mmol) over 10 min and stirred at room temperature for 4 h. The reaction mixture was cooled with an ice water bath and diluted with water (1 mL) and stirred for 10 min. To the stirring solution was added 32% $NH_{3(aq)}$ (3 mL) and stirred for a further 30 min. The solution was concentrated and purified by silica gel chromatography eluting with 5% methanol in chloroform to give a white foam (412, 77%).

^{1}H NMR (300 MHz, CDCl$_3$): δ 9.29 (1H, bs, ArNH), 8.73 (1H, s, ArH), 8.09 (1H, s, ArH), 8.00 (2H, d, *J* = 7.2 Hz, ArH), 7.56-7.61 (1H, m, ArH), 7.47-7.51 (2H, m, ArH), 5.95 (1H, d, *J* = 4.5 Hz, 1' CH), 5.75 (1H, bs, 5' CH$_2$OH), 5.19-5.22 (1H, m, 2' CH), 5.06-5.09 (1H, m, 3' CH), 4.50-4.54 (1H, m, 4' CH), 3.96 (1H, dd, *J* =1.5, 12.3 Hz, 5' CH$_a$),

3.78 (1H, d, J = 12.3 Hz, 5' C**H**$_b$), 1.63 (3H, s, CC**H**$_3$), 1.36 (3H, s, CC**H**$_3$); **^{13}C NMR** (75 MHz, CDCl$_3$): δ 164.9, 152.6, 150.8, 142.8, 133.7, 133.2, 129.1, 128.2, 124.6, 114.5, 94.3, 86.6, 83.5, 81.9, 63.5, 27.8, 25.5.

Methyl 5-[(3a*R*,6*S*,6a*S*)-3-[bis(4-methoxyphenyl)-phenyl-methyl]-2-oxo-3a,4,6,6a-tetrahydro-1*H*-thieno[3,4-*d*]imidazol-6-yl]pentanoate (2.15)[7]
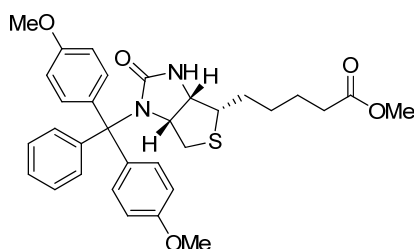
Method 1

To a solution of biotin methyl ester **2.10** (500 mg, 1.94 mmol) in dichloromethane (5 mL) was added 4,4'-dimethoxytrityl chloride (1060 mg, 2.90 mmol) and stirred for 60 min. Excess 4,4'-dimethoxytrityl chloride was quenched with methanol (3 mL) and the reaction mixture was diluted with dichloromethane (40 mL), washed with water (1 x 50 mL) and brine (1 x 50 mL), dried over Na$_2$SO$_4$, filtered and concentrated *in vacuo*. The residue was purified by silica gel chromatography eluting with 2% triethylamine in dichloromethane to give a light yellow solid (380 mg, 35%).

^{1}H NMR (300 MHz, CDCl$_3$): δ 7.28-7.30 (4H, m, Ar**H**), 7.14-7.20(5H, m, Ar**H**), 6.79-6.84 (4H, m, Ar**H**), 5.31 (1H, m, C(O)N**H**), 4.47-4.52 (1H, m, NHC**H**), 3.84 (6H, s, ArOC**H**$_3$), 3.70 (3H, s, COOC**H**$_3$), 3.13-3.21 (1H, m, SC**H**), 2.90 (1H, dd, J = 5.1, 12.6 Hz, SC**H**$_a$), 2.26-2.49 (3H, m, SC**H**$_b$, C**H**$_2$COOCH$_3$), 1.61-1.66 (4H, m, 2 x C**H**$_2$), 1.40-1.45 (2H, m, C**H**$_2$); **^{13}C NMR** (75 MHz, CDCl$_3$): δ 162.3, 158.6, 144.0, 136.0, 131.6, 131.5, 130.0, 127.9, 127.2, 113.2, 73.0, 65.8, 60.0, 55.5, 54.2, 51.9, 39.3, 33.9, 29.1, 28.5, 24.9.

Method 2

To a solution of biotin methyl ester **2.10** (500 mg, 1.94 mmol) in dichloromethane (5 mL) were added 4,4'-dimethoxytrityl chloride (1060 mg, 2.90 mmol) and 4-DMAP (236 mg,

1.94 mmol) stirred for 60 min. Work up was in accordance to method 1 (554 mg, 51%). ^{1}H NMR consistent with method 1 and literature.[7]

(3a*R*,6*S*,6a*S*)-3-[Bis(4-methoxyphenyl)-phenyl-methyl]-6-(5-hydroxypentyl)-3a,4,6,6a-tetrahydro-1*H*-thieno[3,4-*d*]imidazol-2-one (2.16)[7]
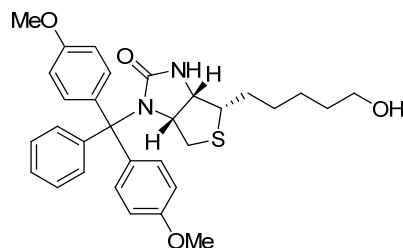
DMTr-biotin methyl ester **2.15** (200 mg, 0.357 mmol) was reduced using general procedure **B1** and purified by silica gel chromatography eluting with 1% methanol in dichloromethane to give a white solid (169 mg, 89%).

^{1}H NMR (300 MHz, CDCl$_3$): δ 7.28-7.31(4H, m, Ar**H**), 7,14-7,21 (5H, m, Ar**H**), 6.80-6.83 (4H, m, Ar**H**), 4.74 (1H, m, C(O)N**H**), 4.34-4.38 (2H, m, 2 x NHC**H**), 3.79 (6H, s, ArOC**H$_3$**), 3.63 (2H, t, *J* = 6.3 Hz, C**H$_2$**OH), 3.10-3.17 (1H, m, SC**H**), 2.48 (1H, d, *J* = 12.6 Hz, SC**H$_b$**), 2.29 (1H, dd, *J* = 5.4, 12.6 Hz, SC**H$_a$**), 1.34-1.72 (8H, m, C**H$_2$**); **^{13}C NMR** (75 MHz, CDCl$_3$): δ 162.3, 158.6, 144.0, 136.0, 131.6, 131.5, 130.0, 127.9, 127.2, 113.2, 73.0, 65.8, 60.0, 55.5, 54.2, 51.9, 39.3, 33.9, 29.1, 28.5, 24.9.

_N_-[9-[(3a*R*,4*R*,6*R*,6a*R*)-6-[[(Diisopropylamino)-methoxy-phosphanyl]oxymethyl]-2,2-dimethyl-3a,4,6,6a-tetrahydrofuro[3,4-*d*][1,3]dioxol-4-yl]purin-6-yl]benzamide (2.17)[12]
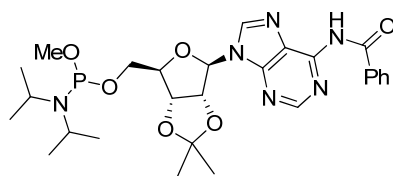
Adenosine **2.12** (200 mg, 0.487 mmol) was phosphitylated using *N,N* - Diisopropylmethylphosphonamidic chloride (59 mg, 0.511 mmol) following general

procedure **C1** and purified by silica gel chromatography eluting with 12:8:1 hexane/chloroform/triethylamine to white oil (187 mg, 67%).

¹H NMR (300 MHz, CDCl₃): δ 9.36 (0.5H, bs, ArN**H**(C(O)), 8.81 (0.5H, s, Ar**H**), 8.80(0.5, s, Ar**H**), 8.40 (0.5H, s, Ar**H**), 8.34 (0.5H, s, Ar**H**), 8.03 (2H, s, *J* = 8.4 Hz, Ar**H**), 7.47-7.61 (3H, m, Ar**H**), 6.29 (0.5H, d, *J* = 3.0 Hz, 5' C**H**), 6.19 (0.5H, d, *J* = 2.7 Hz, 5' C**H**), 5.23-5.28 (1H, m, 2' C**H**), 4.40-4.98 (1H, m, 3' C**H**), 3.43-3.84 (4H, m, 5' C**H₂**, 2 x C**H**(CH₃)₂), 3.34 (1.5H, d, *J* = 1.8 Hz, POC**H₃**), 3.30 (1.5H, d, *J* = 1.8 Hz, POC**H₃**), 1.21 (3H, s, CC**H₃**), 1.20 (3H, s, CC**H₃**), 1.18 (3H, s, CC**H₃**), 1.17 (3H, s, CC**H₃**).

5-Ethylsulfanyl-1*H*-tetrazole (2.18)[13]
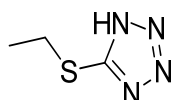
To a suspension of n-ethylthiocyanate (500 mg, 5.75 mol), sodium azide (485 mg, 7.47 mol), ammonium chloride (426 mg, 8.05 mol) and hexadecyltrimethylammonium bromide (72 mg, 0.2 mmol) were stirred in a mixture of water (6 mL) and toluene (1 mL) and stirred at 75 °C for 72 h. The reaction mixture was cooled, acidified with 12 M aqueous HCl to pH<2 (as judge by universal indicator paper) and stirred for 12 h with an ice bath. The precipitate was filtered, washed with ice water (3 x 10 mL) and dried *in vacuo* to give a white crystalline solid (403 mg, 54 %). ¹H NMR spectra was consistent with literature report.[13]

5-[(3a*S*,4*S*,6a*R*)-2-Oxo-1,3,3a,4,6,6a-hexahydrothieno[3,4-d]imidazol-4-yl]pentyl [(2*R*,3*S*,4*R*,5*R*)-5-(6-aminopurin-9-yl)-3,4-dihydroxy-tetrahydrofuran-2-yl]methyl methyl phosphate (2.20)
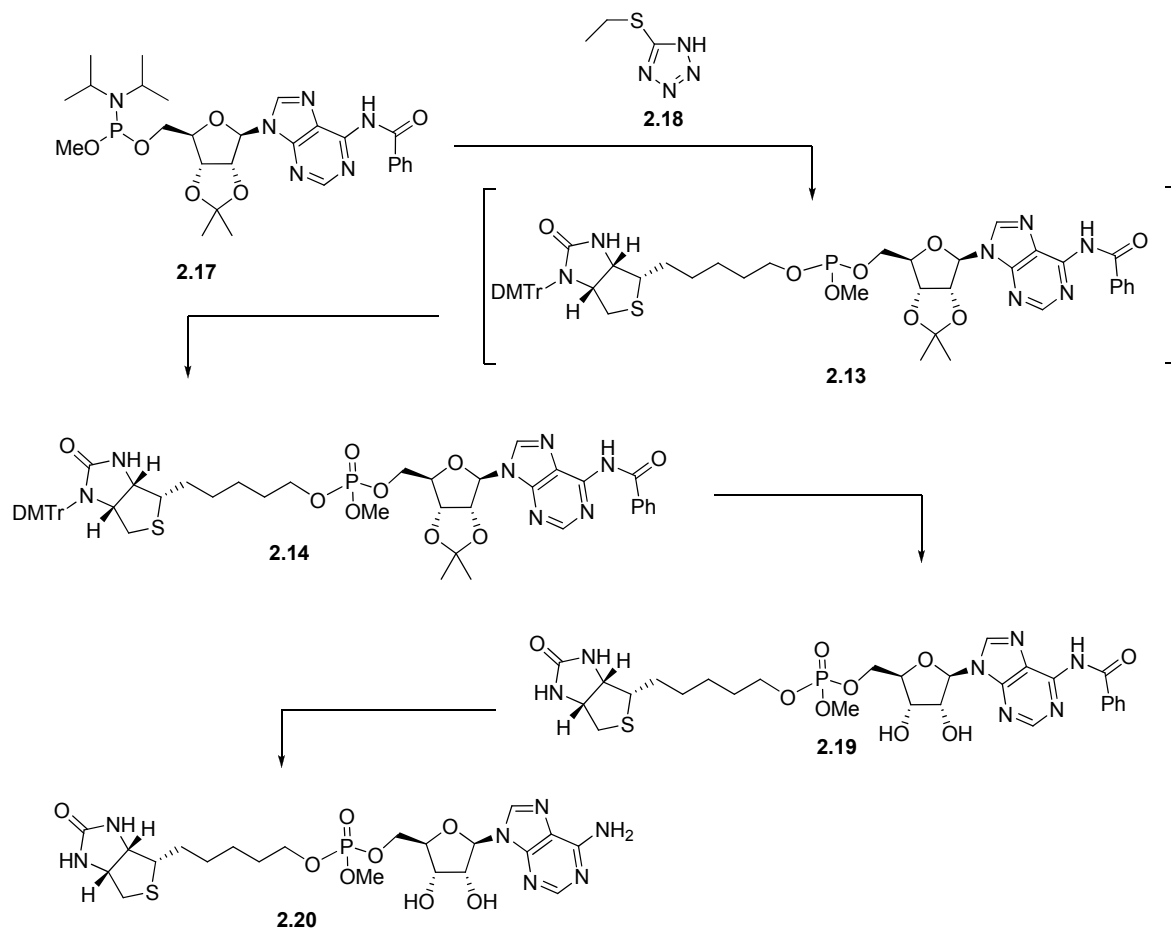
DMtr-biotinol **2.16** (100 mg, 0.19 mmol), adenosine **2.17** (118 mg, 0.21 mmol) in dry acetonitrile (2 mL) was added 2-ETT **2.18** (49 mg, 0.38 mmol) and the solution was stirred for 1 h under nitrogen atmosphere. The reaction mixture was monitored by TLC and upon consumption of compound **2.16**, was added 5 M *tert*-butyl hydrogen peroxide (0.38 ml, 1.88 mmol) and stirred for 15 min. The reaction mixture was poured into water (15 mL) and extracted with dichloromethane (5 x 15 mL). The organic layers were pooled, washed with brine (1 x 75 mL), dried over MgSO$_4$, filtered and concentrated *in vacuo*. The residue was purified with silica gel chromatography eluting with 5% methanol in dichloromethane gave compound **2.19** as a light yellow solid (112 mg, 59%).

^{1}H NMR (300 MHz, CDCl$_3$): δ 10.98 (0.5H, bs, ArN**H**),10.52 (0.5H, bs, Ar**H**), 8.70 (0.5H, s, Ar**H**), 8.67 (0.5H, s, Ar**H**), 8.11 (0.5H, s, Ar**H**), 7.9-7.94 (2H, m, Ar**H**), 7.09-7.25

(12H, m, Ar**H**), 6.99 (0.5H, bs, C(O)N**H**), 6.70-6.76 (4H, m, Ar**H**), 6.39 (0.5H, bs, C(O)N**H**), 6.23 (0.5H, d, J = 2.1 Hz, 1' C**H**), 6.20 (0.5H, d, J = 2.1 Hz, 1' C**H**), 5.61 (0.5H, dd, J = 2.1, 6.3 Hz, 2' C**H**), 5.57 (0.5H, dd, J = 2.1, 6.3 Hz, 2' C**H**), 5.33 (0.5H, dd, J = 2.7, 6.3 Hz, 3' C**H**), 5.30 (0.5H, dd, J = 2.7, 6.3 Hz, 3' C**H**), 3.98-4.51 (5H, m, 5' C**H₂**, 4' C**H**, 2 x NHC**H**, POC**H₂**), 3.74-2.78 (9H, m, 2 x POC**H₃**, 2 x ArOC**H₃**), 3.10-3.18 (1H, m, SC**H**), 2.41 (1H, dd, J = 4.5, 13.2 Hz, SC**Hₐ**), 2.23-2.29 (1H, m, SC**H_b**), 1.62-1.75 (5H, CC**H₃**, C**H₂**), 1.38-1.45 (5H, CC**H₃**, C**H₂**), 1.26-1.33 (4H, m, C**H₂**); **¹³C NMR** (75 MHz, CDCl₃): δ 162.4, 162.1, 158.6, 153.0, 151.7, 144.0, 143.0, 142.9, 136.0, 133.0, 132.7, 132.6, 131.6, 130.0, 129.3, 129.0, 128.6, 128.4, 127.8, 127.7, 127.2, 114.9, 113.0, 92.2, 84.5, 82.4, 73.1, 68.4, 65.9, 60.6, 54.7, 46.2, 39.4, 36.8, 30.4, 30.1, 29.3, 27.5, 25.7.

To a solution of compound **2.14** (50 mg, 0.05 mmol) in dichloromethane (1 mL) was added TFA (0.1 mL) and the solution was stirred for 3 h. The reaction mixture was concentrated *in vacuo* and the residue was purified by silica gel chromatography eluting with 7% methanol in dichloromethane gave **2.19** as a white foam (27 mg, 81%).

¹H NMR (300 MHz, CDCl₃): δ 8.70 (1H, s, Ar**H**), 8.32 (1H, s, Ar**H**), 8.01 (2H, d, J = 7.5 Hz, Ar**H**), 7.45-7.59 (3H, m, Ar**H**), 6.10 (1H, d, J = 3.9 Hz, 1' C**H**), 6.00 (0.25H, bs, C(O)N**H**), 5.81 (0.25H, bs, C(O)N**H**), 4.59-4.65 (1H, m, 2' C**H**), 4.16-4.46 (6H, m, 2 x NHC**H**, 3' C**H**, 4' C**H**, 5' C**H₂**), 3.92-4.03 (2H, m, POC**H₂**), 3.69 (3H, d, J = 11.1 Hz, POC**H₃**), 3.04-3.12 (1H, m, SC**H**), 2.76-2.83 (1H, m, SC**Hₐ**), 2.59 (1H, dd, J = 7.5, 12.9 Hz, SC**H_b**), 1.26-1.66 (8H, m, C**H₂**); **LRMS** calcd. for (M + H) C₂₈H₃₇N₇O₉PS: requires 678.2, found 678.3.

To a solution of compound **2.19** (15 mg, 0.03 mmol) in 1:1 methanol and tetrahydrofuran (0.8 mL) was added 32% aqueous ammonium solution (0.4 mL) and stirred o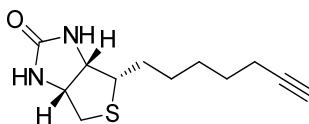vernight. The reaction mixture was concentrated *in vacuo* and purified by silica gel chromatography eluting with 20% methanol in dichloromethane to give a white solid (11 mg, 87%).

¹H NMR (300 MHz, DMSO-d₆): δ 8.34 (1H, s, Ar**H**), 8.20 (1H, s, Ar**H**), 7.41 (2H, bs, ArN**H₂**), 6.60 (1H, d, J = 8.7 Hz, CHN**H**), 6.44 (1H, bs, C(O)N**H**), 5.97 (1H, d, J = 5.1 Hz, 1' C**H**), 5.71 (1H, bs, O**H**, 5.51 (1H, bs, O**H**), 4.65-4.74 (1H, m, 2' C**H**), 4.12-4.38 (6H, m, 3' C**H**, 4' C**H**, 2 NHC**H**, 5' C**H₂**), 3.92-3.98 (2H, m, POC**H₂**), 3.69 (1.5H, d, J = 5.4 Hz, POC**H₃**), 3.65 (1.5H, d, J = 5.4 Hz, POC**H₃**), 3.09-3.16 (1H, m, SC**H**), 2.87 (1H,

dd, J = 5.1, 12.3 Hz, SCH_a), 2.62 (1H, d, J = 12.3 Hz, SCH_b), 1.22-1.69 (8H, m, CH_2);
^{31}**P NMR** (32 MHz, CDCl$_3$): δ 1.48.

7.4 Experimental work as described in Chapter 3

Pentamethylcyclopentadienylbis(triphenylphosphine)ruthenium(II)   chloride (1.20)[14,15]
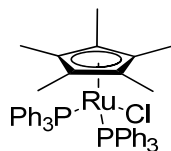
To a degassed solution of ethanol (2.5 mL) were added ruthenium trichloride hydrate (150 mg, 0.66 mmol) and pentamethylcyclopentadiene (225 mg, 1.65 mmol) and the solution was reflux for 6 h under a nitrogen atmosphere. The reaction mixture was cooled to ambient temperature and the precipitate was filtered, washed with cooled ethanol (2 x 10 mL) and diethyl ether (2 x 10 mL) and dried *in vacuo* to give compound **3.27** a dark orange solid (107 mg, 58%). Dry ethanol (2 mL) was purged with nitrogen and to the solvent were added ruthenium **3.27** (100 mg, 0.31 mmol) and triethylphosphine (481 mg, 1.84 mmol). The reaction mixture was refluxed for 24 h and was subsequently allowed to cool to ambient temperature. The precipitate was filtered and washed with hexane (2 x 10 mL) to give an orange solid (127 mg, 51%).

^{1}H NMR (300 MHz, CDCl$_3$): δ 6.8 – 7.8 (m, 30H, Ar-H), 1.05 (15H, s, CH$_3$); **^{31}P NMR** (32 MHz, C$_6$D$_6$): δ 41.53.

(3a*S*,4*S*,6a*R*)-4-[5-[1-[[(2*R*,3*S*,4*R*,5*R*)-5-(6-Aminopurin-9-yl)-3,4-dihydroxy-tetrahydrofuran-2-yl]methyl]triazol-4-yl]pentyl]-1,3,3a,4,6,6a-hexahydrothieno[3,4-*d*]imidazol-2-one (3.08)
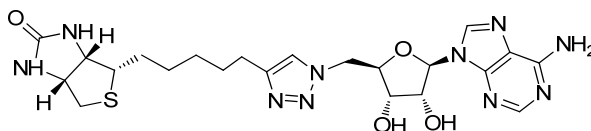
Method 1

To a solution of triazole **3.25** (15 mg, 0.03 mmol) in dichloromethane (0.9 mL) was added TFA (0.1 mL) and stirred for 6 h. The reaction mixture was concentrated *in vacuo* and

purified by silica gel chromatography using 20% methanol in dichloromethane to give a white solid (6 mg, 43%).

¹H NMR (300 MHz, DMSO-d₆): δ 8.22 (1H, s, Ar**H**), 8.15 (1H, s, Ar**H**), 7.67 (1H, s, Ar^{tri}**H**), 7.37 (2H, bs, ArN**H₂**), 6.54 (1H, bs, C(O)N**H**), 6.38 (1H, bs, C(O)N**H**), 5.90 (1H, d, J = 5.4 Hz, 1' C**H**), 5.67 (1H, bs, O**H**), 5.54 (1H, bs, O**H**), 4.59-4.73 (3H, m), 4.28-4.33 (1H, m, NHC**H**), 4.20-4.27 (2H, m, 5' C**H₂**), 4.11-4.15 (1H, m, NHC**H**), 3.05-3.11 (1H, m, SC**H**), 2.81 (1H, dd, J = 5.1, 12.3 Hz, SC**H₂**), 2.50-2.59 (3H, m (under DMSO residual peak), ArC^{tri}**CH₂**, SC**H**$_b$), 1.65-1.211 (8H, m, 4 x C**H₂**); **¹³C NMR** (150 MHz, DMSO-d₆): δ 162.7, 156.1, 152.6, 149.2, 146.7, 139.8, 122.5, 119.2, 87.7, 82.3, 72.5, 71.1, 70.8, 61.1, 59.2, 55.5, 51.0, 40.0, 28.6, 28.3, 28.2, 24.8; **HRMS** calcd. for (M+ H) C₂₂H₃₁N₁₀O₄S: requires 531.2251, found 531.2231.

Method 2 (See chapter 3, table 1 entry 8)

To a suspension of alkyne **3.12** (24 mg, 0.10 mmol) and azide **3.15** (27 mg, 0.09 mmol) in 1:1 acetonitrile and water (2.5 mL) were added a solution of Cu₂SO₄.5H₂O (2.3 mg, 0.009 mmol) and sodium ascorbate (3.6 mg, 0.018 mmol) in 0.23 mL of water and stirred at ambient temperature for 4h. The reaction mixture was concentrated *in vacuo* and the resulting residue was purified by silica gel chromatography using 20% methanol in dichloromethane to give only trace amounts of the title compound.

(3a*S*,4*S*,6a*R*)-4-Hept-6-ynyl-1,3,3a,4,6,6a-hexahydrothieno[3,4-*d*]imidazol-2-one (3.12)[16]

Biotin bromide **3.19** (1.10 g, 3.75 mmol) was treated with 90% lithium acetylide EDA complex (0.959 g, 9.39 mmol) and following general procedure **F1**. The residue was purified by silica gel chromatography eluting with 4% methanol in dichloromethane to give a white solid (0.679 g, 71%).

---

¹H NMR (300 MHz, CDCl₃): δ 5.30 (1H, bs, C(O)N**H**), 5.19 (1H, s, C(O)N**H**), 4.50-4.54 (1H, NHC**H**), 4.31 (1H, ddd, J = 1.5, 4.6, 7.8 Hz, NHC**H**), 3.13-3.20 (1H, m, SC**H**), 2.93 (1H, dd, J = 5.1, 12.8 Hz, SC**H**$_a$), 2.74 (1H, d, J = 12.8 Hz, SC**H**$_b$), 2.19 (2H, td, J =6.8, 2.6 Hz, C**H₂**C≡CH), 1.94 (0.6H, t, J = 2.6 Hz, CH₂C≡C**H**), 1.64-1.71 (2H, m, C**H₂**), 1.39-1.56 (6H, m, 3 x C**H₂**); **¹³C NMR** (75 MHz, CDCl₃): δ 163.3, 84.7, 68.6, 62.2, 60.3, 55.7, 40.8, 28.8, 29.8, 28.4, 18.5; **¹³C NMR** (75 MHz, DMSO-d₆): δ 162.6, 84.5, 70.96, 61.0, 59.2, 55.4, 39.7, 28.2, 28.1, 28.0, 27.7, 17.6.

Ditert-butyl   (3a*S*,4*S*,6a*R*)-4-hept-6-ynyl-2-oxo-3a,4,6,6a-tetrahydrothieno[3,4-*d*]imidazole-1,3-dicarboxylate (3.13)[16]
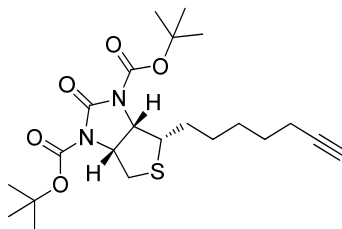
Biotin alkyne **3.12** (100 mg, 0.42 mmol), di-*tert*-butyl-dicarbonate (228 mg, 1.05 mmol), triethylamine (107 mg, 1.05 mmol) and 4-DMAP (102 mg, 0.84 mmol) were dissolved in dichloromethane (2 mL) and stirred for 36 h under nitrogen atmosphere. The reaction mixture was diluted with dichloromethane (45 mL), washed with water (1 x 50 mL) and brine (1 x 50 mL), dried over Na₂SO₄ and concentrated *in vacuo*. The residue was purified by silica gel chromatography eluting with 15% ethyl acetate and petroleum ether to give a white solid (99 mg, 54%).

¹H NMR (300 Mhz, CDCl₃): δ 4.48-4.61 (2H, m, 2 x NC**H**), 3.43-3.50 (1H, m, SC**H**), 3.38 (1H, dd, J = 6.3, 12.9 Hz, SC**H**$_a$), 2.96 (1H, dd, J = 5.7, 12.9 Hz, SC**H**$_b$), 2.67 (2H, td, J = 7.1, 2.6 Hz, C**H₂**C≡CH), 2.02 (1H, t, J = 2.6 Hz, CH₂C≡C**H**), 1.53 (9H, s, C(C**H₃**)₃), 1.52 (9H, s, C(C**H₃**)₃), 1.49-1.60 (8H, m, C**H₂**); **¹³C NMR** (75 MHz, CDCl₃): δ 150.1, 150.0, 148.9, 84.4, 83.9, 83.8, 68.5, 60.4, 58.2, 52.4, 36.6, 28.5, 28.2, 28.1, 28.1, 27.8, 27.7, 18.4.

Attempted synthesis of (3a*S*,4*S*,6a*R*)-4-(5-oxohept-6-ynyl)-1,3,3a,4,6,6a-hexahydrothieno[3,4-d]imidazol-2-one (3.14)
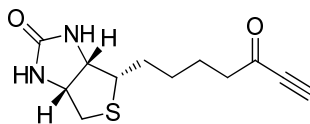
Method 1

A cooled solution of Weinreb amide **3.22** (20 mg, 0.070 mmol) in THF (1 mL) was added dropwise a solution of lithium acetylide ethylene diamine complex (8 mg, 0.077 mmol) in THF (1 mL) and stirred at 0 °C for 3 h under nitrogen atmosphere. The reaction mixture was brought to ambient temperature and stirred for a further 3 h. The reaction mixture was diluted with dichloromethane (25 mL) and washed with water (1 x 25 mL) and brine (1 x 25 mL), dried over Na_2SO_4 and concentrated *in vacuo*. TLC eluting with 10% methanol in dichloromethane indicated a complex mixture.

Method 2

A cooled solution of Weinreb amide **3.22** (20 mg, 0.070 mmol) in THF (1 mL) was added dropwise a solution of 0.5 M ethylnyl magnesium bromide in THF (0.15 ml, 0.076 mmol) and stirred at 0 °C for 3 h. Work up according to method 1. A complex mixture was obtained as judge by TLC.

(2*R*,3*R*,4*S*,5*R*)-2-(6-Aminopurin-9-yl)-5-(azidomethyl)tetrahydrofuran-3,4-diol (3.15)[17]
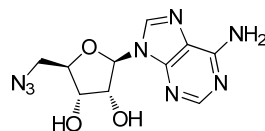
To a solution of azide **3.16** (100 mg, 0.30 mmol) in dichloromethane (1 mL) were added TFA (0.8 mL) and water (0.2 mL) and stirred for 2 h. The reaction mixture concentrated *in vacuo* and purified by silica gel chromatography eluting with 20% methanol in dichloromethane to give a glassy solid (69 mg, 78%).

^{1}**H NMR** (300 MHz, DMSO-d$_6$): δ 8.41 (1H, s, Ar**H**), 8.21 (1H, s, Ar**H**), 7.35 (2H, bs, ArN**H$_2$**), 5.95 (1H, d, *J* = 5.4 Hz, 1' **CH**), 4.78 (1H, t (apparent), *J* = 5.4 Hz, 4' **CH**), 4.21-4.25 (1H, m, **CH**), 4.05-4.09 (1H, m, **CH**), 3.71 (1H, dd, *J* = 7.2, 13.2 Hz, 5' **CH$_a$**), 3.57 (1H, dd, *J* = 3.9, 13.2 Hz, 5' **CH$_b$**); ^{13}**C NMR** (75 MHz, DMSO-d$_6$): δ 156.1, 152.7, 149.4, 140.0, 119.2, 87.8, 83.0, 77.7, 71.0, 51.7.

9-[(3a*R*,4*R*,6*R*,6a*R*)-6-(Azidomethyl)-2,2-dimethyl-3a,4,6,6a-tetrahydrofuro[3,4-*d*][1,3]dioxol-4-yl]purin-6-amine (3.16)[18]
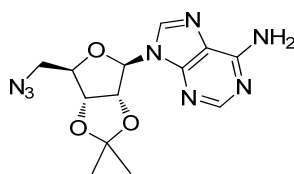
Method 1

To a solution of azide **3.17** (200 mg, 0.45 mmol) in 1:1 MeOH/THF (5 mL) was added 1.5 M lithium hydroxide solution (2.5 mL) and stirred overnight. The reaction mixture was concentrated *in vacuo* and purified by silica gel chromatography using 5% methanol in dichloromethane to give a white solid (97 mg, 64%). ^{1}H NMR consistent with literature reports[18] and method 2.

Method 2 (Mitsunobu reaction)

To a solution of triphenylphosphine (512 mg, 1.95 mmol) cooled at 0 $^{\circ}$C was added diethyl azo dicarboxylate (311 mg, 1.79 mmol) and stirred for 10 min under a nitrogen atmosphere. The mixture was allowed to warm to ambient temperature and was added dropwise diphenylphosphoryl azide (474 mg, 1.95 mmol) over 5 min, followed by adenosine **2.02** (500 mg, 1.62 mmol). The reaction mixture was shielded from light and stirred for 36 h. The resulting precipitate was filtered and washed with petroleum ether. The filtrate was concentrated *in vacuo* and purified by silica gel chromatography using 8% methanol in dichloromethane to give a white foam (422 mg, 78%).

^{1}**H NMR** (300 MHz, CDCl$_3$): δ 8.34 (1H, s, Ar**H**), 7.91 (1H, s, Ar**H**), 6.21 (2H, bs, ArN**H$_2$**), 6.11 (1H, d, *J* = 2.1 Hz, 1' **CH**), 5.46 (1H, dd, *J* = 2.1, 6.3 Hz, 2' **CH**), 5.06 (1H,

dd, J = 3.3, 6.3 Hz, 3' **CH**), 4.37 (1H, dt, J = 3.3, 5.7 Hz, 4' **CH**), 3.57 (2H, dd, J = 3.6, 6.3 Hz, 5' **CH₂**), 1.60 (3H, s, CC**H₃**), 1.38 (3H, CC**H₃**); [13]**C NMR** (75 MHz, CDCl₃): δ 156.01, 153.36, 149.35, 140.02, 120.46, 114.91, 90.81, 85.84, 84.24, 82.23, 52.48, 27.30, 25.51.

N-[9-[(3a*R*,4*R*,6*R*,6a*R*)-6-(Azidomethyl)-2,2-dimethyl-3a,4,6,6a-tetrahydrofuro[3,4-*d*][1,3]dioxol-4-yl]purin-6-yl]benzamide (3.17)[17]
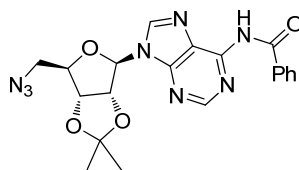
To a solution of adenosine tosylate **3.23** (500 mg, 0.88 mmol) in DMF (5 mL) was added sodium azide (86 mg, 1.33 mmol) and stirred overnight under nitrogen atmosphere. The reaction mixture was poured into water (100 mL) and extracted with dichloromethane (3 x 100 mL). The organic layer were pooled, washed with water (2 x 200 mL) and brine (1 x 200 mL), dried over Na₂SO₄, filtered and concentrated *in vcauo*. The residue was purified by silica gel chromatography eluting with 2% methanol in dichloromethane to give a white solid (304 mg, 79 %).

[1]**H NMR** (300 MHz, CDCl₃): δ 9.05 (1H, bs, N**H**), 8.79 (1H, s, Ar**H**), 8.07 (1H, s, Ar**H**), 8.12 (1H, d, J = 7.2 Hz, Ar**H**), 7.82 (1H, d, J = 8.4 Hz, Ar**H**), 7.42-7.65 (3H, m, Ar**H**), 5.95 (1H, d, J = 4.8 Hz, 1' **CH**), 5.22-5.25 (1H, m, 2' **CH**), 5.12-5.14 (1H, m, 3' **CH**), 4.55-4.56 (1H, m, 4' **CH**), 3.97-4.02 (1H, m, 5' **CH**ₐ), 3.78-3.85 (1H, m, 5' **CH**ᵦ), 1.66 (3H, s, CC**H₃**), 1.39 (3H, s, CC**H₃**).

5-[(3a*S*,4*S*,6a*R*)-2-Oxo-1,3,3a,4,6,6a-hexahydrothieno[3,4-*d*]imidazol-4-yl]pentyl   4-methylbenzenesulfonate (3.18)[19]
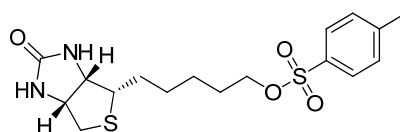
Biotinol **2.05** (2.5 g, 10.8 mmol) was tosylated with tosyl chloride (3.10 g, 16.3 mmol) and following general procedure **D1** to give a white solid (2.79 g, 67%). >95% purity as judge by ^{1}H NMR spectroscopy.

^{1}H NMR (300 MHz, CDCl$_3$): δ 7.78 (2H, d, J = 8.7 Hz, Ar**H**), 7.35 (2H, d, J =8.7 Hz, Ar**H**), 6.09 (1H, bs, C(O)N**H**), 5.47 (1H, bs, C(O)N**H**),4.47-4.51 (1H, m, NHC**H**), 4.26-4.30 (1H, m, NHC**H**), 4.01 (2H, t, J = 6.3 Hz, OC**H$_2$**), 3.07-3.14 (1H, m, SC**H**), 2.89 (1H, dd, J = 5.1, 12.6 Hz, SC**H$_a$**), 2.73 (1H, d, J = 12.6 Hz, SC**H$_b$**), 2.45 (3H, s, ArC**H$_3$**), 1.60-1.69 (4H, m, 2 x C**H$_2$**), 1.33-1.39 (4H, m, 2 x C**H$_2$**); **^{13}C NMR** (75 MHz, CDCl$_3$): 164.0, 145.0, 133.2, 130.1, 128.1, 70.84, 62.1, 60.3, 55.8, 40.8, 28.8, 28.6, 28.5, 25.6, 21.9.

(3a*S*,4*S*,6a*R*)-4-(5-Bromopentyl)-1,3,3a,4,6,6a-hexahydrothieno[3,4-*d*]imidazol-2-one (3.19)[16]
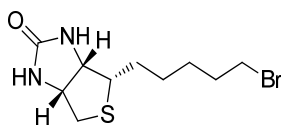
Biotin tosylate **3.18** (2.0 g, 5.21 mmol) was brominated with lithium bromide (0.90 g, 10.4 mmol) and following general procedure **E1**. The residue was purified by silica gel chromatography eluting with 5% methanol in dichloromethane to give a white solid (1.16 g, 76%).

^{1}H NMR (300 MHz, CDCl$_3$): δ 5.51 (1H, bs, C(O)N**H**), 5.21 (1H, bs, C(O)N**H**), 4.49-4.54 (1H, m, NHC**H**), 4.31 (1H, ddd, J = 1.5, 4.6, 7.8 Hz, NHC**H**), 3.41 (2H, t, J = 6.7 Hz, C**H$_2$**Br), 3.13-3.20 (1H, m, SC**H**), 2.93 (1H, dd, J = 5.1, 12.8 Hz, SC**H$_a$**), 2.74 (1H, d, J = 12.8 Hz, SC**H$_b$**), 1.83-1.92 (2H, m, C**H$_2$**), 1.65-1.72 (2H, m, C**H$_2$**), 1.43-1.53 (4H, m, 2 x C**H$_2$**); **^{13}C NMR** (75 MHz, CDCl$_3$), 163.5, 62.3, 60.3, 55.7, 40.8, 34.0, 32.7, 28.8, 28.5, 28.3.

Attempted synthesis of 5-[(3a*S*,4*S*,6a*R*)-2-oxo-1,3,3a,4,6,6a-hexahydrothieno[3,4-*d*]imidazol-4-yl]pentanal (3.20)
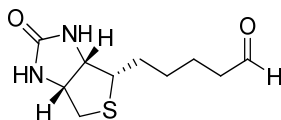
To a solution of biotinol **2.07** (100 mg, 0.43 mmol) in dry dichloromethane (5 mL) was added Dess-Martin periodinane (202 mg, 0.48 mmol) and stirred at 0 °C under nitrogen atmosphere and until consumption of starting material biotinol (as judged by TLC, using 7% methanol in dichloromethane). The reaction mixture was quenched with saturated aqueous sodium bicarbonate (20 mL) and extracted with dichloromethane (3 x 25 mL). The organic layers were pooled, washed with brine (1 x 75 mL), dried over Na_2SO_4 and concentrated *in vacuo*. ^{1}H NMR spectroscopy indicated a complex mixture, whilst purification by silica gel chromatography (3% methanol in dichloromethane) did not isolation target compound.

5-[(3a*S*,4*S*,6a*R*)-2-Oxo-1,3,3a,4,6,6a-hexahydrothieno[3,4-*d*]imidazol-4-yl]-*N*-methoxy-*N*-methyl-pentanamide (3.22)
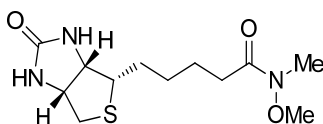
Biotin 1.01 (100 mg, 0.41 mmol), EDCI (69 mg, 0.45 mmol), diisopropylethylamine (158 mg, 1.23 mmol) and N, O- dimethylhydroxylamide hydrochloride (44 mg, 0.45 mmol) were dissolved in DMF (1.5 mL) and stirred for 12 h under nitrogen atmosphere. The reaction mixture was diluted with dichloromethane (30 mL), washed with 0.5M aqueous HCl (2 x 30 mL), saturated aqueous sodium bicarbonate (2 x 30 mL), water (1 x 30 mL) and brine (1 x 30 mL), dried over Na_2SO_4, filtered and concentrated *in vacuo*. The residue was purified by silica gel chromatography eluting with 12% methanol in dichloromethane to give a light brown solid (51 mg, 43%).

^{1}**H NMR** (300 MHz, CDCl$_3$): δ 6.44 (1H, bs, C(O)N**H**), 6.36 (1H, bs, C(O)N**H**), 4.28-4.33 (1H, m, NHC**H**), 4.11-4.15 (1H, m, NHC**H**), 3.65 (3H, s, OC**H**$_3$), 3.13-3.18 (1H, m, SC**H**),

3.08 (3H, s, NCH_3), 2.82 (1H, dd, J =5.1, 12.3 Hz, SCH_a), 2.58 (1H, d, J = 12,3 Hz, SCH_b), 2.36 (2H, t, J = 7.2 Hz, C(O)CH_2), 1.24-1.64 (3H, m, CH_2).

[(3a*R*,4*R*,6*R*,6a*R*)-4-(6-Benzamidopurin-9-yl)-2,2-dimethyl-3a,4,6,6a-tetrahydrofuro[3,4-*d*][1,3]dioxol-6-yl]methyl 4-methylbenzenesulfonate (3.23)[20]
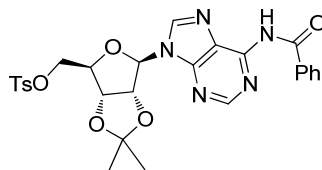
Adenosine **2.12** (500 mg, 1.22 mmol) was tosylated using tosyl chloride (346 mg, 1.82 mmol) following general procedure **D1** and purified by silica gel chromatography eluting with 5% methanol in dichloromethane to give a white foam (515 mg, 75%).

^{1}H NMR (300 MHz, CDCl$_3$): δ 9.01 (1H, s, Ar**H**), 8.70 (1H, s, Ar**H**), 8.60 (1H, s, ArN**H**), 8.00 − 8.08 (4H, m, Ar**H**), 7.37-7.69 (5H, m, Ar**H**), 6.13 (1H, d, J = 1.8 Hz, 1' C**H**), 5.36 (1H, dd, J = 1.8, 6.3 Hz, 2' C**H**), 5.05 (1H, dd, J = 3.0, 6.3 Hz, 3' C**H**), 4.47-4.54 (1H, m, 4' C**H**), 4.27 (1H, dd, J = 4.2, 10.8 Hz, 5' C**H**$_a$), 4.21 (1H, dd, J = 5.7, 10.8 Hz, 5' C**H**$_b$), 2.38 (3H, s, ArC**H**$_3$), 1.60 (3H, s, CC**H**$_3$), 1.37 (3H, s, CC**H**$_3$).

Attempted synthesis of Ditert-butyl (3a*S*,4*S*,6a*R*)-4-[5-[1-[[(3a*R*,4*R*,6*R*,6a*R*)-4-(6-benzamidopurin-9-yl)-2,2-dimethyl-3a,4,6,6a-tetrahydrofuro[3,4-*d*][1,3]dioxol-6-yl]methyl] triazol-4-yl]pentyl]-2-oxo-3a,4,6,6a-tetrahydrothieno[3,4-*d*]imidazole-1,3-dicarboxylate (3.24)
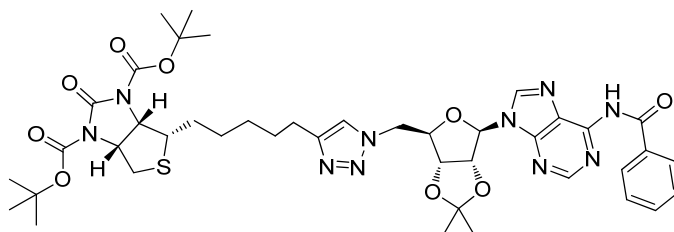
To a suspension of alkyne **3.13** (22 mg, 0.050 mmol) and azide **3.15** (20 mg, 0.046 mmol) in 1:1 *tert*-butanol and water (2 mL) were added a solution of Cu$_2$SO$_4$.5H$_2$O (0.6 mg,

0.0023 mmol) and sodium ascorbate (1.4 mg, 0.0069 mmol) in 0.1 mL of water and the mixture was stirred at ambient temperature for 4h. The reaction was monitored by TLC eluting with 5% methanol in dichloromethane. A complex mixture was obtained as judged by TLC and ^{1}H NMR spectroscopy (300 MHz, CDCl$_3$).

(3a*S*,4*S*,6a*R*)-4-[5-[1-[[(3a*R*,4*R*,6*R*,6a*R*)-4-(6-aminopurin-9-yl)-2,2-dimethyl-3a,4,6,6a-tetrahydrofuro[3,4-d][1,3]dioxol-6-yl]methyl]triazol-4-yl]pentyl]-1,3,3a,4,6,6a-hexa hydrothieno[3,4-d]imidazol-2-one (3.25)
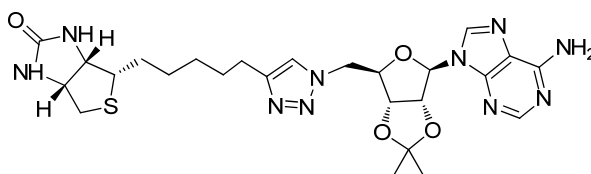
Method 1a (See chapter 3, table 2 entry 8).

To a suspension of alkyne **3.12** (16 mg, 0.066 mmol) and azide **3.16** (20 mg, 0.06 mmol) in 1:2 acetonitrile and water (1.5 mL) was added copper nano powder (1 mg, 0.02 mmol). The reaction mixture was sonicated for 15 min and subsequently stirred at 35 ^{o}C for 6 h. The reaction mixture was concentrated *in vacuo* and the resulting residue was purified by silica gel chromatography eluting with 10% methanol in dichloromethane to give a white solid (25 mg, 73%).

^{1}H NMR (300 MHz, CDCl$_3$): δ 8.21 (1H, s, Ar**H**), 7.74 (1H, bs, C(O)N**H**), 7.53 (1H, s, Ar**H**), 7.07 (1H, s, Ar^{tri}**H**), 6.93 (2H, bs, ArN**H$_2$**), 6.00 (1H, d, *J* = 3.6 Hz, 1' C**H**), 5.27 (1H, dd, *J* = 3.6, 8.8 Hz, 2' C**H**), 5.05 (1H, bs, C(O)N**H**), 5.01 (1H, dd, *J* = 3.9, 8.8 Hz, 3' C**H**), 4.91 (1H, dd, *J* = 5.4, 14.4 Hz, 5' C**H$_a$**), 4.52-4.63 (3H, m, 5' C**H$_b$**, 4' C**H**, NHC**H**), 4.35-4.40 (1H, NHC**H**), 3.15-3.22 (1H, SC**H**), 2.93 (1H, dd, *J* = 4.8, 12.9 Hz, SC**H$_a$**), 2.67-2.78 (2H, SC**H$_b$**, ArC^{tri}C**H$_a$**), 2.48-2.50 (1H, ArC^{tri}C**H$_b$**), 1.25-1.77 (14H, m); **^{13}C NMR** (75 MHz, CDCl$_3$): δ 164.3, 156.6, 153.4, 149.5, 148.1, 139.5, 123.2, 115.8, 90.1, 83.3, 82.9, 80.6, 63.0, 60.3, 56.3, 50.5, 40.9, 29.5, 29.2, 28.6, 27.5, 25.8, 25.7; **HRMS** calcd. for (M+ H) C$_{25}$H$_{35}$N$_{10}$O$_4$S: requires 571.2564, found 571.2564. **HPLC** R$_t$ = 20.1 min.
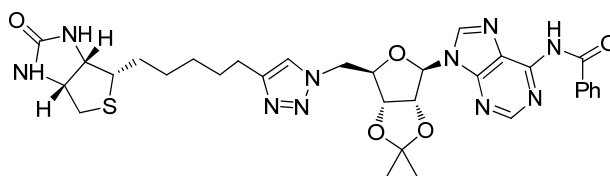
Method 1b (See chapter 3, table 2 entry 1)

To a suspension of alkyne **3.12** (16 mg, 0.066 mmol) and azide **3.16** (20 mg, 0.060 mmol) in 1:2 dichloromethane and water (1.5 mL) was added a 1 cm piece of copper wire and the mixture was stirred at ambient temperature for 6 h. The copper wire was removed and the reaction mixture was concentrated *in vacuo*. The resulting residue was purified by silica gel chromatography using 10% methanol in dichloromethane to give a white solid (8 mg, 23%). ^{1}H NMR spectra was consistent with method 1a.

Method 1c (See chapter 3, table 2 entry 2)

Following the modified procedure outline in method 4 but using 2:1 acetonitrile and water (1.5 mL) solvent system gave the title compound (9 mg, 27%). ^{1}H NMR spectra was consistent with method 1a.

Method 1d (See chapter 3, table 2 entry 3)

Following the modified procedure outline in method 4 but using a piece of copper turning and 2:1 acetonitrile and water (1.5 mL) gave the title compound (12 mg, 35%). ^{1}H NMR spectra was consistent with method 1a.

Method 1e (See chapter 3, table 2 entry 4)

Following the modified procedure outline in method 4 but using copper nano powder (1 mg, 0.016 mmol) and 2:1 acetonitrile and water (1.5 mL) gave the title compound (16 mg, 47%). ^{1}H NMR spectra was consistent with method 1a.

Method 1f (See chapter 3, table 2 entry 5)

Following the modified procedure outline in method 4 but using and using copper nano powder (1 mg, 0.016 mmol) and 2:1 dichloromethane and water (1.5 mL) gave the title compound (8 mg, 23%). ^{1}H NMR spectra was consistent with method 1a.

Method 1g (See chapter 3, table 2 entry 6)

To a suspension of alkyne **3.12** (16 mg, 0.066 mmol) and azide **3.16** (20 mg, 0.060 mmol) in 1:2 acetonitrile and water (1.5 mL) was added copper nano powder (1 mg, 0.016 mmol) and the mixture was stirred at 35 ^{o}C for 6 h. The reaction mixture was concentrated *in*

vacuo and the resulting residue was purified by silica gel chromatography eluting with 10% methanol in dichloromethane to give a white solid (22 mg, 67%). ^{1}H NMR spectra was consistent with method 1a.

Method 1h (See chapter 3, table 2 entry 7).

To a suspension of alkyne **3.12** (16 mg, 0.066 mmol) and azide **3.16** (20 mg, 0.060 mmol) in 1:2 acetonitrile and water (1.5 mL) were added copper nano powder (1 mg, 0.016 mmol) and triethylamine hydrochloride (2 mg, 0.015 mmol) and the mixture was stirred at 35 ^{o}C for 6 h. The reaction mixture was concentrated *in vacuo* and the resulting residue was purified by silica gel chromatography eluting with 10% methanol in dichloromethane to give a white solid (22 mg, 67%). ^{1}H NMR spectra was consistent with method 1a.

Method 2a (See chapter 3, table 1 entry 6)

To a suspension of alkyne **3.12** (24 mg, 0.10 mmol) and azide **3.16** (30 mg, 0.09 mmol) in 1:1 acetonitrile and water (2.5 mL) were added a solution of $Cu_2SO_4.5H_2O$ (2.3 mg, 0.01 mmol) and sodium ascorbate (3.6 mg, 0.02 mmol) in 0.23 mL of water and the mixture was stirred at ambient temperature for 4 h. The reaction mixture was concentrated *in vacuo* and the resulting residue was purified by silica gel chromatography eluting with 10% methanol in dichloromethane to give a white solid (5 mg, 10%). ^{1}H NMR spectra was consistent with method 1a.

Method 2b (See chapter 3, table 1 entry 7)

Following the modified procedure outline in method 2 but using 1:1 dichloromethane and water (2.5 mL) gave the title compound (7 mg, 14%). ^{1}H NMR spectra was consistent with method 1a.

Method 2c (See chapter 3, table 1 entry 9)

To a solution of alkyne **3.12** (48 mg, 0.20 mmol) and azide **3.16** (60 mg, 0.18 mmol) in 1:1 acetonitrile (7 mL) was added copper(I) iodide (3 mg, 0.01 mmol) and the mixture was stirred under overnight under nitrogen atmosphere. TLC eluting with 10% methanol in dichloromethane indicated target product was not present in the reaction mixture. ^{1}H NMR spectra was consistent with method 1a.

Method 3

To a solution of triazole **3.26** (50 mg, 0.074 mmol) in 1:1 THF and methanol (2 mL) was added 32% ammonium solution (1 mL) and the mixture was stirred overnight. The reaction mixture was concentrated *in vacuo* and purified by silica gel chromatography using 10% methanol in dichloromethane to give a white solid (20 mg, 47%). ^{1}H NMR spectra was consistent with method 1a.

_N_-[9-[(3a_R_,4_R_,6_R_,6a_R_)-6-[[4-[5-[(3a_S_,4_S_,6a_R_)-2-Oxo-1,3,3a,4,6,6a-hexahydrothieno[3,4-_d_]imidazol-4-yl]pentyl]triazol-1-yl]methyl]-2,2-dimethyl-3a,4,6,6a-tetrahydrofuro[3,4-_d_][1,3]dioxol-4-yl]purin-6-yl]benzamide (3.26)

Method 1a (see chapter 3, table 1, entry 2)

To a suspension of alkyne **3.12** (12 mg, 0.050 mmol) and azide **3.17** (20 mg, 0.046 mmol) in 1:1 *tert*-butanol and water (2 mL) were added a solution of $Cu_2SO_4.5H_2O$ (0.6 mg, 0.0023 mmol) and sodium ascorbate (1.4 mg, 0.0069 mmol) in water (0.1 mL) and the mixture was stirred at ambient temperature for 4h. The reaction was monitored by TLC using 5% methanol in dichloromethane. TLC revealed only starting material present.

Method 1b (see chapter 3, table 1, entry 3)

To a suspension of alkyne **3.12** (18 mg, 0.076 mmol) and azide **3.17** (30 mg, 0.068 mmol) in 1:1 *tert*-butanol and water (2.5 mL) were added a solution of $Cu_2SO_4.5H_2O$ (1.7 mg, 0.0069 mmol) and sodium ascorbate (2.7 mg, 0.014 mmol) in 0.17 mL of water and the reaction mixture was stirred at ambient temperature for 4h. The reaction mixture was concentrated *in vacuo* and the resulting residue was purified by silica gel chromatography eluting with 7% methanol in dichloromethane to give a white solid (2 mg, 4%). ^{1}H NMR spectra was consistent with method 1d.

Method 1c (see chapter 3, table 1, entry 4)

Following the modified procedure outline in method 2 but using 1:1 acetonitrile and water (2.5 mL) gave the title compound (5 mg, 11%). ^{1}H NMR spectra was consistent with method 1d.

Method 1d (see chapter 3, table 1, entry 5)

Following the modified procedure outline in method 2 but using 1:1 dichloromethane and water (2.5 mL) gave the title compound (4 mg, 9%).

^{1}H NMR (300 MHz, CDCl$_3$): δ 10.16 (1H, bs, N**H**), 8.61 (1H, s, Ar**H**), 8.00-8.05 (3H, m, 3 x Ar**H**), 7.40-7.53 (3H, m, 3 x Ar**H**), 7.00 (1H, s, Ar^{tri}**H**), 6.52 (1H, bs, C(O)N**H**), 6.01 (1H, d, *J* = 2.8 Hz, 1' **CH**), 5.41 (1H, dd, *J* = 2.8, 5.5 Hz, 2' **CH**), 5.11 (1H, dd, *J* = 4.6, 6.6 Hz, 3' **CH**), 4.43-4.93 (5H, m), 4.30-4.35 (1H, m, NHC**H**), 3.09-3.18 (1H, m, SC**H**), 2.89 (1H, dd, *J* = 4.8, 12.8 Hz, SC**H$_a$**), 2.50-2.68 (3H, m, SC**H$_b$**, ArC^{tri}C**H$_2$**), 1.25-1.69 (14H, m); **^{13}C NMR** (75 Mhz, CDCl$_3$): δ 165.9, 164.0, 152.5, 151.7, 150.9, 148.3, 142.8, 133.4, 133.0, 128.8, 128.8, 124.9, 122.7, 115.7, 90.4, 84.3, 83.3, 80.8, 62.4, 60.2, 55.9, 50.7, 40.7, 29.3, 29.0, 28.8, 27.4, 25.6. **LRMS** calcd. for (M+H) C$_{32}$H$_{38}$N$_{10}$O$_5$S: requires 675.78, found 675.6.

(5-Phenyltriazol-1-yl)methyl 2,2-dimethylpropanoate (3.31)
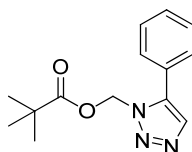
To a solution of azido methyl pivalate **3.29** (50 mg, 0.32 mmol) and phenylacetylene (36 mg, 0.35 mmol) in freshly distilled THF (5 mL) was added Cp*Ru(PPh$_3$)$_2$Cl (13 mg, 0.02 mmol) and the mixture was stirred at reflux for 2 h. The reaction mixture was cooled and diluted with dichloromethane (20 mL), washed with water (1 x 25 mL) and brine (1 x 25 mL), dried over Na$_2$SO$_4$, filtered and concentrated *in vacuo*. The residue was purified with 20% ethyl acetate in petroleum ether to give a white solid (72 mg, 87%).

^{1}**H NMR** (300 MHz, CDCl$_3$): δ 7.72 (1H, s, Ar^{tri}**H)**, 7.45-7.47 (3H, m, Ar**H**), 7.36-7.38 (2H, m, Ar**H**), 5.02 (2H, s, OC**H$_2$**N), 1.37 (9H, s, C(C**H$_3$**)$_3$); ^{13}**C NMR** (75 MHz, CDCl$_3$): δ 165.8, 138.9, 133.2, 130.1, 129.4, 128.9, 127.0, 83.8, 50.4, 28.1.

(3a*S*,4*S*,6a*R*)-4-[5-[3-[[(3a*R*,4*R*,6*R*,6a*R*)-4-(6-Aminopurin-9-yl)-2,2-dimethyl-3a,4,6,6a-tetrahydrofuro[3,4-*d*][1,3]dioxol-6-yl]methyl]triazol-4-yl]pentyl]-1,3,3a,4,6,6a-hexahydro thieno[3,4-*d*]imidazol-2-one (3.32)
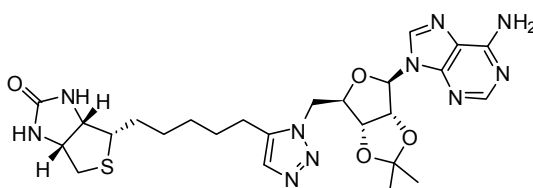
Method 1a (see chapter 3, table 3, entry 1)

To a solution of biotin alkyne **3.12** (20 mg, 0.08 mmol) and adenosine azide **3.16** (31 mg, 0.09 mmol) in THF (2.5 mL) was added Cp*Ru(PPh$_3$)$_2$Cl (1 mg, 0.001 mmol) and the solution was refluxed under nitrogen atmosphere for 4h. The reaction mixture was cooled, diluted with dichloromethane (25 mL), washed with water (1 x 25 mL) and brine (1 x 25 mL), dried over Na$_2$SO$_4$, filtered and concentrated *in vacuo*. The residue was purified by silica gel chromatography eluting with 8% methanol in dichloromethane to give a light yellow solid (5 mg, 10%).

^{1}**H NMR** (600 MHz, CDCl$_3$): δ 8.31 (1H, s, Ar**H**), 7.80 (1H, s, Ar**H**), 7.78 (1H, bs, C(O)N**H**), 7.30 (1H, s, Ar^{tri}**H**), 7.09 (2H, bs, ArN**H$_2$**), 6.04 (1H, s, 1' **CH**), 5.86 and 5.83 (1H, bd, C(O)N**H**), 5.42 (1H, d, *J* = 6.0 Hz, 2' **CH**), 5.33 (1H, dd, *J* = 2.4, 6.0 Hz, 3' **CH**), 4.69-4.84 (3H, m, 5' **CH$_2$**, 4' **CH**), 4.59-4.61 (1H, m, NHC**H**), 4.37-4.39 (1H, m, NHC**H**); 3.12 (1H, m, SC**H**), 2.95 (1H, dd, *J* = 4.8, 12.6 Hz, SC**H$_a$**), 2.71 (1H, d, *J* = 12.6 Hz, SC**H$_b$**), 1.76-1.90 (2H, m), 1.60 (3H, s, CC**H$_3$**), 1.40 (3H, s, CC**H$_3$**), 1.39-1.29 (6H, m, C**H$_2$**, ArC^{tri}C**H$_2$**), 0.87-0.92 (1H, m), 0.47-0.53 (1H, m); ^{13}**C NMR** (150 MHz, CDCl$_3$): 164.5, 156.5, 153.0, 148.6, 143.9, 138.2, 131.7, 120.2, 114.6, 110.0, 91.4, 82.3, 84.5, 82.5, 62.2, 60.1, 56.1, 40.7, 30.3, 29.2, 29.1, 28.1, 27.1, 25.4, 23.0; **HRMS** calcd. for (M + H) C$_{25}$H$_{35}$N$_{10}$O$_4$S: requires 571.2564, found 571.2586. **HPLC** R$_t$ = 20.1 min.

Method 1b (see chapter 3, table 3, entry 2)

To a solution of biotin alkyne **3.12** (20 mg, 0.08 mmol) and adenosine azide **3.16** (31 mg, 0.09 mmol) in THF (2.5 mL) was added Cp*Ru(P(Ph$_3$)$_2$Cl (4 mg, 0.005 mmol) and the solution refluxed under nitrogen for 4h. The reaction was purified according to method 1a to give a light yellow solid (11 mg, 23%). ^{1}H NMR spectra consistent with method 1a.

Method 1c (see chapter 3, table 3, entry 3)

To a solution of biotin alkyne **3.12** (20 mg, 0.08 mmol) and adenosine azide **3.16** (31 mg, 0.09 mmol) in THF (2.5 mL) was added Cp*Ru(PPh$_3$)$_2$Cl (7 mg, 0.01 mmol) and the solution refluxed under nitrogen for 4 h. The reaction was purified according to method 1a to give a light yellow solid (11 mg, 23%). ^{1}H NMR spectra consistent with method 1a.

Method 1d (see chapter 3, table 3, entry 4)

To a solution of biotin alkyne **3.12** (20 mg, 0.08 mmol) and adenosine azide **3.16** (31 mg, 0.09 mmol) in THF (2.5 mL) was added Cp*Ru(PPh$_3$)$_2$Cl (13 mg, 0.02 mmol) and the solution refluxed under nitrogen atmosphere for 4 h. The reaction was purified according to method 1a to give a light yellow solid (12 mg, 25%). ^{1}H NMR spectra consistent with method 1a.

Method 1f (see chapter 3, table 3, entry 5)

To a solution of biotin alkyne **3.12** (20 mg, 0.08 mmol) and adenosine azide **3.16** (31 mg, 0.09 mmol) in THF (2.5 mL) was added Cp*Ru(PPh$_3$)$_2$Cl (13 mg, 0.02 mmol) and the solution refluxed under nitrogen atmosphere for 12 h. The reaction was purified according to method 1a to give a light yellow solid (14 mg, 29%). ^{1}H NMR spectra consistent with method 1a.

Method 1g (see chapter 3, table 3, entry 6)

To a solution of biotin alkyne **3.12** (20 mg, 0.08 mmol) and adenosine azide **3.16** (31 mg, 0.09 mmol) in anhydrous DMF (2.5 mL) was added Cp*Ru(PPh$_3$)$_2$Cl (13 mg, 0.02 mmol) and the solution was stirred at 80 ^{o}C under nitrogen atmosphere for 8 h. The reaction was purified according to method 1 to give a light yellow solid (17 mg, 35%). ^{1}H NMR spectra consistent with method 1a.

Method 1h (see chapter 3, table 3, entry 7)

To a solution of biotin alkyne **3.12** (20 mg, 0.08 mmol) and adenosine azide **3.16** (31 mg, 0.09 mmol) in 1:1 anhydrous DMF and THF (2.5 mL) was added Cp*Ru(PPh$_3$)$_2$Cl (13 mg, 0.02 mmol) and the solution was stirred at 70 ^{o}C under nitrogen atmosphere for 8 h. The reaction was purified according to method 1a to give a light yellow solid (25 mg, 52%). ^{1}H NMR spectra consistent with method 1a.

Method 1i (see chapter 3, table 3, entry 8)

To a solution of biotin alkyne **3.12** (20 mg, 0.08 mmol) and adenosine azide **3.16** (31 mg, 0.09 mmol) in 1:1 anhydrous DMF and THF (2.5 mL) was added Cp*Ru(P(Ph$_3$)$_2$Cl (7 mg, 0.01 mmol) and the solution was stirred at 70 ^{o}C under nitrogen atmosphere for 8 h. The reaction was purified according to method 1a to give a light yellow solid (20 mg, 40%). ^{1}H NMR spectra consistent with method 1a.

7.5 Experimental work as described in chapter 4

(3a*S*,6a*R*)-4-[5-[1-[4-(6-Aminopurin-9-yl)butyl]triazol-4-yl]pentyl]-1,3,3a,4,6,6a-hexahydrothieno[3,4-*d*]imidazol-2-one (4.01)
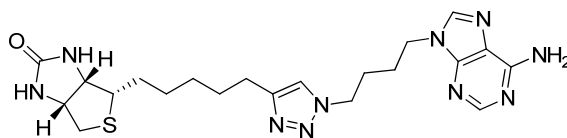
Biotin alkyne **3.12** (31 mg, 0.13 mmol) was reacted with azide **4.20** (36 mg, 0.14 mmol) and Cu nanopowder (2 mg, 0.03 mmol) using General Procedure **G1**. The crude material was purified by flash chromatography on silica eluting with 8% methanol in dichloromethane to give a crystalline white solid (46 mg, 73%).

MP: 106 - 108 °C; **^{1}H NMR** (600 MHz; DMSO-d^6): δ 8.12 (1H, s, Ar**H**), 8.11 (1H, s, Ar**H**), 7.86 (1H, s, Ar^{tri}**H**), 7.20 (2H, bs, ArN**H$_2$**), 6.52 (1H, bs, C(O)N**H**), 6.40 (1H, bs, C(O)N**H**), 4.34-4.38 (3H, m, ArN^{tri}**CH$_2$**, NHC**H**), 4.34-4.38 (3H, m, Ar^{ad}**CH$_2$**, NHC**H**), 3.12-3.16 (m, 1H, SC**H**), 3.12-3.16 (1H, dd, *J* = 4.8, 12.0 Hz, SC**H$_a$**), 2.59-2.64 (3H, m, SC**H$_b$**, ArC^{tri}**CH$_2$**), 1.76-1.80 (4H, m, 2 x C**H$_2$**), 1.28-1.67 (8H, m, 4 x C**H$_2$**); **^{13}C NMR** (150 MHz; DMSO-d^6): 162.8, 156.0, 152.4, 149.5, 146.8, 140.8, 121.8, 118.7, 61.2, 59.2, 55.6, 48.5, 42.2, 40.0, 28.8, 28.6, 28.5, 28.3, 27.0, 26.7, 25.1; **HRMS** calcd. for (M + H) $C_{21}H_{31}N_{10}OS$: requires 471.2403, found 471.2450; **HPLC** R_t = 18.5 min.

(3a*S*,6a*R*)-4-[5-[1-[2-(6-Aminopurin-9-yl)ethyl]triazol-4-yl]pentyl]-1,3,3a,4,6,6a-hexahydrothieno[3,4-*d*]imidazol-2-one (4.02)
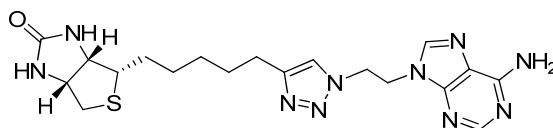
Biotin alkyne **3.12** (15 mg, 0.063 mmol) was reacted with azide **4.18** (15 mg, 0.069) and Cu nanopowder (1 mg, 0.01 mmol) using General Procedure **G1**. The residue was purified by silica gel chromatography on silica eluting with18% methanol in dichloromethane to give a crystalline off white solid (12 mg, 41%).

MP: 222 - 224 °C; **¹H NMR** (300 MHz; DMSO-d⁶): δ 8.16 (1H, s, Ar^ad**H**), 7.85 (1H, s, Ar^ad**H**), 7.45 (1H, s, Ar^tri**H**), 7.33 (2H, bs, ArN**H₂**), 6.73 (1H, bs, C(O)N**H**), 6.45 (1H, bs, C(O)N**H**), 4.86 (2H, t, J = 5.4 Hz, ArC^tri**CH₂**), 4.68 (2H, t, J = 5.4 Hz, Ar^ad**CH₂**), 4.37-4.39 (1H, m, NHC**H**), 4.22-4.23 (1H, m, NHC**H**), 3.15-3.18 (1H, m, SC**H**), 2.90 (1H, dd, J = 4.8, 12.3 Hz, SC**H_a**), 2.56-2.66 (3H, m, SC**H_b**, ArN^tri**CH₂**), 1.62-1.67 (2H, m, C**H₂**), 1.24-1.57 (8H, m, 4 x C**H₂**); **¹³C NMR** (150 MHz; DMSO-d⁶): δ 162.9, 155.9, 152.4, 149.4, 146.9, 140.4, 121.9, 118.4, 61.1, 59.2, 55.6, 48.5, 43.0, 39.9, 28.7, 28.4, 28.3, 28.2, 24.8; **HRMS** calcd. for (M + H) $C_{19}H_{27}N_{10}OS$: requires 443.2090, found 443.2094; **HPLC** R_t = 17.8 min.

(3a*S*,6a*R*)-4-[5-[1-[3-(6-Amino-4,5-dihydropurin-9-yl)propyl]triazol-4-yl]pentyl]-1,3,3a,4,6, 6a-hexahydrothieno[3,4-*d*]imidazol-2-one (4.03)
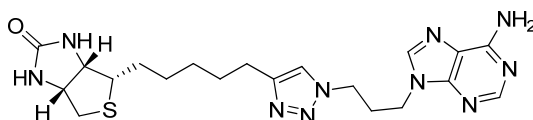
Biotin alkyne **3.12** (15 mg, 0.063 mmol) was reacted with azide **4.19** (16 mg, 0.069 mmol) and Cu nanopowder (1 mg, 0.016 mmol) using General Procedure **G1**. The crude material was purified by flash chromatography on silica eluting with 12% methanol in dichloromethane to give a crystalline white solid (19 mg, 65%).

MP: 156 - 157 °C; **¹H NMR** (600 MHz; 5% CD₃OD, CDCl₃): δ 8.28 (1H, s, ArH), 7.93 (1H, s, ArH), 7.43 (1H, s, Ar^tri**H**), 6.54 (0.25H, bs, ArN**H₂**, exchanged with solvent), 5.91 (1H, bs, C(O)N**H**, exchanged with solvent), 5.73 (0.25H, bs, N**H**, exchanged with solvent), 4.50-4.52 (0.25H, m, C**H**NH), 4.36-4.41 (2H, m, ArN^tri**CH₂**), 4.23 (1H, m, C**H**NH), 4.27 (2H, t, J = 7.2 Hz, Ar^ad**CH₂**), 3.16-3.19 (1H, m, SC**H**), 2.92 (1H, dd, J = 4.8, 13.2 Hz, SC**H_a**), 2.74 (1H, d, J = 4.8 Hz, SC**H_b**), 2.61 (2H, t, J = 7.2 Hz, ArC^tri**CH₂**), 2.43-2.45 (2H, m CH₂C**H₂**CH₂), 1.50-1.65 (4H, m, C**H₂**), 1.28-1.40 (8H, m, 4 x C**H₂**); **¹³C NMR** (150 MHz; 5% CD₃OD, CDCl₃): δ 164.1, 155.7, 152.8, 149.5, 148.4, 140.9, 121.4, 119.1, 62.2, 60.1, 55.8, 46.9, 41.0, 40.4, 30.0, 29.0, 28.9, 28.8, 28.5, 25.2; **HRMS** calcd. for (M + H) $C_{20}H_{29}N_{10}OS$: requires 457.2247, found 457.2269; **HPLC** R_t = 18.0 min.

(3a*S*,6a*R*)-4-[5-[1-[5-(6-Aminopurin-9-yl)pentyl]triazol-4-yl]pentyl]-1,3,3a,4,6,6a-hexahydrothieno[3,4-*d*]imidazol-2-one (4.04)
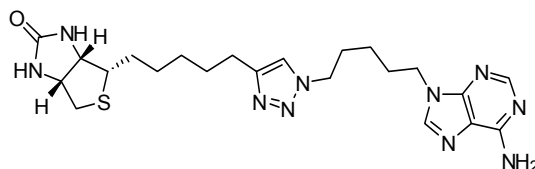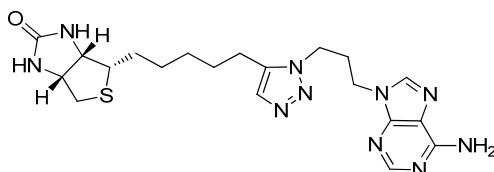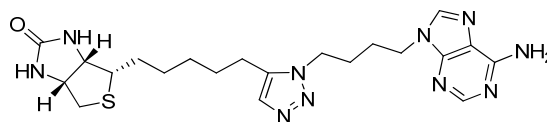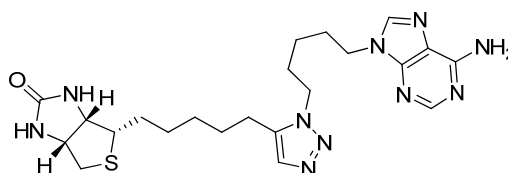

Biotin acetylene **3.12** (21 mg, 0.088 mmol) was reacted with azide **4.21** (25 mg, 0.10 mmol) and Cu nanopowder (1 mg, 0.02 mmol) using General Procedure **G1**. The crude material was purified by flash chromatography on silica eluting with 8% methanol in dichloromethane to give a crystalline white solid (33 mg, 74%).

MP: 101 - 103 °C; **FT-IR** (ATR) ν_{max}: 3202, 2928, 2854, 1708, 1688, 1646, 1604 cm^{-1}; **^{1}H NMR** (300 MHz; 1% CD$_3$OD, CDCl$_3$): δ 8.27 (1H, s, Ar^{ad}**H**), 7.73 (1H, s, Ar^{tri}**H**), 7.20 (1H, s, Ar^{ad}**H**), 4.48-4.53 (1H, dd, J = 4.8, 7.8 Hz, NHC**H**), 4.28-4.36 (3H, m, Ar^{ad}C**H$_2$**, NHC**H**), 4.13-4.19 (2H, m, Ar^{tri}C**H$_2$**), 3.14-3.20 (1H, SC**H**), 2.94 (1H, dd, J = 4.8, 12.7 Hz, SC**H$_a$**), 2.72 (1H, d, J = 12.7, SC**H$_b$**), 2.66 (2H, t, J = 7.8 Hz, ArN^{tri}C**H$_2$**), 1.26-1.96 (14H, m, C**H$_2$**); **^{13}C NMR** (75 MHz; DMSO-d^6): δ 162.8, 155.9, 152.3, 149.5, 140.8, 137.1, 131.3, 118.6, 61.0, 59.2, 55.5, 46.5, 42.6, 29.0, 28.89, 28.61, 28.27, 28.20, 27.39, 23.01, 22.05; **HPLC** R$_t$ = 19.0 min.

(3a*S*,4*S*,6a*R*)-4-[5-[3-[2-(6-Aminopurin-9-yl)ethyl]triazol-4-yl]pentyl]-1,3,3a,4,6,6a-hexahydrothieno[3,4-*d*]imidazol-2-one (4.05)
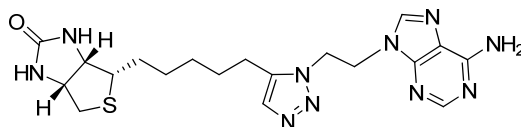
Biotin alkyne **4.16** (15 mg, 0.045 mmol) was reacted with azide **4.18** (16 mg, 0.05 mg) and Cp*Ru(PPh$_3$)$_2$Cl (1 mg, 0.02 mmol) using General Procedure **H1**. The crude material was purified by flash chromatography on silica eluting with 15% MeOH in DCM to yield a white solid, (13 mg, 41%).

^{1}H NMR (300 MHz, DMSO-d$_6$): δ 8.17 (1H, s, Ar**H**), 7.81 (1H, s, Ar**H**), 7.48 (1H, s, Ar^{tri}**H**), 7.92 (2H, bs, ArN**H$_2$**), 6.53 (1H, bs, C(O)N**H**), 6.43(1H, bs, C(O)N**H**), 4.77-4.81

(2H, m, ArN^{tri}C**H$_2$**), 4.64-4.68 (2H, m, ArC**H$_2$**), 4.34-4.39 (1H, m, NHC**H**), 4.17-4.21 (NHC**H**), 3.14-3.22 (1H, m, SC**H**), 2.88 (1H, dd, J = 5.4, 12.6 Hz, SC**H$_a$**), 2.63 (1H, d, J = 12.6 Hz, SC**H$_b$**), 2.35 (2H, t, J = 7.8 Hz, ArC^{tri}C**H$_2$**), 1.20-1.66 (8H, m, 4 x C**H$_2$**); ^{13}**C NMR** (150 MHz, DMSO-d$_6$): δ 162.7, 155.9, 152.2, 149.5, 137.9, 134.9, 131.4, 118.6, 61.1, 59.2, 55.5, 45.9, 42.9, 40.0, 28.5, 28.2, 28.1, 27.1, 21.7; **HRMS** calcd. for (M + H) C$_{19}$H$_{27}$N$_{10}$OS: requires 443.2090, found 443.2127; **HPLC** R$_t$ = 17.5 min.

(3a*S*,4*S*,6a*R*)-4-[5-[3-[3-(6-Aminopurin-9-yl)propyl]triazol-4-yl]pentyl]-1,3,3a,4,6,6a-hexahydrothieno[3,4-*d*]imidazol-2-one (4.06)
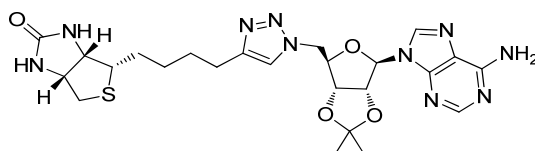

Biotin acetylene **3.12** (24 mg, 0.11 mmol) was reacted with azide **4.19** (26 mg, 0.11 mmol) and Cp*Ru(PPh$_3$)$_2$Cl (16 mg, 0.02 mmol) using General Procedure **H1**. The crude material was purified by flash chromatography on silica using 10% MeOH in DCM to yield a white solid, (25 mg, 52%).

MP: 204 - 206 °C; ^{1}**H NMR** (300 MHz, DMSO-d$_6$): δ 8.13 (1H, s, Ar**H**), 8.12 (1H, s, Ar**H**), 7.49 (1H, s, Ar^{tri}**H**), 7.22 (2H, bs, ArN**H$_2$**), 6.50 (1H, bs, C(O)N**H**), 6.36 (1H, bs, C(O)N**H**), 4.29-4.32 (1H, m, NHC**H**), 4.26 (2H, t, J = 7.2 Hz, ArN^{tri}C**H$_2$**), 4.20 (2H, t, J = 7.2 Hz, ArC**H$_2$**), 4.12-4.14 (1H, m, NHC**H**), 3.07-3.10 (1H, m, SC**H**), 2.82 (1H, dd, J = 7.8, 12.6 Hz, SC**H$_a$**), 2.57 (1H, d, J = 12.6 Hz, SC**H$_b$**), 2.52 (2H, t, J = 7.2 Hz, ArC^{tri}C**H$_2$**), 2.35-2.40 (2H, m, C**H$_2$**), 1.22-1.61 (8H, m, 4 x C**H$_2$**); ^{13}**C NMR** (150 MHz; DMSO-d^6): δ 162.7, 155.9, 152.7, 149.5, 141.1, 137.2, 131.2, 118.8, 61.0, 59.2, 55.4, 44.2, 40.5, 29.4, 28.6, 28.2, 27.3, 22.0; **HRMS** calcd. for (M + H) C$_{20}$H$_{29}$N$_{10}$OS: requires 457.2247, found 457.2269.

(3a*S*,4*S*,6a*R*)-4-[5-[1-[4-(6-Aminopurin-9-yl)butyl]triazol-4-yl]pentyl]-1,3,3a,4,6,6a-hexahydrothieno[3,4-*d*]imidazol-2-one (4.07)

Biotin acetylene **3.12** (41 mg, 0.17 mmol) was reacted with azide **4.20** (47 mg, 0.19 mmol) and Cp*Ru(PPh$_3$)$_2$Cl (27 mg, 0.03 mmol) using General Procedure **H1**. The crude material was purified by flash chromatography on silica eluting with 7% methanol in dichloromethane to give a white solid (46 mg, 55%).

MP: 214 – 216 °C; **^{1}H NMR** (600 MHz; 1% CD$_3$OD, CDCl$_3$): δ 8.20 (1H, s, Ar**H**), 7.76 (1H, s, Ar**H**), 7.37 (1H, s, Ar^{tri}**H**), 6.14 (1H, bs, C(O)N**H**), 5.58 (1H, bs, C(O)N**H**), 4.47 (1H, dd, *J* = 4.8, 7.8 Hz, NHC**H**), 4.13-4.29 (5H, m, ArC**H$_2$**, ArN^{tri}C**H$_2$**, NHC**H**), 3.08-3.12 (1H, m, SC**H**), 2.88 (1H, dd, *J* = 5.4, 12.9 Hz, SC**H$_b$**), 2.69 (1H, d, *J* = 12.9 Hz, SC**H$_a$**), 1.81-1.89 (2H, m, ArC^{tri}C**H$_2$**), 1.26-1.68 (10H, m, 5 x C**H$_2$**);**^{13}C NMR** (150 MHz; DMSO-d^6): 163.9, 155.6, 152.6, 149.4, 140.1, 137.1, 131.7, 118.8, 72.2, 62.0, 59.9, 46.7, 43.0, 40.3, 29.0, 28.7, 28.5, 27.8, 27.0, 26.7, 22.8; **HRMS** calcd. for (M + H) C$_{21}$H$_{31}$N$_{10}$OS: requires 471.2403, found 471.2440; **HPLC** R$_t$ = 18.2 min.

(3a*S*,6a*R*)-4-[5-[3-[5-(6-Aminopurin-9-yl)pentyl]triazol-4-yl]pentyl]-1,3,3a,4,6,6a-hexahydrothieno[3,4-*d*]imidazol-2-one (4.08)

Biotin acetylene **3.12** (32 mg, 0.13 mmol) was reacted with alkyl adenine **4.21** (39 mg, 0.15 mmol) and Cp*Ru(PPh$_3$)$_2$Cl (21 mg, 0.027 mmol) using General Procedure **H1**. The crude material was purified by flash chromatography on silica using 5% methanol in dichloromethane to give a white solid (32 mg, 48%).

MP: 113 - 116 °C; **^{1}H NMR** (300 MHz; DMSO-d^6): δ 8.12 (1H, s, Ar^{ad}**H**), 8.11 (1H, s, Ar^{ad}**H**), 7.77 (1H, s, Ar^{tri}**H**), 7.20 (2H, bs, ArN**H$_2$**), 6.49 (1H, bs, C(O)N**H**), 6.38 (1H, bs,

C(O)N**H**), 4.24-4.32 (3H, m, NHCHC**H₂**S, Ar^(tri)C**H₂**), 4.09-4.14 (3H, m, NHC**H**CH(CH₂)S, Ar^(tri)C**H₂**), 3.06-3.17 (1H, m, CH₂SC**H**CH₂), 2.83 (1H, dd, J = 5.1, 12.3 Hz, , CHSC**H**_aCH), 2.54-2.59 (3H, m, CHSC**H**_aCH, C**H₂**CH₂Ar^(tri)), 1.77-1.86 (4H, m, Ar^(ad)CH₂C**H₂**C**H₂**), 1.13-1.57 (10H, m, C**H₂**C**H₂**); **¹³C NMR** (75 MHz; DMSO-d⁶): δ 162.8, 156.2, 152.5, 149.5, 146.8, 140.8, 121.6, 118.9, 79.2, 62.4, 61.1, 55.6, 48.9, 44.5, 29.1, 28.8, 28.7, 28.6, 28.4, 28.2, 25.0, 22.9; **HPLC** R_t = 19.0 min; **HRMS** calcd. for (M+ H) C₂₂H₃₃N₁₀O₄S: requires 485.2560, found 485.2559.

(3a*S*,4*S*,6a*R*)-4-[4-[1-[[(3aR,4R,6R,6aR)-4-(6-Aminopurin-9-yl)-2,2-dimethyl-3a,4,6,6a-tetrahydrofuro[3,4-*d*][1,3]dioxol-6-yl]methyl]triazol-4-yl]butyl]-1,3,3a,4,6,6a-hexa hydrothieno[3,4-*d*]imidazol-2-one (4.09)
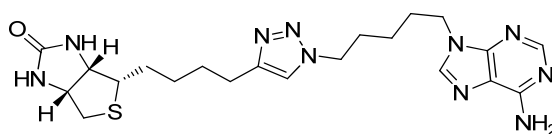

Biotin acetylene **4.16** (15 mg, 0.05 mmol) was reacted with alkyl adenine **3.16** (16 mg, 0.05 mmol) and Cu nanopowder (1 mg, 0.02 mmol) using General Procedure **G1**. The crude material was purified by flash chromatography on silica eluting with 9% methanol in dichloromethane to yield a white solid, (15 mg, 60%).

¹H NMR (600 MHz; 1% CD₃OD, CDCl₃): δ 8.17 (1H, s, Ar**H**), 7.81 (1H, s, Ar**H**), 7.12 (1H, s, Ar^(tri)**H**), 5.93 (1H, d, J = 3.0 Hz, 1' C**H**), 5.48 (1H, dd, J = 3.0, 7.2 Hz, 2' C**H**), 5.02 (0.25H, bs, C(O)N**H**, exchanged with solvent), 4.88 (1H, dd, J = 4.2, 15.0 Hz, 5' C**H**_a), 4.84 (1H, t, J = 6.0 Hz, 3' C**H**), 4.57 (1H, dd, J = 3.0, 15.0 Hz, 5' C**H**_b), 4.53-4.54 (1H, m, C**H**NH), 4.43-4.45 (2H, m, 4' C**H**, C**H**NH), 3.18-3.21 (1H, m SC**H**), 2.96 (1H, dd, J = 5.4, 13.2 Hz, SC**H**_a), 2.74 (1H, d, J = 13.2 Hz, SC**H**_b), 2.66-2.70 (2H, m, ArC^(tri)C**H₂**), 1.70-1.74 (2H, m, C**H₂**), 1.61 (3H, s, CC**H₃**), 1.47-1.51 (4H, m, 2 x C**H₂**), 1.37 (3H, s, CC**H₃**); **¹³C NMR** (150 MHz; 1% CD₃OD, CDCl₃): δ 163.9, 156.4, 152.9, 148.7, 148.0, 140.1, 122.9, 115.8, 89.9, 82.8, 82.0, 79.3, 62.2, 59.7, 55.6, 49.9, 49.8, 40.8, 29.6, 28.8, 28.6, 27.2, 25.3, 25.1.

(3a*S*,4*S*,6a*R*)-4-[6-[1-[[(3a*R*,4*R*,6*R*,6a*R*)-4-(6-Aminopurin-9-yl)-2,2-dimethyl-3a,4,6,6a-tetrahydrofuro[3,4-*d*][1,3]dioxol-6-yl]methyl]triazol-4-yl]hexyl]-1,3,3a,4,6,6a-hexa hydrothieno[3,4-*d*]imidazol-2-one (4.10)
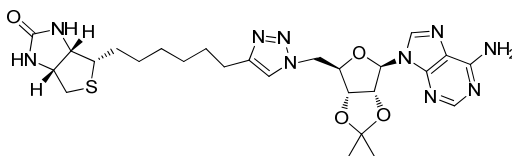
Biotin acetylene **3.12** (10 mg, 0.04 mmol) was reacted with adenosine **3.16** (14 mg, 0.04 mmol) and Cu nanopowder (1 mg, 0.02 mmol) using General Procedure **G1**. The crude material was purified by flash chromatography on silica eluting with 9% methanol in dichloromethane to yield a white solid (16 mg, 69%).

MP: 123 - 128 $^{\circ}$C; **^{1}H NMR** (600 MHz; CDCl$_3$): δ 8.29 (1H, s, Ar**H**), 7.93 (1H, s, Ar**H**), 7.42 (1H, bs, ArN**H**), 7.13 (1H, s, Ar^{tri}**H**), 6.80 (1H, bs, ArN**H**), 6.06 (1H, bs, C(O)N**H**), 5.80 (1H, bs, C(O)N**H**), 5.37 (1H, d, *J* = 4.2 Hz, 1' C**H**), 5.11 (1H, dd, *J* = 4.8, 6.3 Hz, 3' C**H**), 4.82 (1H, dd, *J* = 6.0, 14.4 Hz, 5' C**H$_a$**), 4.68 (1H, dd, *J* = 3.0, 14.4 Hz, 5' C**H$_b$**), 4.58-4.60 (1H, m, 4' C**H**), 4.53-4.55 (1H, m, NHC**H**), 4.35-4.37 (1H, m, NHC**H**), 3.14-3.17 (1H, m, SC**H$_2$**), 2.94 (1H, dd, *J* = 4.8, 12.9 Hz, SC**H$_a$**), 2.75 (1H, d, *J* = 12.9 Hz, SC**H$_b$**), 2.61 (2H, t, *J* = 7.8 Hz, ArC^{tri}C**H$_2$**), 1.46-1.73 (4H, m, 2 x C**H$_2$**), 1.60 (3H, s, CC**H$_3$**), 1.37 (3H, s, CC**H$_3$**), 1.26-1.28 (6H, m, 3 x C**H$_2$**); **^{13}C NMR** (150 MHz; CDCl$_3$): δ 164.4, 156.5, 153.4, 149.3, 148.5, 140.1, 122.6, 120.5, 115.4, 90.7, 84.7, 83.3, 81.3, 77.5, 62.5, 60.3, 56.1, 51.1, 40.9, 29.4, 29.2, 28.9, 28.9, 27.5, 25.7, 25.6; **HRMS** calcd. for (M + H) C$_{26}$H$_{37}$N$_{10}$O$_4$S: requires 585.2720, found 585.2745.

(3a*S*,4*S*,6a*R*)-4-[6-[1-[3-(6-Aminopurin-9-yl)propyl]triazol-4-yl]hexyl]-1,3,3a,4,6,6a-hexahydrothieno[3,4-*d*]imidazol-2-one (4.12)
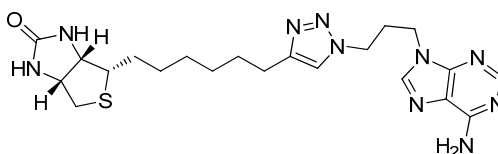
Homobiotin acetylene **4.17** (10 mg, 0.040 mmol) was reacted with alkyl adenine **4.19** (10 mg, 0.044 mmol) and Cu nanopowder (1 mg, 0.017 mmol) using General Procedure **G1**.

The crude material was purified by flash chromatography on silica eluting with 9% MeOH in DCM to give an off white solid (13 mg, 70%).

MP: 104-106 $^{\circ}$C; **^{1}H NMR** (300 MHz; 5% CD$_3$OD, CDCl$_3$): δ 8.30 (1H, s, Ar**H**), 7.90 (1H, s, Ar**H**), 7.41 (1H, s, Ar^{tri}**H**), 4.38-4.52 (1H, m, NHC**H**), 4.31-4.37 (3H, m, NHC**H**, ArN^{tri}C**H$_2$**), 4.26 (2H, t, J = 6.6 Hz, ArC**H$_2$**), 3.15-3.18 (1H, m, SC**H**), 2.93 (1H, dd, J = 5.4, 13.2 Hz, SC**H$_a$**), 2.70-2.74 (3H, m, SC**H$_b$**, ArC^{tri}C**H$_2$**), 2.51-2.55 (2H, m, C**H$_2$**), 1.11-1.69 (10H, m, 5 x C**H$_2$**); **^{13}C NMR** (150 MHz; 5% CD$_3$OD, CDCl$_3$): 163.6, 155.6, 152.9, 149.8, 140.7, 121.2, 118.3, 61.9, 60.0, 55.6, 46.7, 40.9, 40.4, 30.0, 29.6, 29.2, 29.0, 28.9, 28.5, 25.3; **HRMS** calcd. for (M + H) C$_{21}$H$_{31}$N$_{10}$OS: requires 471.2403, found 471.2388**.**

(3a*S*,4*S*,6a*R*)-4-[4-[1-[5-(6-Aminopurin-9-yl)pentyl]triazol-4-yl]butyl]-1,3,3a,4,6,6a-hexahydrothieno[3,4-*d*]imidazol-2-one (4.13)

Norbiotin alkyne **4.16** (15 mg, 0.07 mmol) was reacted with alkyl adenine **4.21** (18 mg, 0.07 mg) and Cu nanopowder (1 mg, 0.02 mmol) using General Procedure **G1**. The crude material was purified by flash chromatography on silica eluting with 9% methanol in dichloromethane to yield a white solid, (21 mg, 67%).

MP: 111 – 114 $^{\circ}$C; **^{1}H NMR** (600 MHz; 5% CD$_3$OD, CDCl$_3$): δ 8.29 (1H, s, Ar**H**), 7.80 (1H, s, Ar**H**), 7.25 (1H, s, Ar^{tri}**H**), 4.50-4.53 (1H, m, NHC**H**), 4.30-4.36 (3H, m, ArN^{tri}C**H$_2$**, NHC**H**), 4.15-4.22 (2H, m, ArC**H$_2$**), 3.17-3.20 (1H, m, SC**H**), 2.93 (1H, dd, J = 5.4, 13.2 Hz, SC**H$_a$**), 2.66 (1H, d, J = 13.2, SC**H$_b$**), 2.65-2.75 (2H, m, ArC^{tri}C**H$_2$**), 1.30-1.96 (14H, m, 7 x C**H$_2$**); **^{13}C NMR** (150 MHz; 5% CD$_3$OD, CDCl$_3$): δ 163.7, 155.1, 151.9, 149.5, 147.8, 140.5, 120.8, 119.0, 62.0, 60.9, 55.4, 49.8, 43.6, 40.5, 29.6, 29.3, 29.1, 28.1, 28.0, 24.6, 23.4; **HRMS** calcd. for (M + H) C$_{21}$H$_{31}$N$_{10}$OS: requires 471.2403, found 471.2402.

(3a*S*,6a*R*)-4-Hex-5-ynyl-1,3,3a,4,6,6a-hexahydrothieno[3,4-*d*]imidazol-2-one (4.16)
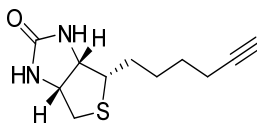
Norbiotin bromide **4.38** (25 mg, 0.09 mmol) was treated according to general procedure **F1** and purified by silica gel chromatography eluting with 5% methanol in dichloromethane to give a white solid (9 mg, 44%).

¹H NMR (300 MHz, CDCl$_3$): δ 5.16 (1H, bs, C(O)N**H**), 5.11 (1H, bs, C(O)N**H**), 4.49-4.53 (1H, m, NHC**H**), 4.30-4.33 (1H, m, NHC**H**), 3.13-3.20 (1H, m, SC**H**), 2.94 (1H, dd, *J* = 5.1, 12.9 Hz, C**H**$_a$S), 2.73 (1H, d, *J* = 12.9 Hz, **CH**$_b$S), 2.21 (2H, dt, *J* = 2.7, 6.75 Hz, C**H₂**C≡CH), 1.97 (1H, t, *J* = 2.7 Hz, CH$_2$C≡C**H**), 1.51-1.70 (6H, m, 3 x C**H₂**); **¹³C NMR (**300 MHz, DMSO-d$_6$): δ 163.2, 84.4, 68.9, 62.2, 60.3, 55.5, 40.8, 28.3 (x2), 28.1, 18.4.

(3a*S*,6a*R*)-4-Oct-7-ynyl-1,3,3a,4,6,6a-hexahydrothieno[3,4-*d*]imidazol-2-one (4.17)
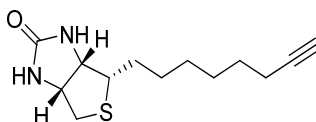
Homobiotin bromide **4.44** (46 g, 0.15 mmol) was treated following general procedure **F1** and purified by silica gel chromatography eluting with 3% methanol in dichloromethane to give a white solid (14 mg, 37%).

¹H NMR (300 MHz, CDCl$_3$): δ 4.79 (2H, bs, 2 x C(O)N**H**), 4.51-4.55 (1H, m C**H**NH), 4.30-4.34 (1H, m, C**H**NH), 3.14-3.20 (1H, m, C**H**S), 2.94 (1H, dd, *J* = 5.1, 12.9 Hz, C**H**$_a$S), 2.73 (1H, d, *J* = 12.6 Hz, C**H**$_b$S), 2.19 (2H, dt, *J* = 2.7, 6.9 Hz, C**H₂**≡CH), 1.95 (1H, d, *J* = 2.7 Hz, CH$_2$≡C**H**), 1.38 − 1.68 (8H, m, 4 x C**H₂**); **¹³C NMR** (150 MHz, CDCl$_3$): δ 162.6, 84.5, 68.3, 61.9, 60.1, 55.4, 40.6, 29.7, 29.4, 28.9, 28.6, 28.4, 18.3; **HRMS** calcd. for (M + H) C$_{13}$H$_{21}$N$_2$OS: requires 253.1375, found 253.1373.

9-(2-Azidoethyl)purin-6-amine (4.18)
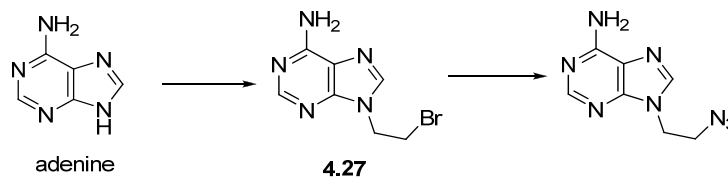
Adenine (500 mg, 3.70 mmol) was alkylated following general procedure **I1**, using 1,2-dibromoethane (1370 mg, 7.41 mmol) and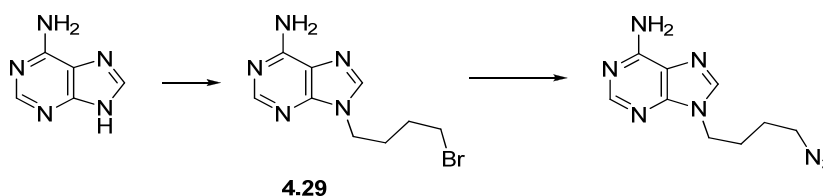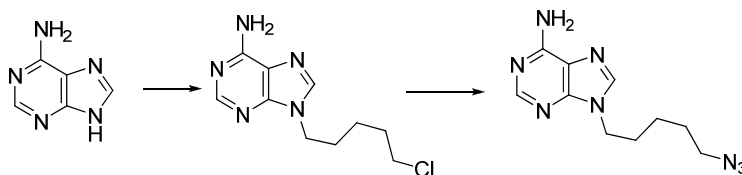 purified by silica gel chromatography eluting with 10% methanol in dichloromethane to give bromide **4.27** as a white solid (640 mg, 72%). Data consistent with literature[21]

FT-IR (ATR) ν_{max}: 3280, 3101, 1667, 1596, 655 cm^{-1}; **^{1}H NMR** (300 MHz; DMSO-d^6): δ 8.17 (1H, s, Ar**H**), 8.15 (1H, s, Ar**H**), 7.27 (2H, bs, Ar**NH$_2$**), 4.56 (2H, t, J = 6.0 Hz, ArC**H$_2$**), 3.94 (2H, t, J = 6.0 Hz, C**H$_2$**Br); **^{13}C NMR** (75 MHz; DMSO-d^6): δ 156.0, 152.5, 149.5, 140.9, 118.7, 44.64, 31.6.

Bromide **4.27** (150 mg, 0.62 mmol) was treated according to general procedure **I2** and purified by silica gel chromatography eluting with 8% methanol in dichloromethane to give a white solid (111 mg, 86%).

FT-IR (ATR) ν_{max}: 3268, 3093, 2097, 1674, 1599, 1574 cm^{-1}; **^{1}H NMR** (300 MHz; DMSO-d$_6$): δ 8.16 (1H, s, Ar**H**) 8.15 (1H, s, Ar**H**), 7.25 (2H, bs, Ar**NH$_2$**), 4.34 (2H, t, J = 6.0 Hz, ArC**H$_2$**), 3.81 (2H, t, J = 6.0 Hz, C**H$_2$**N$_3$); **^{13}C NMR** (75 MHz; 2% CD$_3$OD, CDCl$_3$): δ 156.0, 152.5, 149.6, 140.9, 118.7, 49.7, 42.4; **HRMS** calcd. for (M + H) C$_7$H$_9$N$_8$: requires 205.0950, found 205.0943.

9-(3-Azidopropyl)purin-6-amine (4.19)[22]
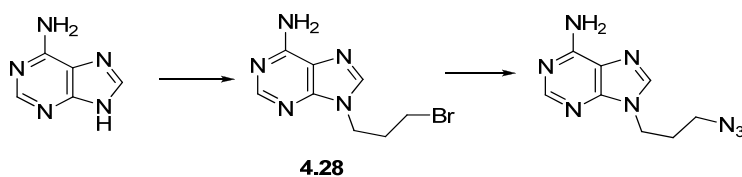
Adenine (250 mg, 1.85 mmol) was alkylated following general procedure **I1**, using 1,3-dibromopropane (737 mg, 3.70 mmol) and purified by silica gel chromatography eluting

with 6% methanol in dichloromethane to give bromide **4.28** as a white solid (178 mg, 38%). Characterisation data consistent with literature[23]

FT-IR (ATR) v_{max}: 3288, 3108, 1661, 1598, 796 cm^{-1}; **^{1}H NMR** (300 MHz; DMSO-d^6): δ 8.14 (2H, s, Ar**H**) 7.22 (2H, bs, ArN**H$_2$**), 4.26 (2H, t, J = 6.6 Hz, ArC**H$_2$**), 3.50 (2H, t, J = 6.3 Hz, C**H$_2$**Br), 2.37 (2H, m, C**H$_2$**CH$_2$Br); **^{13}C NMR** (75 MHz; DMSO-d^6): δ 155.9, 152.4, 149.5, 140.8, 118.8, 41.7, 32.1, 31.3.

Adenine **4.27** (161 mg, 0.63 mmol) was treated according to general procedure **I2** and purified by silica gel chromatography eluting with 5% methanol in dichloromethane to give a white solid (104 mg, 76%).

FT-IR (ATR) v_{max}: 3298, 3131, 2930, 2102, 1662, 1597 cm^{-1}; **^{1}H NMR**(300 MHz; DMSO-d$_6$): δ 8.14 (1H, s, Ar**H**), 8.13 (1H, s, Ar**H**), 7.21 (2H, bs, ArN**H$_2$**), 4.20 (2H, t, J = 7.2 Hz, ArC**H$_2$**), 3.38 (2H, t, J = 7.2 Hz, C**H$_2$**N$_3$), 2.06 (2H, tt, J = 7.2, 7.2 Hz, C**H$_2$**CH$_2$N$_3$); **^{13}C NMR** (75 MHz; 2% CD$_3$OD, CDCl$_3$): δ 155.9, 152.4, 149.6, 140.8, 118.7, 48.1, 40.5, 28.6.

9-(4-Azidobutyl)purin-6-amine (4.20)

4.29

Adenine (251 mg, 1.85 mmol) was alkylated following general procedure **I1**, using 1,4-dibromobutane (789 mg, 3.70 mmol) and purified by silica gel chromatography eluting with 6% methanol in dichloromethane to give bromide **4.29** as a white solid (427 mg, 86%). ^{1}H NMR consistent with literature report.[21]

FT-IR (ATR) v_{max}: 3202, 3108, 2868, 1668, 1605, 1228 cm^{-1}; **^{1}H NMR** (300 MHz; DMSO-d$_6$): δ 8.15 (1H, s, Ar**H**), 8.14 (1H, s, Ar**H**), 7.21 (2H, bs, ArN**H$_2$**), 4.18 (2H, t, J = 6.6 Hz, ArC**H$_2$**), 3.55 (2H, t, J = 6.3 Hz, C**H$_2$**Br), 1.88-1.97 (2H, m, C**H$_2$**), 1.70-1.79 (2H, m, C**H$_2$**); **^{13}C NMR** (75 MHz; 2% CD$_3$OD, CDCl$_3$): δ 155.9, 152.4, 149.6, 140.8, 118.7, 42.0, 34.3, 29.3, 28.1.

Adenine **4.27** (150 mg, 0.56 mmol) was treated according to general procedure **I2** and purified by silica gel chromatography eluting with 8% methanol in dichloromethane to give a white solid (121 mg, 92%).

^{1}H NMR (300 MHz; 2% CD$_3$OD, CDCl$_3$): δ 8.30 (1H, s, Ar**H**) 7.84 (1H, s, Ar**H**), 7.21 (2H, bs, ArN**H$_2$**), 4.25 (2H, t, J = 7.2 Hz, ArC**H$_2$**), 3.36 (2H, t, J = 6.6 Hz, C**H$_2$**N$_3$), 1.95-2.04 (2H, m, C**H$_2$**), 1.58-1.68 (2H, m, C**H$_2$**); **^{13}C NMR**(75 MHz; DMSO-d$_6$): δ 155.9, 152.4, 149.9, 140.8, 118.6, 50.1, 42.4, 26.7, 25.5.

9-(5-Azidopentyl)purin-6-amine (4.21)

Adenine (250 mg, 1.85 mmol) was alkylated following general procedure **I1**, using 1-bromo-5-chloropentane (679 mg, 3.70 mmol) and purified by silica gel chromatography eluting with 5% methanol in dichloromethane to give chloride **4.30** as a white solid (380 mg, 89%).

FT-IR (ATR) ν**$_{max}$**: 3215, 3109, 1608, 1570, 1300 cm^{-1}; **^{1}H NMR** (200 MHz; 5% CD$_3$OD, CDCl$_3$): δ 7.92 (1H, s, Ar**H**), 7.49 (1H, s, Ar**H**), 6.19 (2H, bs, ArN**H$_2$**), 3.85 (2H, t, J = 7.2 Hz, ArC**H$_2$**), 3.15 (2H, t, J = 6.4 Hz, C**H$_2$**Cl), 1.64-1.85 (2H, m, C**H$_2$**), 1.32-1.45 (2H, m, C**H$_2$**); **^{13}C NMR** (75 MHz; 5% CD$_3$OD, CDCl$_3$): δ 155.6, 152.8, 149.8, 140.5, 119.0, 44.6, 43.62, 31.9, 29.1, 24.1.

Adenine **4.30** (110 mg, 0.46 mmol) was treated according to general procedure **I2** and purified by silica gel chromatography eluting with 10% methanol in dichloromethane to give a white solid (95 mg, 84%).

FT-IR (ATR) ν**$_{max}$**: 3211, 3108, 2942, 2089, 1667, 1607, 1572 cm^{-1}; **^{1}H NMR** (200 MHz; 2% CD$_3$OD, CDCl$_3$): δ 8.23 (1H, s, Ar**H**), 7.77 (1H, s, Ar**H**), 6.63 (2H, bs, ArN**H$_2$**), 4.12 (2H, t, J = 7.2 Hz, ArC**H$_2$**), 3.174 (2H, t, J = 6.4 Hz, C**H$_2$**N$_3$), 1.76-1.91 (2H, m, C**H$_2$**CH$_2$Ar), 1.48-1.61 (2H, m, C**H$_2$**CH$_2$N$_3$), 1.32-1.39 (2H, m, CH$_2$C**H$_2$**CH$_2$); **^{13}C NMR**

(75 MHz; 2% CD$_3$OD, CDCl$_3$): δ 155.9, 152.9, 149.9, 140.2, 119.3, 51.1, 43.7, 29.6, 28.3, 23.8; **HRMS** calcd. for (M + H) C$_{10}$H$_{15}$N$_8$: requires 247.1420, found 247.1420

(3a*S*,6a*R*)-4-(4-Aminobutyl)-1,3,3a,4,6,6a-hexahydrothieno[3,4-*d*]imidazol-2-one hydrochloride salt (4.33)[24]
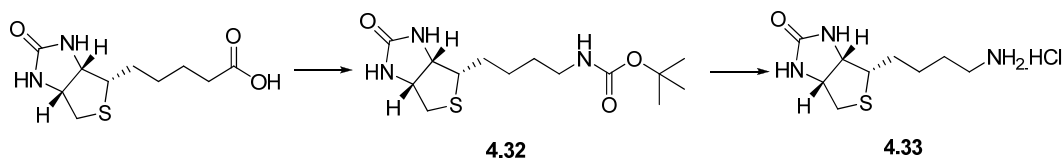

To a suspension of biotin **1.01** (300 mg, 1.23 mmol) were added diphenylphosphoryl azide (320 mg, 1.35 mmol) and triethylamine (136 mg, 1.35 mmol) in 10 mL of dry *tert*-butanol and heated at reflux for 18 h under nitrogen atmosphere. Solvents were evaporated; the residue was dissolved in dichloromethane (50 mL) and washed with water (1 x 50 mL) and brine (1 x 50 mL). The organic layer was dried over Na$_2$SO$_4$, filtered and concentrated *in vacuo*. The crude material was purified by flash chromatography on silica using 4% MeOH in DCM to yield compound **4.32** as a white solid. (197 mg, 51%).

^{1}H NMR (300 MHz, 2% CD$_3$OD, CDCl$_3$): δ 4.48-4.58 (1H, m, NHC**H**), 4.30-4.40 (1H, m, NHC**H**), 3.27-3.38 (1H, m, SC**H**), 3.05-3.18 (2H, m, C**H$_a$**NH), 2.93 (1H, dd, *J* = 4.5, 8.7 Hz, C**H$_b$**S), 1.30-1.80 (6H, m, 3 x C**H$_2$**), 1.44 (9H, s, C(C**H$_3$**)$_3$).

To a solution of compound **4.32** (150 mg, 0.47 mmol) in 5 mL of methanol was added 5 mL of 6N HCl and stirred overnight. The mixture was concentrated *in vacuo*, the precipitate was filtered, washed with de-ionized ice water (2 x 10 mL) and dried with vacuum filtration to yield a white solid (89 mg, 87%).

^{1}H NMR (300 MHz, DMSO-d$_6$): δ 6.47 (1H, bs, C(O)N**H**), 6.37 (1H, bs, C(O)N**H**), 3.08-3.14 (1H, m, C**H**SCH$_2$), 2.85 (1H, dd, *J* = 5.1, 12.6 Hz, CH$_a$SCH), 2.52-2.59 (3H, m, C**H$_2$**NH$_3$, CH$_b$SCH), 1.25-1.64 (6H, m, 3 x C**H$_2$**); **^{13}C NMR** (75 MHz, DMSO-d$_6$): δ 162.7, 61.6, 59.2, 55.5, 40.1, 32.1, 28.4, 28.3, 26.3.

Attempted   synthesis   of   (3a*S*,4*S*,6a*R*)-4-(4-hydroxybutyl)-1,3,3a,4,6,6a-hexahydrothieno[3,4-*d*]imidazol-2-one (4.34)
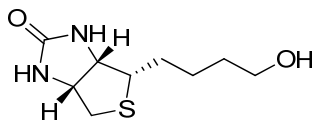
Method 1

To a solution of norbiotin amine hydrochloride **4.33** (50 mg, 0.20 mmol) in 5mL of 1:1 THF and water was added 3 mL of glacial acetic acid and sodium nitrite (41 mg, 0.60 mmol). The reaction was stirred at 50 °C for 48 h and monitored by TLC. The reaction mixture was diluted with water (20 mL) and extracted with dichloromethane (2 x 25 mL). The aqueous layer was concentrated *in vacuo* and ^{1}H NMR was performed on the residue to determine only norbiotin amine **4.33** was present. The organic layer was washed with sodium bicarbonate (1 x 50 mL) and brine (1 x 50 mL), dried over Na_2SO_4, filtered and concentrated *in vacuo*. ^{1}H NMR detected a complex mixture. LRMS of the organic layer did not detect the desired compound.

Method 2

Following the conditions described in method 1. However the reaction was undertaken at 0 °C. ^{1}H NMR of both organic and aqueous layers confirmed the presence of a complex mixture and starting material respectively.

Method 3

To a solution of norbiotin amine **4.33** (50 mg, 0.20 mmol) in water (2 mL) at 60 °C was added 4M NaOH (0.5 mL). Sodium nitroprusside (90 mg, 0.30 mmol) was added in three portions over 30 min and stirred overnight. The reaction mixture was cooled with an ice water bath and 1M HCl (1 mL) was added. The solution was diluted with water (25 mL), extracted with dichloromethane (5 x 25 mL). The organic layers were pooled, dried over Na_2SO_4, filtered and concentrated *in vacuo*. ^{1}H NMR was performed on the resulting residue to give a complex mixture.

(3a*S*,6a*R*)-4-(4-bromobutyl)-1,3,3a,4,6,6a-hexahydrothieno[3,4-*d*]imidazol-2-one (4.38)
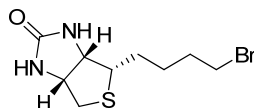
A suspension of biotin **(**121 mg, 0.50 mmol) in anhydrous dichloromethane (10 mL) were added thionyl chloride (243 mg, 1.98 mmol) and DMF (1 mL) and the solution was stirred under nitrogen atmosphere for 1 h. The reaction mixture was concentrated *in vacuo* and used in the following steps (see method 1a-h below).

Method 1a (see chapter 4 table 1 entry 1)

Biotin acid chloride **4.35** (131 mg, 0.50 mmol) and pyrithione sodium salt (82 mg, 0.55 mmol) were suspended in bromotrichloromethane (5 mL) and the mixture was stirred at 80 °C for 4 h. The mixture was cooled and diluted with de-ionized ice water (20 mL) and extracted with dichloromethane (6 x 25 mL). The organic layer was washed with 0.25 M aqueous NaOH (1 x 100 mL), 0.25 M aqueous HCl (1 x 100 mL), water (1 x 100 mL) and brine (1 x 100 mL), dried over Na_2SO_4 and filtered. Activated carbon was added to the solution and stirred for 30 min, filtered over Celite® and washed with dichloromethane (3 x 100 mL). The filtrate was concentrate *in vacuo* and the residue was purified by silica gel flash chromatography eluting with 6% MeOH in DCM to give a white solid (1 mg, 1%). ^{1}H NMR spectra was consistent with method 1h.

Method 1b (see chapter 4 table 1 entry 2)

Biotin acid chloride **4.35** (131 mg, 0.50 mmol) and 2-pyrithione (82 mg, 0.55 mmol) were suspended in bromotrichloromethane (5 mL) and the reaction mixture was subjected to 250 W light (linear tungsten halogen tube) and stirred at ambient temperature for 4 h. The work up procedure followed method 1 to give trace quantities of title compound as judge by TLC.

Method 1c (see chapter 4 table 1 entry 3)

Biotin acid chloride **4.35** (131 mg, 0.50 mmol) and 2-pyrithione (82 mg, 0.55 mmol) were suspended in bromotrichloromethane (5 mL) and the reaction mixture was subjected to 250

W (linear tungsten halogen tube) and the mixture was stirred at 80 ^{o}C for 4 h. The work up procedure followed method 1 to give light yellow solid (1 mg, 1%). ^{1}H NMR spectra was consistent with method 1h.

**Method 1d** (see chapter 4 table 1 entry 4)

Biotin acid chloride **4.35** (131 mg, 0.50 mmol) and 2-pyrithione (82 mg, 0.55 mmol) and azobisisobutyronitrile (16 mg, 0.05 mmol) were suspended in bromotrichloromethane (5 mL) and the mixture was stirred at 80 ^{o}C for 4 h. The work up procedure followed method 1 to give light yellow solid (4 mg, 3%). ^{1}H NMR spectra was consistent with method 1h.

Method 1e (see chapter 4 table 1 entry 5)

Biotin acid chloride **4.35** (131 mg, 0.50 mmol) and 2-pyrithione (82 mg, 0.55 mmol) and 4-DMAP (67 mg, 0.55 mmol) were suspended in bromotrichloromethane (5 mL) and the mixture was stirred at 80 ^{o}C for 4 h. The work up procedure followed method 1 to give light yellow solid (1 mg, 1%). ^{1}H NMR spectra was consistent with method 1h.

Method 1f (see chapter 4 table 1 entry 6)

Biotin acid chloride **4.35** (131 mg, 0.50 mmol) and 2-pyrithione (82 mg, 0.55 mmol) were dissolved in 1:1 DMF and bromotrichloromethane (5 mL) and the solution was stirred at 80 ^{o}C for 4 h. The work up procedure followed method 1 to give light yellow solid (10 mg, 7%). ^{1}H NMR spectra was consistent with method 1h.

Method 1g (see chapter 4 table 1 entry 7)

Biotin acid chloride **4.35** (131 mg, 0.50 mmol) and 2-pyrithione (82 mg, 0.55 mmol) were dissolved in 2:1 DMF and bromotrichloromethane (5 mL) and the solution was stirred at 80 ^{o}C for 4 h. The work up procedure followed method 1 to give light yellow solid (21 mg, 15%). ^{1}H NMR spectra was consistent with method 1h.

Method 1h (see chapter 4 table 1 entry 8)

Biotin acid chloride **4.35** (131 mg, 0.50 mmol) and 2-pyrithione (82 mg, 0.55 mmol) were dissolved in 8:1 DMF and bromotrichloromethane (5 mL) and the solution was stirred at 80 ^{o}C for 4 h. The work up procedure followed method 1 to give light yellow solid (29 mg, 21%).

MP: 146 – 148 °C; **^{1}H NMR** (300 MHz, DMSO-d$_6$): δ 6.49 (1H, bs, N**H**), 6.42 (1H, bs, N**H**), 4.33-4.38 (1H, m, C**H**NH), 4.17-4.21 (1H, m, C**H**NH), 3.68 (2H, t, *J* = 6.6 Hz, C**H$_2$**Br), 3.13-3.19 (1H, m, C**H**S), 2.89 (1H, dd, *J* = 5.1, 12.6 Hz, C**H$_a$**S), 2.70 (1H, d, *J* = 12.6 Hz, C**H$_b$**S), 1.46-1.84 (6H, m, C**H$_2$**); **^{13}C NMR** (75 MHz, DMSO-d$_6$): δ 162.7, 61.0, 59.2, 55.3, 45.2, 39.8, 32.0, 27.6, 25.9.

6-[(3a*S*,6a*R*)-2-Oxo-1,3,3a,4,6,6a-hexahydrothieno[3,4-*d*]imidazol-4-yl]hexanenitrile (4.39)[25]
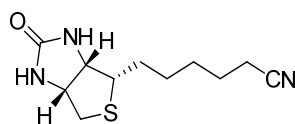
To a solution of biotin tosylate **3.22** (545 mg, 1.42 mmol) in dry DMF (20 mL) was added potassium cyanide (110 mg, 1.70 mmol) and stirred overnight at ambient temperature under a nitrogen atmosphere. The reaction mixture was diluted with dichloromethane (80 mL), washed with water (2 x 100 mL) and brine (1 x 100 mL), dried over Na$_2$SO$_4$, filtered and concentrated *in vacuo*. The residue was purified with silica gel chromatography eluting with 5% methanol in dichloromethane to give a white solid (244 mg, 72%).

^{1}H NMR (300 MHz, DMSO-d$_6$): δ 6.52 (1H, bs, C(O)N**H**), 6.43(1H, bs, C(O)N**H**), 4.34-4.38 (1H, m, NHC**H**), 4.16-4.21 (1H, m, NHC**H**), 3.12-3.18 (1H, m, SC**H**), 2.87 (1H, dd, *J* = 5.1, 12.6 Hz, C**H$_a$**S), 2.63 (1H, d, *J* = 12.6 Hz, C**H$_b$**S), 2.53 (2H, t, *J* = 6.3 Hz, C**H$_2$**CN), 1.35-1.72 (8H, m, 4 x C**H$_2$**); **^{13}C NMR** (75 MHz, DMSO-d$_6$): δ 162.8, 120.8, 61.1, 59.3, 55.5, 39.9, 28.2, 28.1, 27.8, 24.6, 16.1.

6-[(3a*S*,6a*R*)-2-Oxo-1,3,3a,4,6,6a-hexahydrothieno[3,4-*d*]imidazol-4-yl]hexanoic   acid (4.40)[25]
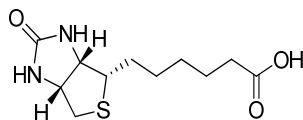
A suspension of biotin nitrile **4.39** (220 mg, 0.92 mmol) in 1 M aqueous NaOH (10 mL) was heated at reflux for 3 h. The reaction mixture was acidified with cooled 6 M aqueous HCl (5 mL) to form a white precipitate. The precipitate was filtered and washed with ice-water (2 x 10 mL) and dried *in vacuo* to give a white solid (228 mg, 96%).

MP>250 °C; **^{1}H NMR (**300 MHz, DMSO-d_6): δ 612.86 (1H, bs, COOH), 6.36 (1H, bs, C(O)NH), 6.27 (1H, bs, C(O)NH), 4.17-4.23 (1H, m, NHC**H**CH$_2$S), 3.99-4.08 (1H, m, NHCHC**H**S), 2.95-3.03 (1H, m, C**H**SCH$_2$), 2.75 (1H, dd, *J* = 4.8, 12.4 Hz, C**H**$_a$SCH), 2.47 (1H, d, *J* = 12.4 Hz, C**H**$_b$SCH), 2.08 (2H, t, *J* = 7.0 Hz, C**H**$_2$OH), 1.10-1.57 (8H, m, 4 x C**H**$_2$); **^{13}C NMR (**75 MHz, DMSO-d_6): δ 174.4, 162.7, 61.0, 59.2, 55.4, 39.7, 33.6, 28.5, 28.2, 28.1, 24.2.

(3a*S*,6a*R*)-4-(6-Hydroxyhexyl)-1,3,3a,4,6,6a-hexahydrothieno[3,4-*d*]imidazol-2-one (4.42)
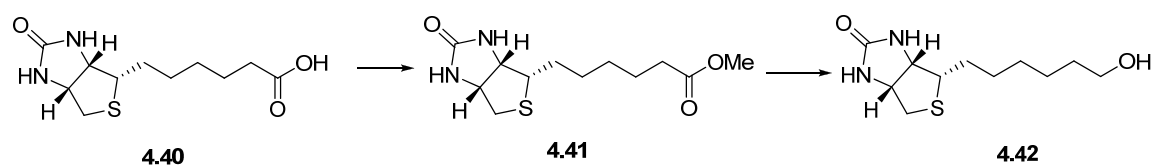
Homobiotin **4.40** (210 mg, 0.81 mmol) was esterified using general procedure **A1** and purified by silica gel chromatography eluting with 5% methanol in dichloromethane to give methyl ester **4.41** as an off white solid (221 mg, 100%).

MP: 168 – 170 °C; **^{1}H NMR** (300 MHz, 2% CD$_3$OD, CDCl$_3$)**:** δ 4.46-4.50 (1H, m, C**H**NH), 4.24-4.30 (1H, m, C**H**NH), 3.64 (1H, s, COOC**H**$_3$), 3.10-3.16 (1H, m, C**H**S), 2.92 (1H, dd, *J* = 4.8, 12.6 Hz, C**H**$_a$S), 2.70 (1H, d, *J* = 12.6 Hz, C**H**$_b$S), 2.29 (2H, t, *J* = 7.5 Hz, C**H**$_2$COOCH$_3$), 1.30-1.65 (8H, m, 4 x C**H**$_2$); **^{13}C NMR** (75 MHz, 2% CD$_3$OD, CDCl$_3$)**:** δ 174.5, 164.0, 62.2, 60.3, 56.0, 51.7, 40.8, 34.2, 29.2, 28.9, 28.6, 24.7.

Homobiotin methyl ester **4.41** (141 mg, 0.52 mmol) was esterified using general procedure **B1** and purified by silica gel chromatography eluting with 8% methanol in dichloromethane to give a white solid (115 mg, 91%).

MP: 158 -161 $^{\circ}$C; **^{1}H NMR** (300 MHz, CD$_3$OD)**:** δ 4.49 (1H, ddd, J = 0.9, 4.8, 6.9 Hz, CHNH), 4.29 (1H, dd, J = 4.5, 7.8 Hz, CHNH), 3.55 (2H, t, J = 6.6 Hz, **CH$_2$**COOCH$_3$), 3.17-3.24 (1H, m, CHS), 2.93 (1H, dd, J = 5.1, 12.8 Hz, CH$_a$S), 2.70 (1H, d, J = 12.8 Hz, CH$_b$S), 1.29-1.78 (8H, m, 4 x CH$_2$); **^{13}C NMR** (75 MHz, CD$_3$OD)**:** δ 156.1, 54.0, 53.4, 52.1, 47.7, 31.5, 24.0, 21.0, 20.9, 20.3, 17.3; **HRMS** calcd. for (M + H) C$_{11}$H$_{21}$N$_2$O$_2$S: requires 245.1324, found 245.1357.

(3aS,6aR)-4-(6-Bromohexyl)-1,3,3a,4,6,6a-hexahydrothieno[3,4-d]imidazol-2-one (4.44)
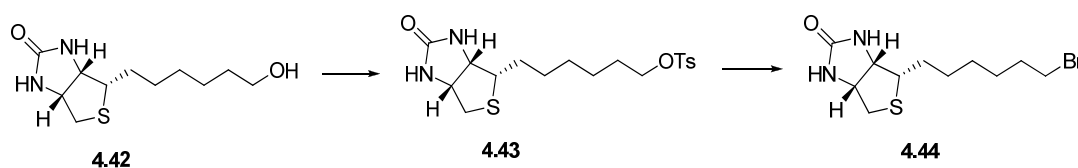
Homobiotinol **4.42** (122 mg, 0.50 mmol) was tosylated using general procedure **D1** to give crude tosylate **4.43** as a yellow solid. Homobiotinol tosylate **4.43** was brominated using general procedure **E1** and purified by silica gel chromatography eluting with 4% methanol in dichloromethane to give a white solid (78 mg, 51%).

MP: 159 – 161 $^{\circ}$C; **^{1}H NMR** (300 MHz, CDCl$_3$)**:** δ 5.30 (1H, s, CHN**H**), 5.15 (1H, s, CHN**H**), 4.50-4.54 (1H, m CHN**H**), 4.30-4.34 (1H, m CHN**H**), 3.41 (2H, t, J = 6.9 Hz, CH$_2$Br), 3.14-3.21 (1H, m CHSCH$_2$), 2.94 (1H, dd, J = 5.1, 12.8 Hz, CH$_a$SCH), 2.74 (1H, d, J = 12.8 Hz, CH$_b$SCH), 1.83-1.90 (2H, m, CH$_2$), 1.30-1.68 (4H, m, CH$_2$); **^{13}C NMR** (300 MHz, CDCl$_3$): δ 163.4, 62.2, 60.3, 55.7, 40.8, 34.2, 32.8, 29.1, 28.9, 28.8, 28.1; **HRMS** calcd. for (M + H) C$_{11}$H$_{20}$BrN$_2$OS: requires 307.0480, found 307.0478.

7.6 Experimental work as described in chapter 5

(3a*S*,6a*R*)-4-(5-Aminopentyl)-1,3,3a,4,6,6a-hexahydrothieno[3,4-*d*]imidazol-2-one (5.01)[26]
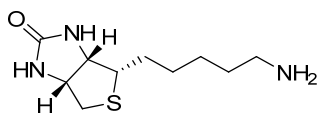
To a solution of biotin azide **5.07** (80 mg, 0.31 mmol) in THF (2 mL) was added triphenylphosphine (106 mg, 0.41 mmol) and the solution was stirred at ambient temperature for 1 h, followed by addition of water (2 mL) and stirred for a further 3 h at 60 °C. The reaction mixture was filtered and the filtrand was diluted with water (20 mL) and extracted with dichloromethane (3 x 25 mL). The organic layer were pooled, dried over Na$_2$SO$_4$, filtered and concentrated *in vacuo*. The residue was purified by silica gel chromatography eluting with 10% methanol in dichloromethane to give a white solid (13 mg, 18%).

^{1}H NMR (300 MHz, CDCl$_3$): 6.51 (0.5H, bs, C(O)NH), 6.41 (0.5H, bs, C(O)NH), 4.33-4.38 (1H, m, NHCH), 4.15-4.20 (1H, m, NHCH), 3.59 (2H, bs, NH$_2$), 3.14-3.16 (1H, m, SCH), 2.87 (1H, dd, *J* = 7.5, 12.6 Hz, SCH$_a$), 2.56-2.64 (3H, m, SCH$_b$, CH$_2$NH$_2$), 1.25-1.74 (8H, m, 4 x CH$_2$); **^{13}C NMR** (300 MHz, DMSO-d$_6$): 163.1, 79.6, 61.4, 59.6, 55.9, 41.35, 32.4, 28.9, 28.7, 26.7; **HRMS** calcd. for (M$^+$ + H) C$_{11}$H$_{20}$N$_2$OSNa: requires 230.1322, found 2230.1319.

(3a*S*,6a*R*)-4-Hexyl-1,3,3a,4,6,6a-hexahydrothieno[3,4-*d*]imidazol-2-one (5.02)[27]
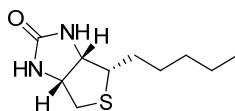
To a solution of biotin tosylate **3.18** (52 mg, 0.14 mmol) in anhydrous THF (2 mL) was added lithium aluminium hydride (15 mg, 0.41 mmol) and the solution was stirred under reflux for 3 h. The reaction mixture was cooled to ambient temperature and were added methanol (1 mL) and saturated aqueous sodium sulphate (2 mL), followed by concentration *in vacuo* and dissolving with 1:1 dichloromethane and methanol (15 mL) and

stirring for 30 min. The solution was filtered and the filtrate was concentrated *in vacuo* and purified by silica gel chromatography eluting with 3% methanol in dichloromethane to give an off white solid (16 mg, 56%).

1H NMR (300 MHz, CDCl$_3$): δ 5.27 (1H, bs, C(O)NH), 5.16 (1H, bs, C(O)NH), 4.49-4.53 (1H, m, NHCH); 4.29-4.33 (1H, m, NHCH), 3.14-3.20 (1H, m, SCH), 2.94 (1H, dd, J = 4.8, 12.6 Hz, SCH$_a$), 2.73(1H, d, J = 12.6 Hz, SCH$_b$), 1.62-1.70 (2H, m, CH$_2$), 1.28-1.45 (4H, m, CH$_3$), 0.89 (3H, t, J = 6.6 Hz, CH$_3$); **13C NMR** (300 MHz, DMSO-d$_6$): δ 163.16, 62.23, 60.41, 55.81, 40.92, 31.93, 29.52, 29.34, 28.98, 22.90, 14.39.

(3a*S*,6a*R*)-4-heptyl-1,3,3a,4,6,6a-hexahydrothieno[3,4-d]imidazol-2-one (5.03)
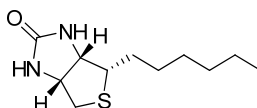
To a solution of homobiotin tosylate **4.43** (5 mg, 0.013 mmol) in anhydrous THF (1 mL) was added lithium aluminium hydride (3 mg, 0.079 mmol) and the solution was stirred under reflux for 3 h. The reaction mixture was cooled to ambient temperature and were added methanol (1 mL) and saturated aqueous sodium sulphate (2 mL), followed by concentration *in vacuo* and dissolving with 1:1 dichloromethane and methanol (15 mL) and stirring for 30 min. The solution was filtered and the filtrate was concentrated *in vacuo* and purified by silica gel chromatography eluting with 3% methanol in dichloromethane to give an off white solid (2 mg, 69%).

1H NMR (300 MHz, CDCl$_3$): δ 4.93 (1H, bs, C(O)NH), 4.86 (1H, bs, C(O)NH), 4.50-4.54 (1H, m, NHCH); 4.32 (1H, ddd, J = 1.5, 4.5, 7.5 Hz, NHCH), 3.19 (1H, dt, J = 4.5, 7.5 Hz, SCH), 2.94 (1H, dd, J = 5.1, 12.9 Hz, SCH$_a$), 2.73 (1H, d, J = 12.9 Hz, SCH$_b$), 1.63-1.68 (2H, m, CH$_2$), 1.26-1.45 (6H, m, CH$_3$), 0.89 (3H, t, J = 6.9 Hz, CH$_3$); **13C NMR** (75 MHz, DMSO-d$_6$): δ 163.1, 62.2, 60.4, 55.8, 40.9, 31.93, 29.5, 29.3, 29.0, 22.9, 14.4; **HRMS** calcd. for (M + H) C$_{11}$H$_{21}$N$_2$OS: requires 229.1374 found 229.1369.

(3a*S*,6a*R*)-4-[5-(1*H*-Triazol-4-yl)pentyl]-1,3,3a,4,6,6a-hexahydrothieno[3,4-*d*]imidazol-2-one (5.04)
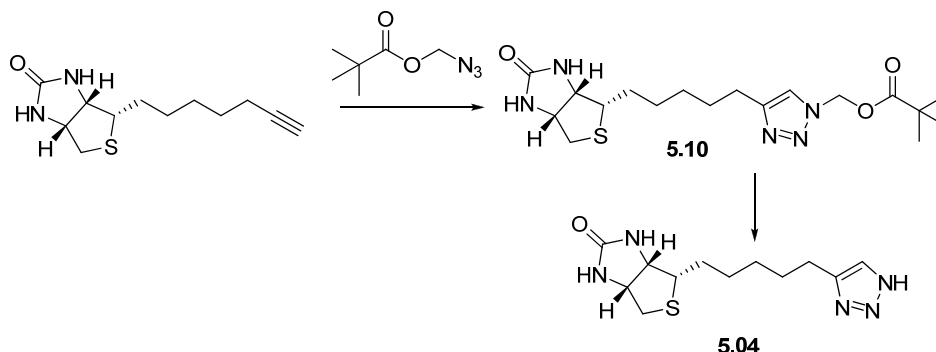

Biotin acetylene **3.12** (32 mg, 0.13 mmol) was reacted with azidomethylpivalate **5.09** (23 mg, 0.15 mmol) according to general procedure **G1**. The crude material was purified by flash chromatography on silica eluting with 5% methanol in dichloromethane to give 1,4-triazole **5.10** as a white solid (25 mg, 48%).

¹H NMR (300 MHz, CDCl₃): δ 7.53 (1H, s, ArH), 6.19 (2H, s, OCH₂), 5.62 (1H, bs, C(O)NH), 5.24 (1H, bs, C(O)NH), 4.49 − 4.53 (1H, m, NHCH), 4.28 − 4.33 (1H, m, NHCH), 3.12-3.18 (1H, m, SCH), 2.90 (1H, dd, J = 4.8, 12.6 Hz, SCH_a), 2.69 − 2.74 (3H, m, SCH_b, ArCH₂), 1.67-1.76 (4H, m, 2 x CH₂), 1.34-1.52 (4H, m, 2 x CH₂), 1.18 (9H, s, CCH₃); **¹³C NMR** (75 MHz, CDCl₃): δ 178.2, 163.9, 149.0, 122.4, 69.9, 62.3, 60.4, 56.0, 40.8, 39.1, 29.3, 29.1, 29.0, 28.8, 27.1, 25.6.

To a solution of 1,4-triazole **5.10** (20 mg, 0.063 mmol) in 1:1 methanol and THF (2 mL) was added 32% ammonia solution (2 mL) and stirred at ambient temperature overnight. The reaction mixture was concentrated *in vacuo* and purified by silica gel chromatography eluting with 15% methanol in dichloromethane to give a white solid (8 mg, 43%).

¹H NMR (300 MHz, CDCl₃): δ 7.62 (1H, s, Ar**H**), 6.47 (1H, bs, C(O)N**H**), 6.39 (1H, bs, C(O)N**H**), 4.33-4.37 (1H, m, NHC**H**), 4.14-4.20 (1H, m, NHC**H**), 3.10-3.19 (1H, m, SC**H**), 2.86 (1H, dd, J = 8.7, 12.0 Hz, SCH_a), 2.60-2.69 (3H, m, SCH_b, ArCH₂), 1.30-1.72 (8H, m, 4 x C**H₂**); **HRMS** calcd. for (M + H) C₁₂H₂₀N₅OS: requires 282.1389, found 282.1381.

(3a*S*,6a*R*)-4-Hept-6-ynyl-5,5-dioxo-1,3,3a,4,6,6a-hexahydrothieno[3,4-*d*]imidazol-2-one (5.05)
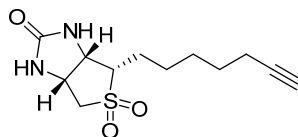
To a solution of biotin alkyne **3.12** (69 mg, 0.29 mmol) in 9:1 anhydrous dichloromethane and anhydrous DMF (2 mL) was added >77% *m*-CPBA (194 mg, 0.87 mmol) and the solution was stirred for 1h. The reaction mixture was diluted with dichloromethane (25 mL), washed with saturated aqueous sodium bicarbonate (1 x 25 mL), water (1 x 25 mL) and brine (1 x 25 mL), dried over Na_2SO_4, filtered and concentrated *in vacuo*. The residue was purified by silica gel chromatography eluting with 15% methanol in dichloromethane to give a white solid (48 mg, 61%).

^{1}H NMR (600 MHz, DMSO-d_6): δ 6.66 (1H, bs, C(O)N**H**), 6.59 (1H, bs, C(O)N**H**), 4.32-4.39 (2H, m, NHC**H**), 3.23-3.34 (1H, m, SC**H** (under H_2O peak)), 3.15-3.09 (1H, m, SC**H**), 2.97 (1H, d, *J* = 14.4 Hz, SC**H$_b$**), 2.70 (1H, m, CC**H**), 2.11 (2H, m, C**H$_2$**CCH), 1.53-1.66 (2H, m, C**H$_2$**), 1.31-1.47 (6H, m, C**H$_2$**); **^{13}C NMR** (300 MHz, DMSO-d_6): δ 167.0, 84.5, 71.2, 60.3, 54.2, 53.5, 48.9, 28.0, 27.6, 25.4, 21.3, 17.8; **HRMS** calcd. for (M + H) $C_{12}H_{19}N_2O_3S$: requires 271.11164, found 271.11097

(4*S*,5*R*)-4-Methyl-5-(oct-7-ynyl)imidazolidin-2-one (5.06b)
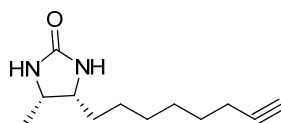
Bromide **5.14** (86 mg, 0.32 mmol) was reacted according to general procedure **F1**. The residue was purified by silica gel chromatography eluting with 5% methanol in dichloromethane to give an orange powder (34 mg, 50%).

MP: 95-97°C; **^{1}H NMR** (300 MHz, CDCl$_3$): δ 1.14 (3H, d, *J* = 6.3 Hz), 1.25-1.59 (10H, m), 1.95 (1H, dt, *J* = 2.55, 0.9 Hz), 2.19 (1H, ddd, *J* = 6.9, 6.9, 2.7 Hz), 3.67-3.73 (1H, m), 3.85 (1H, ddd, *J* = 13.8, 6.6, 6.6 Hz), 4.36 (1H, s), 4.54 (1H, s); **^{13}C NMR** (300 MHz,

DMSO-d_6): δ 163.8, 84.4, 68.1, 56.0, 51.2, 40.8, 29.5, 28.9, 28.4, 28.2, 26.2, 18.2, 15.6; **HRMS** calcd. for (M + Na) $C_{12}H_{20}ON_2Na$: requires 231.1473, found 231.1470.

(3a*S*,6a*R*)-4-(5-Azidopentyl)-1,3,3a,4,6,6a-hexahydrothieno[3,4-*d*]imidazol-2-one (5.07)[28]
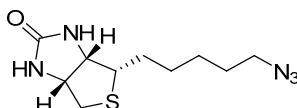
To a solution of biotin tosylate **3.18** (151 mg, 0.39 mmol) in DMF (2 mL) was added sodium azide (32 mg, 0.48 mmol) and solution was stirred overnight under nitrogen atmosphere. The reaction mixture was poured into water (20 mL) and extracted with dichloromethane (3 x 25 mL). The organic layers were pooled and washed with brine (1 x 75 mL), dried over Na_2SO_4, filtered and concentrated *in vacuo*. The residue was purified by silica gel chromatography eluting with 5% methanol in dichloromethane to give a white solid (86 mg, 86%).

^{1}H NMR (300 MHz, CDCl$_3$): 6.57 (1H, bs, C(O)NH), 6.46 (1H, bs, C(O)NH), 4.38-4.42 (1H, m, NHCH), 4.20-4.24 (1H, m, NHCH), 3.40 (2H, t, *J* = 6.9 Hz, CH$_2$N$_3$), 3.16-3.22 (1H, m, SCH), 2.91 (1H, dd, *J* = 5.1, 12.6 Hz, SCH$_a$), 2.66 (1H, d, *J* = 12.6 Hz, SCH$_b$), 1.37-1.78 (8H, m, 4 x CH$_2$); **^{13}C NMR** (300 MHz, DMSO-d_6): δ 164.3, 62.3, 60.4, 55.9, 51.6, 40.6, 28.9, 28.9, 28.7, 26.9.

Azidomethyl 2,2-dimethylpropanoate (5.09)[29]
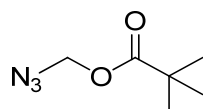
To a solution of chloromethylpivalate (500 mg, 3.33 mmol) in water (5 mL) was added sodium azide (335 mg, 5.00 mmol) and the emulsion was stirred under reflux for 6 h. The reaction mixture was diluted with water (20 mL) and extracted with diethyl ether (3 x 25 mL). The organic layer were pooled and washed with brine (1 x 75 mL), dried over Na_2SO_4, filtered and concentrated *in vacuo* to give a clear oil (377 mg, 72%).

**¹H NMR** (300 MHz, CDCl₃): δ 5.12 (2H, s, **CH₂**), 1.24 (9H, s, **CH₃**).

Methyl 6-((4*R*,5*S*)-5-methyl-2-oxoimidazolidin-4-yl)hexanoate (5.12)
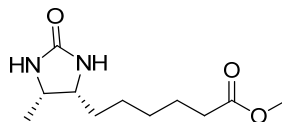
Desthiobiotin **5.11** (200 mg, 0.93 mmol) was reacted according to general procedure **A1**. The residue was purified by silica gel chromatography eluting with 2% methanol in dichloromethane to give a yellow gum (213 mg, 100%).

¹H NMR (300 MHz, CDCl₃): δ 1.20 (3H, d, *J* = 3.15 Hz), 1.31-1.67 (8H, m), 2.33 (2H, t, *J* = 7.5 Hz), 3.67 (3H, s), 3.84-3.86 (1H, m), 3.95-4.04 (1H, m), 6.22 (2H, s); **¹³C NMR** (300 MHz, DMSO-d₆): δ 174.1, 163.6, 56.8, 52.4, 51.6, 33.8, 29.2, 28.9, 26.1, 24.6, 15.5; **HRMS** calcd. for (M + Na) C₁₁H₂₀O₃N₂Na: requires 251.1372, found 251.1385.

(4*R*,5*S*)-4-(6-Hydroxyhexyl)-5-methylimidazolidin-2-one (5.13)
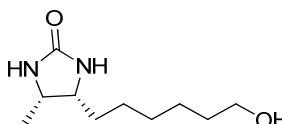
Desthiobiotinol **5.12** (692 mg, 3.03 mmol) was reacted according to general procedure B1. The residue was purified by silica gel chromatography eluting with 10% methanol in dichloromethane to give a white solid (533 mg, 82%).

MP: 78-80°C; **¹H NMR** (300 MHz, CDCl₃): δ 1.33 (3H, d, *J* = 6.6 Hz), 1.25-1.77 (11H, m), 3.62-3.71 (3H, m), 3.84 (1H, ddd, *J* = 13.5, 6.6, 6.6 Hz), 4.69 (1H, s), 5.11 (1H, s); **¹³C NMR** (75 MHz, DMSO-d₆): δ 163.5, 62.6, 56.0, 51.4, 32.5, 29.5, 29.1, 26.4, 25.5, 15.7; **HRMS** calcd. for (M + Na) C₁₀H₂₀O₂N₂Na: requires 223.1422, found 223.1432.

(4*R*,5*S*)-4-(6-Bromohexyl)-5-methylimidazolidin-2-one (5.14)
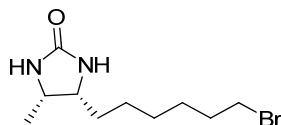
To a stirred solution of triphenylphosphine (1.2 eq) and 2,3-dichloro-5,6-dicyano-*p*-benzoquinone (DDQ) (1.2 eq) in dry dichloromethane (10 mL / 100 mg of DDQ) under a stream of nitrogen at ambient temperature was added tetrabutylammonium bromide (1.2 eq) followed by addition of the appropriate alcohol (1 eq) and stirred for 1 h. Volatiles where removed *in vacuo* and the crude residue purified to furnish an orange powder (113 mg, 89%).

MP: 113-115°C; **^{1}H NMR** (300 MHz, CDCl$_3$): δ 1.46 (3H, d, *J* = 6.3 Hz), 1.29-1.47 (8H, m), 1.86 (2H, ddd, *J* = 14.25, 6.9, 6.9 Hz), 3.41 (1H, t, *J* = 6.9 Hz), 3.67-3.74 (1H, m), 3.86 (1H, ddd, *J* = 13.65, 6.6, 6.6 Hz), 4.44 (1H, s), 4.64 (1H, s); **^{13}C NMR** (300 MHz, DMSO-d$_6$): δ 163.1, 56.3, 51.4, 33.8, 32.6, 29.6, 28.7, 28.0, 26.3, 15.8; **HRMS** calcd. for (M + Na) C$_{10}$H$_{19}$O$_2$N$_2$Na: requires 285.0578, found 285.0584.

7.7 Experimental work as described in chapter 6

(3a*S*,4*S*,6a*R*)-4-[5-[1-(3-Phenoxypropyl)triazol-4-yl]pentyl]-1,3,3a,4,6,6a-hexahydrothieno[3,4-d]imidazol-2-one (6.02)
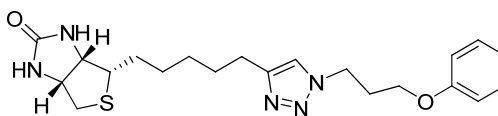
Biotin alkyne **3.12** (21 mg, 0.09 mmol) was reacted with azide **6.16** (18 mg, 0.10 mmol) and Cu nanopowder (1 mg, 0.02 mmol) according to general procedure **G1**. The residue was purified by flash chromatography on silica eluting with 7% methanol in dichloromethane to give a white solid, (21 mg, 57%).

MP: 132 – 135 $^{\circ}$C; **^{1}H NMR** (600 MHz, CDCl$_3$): δ 7.27-7.30 (3H, m, Ar^{tri}**H**, Ar**H**), 6.97 (1H, t, *J* = 7.8 Hz, Ar**H**), 6.88 (2H, d, *J* = 8.4 Hz, Ar**H**), 5.58 (1H, bs, C(O)N**H**), 5.21(1H, bs, C(O)N**H**), 4.55 (2H, t, *J* = 6.6 Hz, ArN^{tri}C**H$_2$**), 4.48-4.50 (1H, NHC**H**), 4.28-4.30 (1H, m, NHC**H**), 3.95 (2H, t, *J* = 6.6 Hz, ArOC**H$_2$**), 3.12-3.15 (1H, m, SC**H**), 2.90 (1H, dd, *J* = 5.4, 13.2 Hz, SC**H$_a$**), 2.71 (1H, d, *J* = 13.2 Hz, SC**H$_b$**), 2.69 (2H, t, *J* = 7.8 Hz, ArC^{tri}C**H$_2$**), 2.38 (2H, m, C**H$_2$**), 1.62-1.71 (4H, m, 2 x C**H$_2$**), 1.37-1.46 (4H, m, 2 x C**H$_2$**); **^{13}C NMR** (150 MHz, CDCl$_3$): δ 163.3, 158.4, 148.1, 129.6, 121.2, 121.1, 114.4, 63.9, 62.0, 60.1, 55.6, 46.8, 40.5, 30.0, 29.0, 29.0, 28.7, 28.5, 25.5; **HRMS** calcd. for (M + H) C$_{21}$H$_{30}$N$_5$O$_2$S: requires 416.2120, found 416.2105.

(3a*S*,4*S*,6a*R*)-4-[5-[1-(4-Phenoxybutyl)triazol-4-yl]pentyl]-1,3,3a,4,6,6a-hexa hydrothieno[3,4-*d*]imidazol-2-one (6.03)
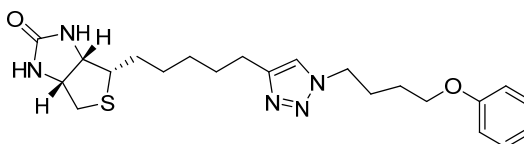
Biotin alkyne **3.12** (18 mg, 0.075 mmol) was reacted with azide **6.16** (16 mg, 0.083 mmol) and Cu nanopowder (1 mg, 0.015 mmol) according to general procedure **G1**. The residue was purified by flash chromatography on silica eluting with 7% methanol in dichloromethane to give a white solid, (21 mg, 64%).

MP: 117 - 120 °C; ¹**H NMR** (300 MHz, CDCl₃): δ 7.25-7.31 (3H, m, Ar^{tri}**H**, Ar**H**), 6.86-6.97 (3H, m, Ar**H**), 5.55 (1H, bs, C(O)N**H**), 5.18 (1H, bs, C(O)N**H**), 4.47-4.51 (1H, m, NHC**H**), 4.41 (2H, t, J = 7.2 Hz, ArN^{tri}C**H₂**), 4.27-4.31 (1H, m NHC**H**), 3.98 (2H, t, J = 6.0 Hz, ArOC**H₂**), 3.11-3.18 (1H, m, SC**H**), 2.90 (1H, dd, J = 5.1, 12.9 Hz, SC**H_a**), 2.67-2.73 (3H, m, SC**H_b**, ArC^{tri}C**H₂**), 2.06-2.16 (2H, m, C**H₂**), 1.63-1.85 (4H, m, 2 x C**H₂**), 1.37-1.50 (4H, m, 2 x C**H₂**); ¹³**C NMR** (75 MHz, CDCl₃): δ 163.5, 158.9, 129.7, 121.0, 120.8, 114.6, 67.0, 62.2, 60.3, 55.9, 50.0, 40.8, 29.3, 28.9, 28.8, 27.5, 26.5, 25.7; **HRMS** calcd. for (M + H) C₂₂H₃₂N₅O₂S: requires 430.2277, found 430.2311.

(3a*S*,4*S*,6a*R*)-4-[5-[1-[3-(1-Naphthyloxy)propyl]triazol-4-yl]pentyl]-1,3,3a,4,6,6a-hexahydrothieno[3,4-*d*]imidazol-2-one (6.04)
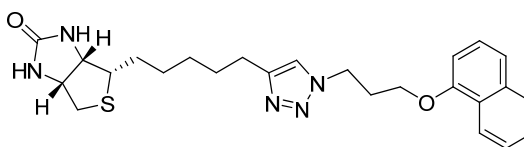
Biotin alkyne **3.12** (16 mg, 0.07 mmol) was reacted with azide **6.22** (17 mg, 0.08 mmol) and Cu nanopowder (1 mg, 0.02 mmol) according to general procedure **G1**. The residue was purified by flash chromatography on silica eluting with 8% methanol in dichloromethane to give a white solid, (11 mg, 35%).

¹**H NMR** (300 MHz, CDCl₃): δ 8.15-8.19 (1H, m, Ar**H**), 7.73-7.76 (1H, m, Ar**H**), 7.26-7.47 (5H, m, Ar**H**, Ar^{tri}**H**), 6.70 (1H, d, J = 6.6 Hz, Ar**H**), 5.15 (1H, bs, C(O)N**H**), 4.86 (1H, bs, C(O)N**H**), 4.59 (2H, t, J = 6.9 Hz, ArN^{tri}C**H₂**), 4.39-4.43 (1H, m, NHC**H**), 4.18-4.23 (1H, m, NHC**H**), 4.07 (2H, t, J = 5.7 Hz, ArOC**H₂**), 3.02-3.08 (1H, m, SC**H**), 2.82 (1H, dd, J = 5.1, 12.6 Hz, SC**H_a**), 2.64 (1H, d, J = 12.6 Hz, SC**H_b**), 2.96 (2H, t, J = 7.5 Hz, ArC^{tri}C**H₂**), 2.43-2.51 (2H, m, C**H₂**), 1.18-1.62 (8H, m, 4 x C**H₂**); ¹³**C NMR** (75 MHz, CDCl₃): δ 163.2, 154.3, 148.3, 134.7, 127.8, 126.7, 126.1, 125.6, 125.5, 121.8, 121.5, 120.9, 104.9, 64.5, 62.1, 60.2, 55.7, 47.3, 40.8, 30.2, 29.3, 29.2, 28.9, 28.7, 25.7; **HRMS** calcd. for (M+ H) C₂₅H₃₂N₅O₂S: requires 466.2277, found 466.2294.

(3a*S*,4*S*,6a*R*)-4-[5-[1-[4-(1-Naphthyloxy)butyl]triazol-4-yl]pentyl]-1,3,3a,4,6,6a-hexahydrothieno[3,4-*d*]imidazol-2-one (6.05)
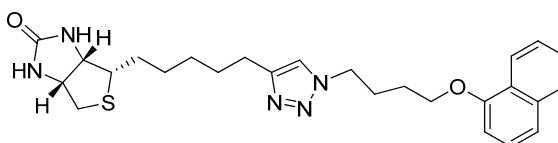
Biotin alkyne **3.12** (16 mg, 0.07 mmol) was reacted with azide **6.23** (18 mg, 0.07 mmol) and Cu nanopowder (1 mg, 0.02 mmol) according to general procedure **G1**. The residue was purified by flash chromatography on silica eluting with 8% methanol in dichloromethane to give a white solid, (14 mg, 41%).

MP: 97 - 98 $^{\circ}$C; **^{1}H NMR** (300 MHz, CDCl$_3$): δ 8.21 – 8.24 (1H, m, Ar**H**), 7.78-7.81 (1H, s, Ar**H**), 7.37-7.50 (4H, m, Ar**H**), 7.29 (1H, s, Ar$^{\text{tri}}$**H**), 6.87 (1H, d, J = 7.5 Hz, Ar**H**), 5.63 (1H, bs, C(O)N**H**), 5.24 (1H, bs, C(O)N**H**), 4.45 (3H, t (apparent), J = 6.9 Hz, ArN$^{\text{tri}}$C**H$_2$**, NHC**H**), 4.23-4.27 (1H, m, NHC**H**), 4.15 (2H, t, J = 6.0 Hz, ArOC**H$_2$**), 3.08-3.14 (1H, m, SC**H**), 2.87 (1H, dd, J = 5.1, 12.6 Hz, SC**H$_a$**), 2.67-2.71 (3H, m, SC**H$_b$**, ARC$^{\text{tri}}$C**H$_2$**), 2.16-2.26 (2H, m, C**H$_2$**), 1.90-2.00 (2H, m, C**H$_2$**), 1.57-1.71 (2H, m, 2 x C**H$_2$**), 1.33-1.48 (2H, m, 2 x C**H$_2$**); **^{13}C NMR** (75 MHz, CDCl$_3$): δ 163.6, 154.6, 134.7, 127.7, 126.6, 126.0, 125.7, 125.4, 122.0, 120.8, 120.5, 104.8, 67.2, 62.2, 55.9, 50.1, 40.7, 29.3 ,29.2, 28.9, 28.7, 27.8, 26.5, 25.7; **HRMS** calcd. for (M+ H) C$_{26}$H$_{34}$N$_5$O$_2$S: requires 480.2433, found 480.2458.

(3a*S*,4*S*,6a*R*)-4-[5-[1-[3-(2-Naphthyloxy)propyl]triazol-4-yl]pentyl]-1,3,3a,4,6,6a-hexahydrothieno[3,4-*d*]imidazol-2-one (6.05)
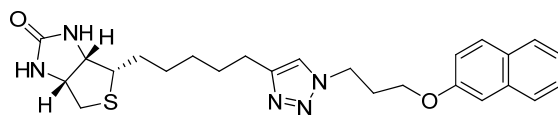
Biotin alkyne **3.12** (20 mg, 0.08 mmol) was reacted with azide **6.24** (21 mg, 0.09 mmol) and Cu nanopowder (1 mg, 0.02 mmol) according to general procedure **G1**. The residue was purified by flash chromatography on silica eluting with 8% methanol in dichloromethane to give a white solid, (20 mg, 51%).

^{1}**H NMR** (300 MHz, CDCl$_3$): δ 7.77 (1H, d, J = 7.5 Hz, Ar**H**), 7.75 (1H, d, J = 8.9 Hz, Ar**H**), 7.71 (1H, d, J = 7.5 Hz, Ar**H**), 7.42-7.47 (1H, m, Ar**H**), 7.32-7.37 (1H, m, Ar**H**), 7.28 (1H, s, Ar^{tri}**H**), 7.14 (1H, dd, J = 2.7, 8.7 Hz, Ar**H**), 7.09 (1H, d, J = 2.7 Hz, Ar**H**), 5.50 (1H, bs, C(O)N**H**), 5.15 (1H, bs, C(O)N**H**), 4.59 (2H, t, J = 6.6 Hz, ArN^{tri}**CH$_2$**), 4.44-4.49 (1H, m, NHC**H**), 4.23-4.27 (1H, m, NHC**H**), 4.07 (2H, t, J = 6.0 Hz, ArOC**H$_2$**), 3.06-3.13 (1H, m, SC**H**), 2.87 (1H, dd, J = 5.1, 12.6 Hz, SC**H$_a$**), 2.65-2.72 (3H, m, SC**H$_b$**, ArC^{tri}**CH$_2$**), 2.41-2.49 (2H, m, **CH$_2$**), 1.62-1.69 (4H, m, 2 x **CH$_2$**), 1.34-1.42 (4H, m, 2 x **CH$_2$**); ^{13}**C NMR** (75 MHz, CDCl$_3$): δ 163.4, 156.6, 148.3, 134.6, 129.8, 129.3, 127.9, 127.0, 126.7, 124.0, 121.5, 118.8, 106.9, 64.3, 62.2, 60.2, 55.9, 47.1, 40.7, 30.1, 29.2, 29.1, 28.9, 25.7.

(3a*S*,4*S*,6a*R*)-4-[5-[1-[4-(2-Naphthyloxy)butyl]triazol-4-yl]pentyl]-1,3,3a,4,6,6a-hexahydrothieno[3,4-*d*]imidazol-2-one (6.07)
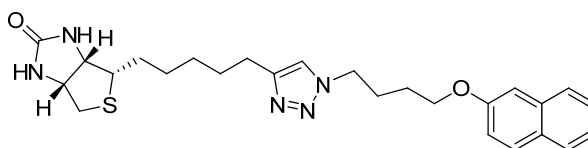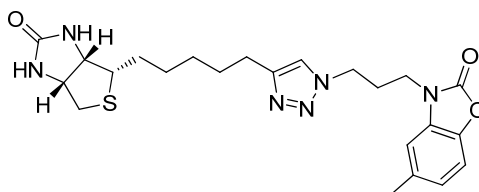

Biotin alkyne **3.12** (18 mg, 0.07 mmol) was reacted with azide **6.25** (20 mg, 0.08 mmol) and Cu nanopowder (1 mg, 0.02 mmol) according to general procedure **G1**. The residue was purified by flash chromatography on silica eluting with 8% methanol in dichloromethane to give a white solid, (26 mg, 74%).

MP: 96 – 98 °C; ^{1}**H NMR** (300 MHz, CDCl$_3$): δ 7.70-7.77 (3H, m, Ar**H**), 7.41-7.46 (1H, m, Ar**H**), 7.31-7.35 (1H, m, Ar**H**), 7.30 (1H, Ar^{tri}**H**), 7.10-7.14 (2H, m, Ar**H**), 5.39 (1H, bs, C(O)N**H**), 5.05 (1H< bs, C(O)N**H**), 4.41-4.50 (3H, m, NHC**H**, ArN^{tri}**CH$_2$**), 4.26-4.30 (1H, m, NHC**H**), 4.10 (2H, t, J = 6.0 Hz, ArOC**H$_2$**), 3.10-3.16 (1H, m, SC**H**), 2.89 (1H, dd, J = 5.4, 12.9 Hz, SC**H$_a$**), 2.67-2.73 (3H, m, SC**H$_b$**, ArC^{tri}**CH$_2$**), 2.11-2.20 (2H, m, **CH$_2$**), 1.83-1.92 (2H, m, **CH$_2$**), 1.63-1.72 (4H, m, 2 x **CH$_2$**), 1.37-1.46 (4H, m, 2 x **CH$_2$**); ^{13}**C NMR** (75 MHz, CDCl$_3$): δ 163.8, 156.8, 148.4, 134.7, 129.6, 129.1, 127.8, 126.9, 126.6, 123.9, 120.8, 118.9, 106.8, 67.1, 62.2, 60.3, 56.0, 50.0, 40.7, 29.3, 29.2, 24.9, 28.7, 27.5, 26.4, 25.7; **HRMS** calcd. for (M+ H) C$_{26}$H$_{34}$N$_5$O$_2$S: requires 480.2433, found 480.2454.

3-[2-[4-[5-[(3a*S*,4*S*,6a*R*)-2-Oxo-1,3,3a,4,6,6a-hexahydrothieno[3,4-*d*]imidazol-4-yl]pentyl]triazol-1-yl]ethyl]-5-methyl-1,3-benzoxazol-2-one (6.08)
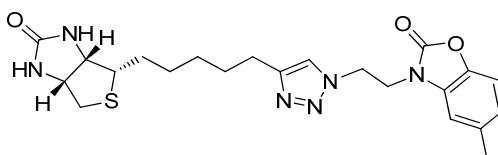
Biotin alkyne **3.12** (21 mg, 0.09 mmol) was reacted with azide **6.31** (21 mg, 0.10 mmol) and Cu nanopowder (1 mg, 0.02 mmol) according to general procedure **G1**. The residue was purified by flash chromatography on silica eluting with 8% methanol in dichloromethane to give a white solid, (26 mg, 65%).

MP: 198 – 200 $^{\circ}$C; ^{1}**H NMR** (300 MHz, DMSO-d$_6$): δ 7.90 (1H, s, Ar^{tri}**H**), 7.22 (1H, d, *J* = 8.1 Hz, Ar**H**), 6.93-6.97 (1H, d, *J* = 8.1 Hz, Ar**H**), 6.78 (1H, s, Ar**H**), 6.50 (1H, bs, C(O)N**H**), 6.43 (1H, bs, C(O)N**H**), 4.73 (2H, t, *J* = 6.3 Hz, ArN^{tri}C**H$_2$**), 4.35-4.39 (1H, m, NHC**H**), 4.28 (2H, t, *J* = 6.3 Hz, NC**H$_2$**), 4.16-4.21 (1H, NHC**H**), 3.12-3.18 (1H, m, SC**H**), 2.88 (1H, dd, *J* = 5.1, 12.3 Hz, SC**H$_a$**), 2.63 (1H, d, *J* = 12.3 Hz, SC**H$_b$**), 2.54-2.59 (2H, m (with DMSO), ArC^{tri}C**H$_2$**), 2.33 (3H, ArC**H$_3$**), 1.26-1.69 (8H, m, 4 x C**H$_2$**); ^{13}**C NMR** (75 MHz, CDCl$_3$): δ 162.8, 153.8, 147.1, 139.8, 133.2, 130.6, 122.6, 122.4, 109.2, 109.1, 61.1, 59.2, 55.6, 47.0, 42.2, 28.9, 28.4, 24.9, 21.1; **HRMS** calcd. for (M+ H) C$_{22}$H$_{29}$N$_6$O$_3$S: requires 457.2022, found 457.2036.

3-[3-[4-[5-[(3a*S*,4*S*,6a*R*)-2-Oxo-1,3,3a,4,6,6a-hexahydrothieno[3,4-*d*]imidazol-4-yl]pentyl]triazol-1-yl]propyl]-5-methyl-1,3-benzoxazol-2-one (6.09)

Biotin alkyne **3.12** (14 mg, 0.06 mmol) was reacted with azide **6.32** (15 mg, 0.06 mmol) and Cu nanopowder (1 mg, 0.02 mmol) according to general procedure **G1**. The residue was purified by flash chromatography on silica eluting with 8% methanol in dichloromethane to give a white solid, (17 mg, 61%).

MP: 134 – 136 °C; **^{1}H NMR** (300 MHz, CDCl$_3$): δ 7.48 (1H, s, Ar^{tri}**H**), 7.08 (1H, d, *J* = 8.1 Hz, Ar**H**), 6.92 (1H, d, *J* = 8.1 Hz, Ar**H**), 6.78 (1H, s, Ar**H**), 5.70 (1H, bs, C(O)N**H**), 5.30 (1H, bs, C(O)N**H**), 4.48-4.52 (1H, m, NHC**H**), 4.40 (2H, t, *J* = 6.6 Hz, ArN^{tri}C**H$_2$**), 4.29-4.33 (1H, m, NHC**H**), 3.87 (2H, t, *J* = 6.6 Hz, NC**H$_2$**), 3.12-3.19 (1H, m, SC**H**), 2.90 (1H, dd, *J* = 5.1, 12.6 Hz, SC**H$_a$**), 2.70-2.74 (3H, m, SC**H$_b$**, ArC^{tri}C**H$_2$**), 2.39-2.47 (5H, m, C**H$_2$**, ArC**H$_3$**), 1.36-1.78 (8H, m, 4 x C**H$_2$**); **^{13}C NMR** (75 MHz, CDCl$_3$): δ 163.6, 155.28, 148.4, 140.9, 134.4, 130.7, 123.4, 121.9, 110.0, 109.1, 62.2, 60.3, 55.9, 47.3, 40.8, 39.5, 29.2, 28.9, 28.7, 28.67, 25.7, 21.8 **HRMS** calcd. for (M + H) C$_{23}$H$_{31}$N$_6$O$_3$S: requires 471.2178, found 471.2198.

3-[4-[4-[5-[(3a*S*,4*S*,6a*R*)-2-Oxo-1,3,3a,4,6,6a-hexahydrothieno[3,4-*d*]imidazol-4-yl]pentyl]triazol-1-yl]butyl]-5-methyl-1,3-benzoxazol-2-one (6.10)
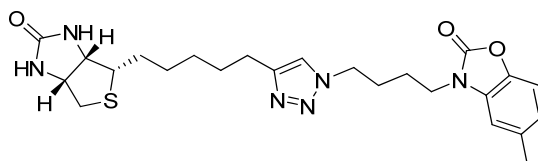
Biotin alkyne **3.12** (21 mg, 0.06 mmol) was reacted with azide **6.33** (24 mg, 0.06 mmol) and Cu nanopowder (1 mg, 0.02 mmol) according to general procedure **G1**. The residue was purified by flash chromatography on silica eluting with 8% methanol in dichloromethane to give a white solid, (29 mg, 68%).

MP: 99 - 101 °C; **^{1}H NMR** (300 MHz, CDCl$_3$): δ 7.32 (1H, s, Ar^{tri}**H**), 7.06 (1H, d, *J* = 8.1 Hz, Ar**H**), 6.90(1H, d, *J* = 8.1 Hz, Ar**H**), 6.77 (1H, m, Ar**H**), 6.22 (1H, bs, C(O)N**H**), 5.81 (1H, bs, C(O)N**H**), 4.46-4.50 (1H, m, NHC**H**), 4.39 (2H, t, *J* = 6.9 Hz, ArN^{tri}C**H$_2$**), 4.26-4.31 (1H, m, NHC**H**), 3.83 (2H, t, *J* = 6.9 Hz, NC**H$_3$**), 3.11-3.17 (1H, m, SC**H**), 2.89 (1H, dd, *J* = 5.1, 12.6 Hz, SC**H$_a$**), 2.66-2.73 (3H, m, SC**H$_b$**, ArC^{tri}C**H$_2$**), 2.39 (3H, s, ArC**H$_3$**), 1.93-2.03 (2H, m, C**H$_2$**), 1.65-1.84 (6H, m, 3 x C**H$_2$**), 1.33-1.43 (4H, m, 2 x C**H$_2$**); **^{13}C NMR** (300 MHz, CDCl$_3$): δ 164.0, 155.1, 148.5, 140.8, 134.1, 130.8, 123.1, 121.0, 109.8, 109.0, 62.2, 60.3, 56.0, 49.3, 41.3, 40.7, 29.3, 29.2, 28.9, 28.7, 27.4, 25.7, 24.8, 21.7; **HRMS** calcd. for (M + H) C$_{24}$H$_{33}$N$_6$O$_3$S: requires 485.2335, found 485.2359.

3-Azidopropoxybenzene (6.16)[30,31]
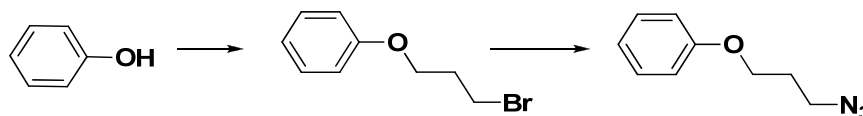
Phenol (215 mg, 2.28 mmol) and 1,3-dibromopropane (686 mg, 3.43 mmol) were reacted according to general procedure **I1** and purified by silica gel chromatography eluting with 25% dichloromethane in petroleum ether to give bromide **6.14** as a clear oil (367 mg, 75%).

FT-IR (ATR) v_{max}: 2926, 1599, 1496, 1240, 690 cm^{-1}; **^{1}H NMR** (300 MHz; CDCl$_3$)**:** δ 7.30 **(**2H, dd, J = 7.2, 8.7 Hz, Ar**H**), 6.89 – 6.98 (3H, m, Ar**H**), 6.92 (2H, d, J = 8.7 Hz, Ar**H**), 4.11 (2H, t, J = 5.7 Hz, ArOC**H$_2$**), 3.62 (2H, t, J = 6.3 Hz, C**H$_2$**Br), 2.33 (2H, tt, J = 5.7, 6.3 Hz, C**H$_2$**); **^{13}C NMR** (300 MHz; CDCl$_3$)**:** δ 129.7, 121.1, 114.7, 65.4, 32.6, 30.3.

Bromide **6.14** (163 mg, 0.76 mmol) was reacted according to general procedure **I2** and purified by silica gel chromatography eluting with 20% dichloromethane in petroleum ether to give a clear oil (122 mg, 89%).

FT-IR (ATR) v_{max}: 2931, 2094, 1496, 1241 cm^{-1}; **^{1}H NMR** (300 MHz; CDCl$_3$)**:** δ 7.35 (2H, dd, J = 8.1, 8.7 Hz, Ar**H**), 7.01 (1H, d, J = 8.7 Hz, Ar**H**), 6.94 (1H, d, J = 8.1 Hz, Ar**H**), 4.07 (2H, t, J = 6.0 Hz, ArOC**H$_2$**), 3.54 (2H, t, J = 6.6 Hz, C**H$_2$**N$_3$), 2.07 (2H, tt, J = 6.0, 6.6 Hz, C**H$_2$**); **^{13}C NMR** (300 MHz; CDCl$_3$): 129.6, 121.0, 114.6, 64.5, 48.4, 28.9.

4-Azidobutoxybenzene (6.17)[30,31]
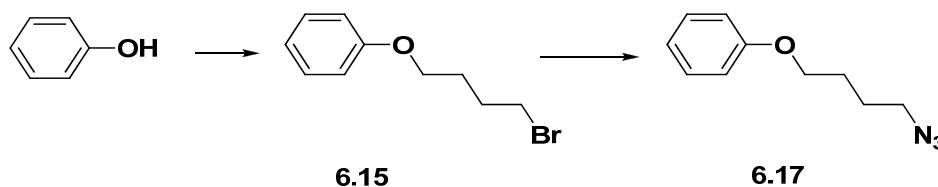
Phenol (230 mg, 2.44 mmol) and 1,4-dibromobutane (785 mg, 3.67 mmol) were reacted according to general procedure **I1** and purified by silica gel chromatography eluting with 25% dichloromethane in petroleum ether to give bromide **6.15** as a clear oil (435 mg, 78%).

FTIR (ATR): 2957, 1488, 1242, 691 cm^{-1}; **^{1}H NMR** (300 MHz; CDCl$_3$)**:** δ 7.30 (2H,dd, J = 8.1, 8.7 Hz, Ar**H**), 6.98 (1H, d, J = 8.1 Hz, Ar**H**), 6.91 (1H, d J = 8.7 Hz, Ar**H**), 4.01 (2H, t, J = 5.7 Hz, OC**H$_2$**), 3.51 (2H, t, J = 6.6 Hz, C**H$_2$**Br), 2.05-2.14 (2H, m , C**H$_2$**), 1.91-2.00 (2H, m, C**H$_2$**); **^{13}C NMR** (300 MHz; CDCl$_3$)**:** δ 129.6, 120.9, 114.6, 66.9, 33.7, 29.7, 27.9.

Bromide **6.15** (178 mg, 0.78 mmol) was reacted according to general procedure **I2** and purified by silica gel chromatography eluting with 20% dichloromethane in petroleum ether to give a clear oil (141 mg, 93%).

FTIR (ATR**):** 2929, 2093, 1496, 1241 cm^{-1}; **^{1}H NMR** (300 MHz; CDCl$_3$)**:** δ 7.30 (2H, dd, J = 7.5, 8.1 Hz, Ar**H**), 6.97 (1H, d, J = 7.5 Hz, Ar**H**), 6.91 (1H, d, J = 8.1 Hz, Ar**H**), 4.00 (2H, t, J = 5.7 Hz, ArOC**H$_2$**), 3.38 (2H, t, J = 6.6 Hz, C**H$_2$**N$_3$), 1.76-1.93 (4H, m, 2 x C**H$_2$**); **^{13}C NMR** (300 MHz; CDCl$_3$): δ 129.7, 121.0, 114.7, 67.2, 51.4, 26.7, 26.0

1-(3-Azidopropoxy)naphthalene (6.22)
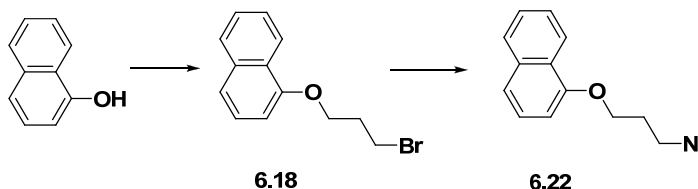
1-Naphthol (361 mg, 2.50 mmol) and 1,3-dibromopropane (752 mg, 3.76 mmol) were reacted according to general procedure **I1** and purified by silica gel chromatography eluting with 15% dichloromethane in petroleum ether to give bromide **6.18** as a clear oil (99 mg, 15%). ^{1}H NMR consistent with literature report[32]

FT-IR (ATR) **ν$_{max}$**: 3053, 2940, 1594, 1270 cm^{-1}; **^{1}H NMR** (300 MHz; CDCl$_3$): δ 8.21-8.24 (1H, m, Ar**H**), 7.76-7.79 (1H, m, Ar**H**), 7.31-7.49 (4H, m, Ar**H**), 6.76-6.78 (1H, m, Ar**H**), 4.21 (2H, t, J = 6.0 Hz, ArOC**H$_2$**), 3.65 (2H, t, J = 6.3 Hz, C**H$_2$**Br), 2.39 (2H, quin, J = 6.3 Hz, C**H$_2$**); **^{13}C NMR** (75 MHz; CDCl$_3$): δ 154.2, 134.4, 127.5, 126.4, 125.8, 125.5, 125.2, 121.8, 120.4, 104.7, 65.4, 32.4, 30.1.

Bromide **6.18** (85 mg, 0.32 mmol) was reacted according to general procedure **I2** and purified by silica gel chromatography eluting with 20% dichloromethane in petroleum ether to give a clear oil (63 mg, 86%).

FT-IR (film) v_{max}: 3054, 2934, 2098, 1580 cm^{-1}; **^{1}H NMR** (300 MHz; CDCl$_3$): δ 8.22-8.25 (1H, m, Ar**H**), 7.78-7.81 (1H, m, Ar**H**), 7.33-7.49 (4H, m, Ar**H**), 6.91 (1H, t, J = 7.5 Hz, Ar**H**), 4.21 (2H, t, J = 6.3 Hz, ArOC**H$_2$**), 3.60 (2H, t, J = 6.6 Hz, C**H$_2$**N$_3$), 2.18 (2H, quin, J = 6.6 Hz, C**H$_2$**); **^{13}C NMR** (75 MHz; CDCl$_3$): δ 154.3, 134.5, 127.5, 126.4, 125.8, 125.5, 125.2, 121.8, 120.4, 104.6, 64.6, 48.4, 28.8.

1-(4-Azidobutoxy)naphthalene (6.23)[32,33]
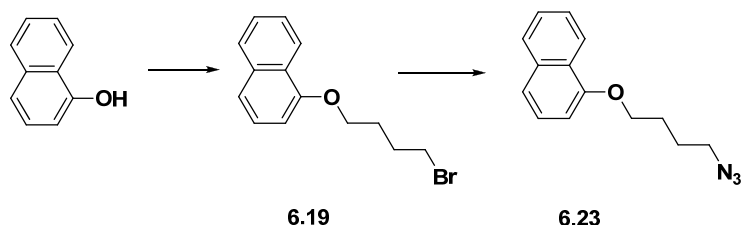
1-Naphthol (178 mg, 1.24 mmol) and 1,4-dibromobutane (397 mg, 1.85 mmol) were reacted according to general procedure **I1** and purified by silica gel chromatography eluting with 15% dichloromethane in petroleum ether to give bromide **6.19** as a clear oil (89 mg, 26%).

FT-IR (film) v_{max}: 3052, 2953, 1580, 1270 cm^{-1}; **^{1}H NMR** (300 MHz; CDCl$_3$): δ 8.24-8.27 (1H, m, Ar**H**), 7.77-7.80 (1H, m, Ar**H**), 7.35-7.51 (4H, m, Ar**H**), 6.78 (1H, dd, J = 0.9, 7.5 Hz, Ar**H**), 4.16 (2H, t, J = 6.3 Hz, ArOC**H$_2$**), 3.54 (2H, t, J = 6.6 Hz, C**H$_2$**Br), 2.03-2.22 (4H, m, 2 x C**H$_2$**); **^{13}C NMR** (75 MHz; CDCl$_3$): δ 154.5, 134.5, 127.5, 126.4, 125.8, 125.6, 125.2, 121.9, 120.2, 104.5, 66.9, 33.6, 29.7, 27.9.

Bromide **6.19** (81 mg, 0.29 mmol) was reacted according to general procedure **I2** and purified by silica gel chromatography eluting with 20% dichloromethane in petroleum ether to give a clear oil (61 mg, 86%).

FT-IR (film) v_{max}: 3053, 2949, 2098, 1595 cm^{-1}; **^{1}H NMR** (300 MHz; CDCl$_3$): δ 8.24-8.27 (1H, m, Ar**H**), 7.77-7.81 (1H, m, Ar**H**), 7.33-7.51 (4H, m, Ar**H**), 6.78 (1H, d, J = 6.6

Hz, Ar**H**), 4.15 (2H, t, J = 6.3 Hz, ArOC**H₂**), 3.40 (2H, t, J = 6.6 Hz, C**H₂**N₃), 1.86-2.05 (4H, m, 4 x C**H₂**); **¹³C NMR** (75 MHz; CDCl₃): δ 154.5, 134.5, 127.5, 126.4, 125.8, 125.6, 121.9, 120.2, 104.5, 67.2, 51.2, 26.6, 25.9.

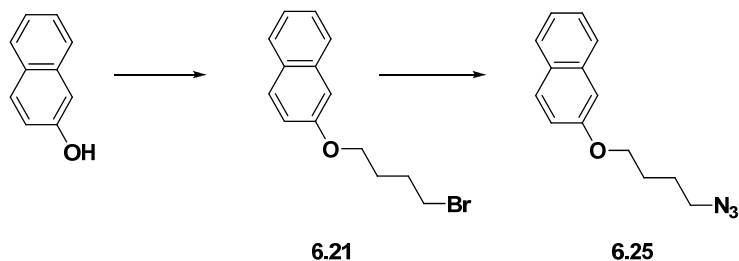## 2-(3-Azidopropoxy)naphthalene (6.24)[34,35]
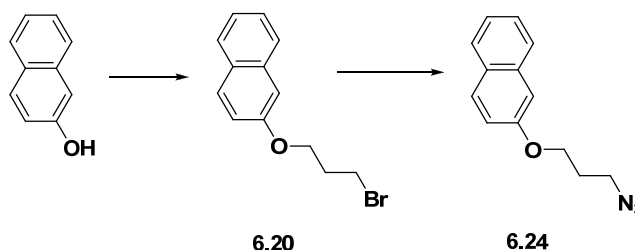
2-Naphthol (412 mg, 2.86 mmol) and 1,3-dibromopropane (858 mg, 4.29 mmol) were reacted according to general procedure **I1** and purified by silica gel chromatography eluting with 15% dichloromethane in petroleum ether to give bromide **6.20** as a white solid (453 mg, 60%).

MP:45-46 °C; **FTIR** (nujol): 3053, 2940, 1594, 1270 cm⁻¹; **¹H NMR** (300 MHz; CDCl₃): δ 7.72-7.78 (3H, m, Ar**H**), 7.41-7.47 (1H, m, Ar**H**), 7.31-7.37 (1H, m, Ar**H**), 7.16 (1H, s, Ar**H**), 7.12 (1H, d, J = 2.7 Hz, Ar**H**), 4.23 (2H, t, J = 6.3 Hz, ArOC**H₂**), 3.66 (2H, t, J = 6.3 Hz, C**H₂**Br), 2.39 (2H, quin, J = 6.3 Hz, C**H₂**); **¹³C NMR** (75 MHz; CDCl₃): δ 156.59, 134.49, 129.44, 129.01, 127.63, 126.73, 126.40, 123.69, 118.76, 106.70, 65.29, 32.34, 30.08.

Bromide **6.20** (121 mg, 0.46 mmol) was reacted according to general procedure **I2** and purified by silica gel chromatography eluting with 20% dichloromethane in petroleum ether to give a clear oil (72 mg, 68%).

FT-IR (ATR) **v_max**: 3057, 2098, 1630, 1601 cm⁻¹; **¹H NMR** (300 MHz; CDCl₃): δ 7.71-7.78 (3H, m, Ar**H**), 7.41-7.47 (1H, m, , Ar**H**), 7.31-7.36 (1H, m, , Ar**H**), 7.11-7.16 (2H, m, , Ar**H**), 4.17 (2H, t, J = 6.0 Hz, ArOC**H₂**), 3.56 (2H, t, J = 6.6 Hz, C**H₂**N₃), 2.12 (2H, quin, J = 6.0 Hz, C**H₂**); **¹³C NMR** (75 MHz; CDCl₃): δ 156.6, 134.5, 129.5, 129.0, 127.6, 126.7, 126.4, 123.7, 118.8, 106.6, 64.5, 48.3, 28.8.

2-(4-Azidobutoxy)naphthalene (6.25)[35]

2-Naphthol (416 mg, 2.89 mmol) and 1,3-dibromopropane (927 mg, 4.33 mmol) were reacted according to general procedure **I1** and purified by silica gel chromatography eluting with 15% dichloromethane in petroleum ether to give bromide **6.21** as a white solid (362 mg, 60%).

MP: 44-46°C. **FTIR (**nujol)**:** 1629, 1596, 1257, 1217 cm^{-1}; **^{1}H NMR** (300 MHz; CDCl$_3$): δ 7.71-7.78 (3H, m, Ar**H**), 7.41-7.46 (1H, m, Ar**H**), 7.30-7.36 (1H, m, Ar**H**), 7.15 (1H, d, J = 2.4 Hz, Ar**H**), 7.12 (1H, s, Ar**H**), 4.11 (2H, t, J = 6.0 Hz, ArOC**H$_2$**), 3.52 (2H, t, J = 6.6 Hz, C**H$_2$**Br), 1.98-2.14 (4H, m, 2 x C**H$_2$**); **^{13}C NMR** (75 MHz; CDCl$_3$): δ 156.79, 134.51, 129.39, 128.93, 127.63, 126.69, 126.36, 123.59, 118.85, 106.51, 66.79, 33.49, 29.51, 27.85.
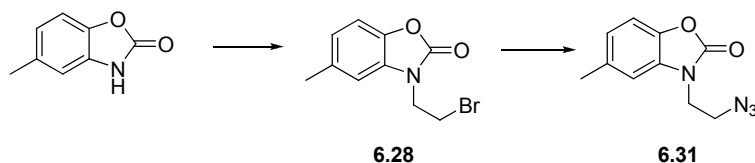
Bromide **6.21** (167 mg, 0.60 mmol) was reacted according to general procedure **I2** and purified by silica gel chromatography eluting with 20% dichloromethane in petroleum ether to give a clear oil (66 mg, 45%).

FT-IR (Nujol) **ν$_{max}$**: 3058, 2094, 1628, 1511 cm^{-1}; **^{1}H NMR** (300 MHz; CDCl$_3$): δ 7.69-7.77 (3H, m, Ar**H**), 7.40-7.46 (1H, m, Ar**H**), 7.29-7.35 (1H, m, Ar**H**), 7.15 (1H, d, J = 2.4 Hz, Ar**H**), 7.12 (1H, s, Ar**H**), 4.09 (2H, t, J = 6.0 Hz, ArOC**H$_2$**), 3.38 (2H, t, J = 6.6 Hz, C**H$_2$**N$_3$), 1.79-1.96 (4H, m, 2 x C**H$_2$**); **^{13}C NMR** (75 MHz; CDCl$_3$): δ 156.8, 134.5, 129.4, 128.9, 127.6, 126.7, 126.3, 123.6, 118.8, 106.5, 67.1, 51.2, 26.4, 25.8.

5-Methyl-3*H*-1,3-benzoxazol-2-one (6.27)[36]
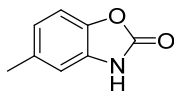
To a solution of 2-amino-cresol (5.10 g, 41.4 mmol) in 50 mL of dichloromethane was added 1,1-carbonyldiimidazole (7.39 g, 45.6 mmol) and the solution was stirred at ambient temperature under nitrogen atmosphere for 45 min. The reaction mixture was poured into water (100 mL) and extracted with dichloromethane (2 x 100 mL). The organic layers were pooled, washed with saturated aqueous sodium bicarbonate (1 x 150 mL), water (1 x 150 mL) and brine (1 x 150 mL), dried over Na$_2$SO$_4$, filtered and concentrated *in vacuo* to give a white solid (5.93 g, 96%). >95% purity as judged by ^{1}H NMR spectroscopy.

^{1}H NMR (300 Mhz, CDCl$_3$): δ 10.07 (1H, bs, N**H**), 7.06 (1H, d, *J* = 8.1 Hz, Ar**H**), 6.90 (1H, s, Ar**H**), 6.87 (1H, d, *J* = 8.1 Hz, Ar**H**), 2.36 (3H, s, ArC**H$_3$**); **^{13}C NMR** (75 MHz, CDCl$_3$): δ 157.0, 142.0, 134.3, 129.6, 123.2, 111.0, 109.7, 21.6.

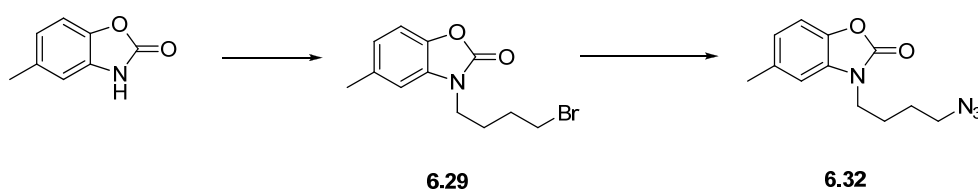## 3-(2-Azidoethyl)-5-methyl-1,3-benzoxazol-2-one (6.31)

2-Benzoxazolone **6.27** (214 mg, 1.44 mmol) and 1,2-dibromoethane (401 mg, 2.15 mmol) was reacted according to general procedure **I1** and was purified by flash chromatography on silica eluting with 25% ethyl acetate in petroleum ether to give bromide **6.28** as a white solid (315 mg, 86%)

FT-IR (ATR) **ν$_{max}$**: 2972, 1765, 1623, 1381 cm^{-1}; **^{1}H NMR** (300 MHz; CDCl$_3$): δ 7.07 (1H, d, *J* = 8.0 Hz, Ar**H**), 6.09 (1H, d, *J* = 8.0 Hz, Ar**H**), 6.86 (1H, s, Ar**H**), 4.19 (2H, t, *J* = 6.6, NC**H$_2$**), 3.65 (2H, t, *J* = 6.6, C**H$_2$**Br), 2.39 (3H, s, ArC**H$_3$**); **^{13}C NMR** (75 MHz; CDCl$_3$): δ 154.5, 140.7, 134.2, 130.8, 123.3, 109.9, 109.1, 43.9, 27.6, 21.7**.**

Bromide **6.28** (156 mg, 0.61 mmol) was reacted according to general procedure **I1** and purified by silica gel chromatography eluting with 20% ethyl acetate in petroleum ether to yield a white solid (128 mg, 95%).

FT-IR (ATR) ν_{max}: 3069, 2932, 2092, 1763 cm^{-1}; **^{1}H NMR** (300 MHz; CDCl$_3$): δ 7.09 (1H, d, J = 8.1 Hz, Ar**H**), 6.93 (1H, d, J = 8.1 Hz, Ar**H**), 6.87 (1H, s, Ar**H**), 3.96 (2H, t, J = 6.0 Hz, NC**H$_2$**), 3.71 (2H, t, J = 6.0 Hz, C**H$_2$**Br), 2.41 (3H, s, ArC**H$_3$**); **^{13}C NMR** (75 MHz; CDCl$_3$): δ 155.0, 141.0, 134.4, 131.2, 123.5, 110.1, 109.3, 49.4, 41.9, 21.9; **HRMS** calcd. for (M+ Na) C$_{10}$H$_{10}$N$_4$NaO$_2$: requires 241.0702, found 241.0695.

3-(3-Azidopropyl)-5-methyl-1,3-benzoxazol-2-one (6.32)

2-Benzoxazolone **6.27** (366 mg, 2.46 mmol) and 1,2-dibromoethane (788 mg, 3.68 mmol) was reacted according to general procedure **I1** and was purified by flash chromatography on silica eluting with 20% ethyl acetate in petroleum ether to yield bromide **6.29** as an off white solid (647 mg, 93%)

FT-IR (ATR) ν_{max}: 2946, 1765, 1623, 1493 cm^{-1}; **^{1}H NMR** (300 MHz; CDCl$_3$): δ 7.07 (1H, d, J = 8.1 Hz, Ar**H**), 6.90 (1H, d, J = 8.1 Hz, Ar**H**), 6.78 (1H, s, Ar**H**), 3.84 (2H, t, J = 6.6 Hz, NC**H$_2$**), 3.43 (2H, t, J = 6.6 Hz, C**H$_2$**Br), 2.39 (3H, s, ArC**H$_3$**), 1.92-1.97 (4H, m, C**H$_2$**); **^{13}C NMR** (75 MHz; CDCl$_3$): δ 155.0, 140.9, 134.1, 131.0, 123.0, 109.8, 108.9, 41.4, 32.9, 29.6, 26.5, 21.7

Bromide **6.29** (112 mg, 0.41 mmol) was reacted according to general procedure **I2** and purified by silica gel chromatography eluting with 20% ethyl acetate in petroleum ether to yield a white solid (81 mg, 83%).

FT-IR (ATR) ν_{max}: 2945, 2100, 1754, 1495, 1240 cm^{-1}; **^{1}H NMR** (300 MHz; CDCl$_3$): δ 7.08 (1H, d, J = 8.4 Hz, Ar**H**), 6.90 (1H, d, J = 8.1 Hz, Ar**H**), 6.83 (1H, s, Ar**H**), 3.90 (2H, t, J = 6.9 Hz, NC**H$_2$**), 3.43 (2H, t, J = 6.9 Hz, C**H$_2$**N$_3$), 2.40 (3H, s, ArC**H$_3$**), 2.03 (2H, m,

CH$_2$); ^{13}**C NMR** (75 MHz; CDCl$_3$): δ 154.9, 140.8, 134.2, 131.1, 123.1, 109.9, 108.2, 48.6, 39.5, 27.4, 21.7; **HRMS** calcd. for (M+ Na) C$_{11}$H$_{12}$N$_4$NaO$_2$: requires 255.0858, found 255.0851.

### 3-(4-Azidobutyl)-5-methyl-1,3-benzoxazol-2-one (6.33)
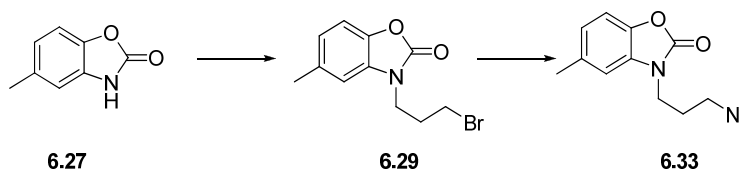
2-Benzoxazolone **6.27** (195 mg, 1.31 mmol) and 1,3-dibromopropane (392 mg, 1.96 mmol) was reacted according to general procedure **I1** and was purified by flash chromatography on silica eluting with 20% ethyl acetate in petroleum ether to yield bromide **6.29** as an off white solid (310 mg, 88%)

FT-IR (ATR) ν$_{max}$: 3068, 2931, 1760, 1623, 1383 cm^{-1}; ^{1}**H NMR** (300 MHz; CDCl$_3$): δ 7.04 (1H, d, *J* = 8.7 Hz, Ar**H**), 6.89 (1H, d, *J* = 8.7 Hz, Ar**H**), 6.87 (1H, s, Ar**H**), 3.94 (2H, t, *J* = 6.6 Hz, NC**H$_2$**), 3.43 (2H, t, *J* = 6.6 Hz, C**H$_2$**Br), 2.38 (3H, s, ArC**H$_3$**), 2.32 (2H, tt, *J* = 6.6, 6.6 Hz, C**H$_2$**) ^{13}**C NMR** (75 MHz; CDCl$_3$): δ 154.8, 140.7, 134.1, 131.1, 123.0, 109.7, 109.0, 40.6, 30.9, 30.0, 21.6.

Bromide **6.29** (256 mg, 0.90 mmol) was reacted according to general procedure **I2** and purified by silica gel chromatography eluting with15% ethyl acetate in petroleum ether to yield a clear oil (205 mg, 91%).

FT-IR (ATR) ν$_{max}$: 2937, 2093, 1762, 1622, 1494 cm^{-1}; ^{1}**H NMR** (300 MHz; CDCl$_3$): δ 7.08 (1H, d, *J* = 8.1 Hz, Ar**H**), 6.91 (1H, d, *J* = 8.1 Hz, Ar**H**), 6.79 (1H, s, Ar**H**), 3.83 (2H, t, *J* = 6.9 Hz, NC**H$_2$**), 3.36 (2H, t, *J* = 6.9 Hz, C**H$_2$**N$_3$), 2.40 (3H, s, ArC**H$_3$**), 1.83-1.93 (2H, m, C**H$_2$**), 1.63-1.72 (2H, m, C**H$_2$**); ^{13}**C NMR** (75 MHz; CDCl$_3$): δ 155.0, 140.9, 134.0, 131.1, 123.0, 109.8, 108.9, 51.0, 41.7, 26.2, 25.2, 21.7; **HRMS** calcd. for (M + Na) C$_{12}$H$_{14}$N$_4$NaO$_2$: requires 269.1015, found 269.1006.

5-[(3a*S*,4*S*,6a*R*)-2-Oxo-1,3,3a,4,6,6a-hexahydrothieno[3,4-*d*]imidazol-4-yl]pentyl 4-(5-methyl-2-oxo-1,3-benzoxazol-3-yl)butyl phosphate (6.34)
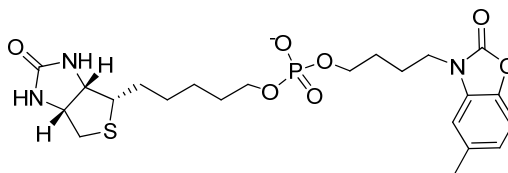
To a solution of phosphotriester **6.39** (25 mg, 0.047 mmol) in dry acetone (5 mL) was added sodium iodide (21 mg, 0.14 mmol) and stirred under reflux for 6 h. The reaction mixture was concentrated *in vacuo* and the residue was purified in two equal portions with HPLC using solvent A (0.1% TFA in water) and solvent B (0.08% TFA, 90% acetonitrile) with gradient of 0 - 0% of solvent B for 5 min, 0%-65% of solvent B for 25 min and 65-90% 10 min of solvent B to give a white solid (17 mg, 68%).

^{1}H NMR (600 MHz, DMSO-d$_6$): 8.27 (1H, bs, OPO**H**), 7.19 (1H, d, *J* = 7.2 Hz, Ar**H**), 7.15 (1H, s, Ar**H**), 6.92 (d, *J* = 7.2 Hz, Ar**H**), 6.42 (1H, bs, C(O)N**H**), 6.33 (1H, bs, C(O)N**H**), 4.28-4.30 (1H, m, NHC**H**), 4.10-4.12 (1H, m, NHC**H**), 3.82-3.85 (2H, m, OPOC**H$_2$**), 3.80 (2H, t, *J* = 6.6 Hz, NC**H$_2$**), 3.76-3.78 (2H, m, OPOC**H$_2$**), 3.06-3.09 (1H, m, SC**H**), 2.80 (1H, dd, *J* = 5.4, 12.6 Hz, SC**H$_a$**), 2.56 (1H, d, *J* = 12.6 Hz, SC**H$_b$**), 2.34 (3H, s, ArC**H$_3$**), 1.74 (2H, m, C**H$_2$**), 1.35-1.64 (6H, m, C**H$_2$**), 1.25-1.34 (4H, m, C**H$_2$**); ^{13}**C NMR**(150 Mhz, DMSO-d$_6$): δ 162.7, 154.0, 139.9, 133.4, 130.9, 122.4, 109.6, 109.2, 65.2, 60.9, 69.2, 55.4, 41.2, 40.0, 34.3, 29.7, 28.2, 28.1, 27.0, 25.1, 23.7, 21.0; ^{31}**P NMR** (32 MHz, D$_2$O): δ -22.4; **HRMS** calcd. for (M+ H) C$_{22}$H$_{33}$N$_3$O$_7$PS: requires 514.1777, found 514.1769.

3-(4-Hydroxybutyl)-5-methyl-1,3-benzoxazol-2-one (6.36)
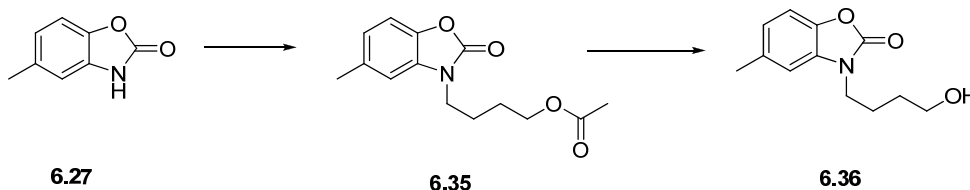
To a solution of 2-benzoxazolone **6.27** (550 mg, 3.69 mmol) in anhydrous DMF (10 mL) were added 4-bromobutyl acetate (1074 mg, 5.53 mmol) and potassium carbonate (764

mg, 5.53 mmol) and stirred under nitrogen atmosphere at ambient temperature. The reaction mixture was diluted with 50 mL of dichloromethane and washed with 0.25 M aqueous HCl (1 x 50 mL), saturated aqueous sodium bicarbonate (1 x 50 mL), water (1 x 50 mL) and brine (1 x 50 mL). The organic layer was dried with Na_2SO_4, filtered and concentrated *in vacuo*. The residue was purified with silica gel chromatography eluting with 30% ethyl acetate in petroleum ether to give acetate **6.36** as a light yellow oil (757 mg, 78%).

^{1}H NMR (200 MHz, CDCl$_3$): δ 7.07 (1H, d, *J* = 8.2 Hz, Ar**H**), 6.90 (1H, d, *J* = 8.2 Hz, Ar**H**), 6.78 (1H, s, Ar**H**), 4.11 (2H, t, *J* = 6.2 Hz, OC**H$_2$**), 3.38 (2H, t, *J* = 7.0 Hz, NC**H$_2$**), 2.40 (3H, s, C(O)C**H$_3$**), 2.04 (3H, s, ArC**H$_2$**), 1.69-1.94 (4H, m, 2 x C**H$_2$**); **^{13}C NMR** (50 MHz, CDCl$_3$): δ 171.2, 158.7, 147.5, 134.0, 131.2, 123.0, 109.9, 108.9, 65.8, 42.0, 26.1, 24.7, 21.7.

To a solution of 2-benzoxazolone **6.35** (311 mg, 1.18 mmol) in THF (3 mL) was added 1M aqueous lithium hydroxide (3 mL) and the solution was stirred overnight. The reaction mixture was diluted with dichloromethane (25 mL), washed with water (1 x 25 mL) and brine (1 x 25 mL), dried over Na_2SO_4 and concentrated *in vacuo*. The residue was purified by silica gel chromatography using 30% ethyl acetate in petroleum ether to give a white solid (170 mg, 65%).

MP: 34 – 36 ^{o}C; **^{1}H NMR** (300 MHz, CDCl$_3$): δ 7.06 (1H, d, *J* = 8.1 Hz, Ar**H**), 6.89 (1H, d, *J* = 8.1 Hz, AR**H**), 6.80 (1H, s, Ar**H**), 3.86 (2H, t, *J* = 7.2 Hz, C**H$_2$**OH), 3.71 (2H, t, *J* = 6.3 Hz, NC**H$_2$**), 2.40 (3H, s, ArC**H$_3$**), 1.89 (2H, m, C**H$_2$**), 1.60-1.69 (2H, m, C**H$_2$**); **^{13}C NMR** (75 MHz, CDCl$_3$) δ 155.2, 140.9, 134.0, 131.2, 123.0, 109.8, 109.1, 62.4, 42.2, 29.6, 24.7, 21.8.

3-[4-[(Diisopropylamino)-methoxy-phosphanyl]oxybutyl]-5-methyl-1,3-benzoxazol-2-one (6.37)
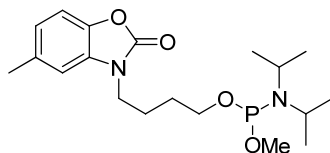

To a solution of 2-benzoxazolone **6.35** (251 mg, 1.14 mmol) and triethylamine (172 mg, 1.70 mmol) in dry dichloromethane (2.5 mL) was reacted with *N,N*-diisopropylmethoxyphosphonamidic (336 mg, 1.70 mmol) according to general procedure **C1**. The residue was obtained as a yellow oil (290 mg) and was used without further purification.

Select Data:

^{1}H NMR (300 MHz, CDCl$_3$): δ 7.08-7.13 (1H, m, Ar**H**), 6.92-6.96 (1H, m, Ar**H**), 6.86 (1H, s, Ar**H**), 4.18 (1H, *quart*, *J* = 6.6 Hz, POC**H**$_a$), 3.85-4.00 (3H, m, POC**H**$_b$, NC**H$_2$**), 3.63 (3H, d, *J* = 12.0 Hz, POC**H$_3$**), 3.28-3.40 (2H, m, 2 x NC**H**), 1.60-2.00 (4H, m, 2 x C**H$_2$**), 1.41 (12H, d, *J* = CHC**H$_3$**); **^{31}P NMR** (75 MHz, CDCl$_3$): δ 4.61.

5-[(3a*S*,4*S*,6a*R*)-2-Oxo-1,3,3a,4,6,6a-hexahydrothieno[3,4-*d*]imidazol-4-yl]pentyl methyl 4-(5-methyl-2-oxo-1,3-benzoxazol-3-yl)butyl phosphate (6.39)
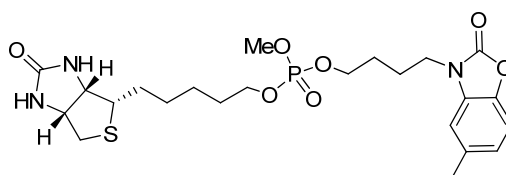
To a solution of phosphite **6.37** (61 mg, 0.16 mmol) and DMtr-biotinol **2.19** (85 mg, 0.16 mmol) in dry acetonitrile (2 mL) was added 2-ETT (42 mg, 0.32 mmol) and stirred at ambient temperature for 4 h under nitrogen atmosphere. 5 M TBHP in decane (0.32 mL) was added and the reaction mixture was stirred for a further 15 min. The solution was diluted with dichloromethane (20 mL) and washed with water (2 x 20 mL) and brine (1 x 20 mL). The organic layer was dried over Na$_2$SO$_4$, filtered and concentrated *in vacuo*. The residue was diluted with dichloromethane (4.75 mL) and TFA (0.25 mL) was added and

stirred for 30 min. The reaction mixture was concentrated *in vacuo* and purified by silica gel chromatography eluting with 5% methanol in dichloromethane to give a clear oil (33 mg, 39%).

¹H NMR (600 MHz, CDCl₃): δ 7.08 (1H, d, *J* = 7.8 Hz, Ar**H**), 6.91 (1H, d, *J* = 7.8 Hz, Ar**H**), 6.81 (1H, s, Ar**H**), 5.71 (1H, bs, C(O)N**H**), 5.12 (1H, bs, C(O)N**H**), 4.51-4.53 (1H, NHC**H**), 4.31-4.34 (1H, NHC**H**), 4.10 (2H, m, NC**H₂**), 4.05 (2H, m, POC**H₂**), 3.85 (2H, t, *J* = 7.2 Hz, POC**H₂**), 5.76 (3H, d, *J* = 11.4 Hz, POC**H₃**), 3.14-3.17 (1H, m, SC**H**), 2.92 (1H, dd, *J* = 5.4, 12.6 Hz, SC**Hₐ**), 2.74 (1H, d, *J* = 12.6 Hz, SC**Hᵦ**), 2.40 (3H, s, ArC**H₃**), 1.88-1.93 (2H, m, C**H₂**), 1.76-1.81 (2H, m, C**H₂**), 1.66-1.72 (4H, m, C**H₂**), 1.42-1.49 (4H, m, C**H₂**); **¹³C NMR** (150 MHz, CDCl₃): δ 163.3, 154.9, 140.7, 133.9, 130.9, 122.9, 109.7, 108.8, 67.8, 67.0, 61.5, 60.1, 55.5, 54.3, 41.6, 40.5, 29.9, 28.6, 28.3, 27.5, 25.3, 24.0, 21.5; **³¹P NMR** (32 MHz, CDCl₃): δ -21.89. **LRMS** calcd. for (M+ H) C₂₃H₃₅N₃O₇PS: requires 528.2, found 528.2.

7.8 References for Experimental

(1)   *Purification of Laboratory Chemicals (4th Edition)*; Armarego, W. L. F.; Perrin, D. D., Eds.; Elsevier, 1997.

(2)   Polyak, S. W.; Chapman-Smith, A.; Brautigan, P. J.; Wallace, J. C. *Journal of Biological Chemistry* **1999**, *274*, 32847.

(3)   Polyak, S. W.; Chapman-Smith, A.; Mulhern, T. D.; Cronan, J. E., Jr.; Wallace, J. C. *J Biol Chem* **2001**, *276*, 3037.

(4)   Cheng, Y.; Prusoff, W. H. *Biochem Pharmacol* **1973**, *22*, 3099.

(5)   Brown, P. H.; Cronan, J. E.; Grøtli, M.; Beckett, D. *Journal of Molecular Biology* **2004**, *337*, 857.

(6)   Debnath, J.; Dasgupta, S.; Pathak, T. *Bioorganic & Medicinal Chemistry* **2010**, *18*, 8257.

(7)   Alves, A. M.; Holland, D.; Edge, M. D. *Tetrahedron Letters* **1989**, *30*, 3089.

(8)   Zatorski, A.; Watanabe, K. A.; Carr, S. F.; Goldstein, B. M.; Pankiewicz, K. W. *Journal of Medicinal Chemistry* **1996**, *39*, 2422.

(9)   *Organophosphorus Reagents: A Practical Approach in Chemistry*; 1 ed.; Williams, D. M. H., V. H.;, Ed.; Oxford University Press: Oxford, 2004; Vol. 1.

(10)   Mugherli, L.; Burchak, O. N.; Balakireva, L. A.; Thomas, A.; Chatelain, F.; Balakirev, M. Y. *Angewandte Chemie International Edition* **2009**, *48*, 7639.

(11)   Jawalekar, A. M.; Meeuwenoord, N.; Cremers, J. G. O.; Overkleeft, H. S.; van der Marel, G. A.; Rutjes, F. P. J. T.; van Delft, F. L. *The Journal of Organic Chemistry* **2007**, *73*, 287.

(12)   Desjardins, M.; Garneau, S.; Desgagnés, J.; Lacoste, L.; Yang, F.; Lapointe, J.; Chênevert, R. *Bioorganic Chemistry* **1998**, *26*, 1.

(13)   LeBlanc, B. W.; Jursic, B. S. *Synthetic Communications* **1998**, *28*, 3591.

(14)   Oshima, N.; Suzuki, H.; Moro-oka, Y. *Chem. Lett.* **1984**, *13*, 1161.

(15)   Boren, B. C.; Narayan, S.; Rasmussen, L. K.; Zhang, L.; Zhao, H.; Lin, Z.; Jia, G.; Fokin, V. V. *Journal of the American Chemical Society* **2008**, *130*, 8923.

(16)   Corona, C.; Bryant, B. K.; Arterburn, J. B. *Organic Letters* **2006**, *8*, 1883.

(17)   Wang, T.; Lee, H. J.; Tosh, D. K.; Kim, H. O.; Pal, S.; Choi, S.; Lee, Y.; Moon, H. R.; Zhao, L. X.; Lee, K. M.; Jeong, L. S. *Bioorganic & Medicinal Chemistry Letters* **2007**, *17*, 4456.

(18)   Comstock, L. R.; Rajski, S. R. *Tetrahedron* **2002**, *58*, 6019.

(19)   DeLaLuz, P. J.; Golinski, M.; Watt, D. S.; Vanaman, T. C. *Bioconjugate Chemistry* **1995**, *6*, 558.

(20)   Guillerm, G.; Guillerm, D.; Vandenplas-Witkowki, C.; Rogniaux, H.; Carte, N.; Leize, E.; Van Dorsselaer, A.; De Clercq, E.; Lambert, C. *Journal of Medicinal Chemistry* **2001**, *44*, 2743.

(21)   Nagahara, T.; Suemasu, T.; Aida, M.; Ishibashi, T.-a. *Langmuir* **2009**, *26*, 389.

(22)   Zhang, Q.; Hua, G.; Bhattacharyya, P.; Slawin, Alexandra M. Z.; Woollins, J. D. *European Journal of Inorganic Chemistry* **2003**, *2003*, 2426.

(23)   Itahara, T. *Journal of the Chemical Society, Perkin Transactions 2* **1998**, 1455.

(24)   Szalecki, W. *Bioconjugate Chemistry* **1996**, *7*, 271.

(25)   Wilbur, D. S.; Hamlin, D. K.; Chyan, M.-K.; Kegley, B. B.; Pathare, P. M. *Bioconjugate Chemistry* **2001**, *12*, 616.

(26)   Wilbur, D. S.; Chyan, M.-K.; Pathare, P. M.; Hamlin, D. K.; Frownfelter, M. B.; Kegley, B. B. *Bioconjugate Chemistry* **2000**, *11*, 569.

(27)   Liu, F.-T.; Leonard, N. J. *Journal of the American Chemical Society* **1979**, *101*, 996.

(28)   Umeda, N.; Ueno, T.; Pohlmeyer, C.; Nagano, T.; Inoue, T. *Journal of the American Chemical Society* **2010**, *133*, 12.

(29)   Loren, J. C.; Krasiński, A.; Fokin, V. V.; Sharpless, K. B. *Synlett* **2005**, *2005*, 2847.

(30)   Huang, L.; Shi, A.; He, F.; Li, X. *Bioorganic & Medicinal Chemistry* **2010**, *18*, 1244.

(31)   Qin, A.; Lam, J. W. Y.; Jim, C. K. W.; Zhang, L.; Yan, J.; Häussler, M.; Liu, J.; Dong, Y.; Liang, D.; Chen, E.; Jia, G.; Tang, B. Z. *Macromolecules* **2008**, *41*, 3808.

(32)   Bymaster, F. P.; Beedle, E. E.; Findlay, J.; Gallagher, P. T.; Krushinski, J. H.; Mitchell, S.; Robertson, D. W.; Thompson, D. C.; Wallace, L.; Wong, D. T. *Bioorganic & Medicinal Chemistry Letters* **2003**, *13*, 4477.

(33)   Li, Z. a.; Zeng, Q.; Li, Z.; Dong, S.; Zhu, Z.; Li, Q.; Ye, C.; Di, C. a.; Liu, Y.; Qin, J. *Macromolecules* **2006**, *39*, 8544.

(34)   Shinde, S. S.; Chi, H. M.; Lee, B. S.; Chi, D. Y. *Tetrahedron Letters* **2009**, *50*, 6654.

(35)   Huang, L.; Luo, Z.; He, F.; Lu, J.; Li, X. *Bioorganic & Medicinal Chemistry*
        2010, *18*, 4475.

(36)   Shankaran, K.; Donnelly, K. L.; Shah, S. K.; Humes, J. L.; Pacholok, S. G.; Grant,
        S. K.; Green, B. G.; MacCoss, M. *Bioorganic & Medicinal Chemistry Letters*
        1997, *7*, 2887.